MOLECULAR BASIS OF BACTERIAL TOLERANCE TO OSMO-CHALLENGING ENVIRONMENTS: THE PLANT GROWTH-PROMOTING BACTERIUM *Gluconacetobacter diazotrophicus* PAL5 AS A MODEL SYSTEM

MARIANA RAMOS LEANDRO

UNIVERSIDADE ESTADUAL DO NORTE FLUMINENSE
DARCY RIBEIRO – UENF

CAMPOS DOS GOYTACAZES - RJ
DEZEMBRO - 2020

MOLECULAR BASIS OF BACTERIAL TOLERANCE TO OSMO-CHALLENGING ENVIRONMENTS: THE PLANT GROWTH-PROMOTING BACTERIUM *Gluconacetobacter diazotrophicus* PAL5 AS A MODEL SYSTEM

MARIANA RAMOS LEANDRO

"Tese apresentada ao Centro de Biociências e Biotecnologia da Universidade Estadual do Norte Fluminense Darcy Ribeiro, como parte das exigências para obtenção do título de Doutor em Biotecnologia Vegetal."

Orientador: Prof. Gonçalo Apolinário de Souza Filho

CAMPOS DOS GOYTACAZES - RJ
DEZEMBRO - 2020

FICHA CATALOGRÁFICA
UENF - Bibliotecas
Elaborada com os dados fornecidos pela autora.

L437 Leandro, Mariana Ramos.

Molecular basis of bacterial tolerance to osmo-challenging environments: The plant growth-promoting bacterium *Gluconacetobacter diazotrophicus* PAL5 as a model system /Mariana Ramos Leandro. - Campos dos Goytacazes, RJ, 2020.

167 f. : il.
Inclui bibliografia.

Tese (Doutorado em Biotecnologia Vegetal) - Universidade Estadual do Norte Fluminense Darcy Ribeiro, Centro de Biociências e Biotecnologia, 2020.
Orientador: Goncalo Apolinario de Souza Filho.

1. Osmotic stress. 2. Salt stress. 3. High-sugar. 4. Proteomics. 5. Mutagenesis. I.Universidade Estadual do Norte Fluminense Darcy Ribeiro. II. Título.

CDD - 660.6

MOLECULAR BASIS OF BACTERIAL TOLERANCE TO OSMO-CHALLENGING ENVIRONMENTS: THE PLANT GROWTH-PROMOTING BACTERIUM *Gluconacetobacter diazotrophicus* PAL5 AS A MODEL SYSTEM

MARIANA RAMOS LEANDRO

"Tese apresentada ao Centro de Biociências e Biotecnologia da Universidade Estadual do Norte Fluminense Darcy Ribeiro, como parte das exigências para obtenção do título de Doutor em Biotecnologia Vegetal."

Aprovada em 17 de dezembro de 2020.

Comissão Examinadora:

Dr. Euan Kevin James (PhD., Biological Sciences) - The James Hutton Institute

Dr. Emanuel Maltempi de Souza (D.Sc., Ciências – Bioquímica) - UFPR

Dr. Fábio Lopes Olivares (D.Sc., Agronomia) - UENF

Prof. Gonçalo A. de Souza Filho (D.Sc., Biociências e Biotecnologia) – UENF (Orientador)

À minha bisavó, Carmelita Maria Conceição da Silva, in memoriam,

dedico.

"Y*ou have within you the strength, the patience,*
and the passion to reach for the stars to change the world."

(Harriet Tubman)

AGRADECIMENTOS

À minha mãe e à minha irmã, pelo amor, exemplo e incentivo que são a principal força impulsora da minha caminhada;

À minha família, minha base, pelo carinho e apoio. Em especial, minha avó Nazaré e meus tios Claudete e Marcelino;

Às minhas companhias de moradia em Campos, Júlia Moreira, Sara Sangi, Léo Silva e Elis Nymeria, pela amizade, pela parceria, pelas horas de conversas, trocas de apoio, e por serem minha segunda família;

Ao professor Gonçalo Apolinário, meu orientador, pela dedicação na orientação, pela amizade e pelos ensinamentos valiosos para minha formação profissional e pessoal;

Aos companheiros de laboratório, em especial: Clara Maia, Danyelle Mayrink, Júlia Moreira, Fabiano Soares e Vivian Pimentel, pela amizade, pelas trocas de conhecimento e por tornarem as manhãs, tardes e noites de trabalho mais agradáveis;

Aos antigos companheiros de laboratório, que já não dividem mais a bancada comigo, mas foram fundamentais na minha formação. Em especial, agradeço ao Leandro Fernandes, a Suzane Ariádina, a Patrícia Rangel, a Tamires Cruz, ao Luciano Vespoli e a Roberta Barbosa pela amizade e ensinamentos;

À Ana Laura Boechat, pela agradável companhia, pelos ensinamentos e contribuições para realização deste trabalho;

Ao Lucas Passamani, Ricardo Reis, Ellen Moura, Felipe Astolpho e professor Vanildo pelos ensinamentos e contribuições para realização deste trabalho;

À técnica do LBT, Telma, pela disponibilidade de sempre;

À equipe responsável pela manutenção, limpeza e segurança da UENF. Em especial, agradeço à dona Carla, pela disponibilidade e contagiante alegria, e ao Uiris, pela disponibilidade e profissionalismo;

Aos doutores Euan James, Emanuel Maltempi e Fábio Olivares por aceitarem fazer parte da banca examinadora desta tese de doutorado;

Ao CNPq, Capes, Finep, Faperj e INCT, pelo apoio financeiro;

À UENF e ao Programa de Pós-graduação em Biotecnologia Vegetal, pela estrutura, pelo apoio e pela oportunidade de realização deste curso;

A todos os professores do Programa de Pós-Graduação em Biotecnologia Vegetal, pelos ensinamentos;

Ao atual coordenador do Programa de Pós-graduação em Biotecnologia Vegetal da UENF, professor Thiago Venâncio, e aos professores Fábio Olivares e Gonçalo Apolinário que o antecederam na coordenação, pela maestria na condução do Programa e parceria com o corpo discente;

À secretária Margareth de Vasconcelos, pela disponibilidade e atenção de sempre;

Ao Núcleo de Estudos em Biotecnologia Vegetal da UENF (GerminAção), pela oportunidade de ter feito parte da equipe e pela troca de experiências e ensinamentos;

E a todos que contribuíram direta ou indiretamente para a conclusão deste trabalho e desta minha etapa profissional.

SUMMARY

ABSTRACT

Bacteria account for most of the biodiversity on Earth. Due to its small size, variations in the environment, such as water availability or nutritional status, can drastically affect bacterial survivance. One of the most recurrent challenges for its survival is the external osmotic fluctuations that can occur due to several factors in the environment, such as dehydration, salinity, and high sugar-conditions. In this sense, the bacteria capable of living under osmo-challenging conditions have great biotechnological potential once they can be a source for new genes and mechanisms of osmotolerance. Among the osmotolerant bacterial species, the plant growth-promoting bacterium *Gluconacetobacter diazotrophicus* stands out as one of the few non-halophiles prokaryotes capable of growth below 0.900_{aw}. However, specific osmotolerance mechanisms that differ *G diazotrophicus* from non-osmotolerant bacteria remain unclear. In this sense, the present work aimed to elucidate the molecular mechanisms regulated in *G. diazotrophicus* in response to different osmo-challenging conditions. To this, we utilized the solutes PEG-400, NaCl, and sucrose to induce osmotic stress, salt stress, and high-sugar environment, respectively, on *G. diazotrophicus*. Bacterial cells exposed to each of these three osmo-challenging conditions were analyzed through morphological, comparative proteomics, and knockout mutagenesis analyses. As a result of the bacterial exposure to osmotic stress (PEG-400), proteomics analyses revealed the regulation of pathways for osmotic adjustment, de novo saturated fatty acids biosynthesis, and uptake of nutrients. The mutagenesis analysis showed that the lack of AccC protein, an essential component of de novo fatty acid biosynthesis, severely affected *G. diazotrophicus* resistance to osmotic stress. Additionally, knock-out mutants for nutrients uptake (Δ*tbdr* and Δ*oprB*) and compatible solutes synthesis (Δ*mtlK* and Δ*otsA*) became more sensitive to osmotic stress. The proteomic analyses of *G. diazotrophicus* exposure to salt stress (NaCl) showed that salt stress modulates proteins involved in iron uptake, outer membrane efflux, osmotic adjustment, cell division and elongation, and protein transport and quality control. The mutagenesis analysis showed that a knock-out mutant for protein quality control (Δ*degP*) was highly sensitive to salt stress. Besides, Δ*tbdr* and Δ*mtlK* became more sensitive to salt stress. This is the first demonstration that DegP protein, a protease with minor chaperone activity, is essential for tolerance to salt stress in *G. diazotrophicus*. The proteomic analyses of *G. diazotrophicus* exposure to high-sugar (sucrose) lead to the identification of regulatory pathways related to sugar metabolism, nutrient uptake,

compatible solute synthesis, amino acid metabolism, and proteolytic system. Mutagenesis analysis revealed that the knock-out mutants Δ*zwf* (sugar metabolism), Δtbdr, ΔmtlK, Δ*pepN* (proteolytic system), Δ*metH* (amino acid metabolism), and Δ*ilvD* (amino acid metabolism), became more sensitive to high-sucrose. By an integrated analysis of our results, we demonstrated that although there are particularities of response to each osmo-challenging condition, there were a significant number of overlapping proteins and mechanisms regulated in *G. diazotrophicus*. Also, we highlight the essential role of the genes *accC* to osmotic stress tolerance, *degP* to salt stress tolerance, and *pepN* to high-sugar resistance in *G. diazotrophicus*. The results obtained in the present work open perspectives about bacterial resistance to osmo-challenging environments and bring new inputs that can be exploited in several application fields, including the industry and agriculture.

Keywords: osmotic stress, salt stress, high-sugar, proteomics, mutagenesis

1. INTRODUCTION

Bacteria are ubiquitous in nature, accounting for most of the biodiversity on Earth (Stevenson *et al.*, 2015). Their habitats vary from water, soil, and air, until extreme environments, such as hydrothermal vents and saturated salt brines (Fenchel and Finlay, 2004). The spatial heterogeneity of bacterial habitats and the temporal dynamics of stress parameters frequently turn the surrounding environment hostile (Stevenson *et al.*, 2015). In this sense, the bacterial ability to survive in a wide range of environments makes them a powerful source of resistance genes and mechanisms for several application fields, including industry and agriculture.

Across bacterial habitats, one of the most recurrent challenges for its survival is the external osmotic fluctuations. This challenge is strictly related to water availability (water activity, a_w), which determines the functionality and viability of living systems (Stevenson *et al.*, 2015). The vast majority of bacterial species on Earth are incapable of multiplying below 0.900 a_w, except archaeal and bacterial halophiles that can multiply until approximately 0.611 a_w (Stevenson *et al.*, 2015).

The semipermeability of the bacterial cytoplasmic membrane, permeable to water but not to most other metabolites, directly contributes to changes in the internal water activity in response to external osmotic fluctuations (Bremer and Krämer, 2019). Hyperosmotic environments, which contain a low water activity, triggers the efflux of water out of bacterial cells, leading to cytoplasmic dehydration and turgor loss (Bremer and Krämer, 2019). On the other hand, the high water activity of hypoosmotic environments causes an excessive influx of water, which affects cellular integrity by the substantial increase in turgor (Csonka, 1989; Bremer and Krämer, 2019).

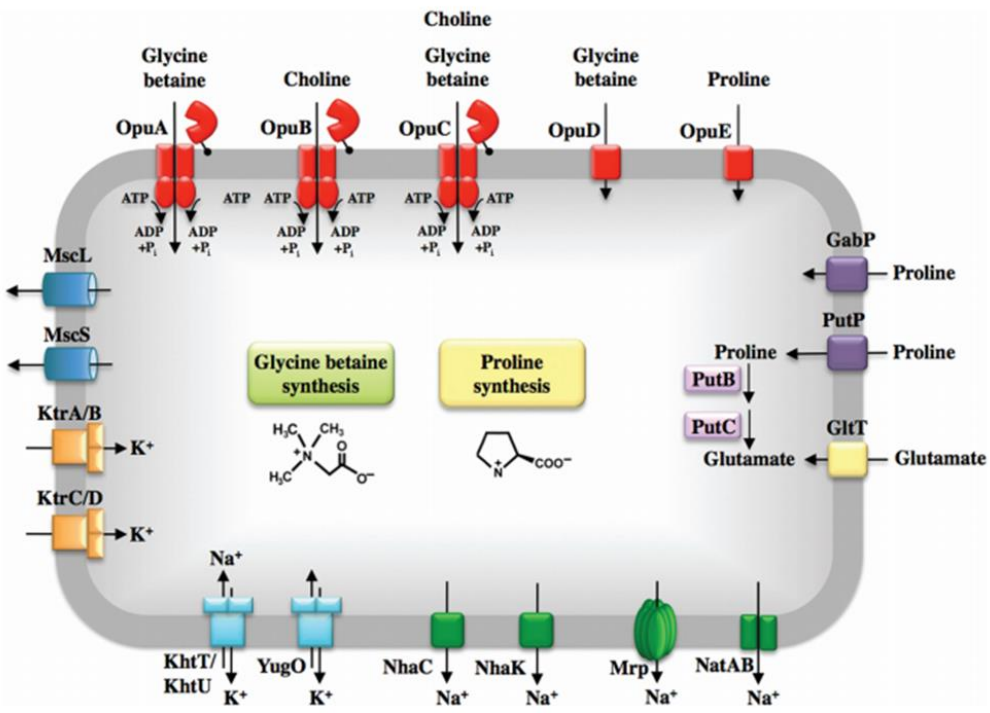

Fig. 1 Overview of the molecular mechanisms cellular components involved in bacterial responses to osmotic stress (Hoffman and Bremer, 2016).

Moreover, the osmotic status of the cytoplasm also affects cellular macromolecules (e.g., proteins), once changes in the concentrations of intracellular components may be harmful to cellular processes (e.g., increase in the concentrations of ions can reach toxic levels) (Paul, 2013). So, both hyper- and hypoosmotic conditions challenge the ability of bacteria to perform vital cellular processes. Therefore, precise osmoadaptation mechanisms are a key factor that determines the ability of bacterial cells to thrive in a variety of environments (Fig. 1).

Several conditions can trigger osmotic stress responses on bacterial cells, such as dehydration and the exposure to high-salt and sugar-rich environments. All of the osmotic stress conditions have in common the disturbance of the status of water activity within bacterial cells (Wood *et al.*, 2009). However, depending on the physicochemical

properties of an osmotic stressor, bacterial cells need to modulate specific response mechanisms to counteract other challenges associated with it.

1. 1 Bacterial responses to osmotic stress

Bacteria did not possess mechanisms to pump water into or out of the cytoplasm actively. Hence, response mechanisms that modulate cellular adjustment to hyper- and hypoosmotic stress indirectly counteract water flux as environmental osmolality fluctuates (Paul, 2013).

In response to hyperosmotic stress, bacterial cells generally increase their intracellular concentration of some molecules, either by *de novo* synthesis and/or import, to reduce the water activity and reestablish cell volume and turgor. The molecules accumulated in such a condition are not greatly inhibitory to cellular processes, and, thus, they are called compatible solutes (Wood et al., 2009). The compatible solutes, also called osmolytes, include sugars (e.g., mannitol, trehalose), amino acids (e.g., proline) and their derivatives (e.g., glycine betaine). Conversely, when bacterial cells are suddenly exposed to hypoosmotic conditions, rapid expulsion of ions and metabolites occurs through the transient opening of mechanosensitive channels. It increases the internal water activity and prevent cell lysis (Wood et al., 2009).

Accumulation of compatible solutes is, in general, the second response of a cell to an hyperosmotic shock; as a first, bacterial cells temporarily increase their intracellular K^+ content as an emergency stress response to decrease water efflux (Bremer and Krämer, 2019). Simultaneously, the cell activates the accumulation of compatible solutes to provide a more stable osmotic adjustment. Then, the increase of such osmolytes in the

cytoplasm allows the export of K^+ to reduce the ionic strength (Held and Sadowski, 2016; Bremer and Krämer, 2019).

Moreover, the adaptation of bacterial cells to different osmotic fluctuations does not only include adjustment and direction of water flow. Bacterial cell envelope needs to sense and respond quickly to environmental osmotic changes to avoid osmotic stress-deleterious effects (Mitchell and Silhavy, 2019). The fortification of peptidoglycan structure by increasing its molecular components and the cellular membrane fluidity adjustment act as essential barriers under osmotic stress, preserving cell turgor and preventing water loss (Van Heijenoort, 2001; Masi et al., 2017).

1. 2 Bacterial responses to salt stress

When hyperosmotic conditions occur due to an increase in external salt concentration, two simultaneous stressing factors are faced by bacterial cells: osmotic stress derived from extracellular solute elevation and ionic stress (Shabala *et al.*, 2009; Oliveira *et al.*, 2016) . The latter refers to the toxicity associated with cellular penetration of ions that affects intracellular ionic balance, protein folding process, cytoplasm pH, and various enzyme activities.

Ion-specific responses vary according to the bacterial species and the ions nature (Oliveira *et al.*, 2016). In some bacterial species, the exposure to high NaCl concentrations leads to a massive Na^+ influx that can cause substantial membrane depolarization, impairing low-affinity K^+ uptake (Shabala *et al.*, 2009). The membrane depolarization can also lead to the efflux of K^+ through voltage-gating K^+ -permeable channels (Shabala *et al.*, 2009). As the permeation of ion channels is normally higher than high-affinity pumps or transporters, these bacterial cells cannot compensate for such

depolarization. This is the case for bacteria species that possesses sensitivity to sodium ion-specific toxicity during salt stress, such as *Escherichia coli* (Shabala *et al.*, 2009).

On the other hand, some bacteria species, as the acidophilic bacteria, possesses positive internal membrane potential (Zammit *et al.*, 2012; Oliveira *et al.*, 2016). To these bacteria, the exposure to NaCl leads to a massive Cl^- and H^+ influx, which causes the acidification of cytoplasm and cell death (Zammit *et al.*, 2012). This is the case for bacteria species that possesses sensitivity to chloride ion-specific toxicity during salt stress.

1. 3 Bacterial responses to high-sugar

High-sugar environments are paradoxical because, whereas they are a resource-rich condition, they can also be hostile to bacterial life. As a solute, sugar reduces water activity, impairing bacterial cell turgor, metabolic activity, and division (Lievens *et al.*, 2015). There are, however, other physicochemical properties of high-sugar environments that can affect bacterial systems.

Sugars can alter the viscosity of both extra- and intracellular compartments, and that viscosity *per se* is a stress parameter that inhibits the bacterial metabolic activities (Lievens *et al.*, 2015). Besides, most of high-sugar environments contains chaotropic solutes (e.g., ethanol, fructose and glycerol), all of which can lead to chaotropicity-mediated stresses that inhibit or prevent bacterial multiplication. So, to live in high-sugar habitats, bacterial cells require mechanisms to counteract such harmful effects. However, in contrast to bacterial response mechanisms to salinized conditions, the cell biology of sugar-tolerant bacterial species at low water activity is poorly understood.

.

1. 4 *Gluconacetobacter diazotrophicus*: a model for study on bacterial responses to osmo-challenging environments

Among the osmotolerant bacterial species, the plant growth-promoting bacterium *Gluconacetobacter diazotrophicus* stands out as one of the few non-halophiles prokaryotes capable of growth below 0.900 a_w (Stevenson *et al.*, 2015). *G. diazotrophicus* is a acidophilic bacterium that was first isolated from sugarcane tissues, where the sucrose content can reach 30% (Cavalcante and Dobereiner, 1988). This bacterium has also been isolated from other sugar-rich plants, such as pineapple (*Ananas comosus*), sweet potato (*Ipomoea batatas*), and coffee plants (*Coffea arabica*) (Madhaiyan *et al.*, 2004; Luna *et al.*, 2010). Among its main beneficial mechanisms as PGPB are the nitrogen fixation, phytohormones production, and nutrient solubilization (Saravanan *et al.*, 2007; Pedraza, 2008; Rodrigues *et al.*, 2016).

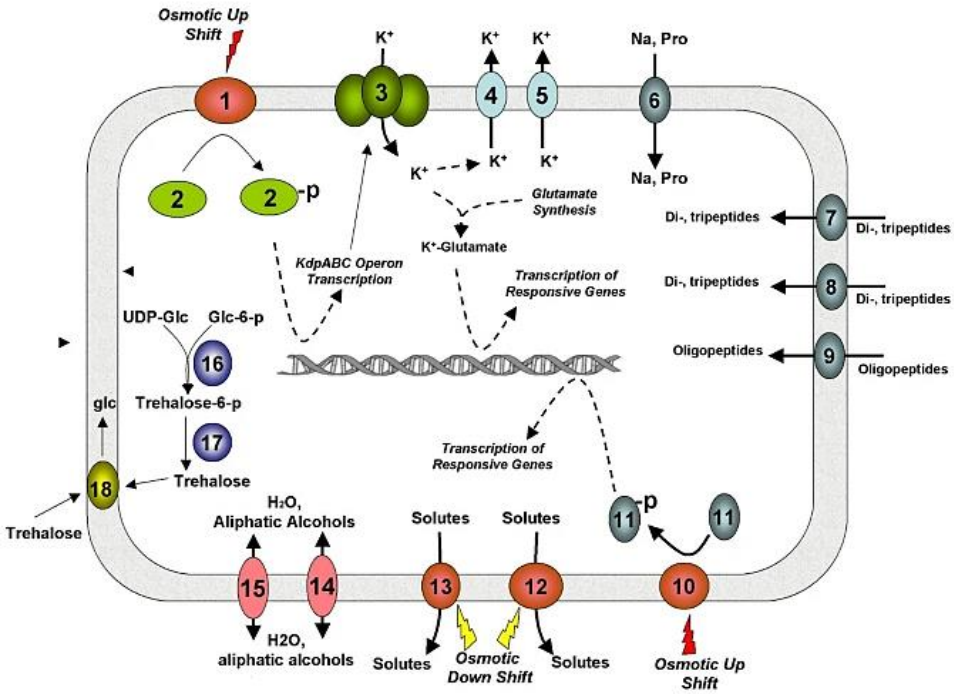

Fig.2 Osmotolerance mechanisms in *G. diazotrophicus*. (1) Sensor protein KdpD. (2) Transcriptional regulatory protein KdpE. (3) Potassium ABC transporter KdpABC. (4) Glutathione-regulated system protein KefB and (5) KefC. (6) Proline/betaine transporter. (7) Dpp ABC transporters for di- and tripeptides. (8) Transporter DtpT. (9) Oligopeptide transporter Opt.

(10) Sensor kinase EnVZ. (11) OmpR. (12) Large conductance mechanosensitive channel MscL (GDI1732). (13) Small conductance mechanosensitive channel MscS. (14) GlpRDFK. (15) GlpDKF. (16) OtsA. (17) OtsB. (18) TreA. Adapted from Bertalan et al. (2009).

The ability to live in osmo-challenge habitats makes *G. diazotrophicus* a promising source of osmotolerance genes. Its genome sequencing allowed the identification of several genes and mechanisms involved in osmotolerance mechanisms, as the *de novo* synthesis of compatible solutes, the import and export of K^+, and the regulation of mechanosensitive channels (Fig.2) (Bertalan *et al.*, 2009). However, these identified osmotolerance mechanisms are also present in several non-osmotolerant bacteria, suggesting that new specific mechanisms of *G diazotrophicus* may control its osmotolerance.

Studies on *G. diazotrophicus* responses to osmo-challenging conditions have suggested the existence of sets of differentially regulated mechanisms in this bacterium depending on the nature of the osmotic stressor. High NaCl concentrations drastically affect *G. diazotrophicus* growth, nitrogenase activity, and other essential enzyme performance, but the addition of glycine betaine in the bacterial growth medium can counteract some of these harmful effects (Tejera *et al.*, 2003; Boniolo *et al.*, 2009). Oliveira et al. (2016) showed that the growth inhibition caused by salinity in *G. diazotrophicus* occurs as a consequence of the Cl ion-specific toxic effect. Moreover, low osmotic stress levels are beneficial for *G. diazotrophicus* multiplication, which can tolerate Na_2SO_4, K_2SO_4, and high-sugar concentrations (Oliveira *et al.*, 2016). To resist these high-sucrose conditions, one of the mechanisms activated by *G. diazotrophicus* cells is the uptake of K^+ through a high-affinity potassium transporter (KupA) (Oliveira *et al.*, 2017).

Although several studies have exploited the mechanisms that confer the osmotolerance feature to *G. diazotrophicus* (Tejera *et al.*, 2003; Boniolo *et al.*, 2009; Velázquez-Hernández *et al.*, 2011; Oliveira *et al.*, 2016; Oliveira *et al.*, 2017), specific osmotolerance systems that differ *G diazotrophicus* from non-osmotolerant bacteria remain unclear. In this sense, the present work aimed to elucidate the molecular mechanisms regulated in *G. diazotrophicus* in response to osmotic stress, salt stress, and high-sugar

To this, we utilized the solutes PEG-400, NaCl, and sucrose to induce osmotic stress, salt stress, and high-sugar environment, respectively. *G. diazotrophicus* cells exposed to each of these three osmo-challenging conditions were analyzed through morphological, comparative proteomics, and knock-out mutagenesis analyses. The results obtained for each condition were organized in the following three independent chapters.

2. CHAPTER 1

COMPARATIVE PROTEOMICS REVEALS ESSENTIAL MECHANISMS FOR OSMOTOLERANCE IN *Gluconacetobacter diazotrophicus* PAL5

2.1 Abstract

Plant growth-promoting bacteria are a promising alternative to improve agricultural sustainability. *Gluconacetobacter diazotrophicus* is an osmotolerant bacterium able to colonize several plant species, including sugarcane, coffee, and rice. Despite its biotechnological potential, the mechanisms controlling such osmotolerance remain unclear. The present study investigated the key mechanisms of resistance to osmotic stress in *G. diazotrophicus*. The molecular pathways regulated by the stress were investigated by comparative proteomics, and proteins essential for resistance were identified by knock-out mutagenesis. Proteomics revealed the regulation of pathways for osmotic adjustment, *de novo* saturated fatty acids biosynthesis, and uptake of nutrients. The mutagenesis analysis showed that the lack of AccC protein, an essential component of *de novo* fatty acid biosynthesis, severely affected *G. diazotrophicus* resistance to osmotic stress. Additionally, knock-out mutants for nutrients uptake (Δ*tbdr* and Δ*oprB*) and compatible solutes synthesis (Δ*mtlK* and Δ*otsA*) became more sensitive to osmotic stress. Together, our results identified specific genes and mechanisms regulated by osmotic stress in an osmotolerant bacterium, shedding light on the essential role of cell envelope and extracytoplasmic proteins for osmotolerance.

Keywords: peg; fatty acid; mutagenesis; proteomics; plant growth-promoting bacteria

2.2 Introduction

During the last decades, the need for sustainable agricultural practices has increased the interest in plant growth-promoting bacteria (PGPB), aiming to reduce the demand for chemical fertilizers. However, the efficiency of PGPBs is dependent on its capacity to survive to several environmental factors, including abiotic stresses and plant-defense substances (de Souza *et al.*, 2015; Karimzadeh *et al.*, 2020). Water deficit is one of the main limiting factors for bacterial survival in the environment, once it promotes osmotic unbalance, affecting its water-cell outflow and cell turgor (Watt *et al.*, 2006; Vriezen *et al.*, 2007).

Bacterial cell envelope, the frontline of bacterial cells, needs to sense and respond quickly to environmental osmotic changes to avoid osmotic stress-deleterious effects (Mitchell and Silhavy, 2019). Proteins of cell envelope are essential to maintain the water balance, nutrient influx, and the efflux of harmful substances (Stenberg *et al.*, 2005; Ghai and Ghai, 2017; Masi *et al.*, 2017). In addition to cell envelope proteins, the fortification of peptidoglycan structure by increasing its molecular components and the cellular membrane fluidity adjustment act as essential barriers under osmotic stress, preserving cell turgor and preventing water loss (Van Heijenoort, 2001; Masi *et al.*, 2017).

Bacteria modify the fatty acid structure and regulate *de novo* biosynthesis of fatty acid biosynthesis to adjust membrane fluidity and adapt the cell to environmental changes (Zhang and Rock, 2008). Osmotic stress can induce bacterial saturated fatty acid accumulation, increase cell membrane packaging, and reduce its fluidity and permeability (Yoon *et al.*, 2015). Two protein groups, Acc and Fab, are essential for bacterial *de novo* saturated fatty acids biosynthetic pathway from Acetyl-CoA (Magnuson *et al.*, 1993). Acc initiates such a pathway by conversion of acetyl-CoA to malonyl-CoA (Lennen and Pfleger, 2012). Then, Fab proteins perform the chain elongation process by converting

malonyl-CoA to malonyl-ACP and the subsequent condensation of acyl groups with malonyl-ACP (Lennen and Pfleger, 2012). The regulation is a precise and highly energy-expensive pathway and determined by saturated fatty acids rate and specific environmental responses (Yoon *et al.*, 2015).

Although bacterial responses to osmotic stress have been widely described, less is known about resistance proteins owned by osmotolerant species. *Gluconacetobacter diazotrophicus* is an osmotolerant PGPB capable of growing under sucrose concentrations above 30% (Cavalcante and Dobereiner, 1988). Such characteristic allows this bacterium to inhabit environments with low water availability and high osmolarity, such as apoplast of sugarcane, and rhizosphere of coffee (Dong *et al.*, 1997; Jimenez-Salgado *et al.*, 1997). Resistance mechanisms of *G. diazotrophicus* to osmotic stress differ from those observed for several other bacterial species, once *G. diazotrophicus* does not accumulate common compatible solutes, as betaines, glutamic acid, and trehalose in such condition (Hartmann *et al.*, 1991). Although several studies demonstrate the effect of osmotic stressors on *G. diazotrophicus* (Hartmann *et al.*, 1991; Tejera *et al.*, 2003; Velázquez-Hernández *et al.*, 2011; De Oliveira *et al.*, 2016), the molecular mechanisms associated to bacterial resistance are poorly understood.

The present study investigated the specific mechanisms of *G. diazotrophicus* resistance to osmotic stress caused by polyethylene glycol (PEG-400). The effects on cell morphology and viability were investigated by epifluorescence microscopy. The molecular mechanisms regulated in response to osmotic stress were investigated by comparative proteomics, and the proteins essential for resistance to osmotic stress were identified by using knock-out mutants.

2.3 Materials and methods

2.3.1 Stock preparation of bacterial strains

The wild-type strain of *G. diazotrophicus* PAl5 used in this study was obtained in the culture collection of the Universidade Estadual do Norte Fluminense Darcy Ribeiro (UENF, Campos dos Goytacazes, Rio de Janeiro State, Brazil). The knock-out mutants of *G. diazotrophicus* PAl5, defective in the synthesis of proteins AccC (A9HEX0 - Δ*accC*), MtlK (A9HBL5 - Δ*mtlK*), OtsA (A9HBU6 - Δ*otsA*), OprB (A9HAM5 - Δ*oprB*), and a TonB-dependent receptor (A9HNM4 - Δ*tbdr*), were obtained from the "*G. diazotrophicus* PAl5 mutant library" of the Laboratório de Biotecnologia - UENF (Aline C. Intorne *et al.*, 2009). These mutants were generated with the EZ-Tn5 <R6Kyori/KAN-2>Tnp insertion kit (Epicentre, Madison, WI, USA). Stock cultures were produced as previously described by Oliveira et al. (2016) (De Oliveira *et al.*, 2016). Specifically, a single colony of each bacterial strain was grown in DYGS medium (1L: 2 g glucose; 2 g yeast extract; 1.5 g peptone; 1.3 g glutamic acid; 500 mg K_2HPO_4; 500 mg $MgSO_4.7H_2O$; pH 6.0) (Rodrigues Neto *et al.*, 1986) under constant agitation (250 rpm min^{-1}, 30 °C) until they reached OD_{600nm} of 1.0. After that, each culture (750 µL) was transferred to microtubes (1.5 mL) and mixed with 100% glycerol (250 µL). Liquid nitrogen was used to freeze tubes before the store at −80 °C.

2.3.2 Osmotic stress assays

Osmotic stress was performed as previously described by Oliveira et al. (2016) [20] with some modifications. Specifically, the polyethylene glycol (PEG, M.W. 400, Sigma Chemical Co., St. Louis, MO, USA) stock solutions were previously prepared at a concentration twice the desired final concentration and autoclaved. 5 mL of cells from 25% glycerol stocks of *G. diazotrophicus* wild-type and insertional mutant strains were

inoculated in 45 mL of DYGS medium within Erlenmeyer flasks (250 mL). The cultures were grown under constant stirring (250 rpm min^{-1}, 30°C) until they reached OD_{600nm} of 1.0. Then, the cultures were centrifuged (15 min; 10.000 g; 25°C), and a fresh two-fold DYGS medium was used to resuspend the cells. The OD_{600nm} of each culture was adjusted to 0.2, and 25 mL of then were mixed with equal volumes of PEG stock solutions in Erlenmeyer flasks (250 mL). The flasks were maintained under constant stirring (250 rpm min^{-1}, 30 °C). The OD_{600nm} reading was performed after 12 h. 2 mL of each culture was separated for microscopy analysis.

2.3.3 Microscopy analyses

2 mL of cell culture of *G. diazotrophicus* submitted to different PEG concentrations were transferred into microtubes (1.5 mL) and centrifuged (3 min; 10.000 g; 25 °C). The supernatants were discarded, and the resultant pellets were washed three times with saline solution [0.85% (w/v) NaCl]. 100 µL of 0.8% (w/v) agarose were added in the center of the glass slides before adding bacterial cells.

For morphological analysis, 5 µL of each washed bacterial suspension were applied onto the solidified agarose in the glass slides, covered with coverslips, and observed in the microscope (Carl Zeiss Axion Imager A.2 Microscope). To capture the images, the software Carl Zeiss Axion Vision Software 4.8.2 was used.

The washed cells were stained for cell viability analysis using the Live/Dead Bacterial Viability Kit (*Bac*LightTM, Thermo Fisher Scientific, U.S.), following fabricant recommendations. Equal volumes of SYTO® and propidium iodide were combined in a microtube (600 µL) to prepare the dye solution. After that, 0.6 µL of the dye mixture was applied in 100 µL of each bacterial suspension and incubated for 15 min in the dark at 23 ºC. Then, 5 µL of each bacterial suspension were applied onto the

solidified agarose in the glass slides, covered with coverslips, and observed in the microscope (Carl Zeiss Axion Imager A.2 Microscope). Six fields of glass slides per treatment were used to count live and dead bacterial cells.

2.3.4 Protein extraction

Three biological samples of *G. diazotrophicus* cells, exposed and non-exposed (control) to 350 mM PEG, were used for protein extract preparation. Each sample corresponded to each treatment sample (20 mL). The extraction methods were performed as described by Damerval et al. (1986) (Damerval *et al.*, 1986) with some modifications. The cells were harvested by centrifugation at 10.000 g at 4 °C for 15 min, and the supernatant was discarded. The resultant pellets were resuspended in a solution (1 mL) containing 10% (w/v) TCA (Sigma-Aldrich, St. Louis, USA) in acetone with 20 mM dithiothreitol (DTT; G.E. Healthcare, Little Chalfont, U.K.). The samples were kept under agitation at 10 °C for 30 min. Then, for protein precipitation, the samples were maintained at -20 °C for 60 min, followed by centrifugation at 16.000 g at 4 ºC for 30 min. The pellets were washed three times with a cooled solution of acetone and 20 mM DTT. The pellets were then dried, and Urea/Thiourea buffer (1 mL) [7 M Urea, 2 M Thiourea, 1% (w/v) DTT, 2% (v/v) Triton X-100, 1 mM PMSF, 5 µM pepstatin] was added to each sample. The samples were then maintained under agitation at 10 °C for 30 min, followed by centrifugation at 16.000 g at 4 °C for 30 min. Supernatants were collected, and the protein concentration of each sample was estimated with 2-D Quant Kit (2-D Quant Kit - G.E. Healthcare Life Sciences).

2.3.4.1 Protein digestion

Protein digestion was performed as described by Passamani et al. (2018) (Passamani *et al.*, 2018) with some modifications. Briefly, total protein (100 µg) from each biological sample was filtered on Amicon Ultra 0.5 -3 K.D. centrifugal filters (Merck Millipore, Darmstadt, Germany) using 50 mM ammonium bicarbonate (pH 8.5; Sigma-Aldrich) as the buffer. After filtration, each sample received 0.2% (v/v) RapiGestR surfactant (25 µL) (Waters, Milford, CT, USA). Each sample was then briefly vortexed and incubated at 80°C for 15 min in a ThermomixerR, and 100 mM DTT (2.5 µL) (Bio-Rad Laboratories, Hercules, CA, USA) was added to each sample. The samples were then vortexed and incubated under agitation (350 rpm min^{-1}) at 60 °C for 30 min, and 300 mM iodoacetamide (2.5 µL) (G.E. Healthcare, Piscataway, NJ, USA) was added. The samples were then vortexed and incubated in the dark at room temperature for 30 min. Each sample received 100 mM DTT (2.5 µL) (Bio-Rad Laboratories) and was incubated at 37 °C for 30 min to quench the iodoacetamide. Then, for protein digestion, each sample received a trypsin solution (20 µL) (50 ng $µL^{-1}$; V5111; Promega, Madison, WI, USA) prepared in 50 mM ammonium bicarbonate and was incubated overnight at 37°C. Aiming to precipitate RapiGestR, 5% (v/v) trifluoroacetic acid (10 µL) (TFA; Sigma-Aldrich) was added to each sample, incubated at 37 °C for 90 min, followed by centrifugation at 16.000 g for 30 min. The samples were then transferred to Total Recovery Vials (Waters), and peptide/sample (1 µg) was used for mass spectrometry analysis.

2.3.4.2 Mass spectrometry analysis

Mass spectrometry analysis was performed as described by Passamani et al. (2018) [24]. Briefly, a nanoAcquity UPLC connected to a Synapt G2-Si HDMS mass spectrometer (Waters) was used for the ESI-LC-MS/MS analysis. For separation, the

samples were loaded on the nanoAcquity UPLC 5-µm C18 trap column (180 µm x 20 mm) at 5 µL min^{-1} for 3 min and then onto the nanoAcquity HSS T3 1.8-µm analytical reverse-phase column (75 µm x 150 mm) at 400 nL min^{-1}. The column temperature was 45 °C. For peptides elution, a binary gradient was used: mobile phase A, containing 0.1% (v/v) formic acid (Sigma-Aldrich) and water (Tedia, Fairfield, USA), and mobile phase B, containing 0.1% (v/v) formic acid and acetonitrile (Sigma-Aldrich). Gradient elution was made by the following steps: 3 min with 7% B, increasing to 40% B until 90.09 min, increasing to 85% B until 94.09 min, keeping constant at 85% B until 98.09 min, decreasing to 7% B until 100.09 min, and keeping constant at 7% B until the end of the run at 108.09 min. Mass spectrometry was accomplished in the positive and resolution mode (V mode), with 35000 FWHM resolution of ion mobility, and data-independent acquisition mode. The ion mobility wave velocity was adjusted to 600 m s^{-1}. The transfer collision energy was up-accumulated from 19 V to 45 V in high-energy mode, the cone and capillary voltages were 30 V and 2,800 V, respectively, and the temperature was 70 °C. The nanoflow gas was calibrated to 0.50 Bar, and the purge gas flow altered from 145 L h^{-1} to 150 L h^{-1}. The parameters of TOF included a scan time of 0.5 s in the continuum mode and a mass range of 50 Da to 2000 Da. Human [Glu1]-fibrinopeptide B (100 fmol µ L^{-1}) (Sigma-Aldrich) was utilized as an external calibrant, and lock mass acquisition was made every 30 s.

2.3.4.3 Proteomic data analyses

For spectral processing and database searching, the software ProteinLynx Global Server (PLGS; version 3.0.2) and ISOQuant were used. The spectral processing on PLGS software was performed using a low-energy threshold of 150 (counts), an elevated energy threshold of 50, and an intensity threshold of 750. Furthermore, adjustments on parameter

analysis were made as follows: two missed cleavages, minimum fragment ion per peptide equal to 3, minimum fragment ion per protein equal to 7, minimum peptide per protein equal to 2, fixed modifications of carbamidomethyl, and variable modifications of oxidation and phosphoryl. The false discovery rate (FDR) for peptide and protein identification was regulated to a maximum of 1%, with a minimum peptide length of six amino acids. The proteomics data were processed against the *G. diazotrophicus* RIOGENE proteome database (www.uniprot.org/proteomes/UP000001176).

The analysis of comparative label-free quantification was performed with ISOQuant software with previously described settings and algorithms (Distler *et al.*, 2014, 2016). The analysis included retention time alignment, exact mass retention time (EMRT), ion mobility spectrometry clustering, protein homology filtering, and data normalization. Aiming to annotate the resulting feature clusters by ISOQuant, the consensus peptide identifications, and identification probabilities were evaluated. The parameters of protein identification in ISOQuant were adjusted to a false discovery rate (FDR) of 1%, a peptide score higher than six, a minimum peptide length of six amino acids, and at least two peptides per protein. The TOP3 identification was used to perform label-free quantification, with the multidimensional normalization process implemented within ISOQuant. The detailed ISOQuant processing parameters configuration is provided in Table S2.

After ISOQuant analysis, only the proteins present or absent (for unique proteins) in all three biological samples were selected for differential abundance analysis. The data were analyzed using Student's t-test (two-tailed). Differentially accumulated proteins (DAPs) ($P < 0.05$) were considered up-accumulated if the fold change (F.C.) was higher than 1.5 and down-accumulated if the F.C. was lesser than 0.667.

The prediction of the subcellular localization (outer membrane, periplasm, cytoplasmic membrane, or cytoplasm) of the identified DAPs was performed using FUEL-mLoc software (http://bioinfo.eie.polyu.edu.hk/FUEL-mLoc/). Additionally, DAPs were manually categorized in protein functional groups based on the information available in the literature.

2.3.5 Reverse genetics analysis

Reverse genetics analysis was performed by the inoculation of 5 mL of cells from glycerol stocks of *G. diazotrophicus* wild-type and insertional mutant strains in 45 mL of LGI medium (1L: 5 g sucrose; 0.2 g K_2HPO_4; 0.6 g KH_2PO_4; 0.2 g $MgSO_4.7H_2O$; 0.02 g $CaCl_2.2H_2O$; 0.002 g $Na_2MoO_4.2H_2O$; 0.01 g $FeCl_3$; pH 6.0) (Vladimir A. Cavalcante and Dobereiner, 1988) within Erlenmeyer flasks (250 mL). After that, cultures were grown under constant stirring (250 rpm min^{-1}, 30 °C) until they reached OD_{600nm} of 1.0. Then, cultures were arranged on a 96-well microplate and plated on LGI solid medium supplemented with PEG with a 96-pin replicator (Boekel, Fisher Scientific, Pittsburgh, PA, USA). The plates were maintained at 30 °C for five days. Then, results were registered.

2.4 Results

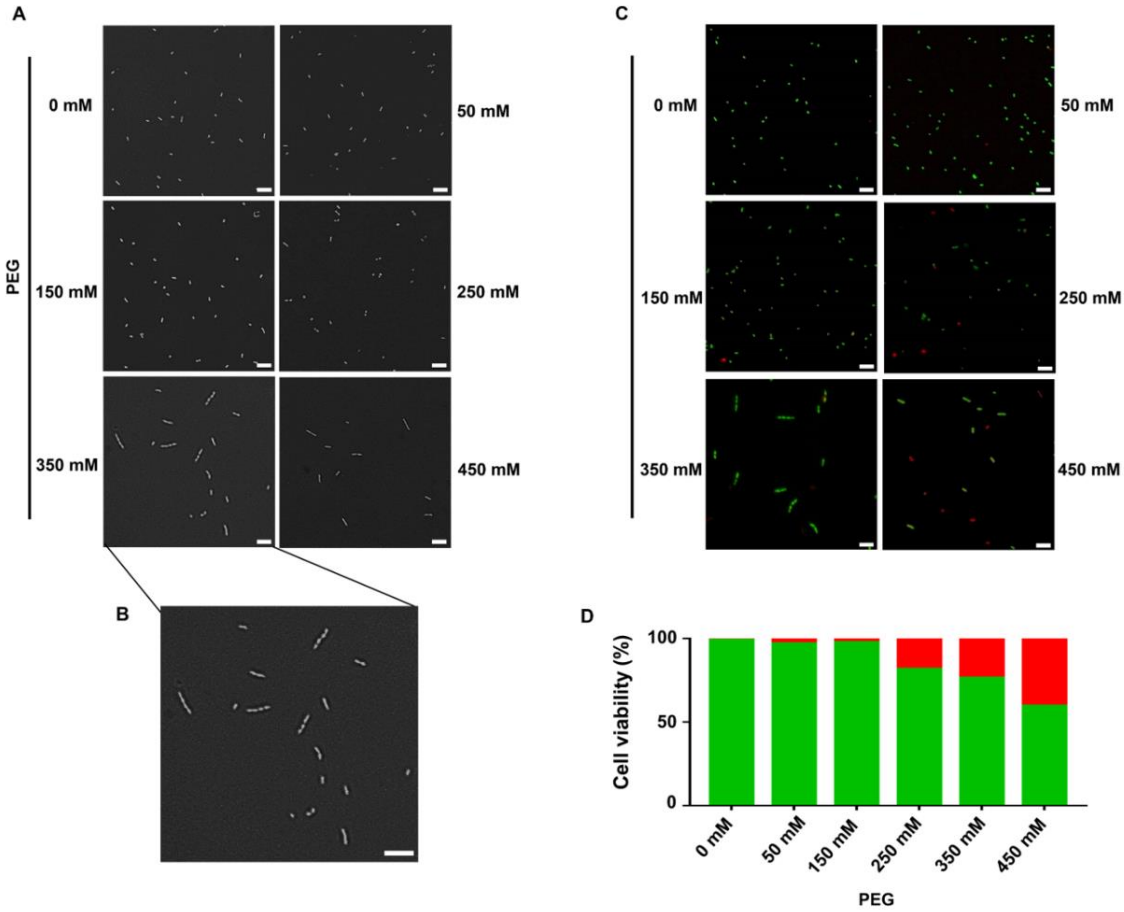

Figure 1. Osmotic stress affects *G. diazotrophicus* morphology and viability. *G. diazotrophicus* was cultivated for 12 h in liquid medium supplemented with different dilutions of PEG-400, and its morphological changes were analyzed (A). The image of *G. diazotrophicus* cells at 350 mM PEG-400 was amplified by 50% (B). The cell viability was analyzed through epifluorescence analysis (C), and the proportion of living (green) and dead (red) cells in the different dilutions of PEG-400 was plotted (D). *Bar* 5 µM.

2.4.1 Osmotic stress affects *G. diazotrophicus* morphology and viability

Aiming to investigate whether osmotic stress affects G. diazotrophicus morphology, bacterial cells were exposed to different dilutions of PEG-400 and analyzed by optical microscopy. Results show that the PEG-400 induces significant morphological changes, with bacterial chains composed by up to four cells, mainly at 350 mM PEG (Fig.

1A, Fig. 1B). The effects of osmotic stress on the cell viability of *G. diazotrophicus were analyzed by* epifluorescence microscopy. PEG dilutions lower than 250 mM induced a proportion of only about 3% of cell death, and even in the higher PEG dilution tested (450 mM), the cell viability was not severely affected (<50% of cell death) (Fig. 1C, Fig. 1D).

These results indicate that the morphological changes caused by osmotic stress in *G. diazotrophicus* are not directly related to cell death. Among the dilutions tested, 350 mM PEG induced the most significant morphological change without causing strong cell death. So, this dilution was selected for the subsequent proteomic analyses.

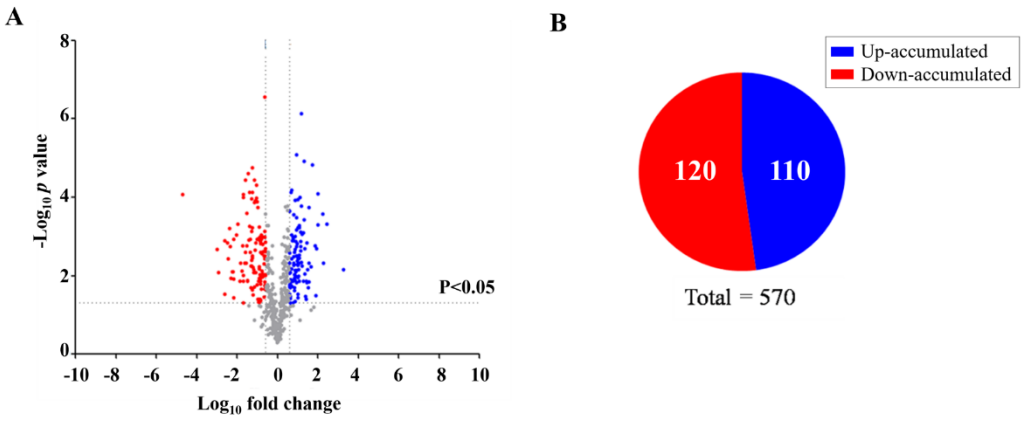

Figure 2. Osmotic stress changes the proteome profile of *G. diazotrophicus*. Volcano plot of all identified proteins (A) and graphical representation of the proportion of differentially accumulates proteins (DAPs) increased and decreased (B) were performed. The spots represent differential abundance (log2 fold change) of identified proteins in the function of statistical significance (-log10 *p* value). Red and blue spots represent DAPs up-accumulated and down-accumulated, respectively, and grey spots represent non-regulated proteins.

2.4.2 Osmotic stress changes the proteome profile of *G. diazotrophicus*

To explore the molecular responses of *G. diazotrophicus* to osmotic stress, total protein extracts from bacterial cells, cultivated during 12 hours in the presence or absence of 350 mM PEG-400, were analyzed by comparative proteomics. A total of 570 proteins

were identified, and 230 (~40%) were differentially accumulated (Table S1, Fig. 2). Among these, 110 proteins were up-accumulated, while 120 were down-accumulated in response to PEG-400 (Fig. 2A; Fig. 2B).

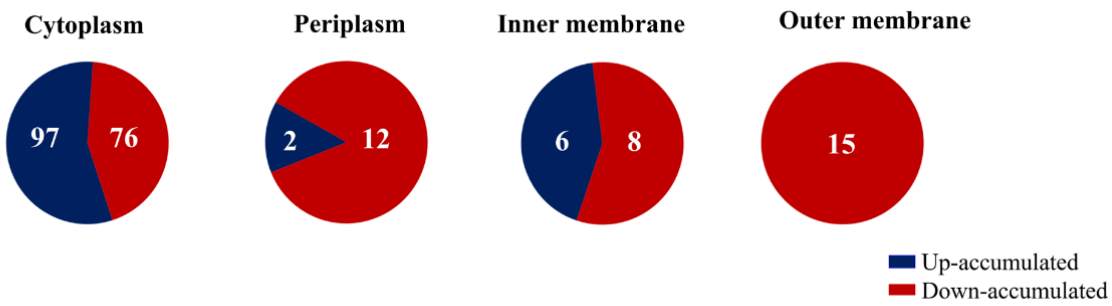

Figure 3. Osmotic stress differentially regulates the protein profile of *G. diazotrophicus* cellular compartments. Identified differentially accumulated proteins (DAPs) were classified by predicted subcellular localization (Cytoplasm; Periplasm; Inner Membrane; Outer Membrane) with FUEL-mLoc software.

2.4.3 Protein profile of cellular compartments during *G. diazotrophicus* response to osmotic stress

Aiming to evaluate the effect of osmotic stress on the proteome of cell compartments, the cellular localization of regulated proteins was predicted. Proteins from periplasm and outer membrane were mostly down-accumulated under osmotic stress (Fig. 3). In periplasm, among 14 regulated proteins, 12 were down-accumulated and two up-accumulated. In the outer membrane, all the 15 regulated proteins were down-accumulated (Fig. 3). Cytoplasmic proteins were mainly up-accumulated, while in the inner membrane, a similar number of proteins were up- and down-accumulated in response to osmotic stress (Fig. 3).

Table 1 Functional protein groups differentially regulated in *G. diazotrophicus* cells exposed to PEG

Accession	Description	Fold Change
a. *Nutrients uptake*		
A9HK76	Iron ABC transporter substrate-binding protein	0.32
A9H7L3	TonB-dependent siderophore receptor	0.41
A9HEU6	TonB-dependent siderophore receptor	0.33
A9HNM4	TonB-dependent receptor	0.18
A9H7L9	TonB-dependent receptor	0.31
A9HDZ9	TonB-dependent receptor	0.31
A9H7M7	TonB-dependent receptor	0.13
A9HE38	TonB-dependent receptor	0.39
A9H932	TonB-dependent receptor	0.53
A9HAM5	Carbohydrate porin (OprB)	0.64
A9HPF6	Carbohydrate porin	0.19
A9HPK6	D-ribose-binding periplasmic protein (RbsB)	0.18
A9HPB9	D-ribose-binding periplasmic protein (RbsB)	0.34
A9HNP0	D-xylose ABC transporter, periplasmic substrate-binding (XylF)	0.24
A9HPM0	Ribose ABC transporter	0.41
A9HPE1	Sugar ABC transporter substrate-binding protein	0.04
A9H577	Sugar ABC transporter substrate-binding protein	0.19
A9HPC7	Sugar ABC transporter substrate-binding protein	0.38
b. *Cell envelope metabolism*		
A9HKU2	3-hydroxyacyl-[acyl-carrier-protein] dehydratase (FabZ)	1.69
A9HEX0	Biotin carboxylase subunit of acetyl-CoA carboxylases (AccC)	1.80
A9HI46	Bifunctional protein (GlmU)	2.75
A9HI49	Glutamine-fructose-6-phosphate aminotransferase (GlmS)	4.67
A9HE46	Acetyl-CoA C-acyltransferase (FadA)	0.42
A9H986	Membrane integrity-associated transporter subunit (PqiC)	0.58
A9HMV6	Polysaccharide export protein (CtrA)	0.66
c. *Osmotic adjustment*		
A9HBU6	Alpha, alpha-trehalose-phosphate synthase (OtsA)	2.11
A9HBL5	Mannitol 2-dehydrogenase (MtlK)	2.3
d. *Cell division*		
A9HLY3	Site-determining protein (MinD)	0.43

2.4.4 Highlighted functional protein groups differentially regulated by osmotic stress in *G. diazotrophicus*

Four functional groups previously described as relevant to bacterial responses/tolerance to osmotic stress and morphological changes were identified through the functional categorization of *G. diazotrophicus* DAPs: nutrients uptake (Yoon *et al.*, 2015), cell envelope metabolism (Yoon *et al.*, 2015; Cesari *et al.*, 2018), osmotic adjustment (Iordachescu and Imai, 2008; Zahid *et al.*, 2015), and cell division (Conti *et al.*, 2015). Details of DAPs in each functional group are described below.

2.4.4.1 Nutrients uptake

Among the extracytoplasmic regulated proteins, we identified nine down-accumulated receptors related to the uptake of iron and other nutrients. Six of those are TonB-dependent receptors - TBDRs (A9H7M7, A9HNM4, A9H7L9, A9HDZ9, A9HE38, and A9H932), two are TonB-dependent siderophore receptors (A9HEU6 and A9H7L3), and one is a periplasmic iron ABC transporter substrate-binding protein (A9HK76) (Table 1).

Additionally, nine transporter proteins involved in sugar uptake identified in our proteomic analysis were down-accumulated (A9HAM5, A9HPF6, A9HPK6, A9HNP0, A9HPM0, A9HPE1, A9HPB9, A9H577, and A9HPC7) (Table 1). These results indicate that osmotic stress has a strong effect on *G. diazotrophicus* nutrients uptake process.

2.4.4.2 Cell envelope metabolism

Seven proteins involved in the biosynthesis and regulation of cell envelope were regulated in response to osmotic stress. Among those, two proteins, FabZ (A9HKU2) and AccC (A9HEX0), involved in *de novo* biosynthesis of fatty acid were up-accumulated (Table 1). Two proteins, GlmS (A9HI46) and GlmU (A9HI49), from the metabolic pathway of UDP-N-acetylglucosamine (UDP-GlcNAc), were also up-accumulated (Table 1). The protein Acetyl-CoA C-acyltransferase (FadA) (A9HE46), a component of the fatty acid oxidation pathway, was down-accumulated (Table 1). Moreover, the proteins PqiC (A9H986) and CtrA (A9HMV6) involved with the export of lipids and capsular lipopolysaccharides, respectively, were down-accumulated. These results reveal the adjustment of cell envelope components during *G. diazotrophicus* response to osmotic stress.

2.4.4.3 Osmotic adjustment

Two proteins involved with compatible solutes synthesis were up-accumulated in our proteomic analysis: alpha, alpha-trehalose-phosphate synthase – OtsA (A9HBU6), and mannitol 2-dehydrogenase – MtlK (A9HBL5) (Table 1). The activation of a small number of proteins involved with the synthesis of compatible solutes suggests that the resistance to osmotic stress in *G. diazotrophicus* may be associated with other molecular mechanisms.

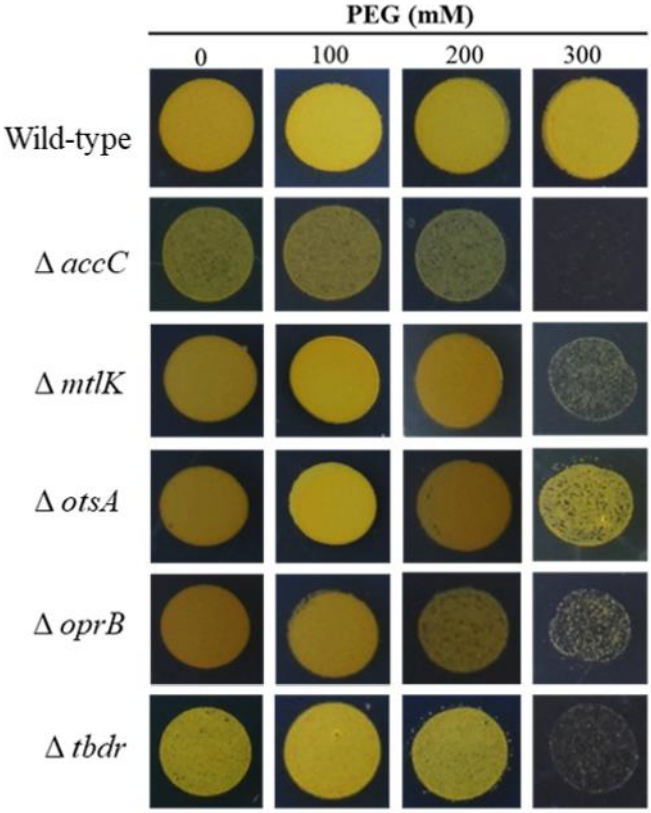

Fig. 4 Reverse genetics analysis revealed essential genes to PEG tolerance in *G. diazotrophicus*. Knock-out mutants of *G. diazotrophicus* defectives in the synthesis of five proteins regulated in our proteomic analysis were selected to perform the osmotic stress tolerance assay. Results were registered after five days of osmotic stress exposure.

2.4.4.4 Cell division

The protein MinD (A9HLY3), an essential component of site-determining cell division, was down-accumulated (Table 1). This result suggests that osmotic stress may affect the efficiency of the cell division process in *G. diazotrophicus*.

2.4.5 Reverse genetics analysis revealed essential proteins for *G. diazotrophicus* resistance to osmotic stress

Specific proteins from the above-mentioned highlighted protein groups were selected to investigate their role on *G. diazotrophicus* resistance to osmotic stress. A reverse genetics approach was applied by obtaining *G. diazotrophicus* knock-out mutants, defective in producing such proteins. The mutant strains, defective for genes related to compatible solute synthesis (Δ*otsA* and Δ*mtlK*), *de novo* biosynthesis of fatty acid (Δ*accC*), sugar uptake (Δ*oprB*), and iron uptake (Δ*tbdr*), were compared to wild-type *G. diazotrophicus* about their growth under several dilutions of PEG-400.

Each mutant presented different sensitivity to osmotic stress (300 mM PEG-400) in comparison to wild-type. The Δ*accC* mutant was the most sensitive to stress, while Δ*otsA* was the less affected (Fig. 4). These results indicate that AccC, MtlK, OtsA, OprB, and TBDR are essential to *G. diazotrophicus* resistance to osmotic stress, with emphasis on AccC.

2.5 Discussion

This study aimed to identify key mechanisms of *G. diazotrophicus* resistance to osmotic stress. Our analysis demonstrated that osmotic stress induces morphological alterations and affects cell viability. Proteomic and reverse genetics approaches revealed that the regulation of proteins involved in the uptake of iron, sugar, and other nutrients, osmotic adjustment, and *de novo* saturated fatty acids biosynthesis are essential to osmotic stress resistance in *G. diazotrophicus*.

Our proteomic data revealed a decrease of several extracytoplasmic proteins in response to osmotic stress, with emphasis on proteins involved in the uptake of nutrients, such as iron and sugar. Protein channels in the outer membrane of Gram-negative bacteria allow the passive diffusion of hydrophilic metabolites with a molecular mass lower than 600 Da, as PEG-400 (Nikaido, 2003). Although *G. diazotrophicus* is not capable of metabolizing PEG (Hartmann *et al.*, 1991), reducing its entry into cells may be a mechanism to avoid deleterious effects inside the cell. The decrease in metabolites uptake, even nutritious ones, is described as a resistance mechanism to avoid the entrance of harmful substances into the bacterial cell under stressful environments, such as toxic compounds and high salinity (Yoon *et al.*, 2015). Reverse genetic analysis showed that knock-out of genes involved with nutrients uptake (*oprB* and *tbdr*) affected *G. diazotrophicus* resistance to osmotic stress. These results indicate that OprB and TBDR activities are essential for bacterial homeostasis during osmotic stress. Their down-accumulation observed in the proteomic analyses may be a mechanism to avoid PEG entry into the cell.

The proteins AccC and FabZ, essential for *de novo* saturated fatty acids biosynthetic pathway (Campbell and Cronan, 2001), were up-accumulated in our proteomic analyses. The increase of saturated fatty acid levels decreases the

unsaturated/saturated fatty acids ratio and, consequently, reduces membrane fluidity (Yoon *et al.*, 2015). The reduction of bacterial membrane fluidity to avoid the entrance of harmful substances into the cells, and to maintain membrane integrity, is an essential mechanism of resistance to high temperature, toxic agents, and osmotic stress (Loffhagen *et al.*, 2002; Murínová and Dercová, 2014; Yoon *et al.*, 2015). Moreover, the protein FadA, responsible for the last step of the fatty acid oxidation pathway (Fujita *et al.*, 2007), was down-accumulated. Our reverse genetic results showed that the lack of AccC severely affects *G. diazotrophicus* resistance to PEG. These results suggest that the decrease in membrane fluidity, as a consequence of the production of saturated fatty acids, is an essential mechanism of osmotic stress resistance in *G. diazotrophicus*.

GlmS and GlmU, two essential proteins of the biosynthetic pathway of UDP-N-acetylglucosamine, were up-accumulated in the proteomic analyses. UDP-GlcNAc is a precursor for peptidoglycan and lipopolysaccharide biosynthesis (Van Heijenoort, 2001). On the other hand, proteins involved with the transport of phospholipids and lipopolysaccharide to the outer membrane (PqiC and CtrA) (Larue *et al.*, 2011; Ekiert *et al.*, 2017) were down-accumulated. Therefore, under osmotic stress, phospholipids and UDP-GlcNAc products would be directed to the inner membrane and peptidoglycan. We hypothesize that *G. diazotrophicus* adjust its peptidoglycan and membranes composition in response to osmotic stress to control internal turgor pressure and decrease membrane permeability.

The modification of cell envelope structures and the down-accumulation of the protein MinD may also be related to the morphological changes observed in *G. diazotrophicus* cells. A common consequence of the decrease in MinD activity is the formation of multiple FtsZ rings, whose morphological effect is the formation of multiple septa in bacterial cells (Levin *et al.*, 1998). Previous work has already shown that ionic

stressors, such as saline stress, cause morphological changes in *G. diazotrophicus* cells (Boniolo *et al.*, 2009; De Oliveira *et al.*, 2016). However, further analyses are necessary to investigate these processes with a non-ionic osmotic stressor such as PEG.

Only two proteins involved with compatible solute synthesis, MtlK and OtsA, were regulated in our proteomic analyses. These proteins are components of the mannitol and trehalose biosynthetic pathways (Iordachescu and Imai, 2008; Ortiz *et al.*, 2017). The knock-out in the *otsA* gene caused a slight reduction in stress resistance, suggesting that this mechanism has little relevance under the conditions tested.

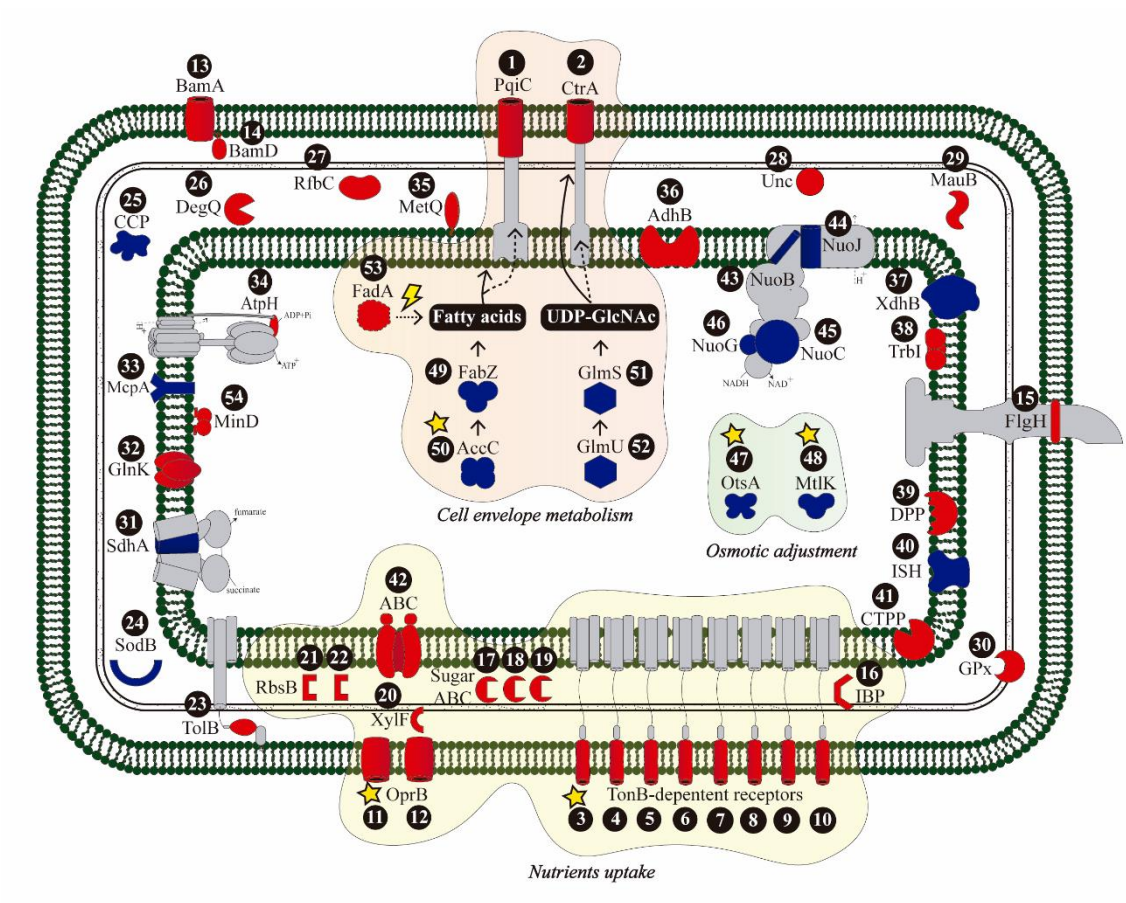

Fig. 5 Schematic illustration of the main responses of *G. diazotrophicus* to osmotic stress. Red and blue forms represent proteins classified as down-accumulated and up-accumulated, respectively, and grey forms represent non-regulated proteins. Yellow stars indicate proteins in which defective mutants were obtained. Dashed arrows indicate activities that were decreased, and continuous arrows indicate activities that were increased. Detailed information on each protein in this scheme is provided in Supporting Information Table S3.

The main pathways regulated in our proteomic analysis, and those revealed as essential for *G. diazotrophicus* osmo-resistance by mutagenesis assays, were summarized in Fig. 5. The model proposes that *G. diazotrophicus* adjusts cell envelope components by increasing the production of fatty acids and UDP-GlcNAc, mainly directed to the inner membrane and peptidoglycan. Such a process decreases bacterial cell permeability and fortifies its resistance against internal turgor pressure. Moreover, *G. diazotrophicus* decreases the accumulation of proteins responsible for the entry of compounds into the cell, avoiding harmful substances. At a lower intensity, the bacteria increase the accumulation of proteins involved with the synthesis of compatible solutes.

Taken together, the results of this study shed light on molecular and morphological aspects of *G. diazotrophicus* resistance to osmotic stress, with emphasis on the regulation of extracytoplasmic proteins and the adjustment of the cell envelope. These findings contribute to the understanding of essential mechanisms regulated in osmotolerant bacteria.

2.6 References

Bastián, F., Cohen, A., Piccoli, P., Luna, V., Bottini*, R., Baraldi, R., and Bottini, R. (1998) Production of indole-3-acetic acid and gibberellins A1 and A3 by Acetobacter diazotrophicus and Herbaspirillum seropedicae in chemically-defined culture media. Plant Growth Regul 24: 7–11.

Bertalan, M., Albano, R., de Pádua, V., Rouws, L., Rojas, C., Hemerly, A., et al. (2009) Complete genome sequence of the sugarcane nitrogen-fixing endophyte Gluconacetobacter diazotrophicus Pal5. BMC Genomics 10: 450.

Boniolo, F.S., Rodrigues, R.C., Delatorre, E.O., da Silveira, M.M., Flores, V.M.Q., and Berbert-Molina, M.A. (2009) Glycine Betaine Enhances Growth of Nitrogen-Fixing Bacteria Gluconacetobacter diazotrophicus PAL5 Under Saline Stress Conditions. Curr Microbiol 59: 593–599.

Campbell, J.W. and Cronan, J.E. (2001) Bacterial Fatty Acid Biosynthesis: Targets for Antibacterial Drug Discovery. Annu Rev Microbiol.

Cavalcante, V.A. and Dobereiner, J. (1988) A new acid-tolerant nitrogen-fixing bacterium associated with sugarcane. Plant Soil 108: 23–31.

Cesari, A.B., Paulucci, N.S., Biasutti, M.A., Morales, G.M., and Dardanelli, M.S. (2018) Changes in the lipid composition of Bradyrhizobium cell envelope reveal a rapid response to water deficit involving lysophosphatidylethanolamine synthesis from phosphatidylethanolamine in outer membrane. Res Microbiol.

Conti, J., Viola, M.G., and Camberg, J.L. (2015) The bacterial cell division regulators MinD and MinC form polymers in the presence of nucleotide. FEBS Lett 589: 201–206.

Damerval, C., De Vienne, D., Zivy, M., and Thiellement, H. (1986) Technical improvements in two-dimensional electrophoresis increase the level of genetic variation detected in wheat-seedling proteins. Electrophoresis 7: 52–54.

Distler, U., Kuharev, J., Navarro, P., Levin, Y., Schild, H., and Tenzer, S. (2014) Drift time-specific collision energies enable deep-coverage data-independent acquisition proteomics. Nat Methods 11: 167–170.

Distler, U., Kuharev, J., Navarro, P., and Tenzer, S. (2016) Label-free quantification in ion mobility-enhanced data-independent acquisition proteomics. Nat Protoc 11: 795–812.

Dong, Z., Mccully, M.E., and Canny, M.J. (1997) Does Acetobacter diazotrophicus Live and Move in the Xylem of Sugarcane Stems ? Anatomical and Physiological Data.

Ekiert, D.C., Bhabha, G., Isom, G.L., Greenan, G., Ovchinnikov, S., Henderson, I.R., et al. (2017) Architectures of Lipid Transport Systems for the Bacterial Outer Membrane. Cell.

Fujita, Y., Matsuoka, H., and Hirooka, K. (2007) Regulation of fatty acid metabolism in bacteria. Mol Microbiol.

Ghai, I. and Ghai, S. (2017) Exploring bacterial outer membrane barrier to combat bad bugs. Infect Drug Resist.

Glick, B.R. (2012) Plant Growth-Promoting Bacteria: Mechanisms and Applications. Scientifica (Cairo).

Hartmann, A., Prabhu, S.R., and Galinski, E.A. (1991) Osmotolerance of diazotrophic rhizosphere bacteria. Plant Soil.

Van Heijenoort, J. (2001) Recent advances in the formation of the bacterial peptidoglycan monomer unit. Nat Prod Rep 18: 503–519.

Intorne, A.C., de Oliveira, M.V. V., Lima, M.L., da Silva, J.F., Olivares, F.L., and de Souza Filho, G.A. (2009) Identification and characterization of Gluconacetobacter diazotrophicus mutants defective in the solubilization of phosphorus and zinc. Arch Microbiol 191: 477–483.

Iordachescu, M. and Imai, R. (2008) Trehalose Biosynthesis in Response to Abiotic Stresses. J Integr Plant Biol 50: 1223–1229.

Jimenez-Salgado, T., Fuentes-Ramirez, L.E., Tapia-Hernandez, A., Mascarua-Esparza, M.A., Martinez-Romero, E., and Caballero-Mellado, J. (1997) Coffea arabica L., a new host plant for Acetobacter diazotrophicus, and isolation of other nitrogen-fixing acetobacteria. Appl Environ Microbiol.

Karimzadeh, J., Alikhani, H.A., Etesami, H., and Pourbabaei, A.A. (2020) Improved Phosphorus Uptake by Wheat Plant (Triticum aestivum L.) with Rhizosphere Fluorescent Pseudomonads Strains Under Water-Deficit Stress. J Plant Growth Regul.

Larue, K., Ford, R.C., Willis, L.M., and Whitfield, C. (2011) Functional and structural characterization of polysaccharide co-polymerase proteins required for polymer export in ATP-binding cassette transporter-dependent capsule biosynthesis pathways. J Biol Chem.

Lennen, R.M. and Pfleger, B.F. (2012) Engineering Escherichia coli to synthesize free fatty acids. Trends Biotechnol.

Lery, L.M.S., Hemerly, A.S., Nogueira, E.M., Von Krüger, W.M.A., and Bisch, P.M. (2011) Quantitative Proteomic Analysis of the Interaction Between the Endophytic Plant-

Growth-Promoting Bacterium Gluconacetobacter diazotrophicus and Sugarcane. Mol Plant-Microbe Interact MPMI 24: 562–576.

Lery, L.M.S., von Krüger, W.M.A., Viana, F.C., Teixeira, K.R.S., and Bisch, P.M. (2008) A comparative proteomic analysis of Gluconacetobacter diazotrophicus PAL5 at exponential and stationary phases of cultures in the presence of high and low levels of inorganic nitrogen compound. Biochim Biophys Acta - Proteins Proteomics.

Levin, P.A., Shim, J.J., and Grossman, A.D. (1998) Effect of minCD on FtsZ ring position and polar septation in Bacillus subtilis. J Bacteriol.

Loffhagen, N., Härtig, C., Benndorf, D., and Babel, W. (2002) Effects of Growth Temperature and Lipophilic Carbon Sources on the Fatty Acid Composition and Membrane Lipid Fluidity of Acinetobacter calcoaceticus 69V. Acta Biotechnol 22: 235–243.

Magnuson, K., Jackowski, S., Rock, C.O., and Cronan, J.E. (1993) Regulation of fatty acid biosynthesis in Escherichia coli. Microbiol Rev.

Masi, M., Réfregiers, M., Pos, K.M., and Pagès, J.M. (2017) Mechanisms of envelope permeability and antibiotic influx and efflux in Gram-negative bacteria. Nat Microbiol.

Mitchell, A.M. and Silhavy, T.J. (2019) Envelope stress responses: balancing damage repair and toxicity. Nat Rev Microbiol 17: 417–428.

Murínová, S. and Dercová, K. (2014) Response mechanisms of bacterial degraders to environmental contaminants on the level of cell walls and cytoplasmic membrane. Int J Microbiol.

Nikaido, H. (2003) Molecular Basis of Bacterial Outer Membrane Permeability Revisited. Microbiol Mol Biol Rev.

Olanrewaju, O.S., Glick, B.R., and Babalola, O.O. (2017) Mechanisms of action of plant growth promoting bacteria. World J Microbiol Biotechnol.

De Oliveira, M.V. V., Intorne, A.C., Vespoli, L. de S., Madureira, H.C., Leandro, M.R., Pereira, T.N.S., et al. (2016) Differential effects of salinity and osmotic stress on the plant growth-promoting bacterium Gluconacetobacter diazotrophicus PAL5. Arch Microbiol 198: 287–294.

Ortiz, M.E., Bleckwedel, J., Fadda, S., Picariello, G., Hebert, E.M., Raya, R.R., and Mozzi, F. (2017) Global Analysis of Mannitol 2-Dehydrogenase in Lactobacillus reuteri CRL 1101 during Mannitol Production through Enzymatic, Genetic and Proteomic Approaches. PLoS One 12: e0169441.

Passamani, L.Z., Bertolazi, A.A., Ramos, A.C., Santa-Catarina, C., Thelen, J.J., and Silveira, V. (2018) Embryogenic Competence Acquisition in Sugar Cane Callus Is Associated with Differential H+-Pump Abundance and Activity. J Proteome Res 17: 2767–2779.

Pedraza, R.O. (2008) Recent advances in nitrogen-fixing acetic acid bacteria. Int J Food Microbiol.

dos Santos, M.F., Muniz de Pádua, V.L., de Matos Nogueira, E., Hemerly, A.S., and Domont, G.B. (2010) Proteome of Gluconacetobacter diazotrophicus co-cultivated with sugarcane plantlets. J Proteomics.

Saravanan, V.S., Madhaiyan, M., Osborne, J., Thangaraju, M., and Sa, T.M. (2008) Ecological Occurrence of Gluconacetobacter diazotrophicus and Nitrogen-fixing Acetobacteraceae Members: Their Possible Role in Plant Growth Promotion. Microb Ecol 55: 130–140.

Saravanan, V.S., Madhaiyan, M., and Thangaraju, M. (2007) Solubilization of zinc compounds by the diazotrophic, plant growth promoting bacterium Gluconacetobacter diazotrophicus. Chemosphere 66: 1794–1798.

de Souza, R., Ambrosini, A., and Passaglia, L.M.P. (2015) Plant growth-promoting bacteria as inoculants in agricultural soils. Genet Mol Biol.

Stenberg, F., Chovanec, P., Maslen, S.L., Robinson, C. V., Ilag, L.L., Von Heijne, G., and Daley, D.O. (2005) Protein complexes of the Escherichia coli cell envelope. J Biol Chem.

Tejera, N.A., Ortega, E., González-López, J., and Lluch, C. (2003) Effect of some abiotic factors on the biological activity of Gluconacetobacter diazotrophicus. J Appl Microbiol 95: 528–535.

Velázquez-Hernández, M.L., Baizabal-Aguirre, V.M., Cruz-Vázquez, F., Trejo-Contreras, M.J., Fuentes-Ramírez, L.E., Bravo-Patiño, A., et al. (2011) Gluconacetobacter diazotrophicus levansucrase is involved in tolerance to NaCl, sucrose and desiccation, and in biofilm formation. Arch Microbiol 193: 137–149.

Vriezen, J.A.C., De Bruijn, F.J., and Nüsslein, K. (2007) Responses of rhizobia to desiccation in relation to osmotic stress, oxygen, and temperature. Appl Environ Microbiol.

Watt, M., Silk, W.K., and Passioura, J.B. (2006) Rates of root and organism growth, soil conditions, and temporal and spatial development of the rhizosphere. In, Annals of Botany.

Yoon, Y., Lee, H., Lee, S., Kim, S., and Choi, K.H. (2015) Membrane fluidity-related adaptive response mechanisms of foodborne bacterial pathogens under environmental stresses. Food Res Int.

Zahid, N., Schweiger, P., Galinski, E., and Deppenmeier, U. (2015) Identification of mannitol as compatible solute in Gluconobacter oxydans. Appl Microbiol Biotechnol 99: 5511–5521.

Zhang, Y.M. and Rock, C.O. (2008) Membrane lipid homeostasis in bacteria. Nat Rev Microbiol.

3. CHAPTER 2

DepP PROTEASE IS ESSENTIAL FOR TOLERANCE TO SALT STRESS IN THE PLANT GROWTH-PROMOTING BACTERIUM *Gluconacetobacter diazotrophicus* PAL5

Abstract

The use of plant growth-promoting bacteria represents an alternative to the massive use of mineral fertilizers in agriculture. However, some abiotic stresses commonly found in the environment, like salinity, can affect the efficiency of this approach. Here, we investigated the key mechanisms involved in the response of the plant growth-promoting bacterium *Gluconacetobacter diazotrophicus* to salt stress by using morphological and cell viability analyses, comparative proteomics, and reverse genetics. Our results revealed that the bacteria produce filamentous cells in response to salt at 100 mM and 150 mM NaCl. However, such a response was not observed at higher concentrations, where cell viability was severely affected. Proteomic analysis showed that salt stress modulates proteins involved in several pathways, including iron uptake, outer membrane efflux, osmotic adjustment, cell division and elongation, and protein transport and quality control. Proteomic data also revealed the repression of several extracytoplasmic proteins, especially those located at periplasm and outer membrane. The role of such pathways in the tolerance to salt stress was analyzed by the use of mutant defectives for Δ*tbdr* (iron uptake), Δ*mtlK* and Δ*otsA* (compatible solutes synthesis), and Δ*degP* (quality control of nascent extracytoplasmic proteins). Δ*degP* presented the highest sensitivity to salt stress, Δ*tbdr*, and Δ*mtlK* also showed increased sensitivity, but Δ*otsA* was not affected. This is the first demonstration that DegP protein, a protease with minor chaperone activity, is essential for tolerance to salt stress in *G. diazotrophicus*. Our data contribute to a better understanding of the molecular bases that control the bacterial response/tolerance to salt stress, shedding light on quality control of nascent extracytoplasmic proteins.

Keywords: Abiotic stress, Protein quality control, Proteome, Mutagenesis

3.1 Introduction

During recent decades, the world demand for mineral fertilizers in agriculture reached 200 million tons per year (FAO-UN, 2017). The intensive use of such fertilizers led to high production costs of agriculture and harmful environmental impacts (Itelima *et al.*, 2018). In this scenario, plant growth-promoting bacteria represent a promising alternative to mineral fertilizers (Adesemoye *et al.*, 2009).

Bacteria, not least those inhabiting soils, are continuously exposed to at least one or more stress parameter(s) (Hallsworth, 2018). Among these, salinity deserves special attention because virtually all soils contain ions, and some are in a state of salinization. Salts reduce water activity, which is a potent determinant of biotic activity for soil bacteria (Stevenson and Hallsworth, 2014). Although several studies about the responses of plant growth-promoting bacteria to salt stress have been conducted, the key mechanisms that regulate these responses remain unclear (Boniolo et al., 2009; Oliveira et al., 2016; Tejera et al., 2003; Velázquez-Hernández et al., 2011).

Gluconacetobacter diazotrophicus is a plant growth-promoting bacterium that colonizes sugar-rich crops such as sugarcane, sweet potato, and pineapple (Cavalcante and Dobereiner, 1988; Saravanan et al., 2008; Tapia-Hernández et al., 2000). Among the beneficial characteristics of this bacterium, we can highlight the production of phytohormones, biological nitrogen fixation, and solubilization of nutrients (Cavalcante and Dobereiner, 1988; Rodrigues et al., 2016; Saravanan et al., 2007). Additionally, *G. diazotrophicus* is one of the few non-halophiles prokaryotes capable of growth below a water activity of 0.900 (Stevenson *et al.*, 2015). However, despite the capacity of *G. diazotrophicus* to survive in osmotically challenging environments, this bacterium is sensitive to salt stress, probably due to ion-specific toxic effects (Oliveira et al. 2016). Although the salt content does not represent a problem for the maintenance of bacterial

life inside the host plants, in the rhizosphere the scenario may be more challenging. The concentration of salt in soils can reach values between 20-40 mM NaCl (low salinity) up to values above 160 mM NaCl (severe salinity) (FAO, 1994). So, in the field, soil salinity can affect plant colonization by PGPBs (Miller and Wood, 1996; Griffiths *et al.*, 2003; Sugawara *et al.*, 2010). Deciphering the molecular basis of salt stress response in this bacterium may contribute to the development of new inoculation technologies for crops cultivated under salinized environments.

High ion concentrations in the environment produce several deleterious effects on bacterial cells, including change in cell shape and in the cytoplasmic pH, and affect the extracytoplasmic protein folding process (Geyter et al., 2016; Oliveira et al., 2016; Saulou-Bérion et al., 2015). Many adaptive responses of Gram-negative bacteria to challenging environments occur in extracytoplasmic compartments (Mitchell and Silhavy, 2019). Salt stress leads to the intense formation of misfolded protein aggregates, which can be lethal to the bacterial cell (Bednarska *et al.*, 2013). Cells activate the protein quality control system during the biogenesis of extracytoplasmic proteins to counteract such effects (Clausen *et al.*, 2011; Lyu and Zhao, 2015).

The quality control system contains both chaperones that perform the correct folding and proteases that degrade any extracytoplasmic misfolded protein (Rollauer *et al.*, 2015). The best-characterized proteins of this system are SurA, SkP, and DegP (Chang, 2016; Mas *et al.*, 2019). SurA and SkP are periplasmic chaperones that deliver nascent extracytoplasmic proteins to the b-barrel-assembly machinery (BAM) complex. BAM complex, in turn, inserts these proteins in the outer membrane (Rollauer *et al.*, 2015). Any misfolded protein in the periplasm is degraded by the protease DegP to prevent the formation of misfolded protein aggregates.

DegP, also called HtrA, is a highly conserved family of proteins that contains homologs in almost all bacterial species, eukaryotic chloroplasts, and mitochondria (Rollauer 2015; Chang 2016). DegP was previously described as a bifunctional protein with chaperone activity, at low temperature, and protease activity, at high temperature (Spiess *et al.*, 1999). However, Ge et al. (2014) demonstrated that DegP had thermodynamic properties ideal for a protease, but ineffective for a chaperone. Moreover, DegP is critical for bacterial resistance to stress and functions by degrading both periplasmic and outer membrane proteins under stress conditions (Zhang *et al.*, 2019). In the plant growth-promoting bacterium *Burkholderia cenocepacia* and in the Gram-positive bacteria *Listeria monocytogenes*, DegP plays an essential role in bacterial growth under osmotic and salt stress, respectively (Wonderling *et al.*, 2004; Flannagan *et al.*, 2007).

The present work aimed to investigate the molecular mechanisms involved in the response/tolerance of *G. diazotrophicus* to salt stress. We analyzed the effects of NaCl on bacterial growth, morphological changes, and cell viability. Comparative proteomic analyses were performed to investigate the main protein groups regulated in *G. diazotrophicus* exposed to salt stress. Using a reverse genetics approach, we used *G. diazotrophicus* knock-out mutants, defective in the regulated pathways of iron uptake, osmotic adjustment, and protein transport and quality control, to verify the correlation between these pathways and stress tolerance.

3.2 Material and Methods

3.2.1 Stock preparation of bacterial strains

G. diazotrophicus PAL5 wild-type was obtained from the culture collection of the Universidade Estadual do Norte Fluminense Darcy Ribeiro (UENF, Campos dos

Goytacazes, Rio de Janeiro State, Brazil). The knock-out mutants of *G. diazotrophicus* PAL5, defective in the production of proteins DegP (A9HEK6, Δ*degP*), MtlK (A9HBL5, Δ*mtlK*), OtsA (A9HBU6, Δ*otsA*), and a TonB-dependent receptor (A9HNM4, Δ*tbdr*), were obtained from the *G. diazotrophicus* PAL5 mutant library of the Laboratório de Biotecnologia - UENF (Aline C Intorne *et al.*, 2009). These mutants were obtained by the utilization of EZ-Tn5 <R6Kyori/KAN-2>Tnp insertion kit (Epicentre, Madison, WI, USA). To produce stock cultures, a single colony of each bacterial strain was grown in DYGS medium (1L: 2 g glucose; 2 g yeast extract; 1.5 g peptone; 1.3 g glutamic acid; 500 mg K_2HPO_4; 500 mg $MgSO_4.7H_2O$; pH 6.0) under constant agitation (250 rpm min^{-1}, 30°C) until it reached OD_{600nm} of 1.0. Then, each culture (750 µL) was transferred to microtubes (1.5 mL) and mixed with 100% glycerol (250 µL). Tubes were frozen using liquid nitrogen and stored at −80°C.

3.2.2 Salt stress assays

Stress assays were performed as described by Oliveira et al. (2016) with some modifications. The NaCl stock solutions were previously prepared at a concentration twice the desired final concentration and autoclaved. Cells (5 mL) from glycerol stocks of *G. diazotrophicus* wild-type and insertional mutants were inoculated in DYGS medium (45 mL) within Erlenmeyer flasks (250 mL). The cultures were grown under constant agitation (250 rpm min^{-1}, 30°C) until they reached OD_{600nm} of 1.0. The cultures were then centrifuged at 10.000 g at 25°C for 15 min, and the cells were resuspended with fresh two-fold DYGS medium. Cultures (25 mL), with OD_{600nm} adjusted to 0.2, were mixed with equal volumes of NaCl stock solutions in Erlenmeyer flasks (250 mL). The flasks were maintained under constant agitation (250 rpm min^{-1}, 30°C). OD_{600nm} reading was performed after 12 h. Cultures (2 mL) were separated for microscopy analysis.

3.2.3 Reverse genetics analysis

To perform reverse genetics analysis, cells (5 mL) from glycerol stocks of *G. diazotrophicus* wild-type and insertional mutants were inoculated in LGI medium (45 mL) (1L: 5 g sucrose; 0.6 g KH_2PO_4; 0.2 g K_2HPO_4; 0.2 g $MgSO_4.7H_2O$; 0.02 g $CaCl_2.2H_2O$; 0.01 g $FeCl_3$; 0.002 g $Na_2MoO_4.2H_2O$; pH 6.0) (Cavalcante and Dobereiner 1988) within Erlenmeyer flasks (250 mL). The cultures were grown under constant agitation (250 rpm min^{-1}, 30°C) until they reached OD_{600nm} of 1.0. The cultures were then placed on a 96-well microplate and plated on LGI solid medium supplemented with NaCl with a 96-pin replicator (Boekel, Fisher Scientific, Pittsburgh, PA, USA). The plates were incubated at 30°C for five days. The results were then registered.

3.2.4 Microscopy analysis

Cell cultures (2 mL), submitted to different salt concentrations, were transferred into microtubes (1.5 mL) and centrifuged at 10.000 g at 25°C for 3 min. The supernatants were discarded, and the pellets were washed three times, with 0.85% (v/v) NaCl. The glass slides were treated with 0.8% (v/v) agarose (100 µL), added in the center of the slides, to avoid bacterial movement during microscopy image capture.

For morphological analysis, after cell wash, each bacterial suspension (5 µL) was applied onto the treated glass slides, covered with coverslips, and observed using Carl Zeiss Axion Imager A.2 Microscope. Images were captured using Carl Zeiss Axion Vision Software 4.8.2.

For cell viability analysis, the washed cells were submitted to the epifluorescence staining method using the Live/Dead Bacterial Viability Kit (*Bac*LightTM, Thermo Fisher Scientific, U.S.), following fabricant recommendations. Briefly, to prepare the dye

solution, equal volumes of SYTO® and propidium iodide were combined in a microtube (600 µL). The dye mixture (0.6 µL) was then added to each bacterial suspension (100 µL), and the mixtures were incubated in the dark at 23ºC for 15 min. Then, each bacterial suspension (5 µL) was applied onto the treated glass slides, covered with coverslips, and observed using Carl Zeiss Axion Imager A.2 Microscope. Live cells were stained in green fluorescence, while dead cells were stained in red fluorescence. For live and dead bacterial cell counts, six fields of glass slides per treatment were analyzed. Details about the cells counted is provided in Table S1.

3.2.5 Protein extraction

Three different biological samples of *G. diazotrophicus* cells, exposed and non-exposed (control) to 150 mM NaCl, were used for protein extract preparation. Each sample corresponded to each treatment sample (20 mL). The extraction methods were performed as described by Damerval et al. (1986) with some modifications. Briefly, the cells were harvested by centrifugation at 10.000 g at 4°C for 15 min, and the supernatant was discarded. The resultant pellets were resuspended in a solution (1 mL) containing 10% (w/v) TCA (Sigma-Aldrich, St. Louis, USA) in acetone with 20 mM dithiothreitol (DTT; GE Healthcare, Little Chalfont, U.K.). The samples were kept under agitation at 10°C for 30 min. Then, for protein precipitation, the samples were maintained at -20°C for 60 min, followed by centrifugation at 16.000 g at 4ºC for 30 min. The pellets were washed three times with a cooled solution of acetone and 20 mM DTT. The pellets were then dried, and Urea/Thiourea buffer (1 mL) [7 M Urea, 2 M Thiourea, 1% (v/v) DTT, 2% (v/v) Triton X-100, 1 mM PMSF, 5 µM pepstatin] was added to each sample. The samples were then maintained under agitation at 10°C for 30 min, followed by centrifugation at 16.000 g at 4°C for 30 min. Supernatants were collected, and the protein

concentration of each sample was estimated with 2-D Quant Kit (2-D Quant Kit - GE Healthcare Life Sciences).

3.2.6 Protein digestion

Proteomic analyses were performed as described by Passamani et al. (2018) with some modifications. Briefly, total protein (100 µg) from each biological sample was filtered on Amicon Ultra 0.5 -3 KD centrifugal filters (Merck Millipore, Darmstadt, Germany) using 50 mM ammonium bicarbonate (pH 8.5; Sigma-Aldrich) as the buffer. After filtration, each sample received 0.2% (v/v) RapiGestR surfactant (25 µL) (Waters, Milford, CT, USA). Each sample was then briefly vortexed and incubated at 80°C for 15 min in a ThermomixerR, and 100 mM DTT (2.5 µL) (Bio-Rad Laboratories, Hercules, CA, USA) was added to each sample. The samples were then vortexed and incubated under agitation (350 rpm min^{-1}) at 60°C for 30 min, and 300 mM iodoacetamide (2.5 µL) (GE Healthcare, Piscataway, NJ, USA) was added. The samples were then vortexed and incubated in the dark at room temperature for 30 min. Each sample received 100 mM DTT (2.5 µL) (Bio-Rad Laboratories) and was incubated at 37°C for 30 min to quench the iodoacetamide. Then, for protein digestion, each sample received a trypsin solution (20 µL) (50 ng $µL^{-1}$; V5111; Promega, Madison, WI, USA) prepared in 50 mM ammonium bicarbonate and was incubated overnight at 37°C. For RapiGestR precipitation, 5% (v/v) trifluoroacetic acid (10 µL) (TFA; Sigma-Aldrich) was added to each sample, and the samples were incubated at 37°C for 90 min, followed by centrifugation at 16.000 g for 30 min. The samples were then transferred to Total Recovery Vials (Waters), and peptide/sample (1 µg) was used for mass spectrometry analysis.

3.2.7 Mass spectrometry analysis

Mass spectrometry analyses were performed as described by Passamani et al. (2018). Briefly, a nanoAcquity UPLC connected to a Synapt G2-Si HDMS mass spectrometer (Waters) was used for the ESI-LC-MS/MS analysis. For separation, the samples were loaded on the nanoAcquity UPLC 5-µm C18 trap column (180 µm x 20 mm) at five µL min^{-1} for 3 min and then onto the nanoAcquity HSS T3 1.8-µm analytical reverse-phase column (75 µm x 150 mm) at 400 nL min^{-1}. The column temperature was 45°C. For peptides elution, a binary gradient was used: mobile phase A, containing 0.1% (v/v) formic acid (Sigma-Aldrich) and water (Tedia, Fairfield, USA), and mobile phase B, containing 0.1% (v/v) formic acid and acetonitrile (Sigma-Aldrich). Gradient elution was made by the following steps: 3 min with 7% (v/v) B, increasing to 40% (v/v) B until 90.09 min, increasing to 85% (v/v) B until 94.09 min, keeping constant at 85% (v/v) B until 98.09 min, decreasing to 7% (v/v) B until 100.09 min, and keeping constant at 7% (v/v) B until the end of the run at 108.09 min. Mass spectrometry was accomplished in the positive and resolution mode (V mode), with 35000 FWHM resolution of ion mobility, and data-independent acquisition mode. The ion mobility wave velocity was adjusted to 600 m s^{-1}, the transfer collision energy was up-accumulated from 19 V to 45 V in high-energy mode, the cone and capillary voltages were 30 V and 2,800 V, respectively, and the temperature was 70°C. The nanoflow gas was calibrated to 0.50 Bar, and the purge gas flow altered from 145 L h^{-1} to 150 L h^{-1}. The parameters of TOF included a scan time of 0.5 s in the continuum mode and a mass range of 50 Da to 2000 Da. Human [Glu1]-fibrinopeptide B (100 fmol µ L^{-1}) (Sigma-Aldrich) was utilized as an external calibrant, and lock mass acquisition was made every 30 s.

3.2.8 Proteomics data analyses

For spectral processing and database searching, the software ProteinLynx Global Server (PLGS; version 3.0.2) and ISOQuant were used. The spectral processing on PLGS software was performed using a low-energy threshold of 150 (counts), an elevated energy threshold of 50, and an intensity threshold of 750. Furthermore, adjustments on parameter analysis were made as follows: two missed cleavages, minimum fragment ion per peptide equal to 3, minimum fragment ion per protein equal to 7, minimum peptide per protein equal to 2, fixed modifications of carbamidomethyl, and variable modifications of oxidation and phosphoryl. The false discovery rate (FDR) for peptide and protein identification was regulated to a maximum of 1%, with a minimum peptide length of six amino acids. The proteomics data were processed against the *G. diazotrophicus* RIOGENE proteome database (www.uniprot.org/proteomes/UP000001176).

The analysis of comparative label-free quantification was performed with ISOQuant software with previously described settings and algorithms (Distler *et al.*, 2014, 2016). Briefly, the analysis included retention time alignment, exact mass retention time (EMRT), ion mobility spectrometry clustering, protein homology filtering, and data normalization. For the annotation of the resulting feature clusters by ISOQuant, the consensus peptide identifications and identification probabilities were evaluated. The parameters of protein identification in ISOQuant were adjusted to a false discovery rate (FDR) of 1%, a peptide score higher than six, a minimum peptide length of six amino acids, and at least two peptides per protein. The TOP3 identification was used to perform label-free quantification with the multidimensional normalization process implemented within ISOQuant. The detailed ISOQuant processing parameters configuration is provided in Table S2.

After ISOQuant analysis, only the proteins that were present or absent (for unique proteins) in all three biological samples were selected for differential abundance analysis. The data were analyzed using Student's t-test (two-tailed). Proteins with $p < 0.05$ were considered differentially accumulated protein (DAP) if their fold change were higher than 1.5 (up-accumulated) or lesser than 0.667 (down-accumulated).

The prediction of the subcellular localization (outer membrane, periplasm, cytoplasmic membrane, or cytoplasm) of the identified differentially accumulated proteins (DAPs) was performed using FUEL-mLoc software (http://bioinfo.eie.polyu.edu.hk/FUEL-mLoc/). Moreover, DAPs were manually categorized in functional groups based on literature information.

3.3 Results

3.3.1 Salt stress affected the morphology, viability and growth rate of *G. diazotrophicus* cells

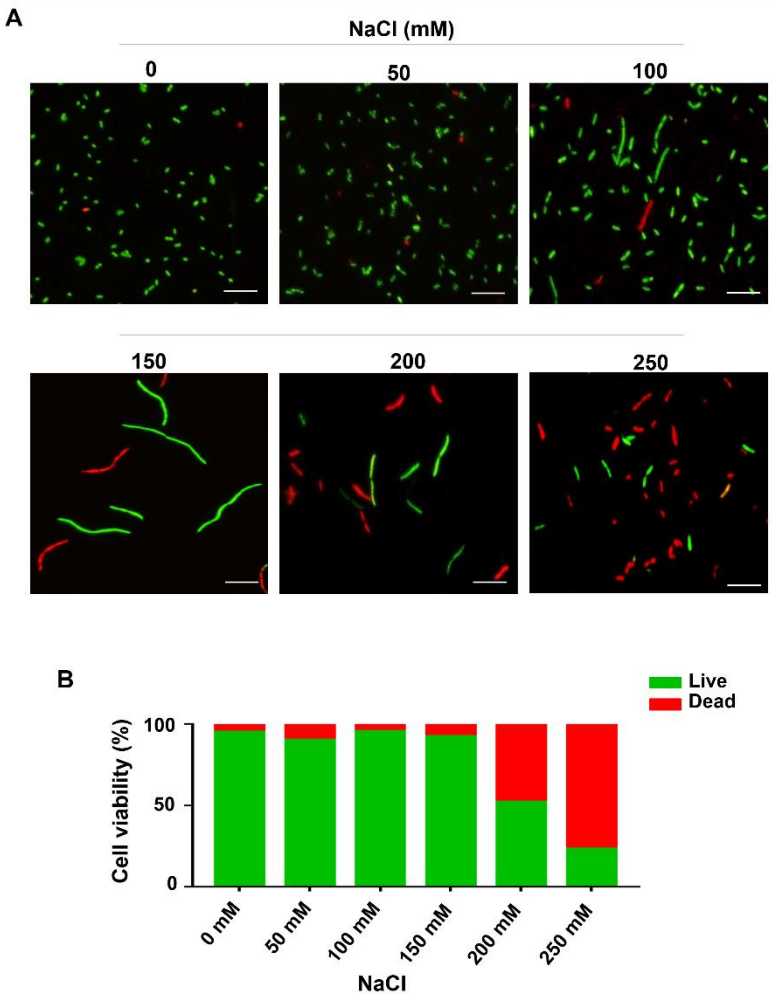

Fig. 1 Salt stress affected *G. diazotrophicus* cells morphology and viability. *G. diazotrophicus* was cultivated for 12 h in liquid medium supplemented with different concentrations of NaCl, and its cell viability was analyzed. *Bar* 5 µm.

Aiming to evaluate the effects of salt stress on cell viability of *G. diazotrophicus*, epifluorescence analyses were performed on cultures previously labeled with fluorescent Live/Dead Bacterial Viability Kit. Results demonstrate that the bacteria show significant morphological changes (filament formation) in response to salt concentrations, mainly at150mM, were about 97% of cells are filamentous (Fig. 1A). This morphological response was reduced at higher concentrations (at 200 and 250 mM NaCl), with about

20% and 5% of filamentous cells, respectively (Fig. 1A, Fig. S1). NaCl concentrations above 150 mM affected cell viability, mainly at 250 mM NaCl, where only approximately 20% of the cells remained viable (Fig. 1B).

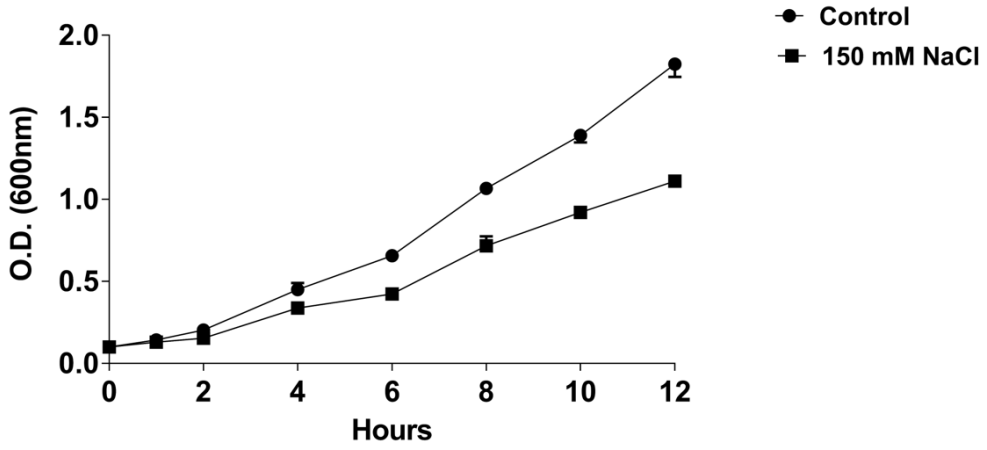

Fig. 2 Salt stress affects the growth rate of *G. diazotrophicus*. *G. diazotrophicus* was cultivated for 12 h in liquid medium supplemented with 150 mM NaCl, and its growth was analyzed every 2 h during the first 12 h of cultivation.

Additionally, once 150 mM NaCl produced the most evident cellular morphological changes without affecting cell viability, we evaluated if this salt concentration affects the growth rate of *G. diazotrophicus*. The results show that 150 mM inhibited cell multiplication by about 30-40% (Fig. 2). This salt concentration was selected for further investigation on the molecular aspects of the bacterial response to salt stress by proteomic analyses.

3.3.2 Salt-induced changes in the proteome profile of *G. diazotrophicus*

We investigated the molecular processes regulated in *G. diazotrophicus exposed* to NaCl by comparative proteomic analyses, using ESI-LC-MS/MS. Five

hundred and seventy-eight proteins were identified (about 15% of *G. diazotrophicus* entire genome coding capacity) (Table S3).

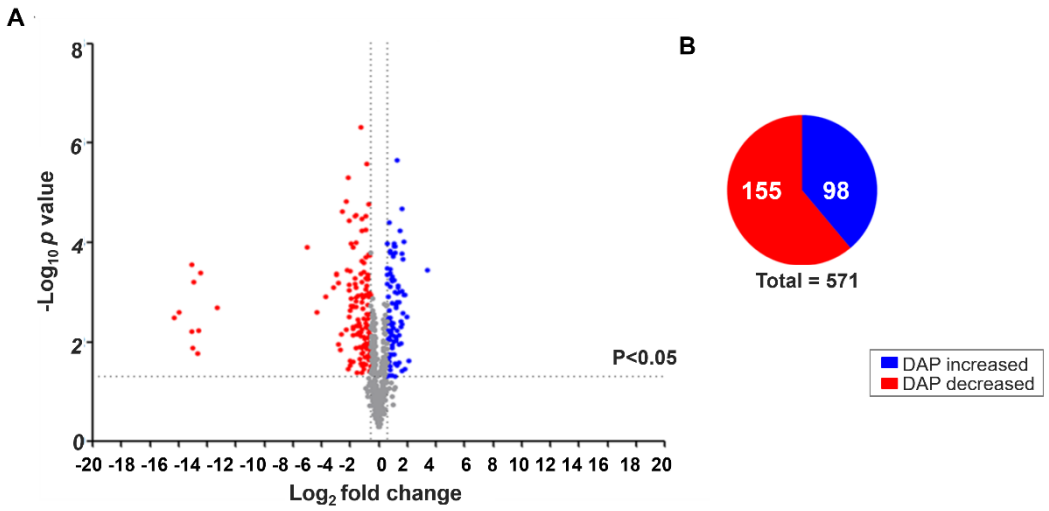

Fig. 3 Salt-induced changes in the proteome profile of *G. diazotrophicus*. All identified proteins are arranged in a volcano plot (a), and the number of differentially accumulated proteins (DAPs) is graphically represented (b). The volcano spots represent differential accumulation ($\log_2$ fold change) of identified proteins in the function of statistical significance ($-\log_{10}$ *p* value). Blue and red spots represent proteins that were up-accumulated and down-accumulated, respectively, and grey spots represent non-regulated proteins.

Among these proteins, two hundred and fifty-three (44%) were differentially accumulated in response to 150 mM NaCl, including 98 proteins up-accumulated, and 155 down-accumulated (Fig. 3A; Fig. 3B). Additionally, ten proteins were absent in *G. diazotrophicus* cells exposed to 150 mM NaCl, compared to non-exposed ones (Table S3).

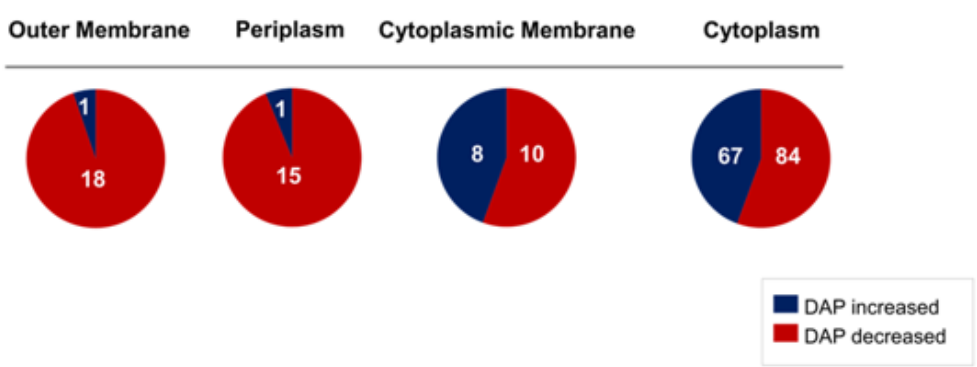

Fig. 4 Salt stress differentially regulates *G. diazotrophicus* protein profile of cellular compartments. Differentially accumulated proteins were classified by predicted subcellular localization (outer membrane, periplasm, cytoplasmic membrane, or cytoplasm) with FUEL-mLoc software.

3.3.3 Salt stress modifies the protein profile of cellular compartments of *G. diazotrophicus*

The differentially accumulated proteins (DAPs) were classified by predicted localization. The results allowed to evaluate the effects of salt stress on the protein profile of the cellular compartments. Regulated proteins were detected in all cell compartments: cytoplasm (151 DAPs), cytoplasmic membrane (18 DAPs), periplasm (16 DAPs), and outer membrane (19 DAPs) (Fig. 4). The proportion of up-accumulated/down-accumulated DAPs was relatively similar in the cytoplasm and cytoplasmic membrane compartments. However, in the extracytoplasmic compartments (periplasm and outer membrane), regulated proteins were mostly down-accumulated. Among 35 DAPs of such compartments, only two were up-accumulated, while 33 were down-accumulated. These results suggest the reduction extracytoplasmic proteins activity as an important response mechanism under salt stress, justifying a more detailed investigation of these processes.

Table 1 Main protein functionalities differentially regulated in *G. diazotrophicus* exposed to NaCl

Accession	Description	Max Score	Predicted Localization	Fold Change
a. Iron uptake				
A9H7L3	TonB-dependent receptor	946,74	Outer Membrane	Unique
A9HNM4	TonB-dependent receptor	844,06	Outer Membrane	Unique
A9H7L9	TonB-dependent receptor	509,80	Outer Membrane	Unique
A9HDZ9	TonB-dependent receptor	481,77	Outer Membrane	Unique
A9H7M7	TonB-dependent receptor	2799,32	Outer Membrane	0,05
A9HEU6	TonB-dependent receptor	8235,52	Outer Membrane	0,13
A9HFL0	TonB-dependent receptor	640,43	Outer Membrane	0,24
A9HE38	TonB-dependent receptor	5189,46	Outer Membrane	0,26
A9HFV5	TonB-dependent receptor	10959,70	Outer Membrane	0,33
A9H932	TonB-dependent receptor	1588,27	Outer Membrane	0,47
b. Osmoprotectants metabolism				
A9HBU6	Alpha,alpha-trehalose-phosphate synthase (OtsA)	1256,87	Cytoplasm	2,12
A9HBL5	Mannitol 2-dehydrogenase (MtlK)	7427,73	Cytoplasm	2,49
A9HM48	Glycine dehydrogenase (GcvP)	414,26	Cytoplasm	1,69
c. Cell division and elongation				
A9H0K4	Cell division protein (FtsZ)	2672,36	Cytoplasmic Membrane	0,57
A9H435	Penicillin-binding protein (PBP)	2675,86	Cytoplasmic Membrane	1,56
d. Efflux pump systems				
A9H3U0	Outer membrane efflux protein	634,49	Outer Membrane	2,66
A9H9Q6	Outer membrane protein efflux protein	1697,59	Outer Membrane	0,65
A9HEG4	Outer membrane protein efflux protein	1199,26	Outer Membrane	0,38

Table 1 (continued)

e. Protein export				
A9HK92	Protein-export protein (SecB)	15074,79	Cytoplasm	1,81
A9HJ83	Protein-export membrane protein(SecG)	3080,96	Cytoplasmic Membrane	1,78
f. Protein quality control				
A9HEK6	Periplasmic serine endoprotease (DegP)	10323,91	Periplasm	1,72
A9HBK9	Periplasmic serine endoprotease (DegQ)	1549,10	Periplasm	0,55

3.3.4 Main protein functionalities differentially regulated in *G. diazotrophicus* exposed to salt stress

The functional categorization of *G. diazotrophicus* proteins differentially accumulated in response to salt allowed the identification of four functional groups previously reported in other bacterial species as relevant to salt stress responses/tolerance and morphological responses: (I) iron uptake and outer membrane efflux (Hoffmann *et al.*, 2002; Martinez *et al.*, 2009), (II) osmotic adjustment (Iordachescu and Imai, 2008; Zahid *et al.*, 2015), (III) cell division and elongation (Errington *et al.*, 2003; Popham and Young, 2003a), and (IV) protein transport and quality control (Wonderling *et al.*, 2004; Flannagan *et al.*, 2007). Details of DAPs in each functional group are given below.

3.3.4.1 Iron uptake and Outer Membrane efflux proteins

In our proteomic analyses, 16 membrane transporters/receptors were regulated. Among those, eight TonB-dependent receptors (TBDRs) (A9HNM4, A9H7L9, A9HDZ9, A9H7M7, A9HFL0, A9HE38, A9HFV5, and A9H932), and two TonB-dependent siderophore receptors (A9H7L3 and A9HEU6) were down-accumulated (Table 1). Moreover, three outer membrane proteins involved in the efflux of potentially harmful substances, such as drugs and ions, were regulated, including two down-accumulated (A9H9Q6 and A9HEG4) and one up-accumulated (A9H3U0) (Table 1). These results suggest that salt stress reduces bacterial iron uptake and the efflux of harmful substances in *G. diazotrophicus* cells.

3.3.4.2 Osmotic adjustment

Only two proteins directly involved in the synthesis of compatible solutes were up-accumulated: mannitol 2-dehydrogenase – MtlK (A9HBL5), and alpha, alpha-

trehalose-phosphate synthase – OtsA (A9HBU6) (Table 1). This result suggests that 150 mM NaCl does not cause relevant osmotic stress on *G. diazotrophicus*.

3.3.4.3 Cell division and elongation proteins

In agreement with the morphological changes observed by microscopy analysis of *G. diazotrophicus* cells exposed to salt stress (Fig. 1), two DAPs involved in cell division and elongation were identified during our proteomic analyses. Among these, the cell division protein - FtsZ (A9H0K4) was down-accumulated, while the penicillin-binding protein – PBP (A9H435), involved in cell elongation, was up-accumulated in response to salt stress (Table 1). Therefore, these results indicate that salt stress represses cell division and simultaneously induces cell elongation.

3.3.4.4 Protein transport and quality control

Four proteins involved in the transport and quality control of extracytoplasmic proteins were regulated. Among those, two proteins that compose the bacterial Sec translocon complex were up-accumulated in *G. diazotrophicus* cells exposed to salt stress: SecB (A9HK92) and SecG (A9HJ83) (Table 1). Sec translocon is involved in the translocation of proteins from the cytoplasm to the extracytoplasmic compartments. Additionally, two periplasmic proteins with protease and chaperone activities, that prevent misfolded protein accumulation were regulated: DegP (A9HEK6) was up-accumulated, while DegQ (A9HBK9) was down-accumulated (Table 1).

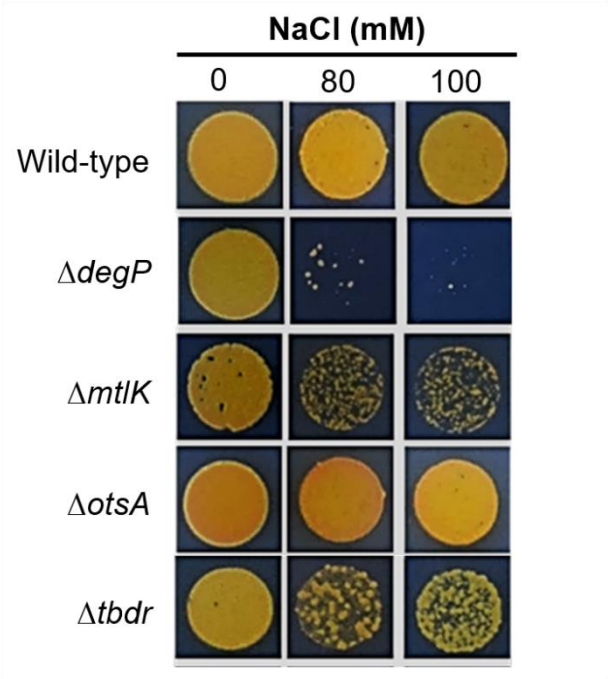

Fig. 5 Reverse genetics analysis reveals essential genes for salt tolerance in *G. diazotrophicus.* Insertional mutants of *G. diazotrophicus,* defective in the production of four proteins regulated in our proteomic analyses, were selected to perform salt stress tolerance assay. Results were registered after five days of salt stress exposure.

3.3.5 Reverse genetics and microscopy analysis revealed the essential role of the protein DegP in the growth and viability of *G. diazotrophicus* under salt stress

In order to investigate if the above-mentioned protein functionalities are important for *G. diazotrophicus* tolerance to salt stress, a reverse genetics approach was applied. *G. diazotrophicus* knock-out mutants, defective for the synthesis of proteins related to iron uptake (Δ*tbdr*), compatible solutes synthesis (Δ*mtlK* and Δ*otsA*), and quality control of nascent extracytoplasmic proteins (Δ*degP*) were compared to wild-type during the response to salt stress.

The mutants Δ*tonB*, Δ*mtlK*, and Δ*degP*, compared to the wild-type strain, showed increased sensitivity to NaCl, while the growth of Δ*otsA* was not affected. Among those,

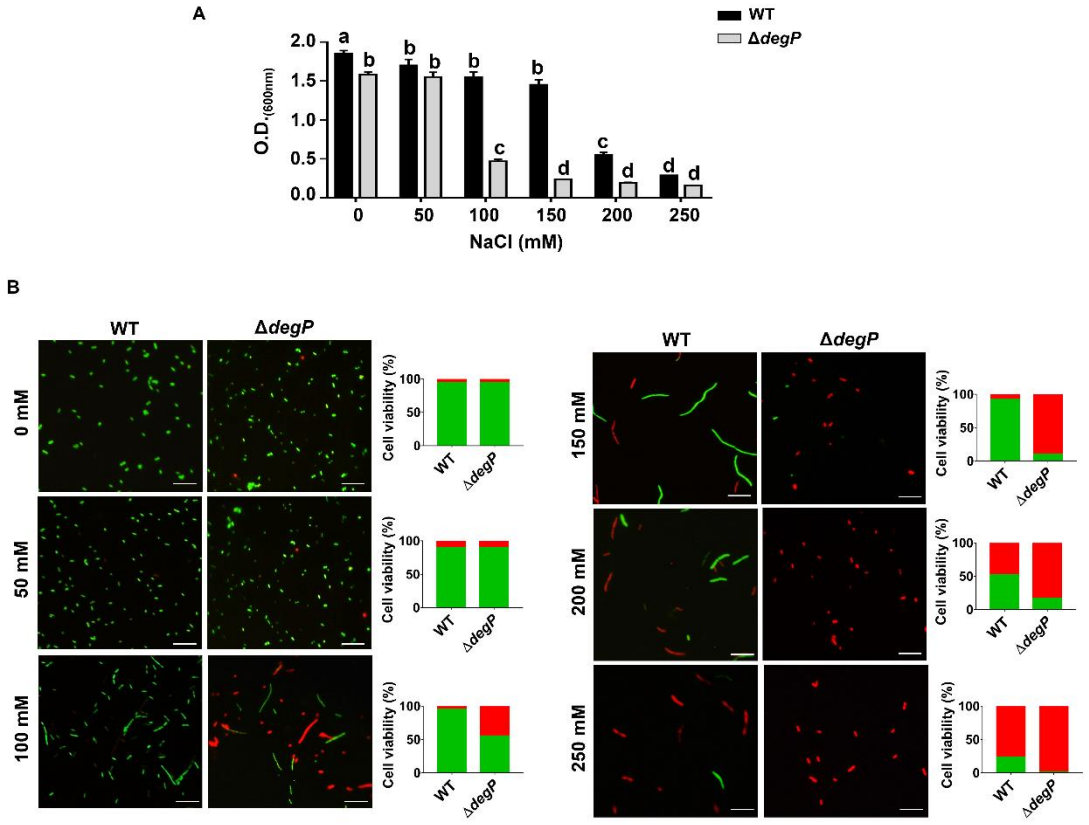

Δ*degP* was the most affected by NaCl and showed growth inhibition even at the lowest concentration of NaCl tested (Fig. 5).

Fig. 6 Lack of DegP affects the tolerance of *G. diazotrophicus* to salt stress. Δ*degP* was cultivated for 12 h in liquid medium supplemented with different concentrations of NaCl, and its growth performance (a) and cell viability (b) were analyzed. The mean of three replications for each treatment was calculated and used for statistical analysis. Means with different letters are significantly different from each other at 1% probability level by Tukey test. *Bar* 5 µm.

Moreover, the relevance of DegP on bacterial growth and cellular morphology/viability during salt stress was investigated by microscopy. The results confirm that the growth of Δ*degP* is severely affected compared to the wild-type strain (Fig. 6A). Additionally, under control condition (without salt) the growth of Δ*degP* was

lower than the wild-type strain, suggesting that DegP is also important to *G. diazotrophicus* growth under normal culture conditions (Fig. 6A).

Results also show that Δ*degP* forms cell filaments in response to salt stress like wild-type strain. However, while in wild-type filamentous cells were observed mainly at 150 mM NaCl, in Δ*degP* filamentous cells were observed mainly at 100 mM NaCl, where about 80% of cells are filamentous (Fig. 6B).

These results demonstrate that DegP is essential for the tolerance of *G. diazotrophicus* to salt stress.

3.4 Discussion

In the present study, microscopy, proteomics, and reverse genetics analyses allowed us to identify the morphological changes and key protein groups involved in the tolerance of *G. diazotrophicus* to salt stress. Among these, proteins related to iron uptake, osmotic adjustment, and extracytoplasmic protein quality control shown to be essential for such tolerance. The results highlighted the morphological and molecular aspects involved in the adaptation of this plant growth-promoting bacterium to salt stress.

Our epifluorescence analyses demonstrated the effects of salt stress on the viability and morphology of *G. diazotrophicus* cells. NaCl concentrations, lower than 150 mM, induced cell filamentation without affect cell viability. Morphological plasticity under specific stress conditions is essential for maintaining the population of several bacterial species (Justice *et al.*, 2008). In *Gluconacetobacter europaeus*, the increase in cell size has been proposed as a survival strategy by reduction of relative area in contact with the stressor agent (Trček *et al.*, 2007). Cell viability is strongly affected at NaCl concentrations higher than 150 mM, where *G. diazotrophicus* do not form filaments.

Such evidence allows hypothesizing that cell filamentation may be a tolerance strategy in *G. diazotrophicus*.

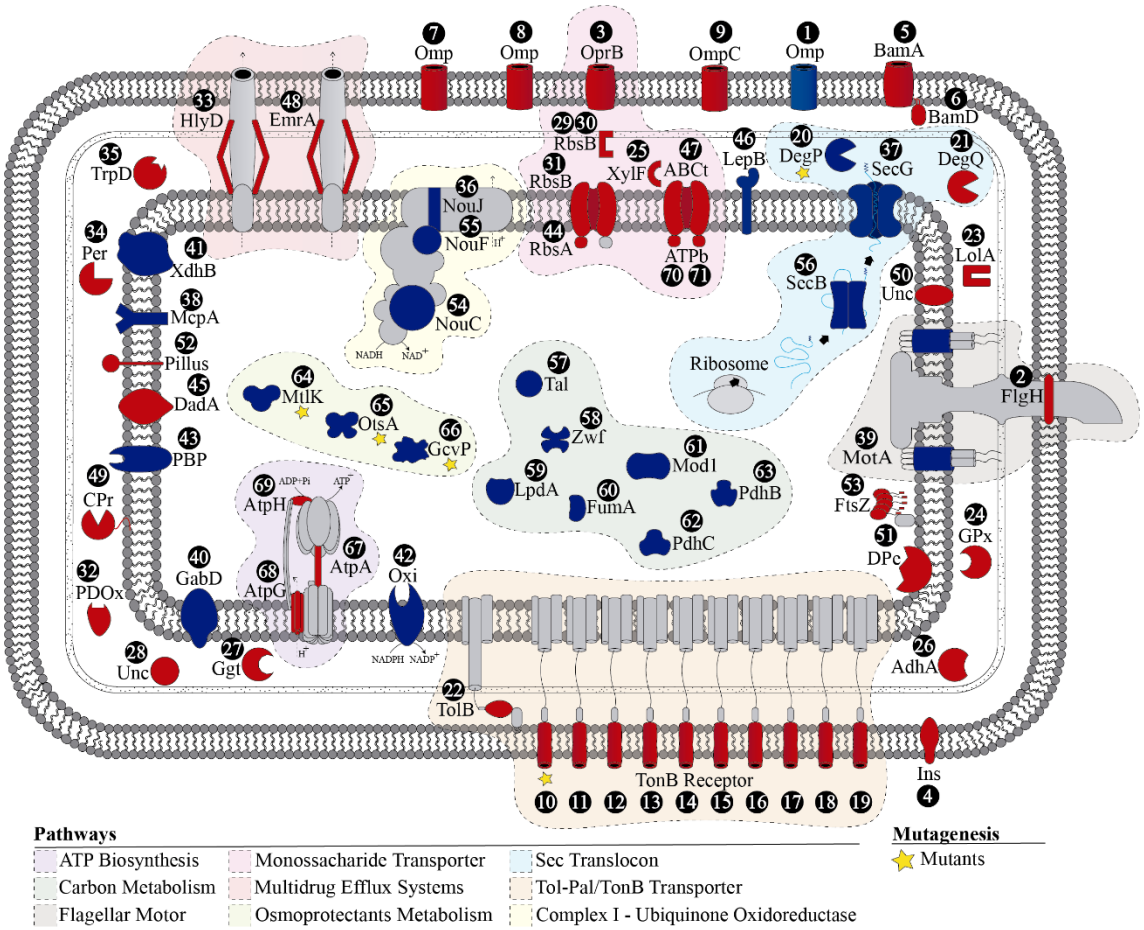

Fig. 7 Schematic illustration of the main responses of *G. diazotrophicus* to salt stress. Red and blue forms represent proteins classified as down-accumulated and up-accumulated, respectively, and grey forms represent non-regulated proteins. Yellow stars indicate proteins in which defective mutants were obtained.

Proteomic approaches have been used to understand molecular aspects of bacterial response to stress (Hoyer *et al.*, 2018; Tang *et al.*, 2018; Barcarolo *et al.*, 2019; Wright *et al.*, 2019). Our analyses revealed several changes in the protein profile of *G. diazotrophicus* in response to salt stress. Figure 7 summarizes all extracytoplasmic proteins that were regulated and cytoplasmic pathways exploited in this study. A general

response observed in our proteomic analysis was the down-regulation of extracytoplasmic proteins of *G. diazotrophicus*. In Gram-negative bacteria, the negative regulation of extracytoplasmic proteins is a response associated with exposition to antibiotics. The consequence of this process is a decrease in outer membrane permeability (Lin *et al.*, 2010).

A small number of proteins related to the synthesis of compatible solutes were regulated in our proteomic analyses, indicating that 150 mM NaCl causes a low level of osmotic stress in this bacterium. Such results are in line with various studies that demonstrated that *G. diazotrophicus* is highly resistant to osmotic stresses (Oliveira et al., 2016; Hartmann et al., 1991; Tejera et al., 2003; Velázquez-Hernández et al., 2011). Only two proteins, MtlK and OtsA, directly involved in the synthesis of compatible solutes, were up-accumulated. MtlK and OtsA participate in the biosynthesis of mannitol and trehalose, respectively, which are two widely characterized compatible solutes (Iordachescu and Imai, 2008; Ortiz *et al.*, 2017). Although no studies demonstrated that *G. diazotrophicus* accumulates mannitol or trehalose under osmotic stress, our reverse genetics analysis revealed that the mutant MtlK is slightly more sensitive to NaCl compared to the wild-type. The mutation in OtsA does not affect the tolerance. Therefore, such pathways are not essential for *G. diazotrophicus* tolerance to salt stress at NaCl concentrations tested. Hartamann et al. (1991) showed that sucrose was the only organic solute accumulated in *G. diazotrophicus* when exposed to osmotic stress. So, further analyses are necessary to investigate the role of MtlK for *G. diazotrophicus* tolerance to salt stress.

The formation of filamentous cells, observed by microscopy, was supported by proteomic results. Two proteins that modulate such process were regulated: PBP was up-accumulated, while FtsZ was down-accumulated. PBPs directly participate in deciding

when and where the cell must elongate and divide (Popham and Young, 2003b). The switch between these decisions is controlled by FtsZ (Popham and Young 2003). When FtsZ accumulation increases, the cell enters the division process; however, when its accumulation decreases, the cell activates the elongation process and does not divide (Popham and Young 2003). The opposite regulation of these two proteins, therefore, is in line with the formation of elongated cells, as observed during salt stress.

Iron is an essential nutrient for most bacteria, especially the nitrogen-fixing ones (de Paula Soares *et al.*, 2015). In our proteomic analyses, 10 TonB-dependent receptors, potentially involved with iron-uptake, were down-accumulated. Previous studies demonstrate that salinity induces iron limitation responses in *Bacillus subtilis* (Hoffmann *et al.*, 2002). Soares et al. (2015) showed that a Tn5 insertion in the *tonB* gene promoter of *G. diazotrophicus* affected its nitrogenase activity and biofilm formation. Thus, our proteomic analyses suggest that salt stress might lead to iron limitation in *G. diazotrophicus*, affecting many iron-dependent mechanisms, as biological nitrogen fixation. On the other hand, in contrast with the TonB-dependent receptors down-accumulation observed in our proteomic data, the lack of a TonB-dependent receptor increases *G. diazotrophicus* sensitivity to salt stress. This result indicates that a moderate level of TonB-dependent receptors is essential for cellular iron homeostasis during salt stress.

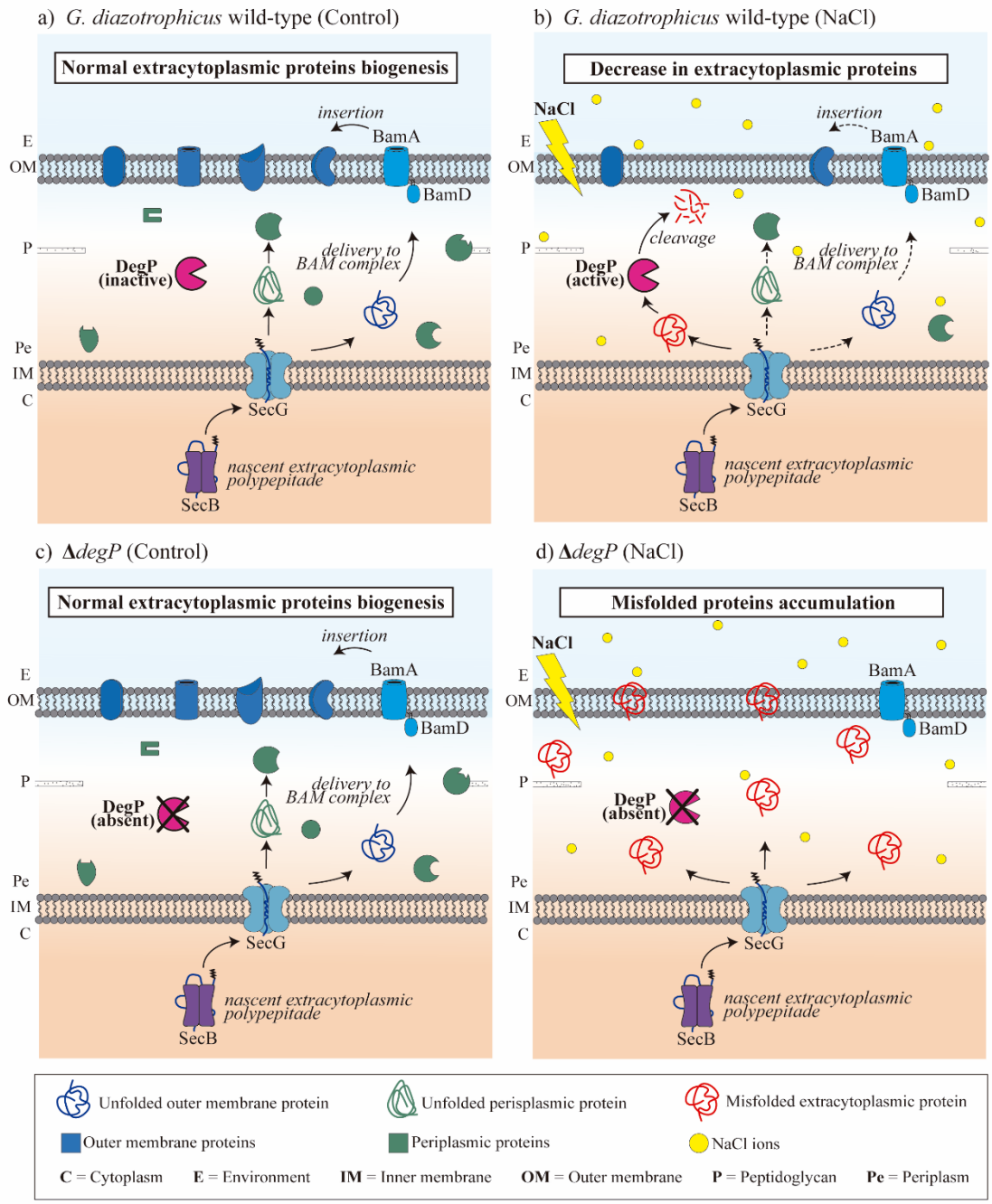

Fig. 8 Hypothesis for the essential role of DegP to *G. diazotrophicus* tolerance to salt stress. Under favorable conditions, DegP does not participate in the production of extracytoplasmic proteins (a, c). Nevertheless, under salt stress conditions, *G. diazotrophicus* wild-type activates/accumulates DegP in order to degrade misfolded proteins, which leads to a decrease in the number of extracytoplasmic proteins (b). On the other hand, Δ*degP* is impaired in the degradation of misfolded proteins and accumulates misfolded proteins under salt stress conditions, which drastically affects its survival (d). Solid arrows represent processes that occur most frequently in a condition, while dashed arrows represent processes that occur less often.

Despite the significant down-regulation of most extracytoplasmic proteins by salt stress, the proteins SecB and SecG, components of the Sec translocon machinery, were up-accumulated in our proteomic analyses. Additionally, the periplasmic protease DegP was also up-accumulated. Although the Sec translocon is the main protein transport system involved in the biogenesis of extracytoplasmic proteins in Gram-negative bacteria (Kudva *et al.*, 2013), NaCl ion-toxic effects may impair the extracytoplasmic protein folding process. In this way, the increase of DegP may be a strategy to degrade the proteins misfolded due to the ion-toxic effect of NaCl. Moreover, the increase in Sec translocon machinery components would be a compensatory mechanism, activated to replace the extracytoplasmic proteins misfolded/degraded under salt stress.

Our hypothesis for the essential role of DegP to *G. diazotrophicus* tolerance to salt stress is summarized in a schematic illustration (Fig. 8): under favorable conditions, DegP is not essential for *G. diazotrophicus* growth and maintenance of cellular viability. Nevertheless, under salt stress conditions, the entrance of NaCl ions in *G. diazotrophicus* cells trigger the misfolding of nascent extracytoplasmic proteins. *G. diazotrophicus* activates DegP protease to prevent the accumulation of misfolded protein. Consequently, the amount of extracytoplasmic proteins decreases, affecting various processes dependent on extracytoplasmic protein activity. On the other hand, *G. diazotrophicus* Δ*degP* knock-out mutant is impaired in the degradation of misfolded proteins. Thus, Δ*degP* accumulates misfolded proteins under salt stress conditions, which drastically affects its survival. Further analyses will be important to investigate in deep if salt stress impairs folding of *G. diazotrophicus* extracytoplasmic proteins, either globally or by targeting specific proteins.

Conclusions

Our results contribute to a better understanding of the molecular bases of *G. diazotrophicus* response/tolerance to salt stress, shedding light on the importance of quality control of nascent extracytoplasmic proteins. This is the first work to show that DegP is essential to tolerance to salt stress in *G. diazotrophicus*. Further studies addressing similar mechanisms in other plant growth-promoting bacteria may provide new acknowledge about essential components of salt stress tolerance and contribute to the expansion of its use in salinized soils.

3.5 References

Adesemoye, A.O., Torbert, H.A., Kloepper, J.W., 2009. Plant growth-promoting rhizobacteria allow reduced application rates of chemical fertilizers. Microb. Ecol. 58, 921–929. https://doi.org/10.1007/s00248-009-9531-y

Barcarolo, M.V., Garavaglia, B.S., Thomas, L., Marondedze, C., Gehring, C., Gottig, N., Ottado, J., 2019. Proteome changes and physiological adaptations of the phytopathogen Xanthomonas citri subsp. citri under salt stress and their implications for virulence. FEMS Microbiol. Ecol. 95. https://doi.org/10.1093/femsec/fiz081

Bednarska, N.G., Schymkowitz, J., Rousseau, F., Van Eldere, J., 2013. Protein aggregation in bacteria: The thin boundary between functionality and toxicity. Microbiol. (United Kingdom). https://doi.org/10.1099/mic.0.069575-0

Boniolo, F.S., Rodrigues, R.C., Delatorre, E.O., da Silveira, M.M., Flores, V.M.Q., Berbert-Molina, M.A., 2009. Glycine Betaine Enhances Growth of Nitrogen-Fixing Bacteria Gluconacetobacter diazotrophicus PAL5 Under Saline Stress Conditions. Curr. Microbiol. 59, 593–599. https://doi.org/10.1007/s00284-009-9479-7

Cavalcante, V. A., Dobereiner, J., 1988. A new acid-tolerant nitrogen-fixing bacterium associated with sugarcane. Plant Soil 108, 23–31. https://doi.org/10.1007/BF02370096

Chang, Z., 2016. The function of the DegP (HtrA) protein: Protease versus chaperone. IUBMB Life 68, 904–907. https://doi.org/10.1002/iub.1561

Clausen, T., Kaiser, M., Huber, R., Ehrmann, M., 2011. HTRA proteases: Regulated proteolysis in protein quality control. Nat. Rev. Mol. Cell Biol. https://doi.org/10.1038/nrm3065

Damerval, C., De Vienne, D., Zivy, M., Thiellement, H., 1986. Technical improvements in two-dimensional electrophoresis increase the level of genetic variation detected in wheat-seedling proteins. Electrophoresis 7, 52–54. https://doi.org/10.1002/elps.1150070108

De Geyter, J., Tsirigotaki, A., Orfanoudaki, G., Zorzini, V., Economou, A., Karamanou, S., 2016. Protein folding in the cell envelope of Escherichia coli. Nat. Microbiol. 1. https://doi.org/10.1038/nmicrobiol.2016.107

De Oliveira, M.V. V., Intorne, A.C., Vespoli, L. de S., Madureira, H.C., Leandro, M.R., Pereira, T.N.S., Olivares, F.L., Berbert-Molina, M.A., De Souza Filho, G.A., 2016. Differential effects of salinity and osmotic stress on the plant growth-promoting bacterium Gluconacetobacter diazotrophicus PAL5. Arch. Microbiol. 198, 287–294. https://doi.org/10.1007/s00203-015-1176-2

de Paula Soares, C., Rodrigues, E.P., de Paula Ferreira, J., Simões Araújo, J.L., Rouws, L.F.M., Baldani, J.I., Vidal, M.S., 2015. Tn5 insertion in the tonB gene promoter affects iron-related phenotypes and increases extracellular siderophore levels in Gluconacetobacter diazotrophicus. Arch. Microbiol. 197, 223–233. https://doi.org/10.1007/s00203-014-1045-4

Distler, U., Kuharev, J., Navarro, P., Levin, Y., Schild, H., Tenzer, S., 2014. Drift time-specific collision energies enable deep-coverage data-independent acquisition proteomics. Nat. Methods 11, 167–170. https://doi.org/10.1038/nmeth.2767

Distler, U., Kuharev, J., Navarro, P., Tenzer, S., 2016. Label-free quantification in ion mobility-enhanced data-independent acquisition proteomics. Nat. Protoc. 11, 795–812. https://doi.org/10.1038/nprot.2016.042

Errington, J., Daniel, R.A., Scheffers, D.-J., 2003. Cytokinesis in Bacteria. Microbiol. Mol. Biol. Rev. https://doi.org/10.1128/mmbr.67.1.52-65.2003

FAO-UN, 2017. World fertilizer trends and outlook to 2020. Food Agric. Organ. United Nations.

FAO, 1994. FAO IRRIGATION AND DRAINAGE PAPER: Water Quality for Agriculture, FAO of the UNITED NATIONS, Rome, Italy.

Flannagan, R.S., Aubert, D., Kooi, C., Sokol, P.A., Valvano, M.A., 2007. Burkholderia cenocepacia Requires a Periplasmic HtrA Protease for Growth under Thermal and Osmotic Stress and for Survival In Vivo †. Infect. Immun. 75, 1679–1689. https://doi.org/10.1128/IAI.01581-06

Ge, X., Wang, R., Ma, J., Liu, Y., Ezemaduka, A.N., Chen, P.R., Fu, X., Chang, Z., 2014. DegP primarily functions as a protease for the biogenesis of β-barrel outer membrane proteins in the Gram-negative bacterium Escherichia coli. FEBS J. 281, 1226–1240. https://doi.org/10.1111/febs.12701

Griffiths, R.I., Whiteley, A.S., O'Donnell, A.G., Bailey, M.J., 2003. Physiological and Community Responses of Established Grassland Bacterial Populations to Water Stress. Appl. Environ. Microbiol. https://doi.org/10.1128/AEM.69.12.6961-6968.2003

Hallsworth, J.E., 2018. Stress-free microbes lack vitality. Fungal Biol. https://doi.org/10.1016/j.funbio.2018.04.003

Hartmann, A., Prabhu, S.R., Galinski, E.A., 1991. Osmotolerance of diazotrophic rhizosphere bacteria. Plant Soil. https://doi.org/10.1007/BF02187440

Hoffmann, T., Schütz, A., Brosius, M., Völker, A., Völker, U., Bremer, E., 2002. High-salinity-induced iron limitation in Bacillus subtilis. J. Bacteriol. https://doi.org/10.1128/JB.184.3.718-727.2002

Hoyer, J., Bartel, J., Gómez-Mejia, A., Rohde, M., Hirschfeld, C., Heß, N., Sura, T., Maaß, S., Hammerschmidt, S., Becher, D., 2018. Proteomic response of Streptococcus pneumoniae to iron limitation. Int. J. Med. Microbiol. 308, 713–721. https://doi.org/10.1016/j.ijmm.2018.02.001

Intorne, A.C., De Oliveira, M. V V, Lima, M.L., da Silva, J.F., Olivares, F.L., de Souza Filho, G.A., Oliveira, Marcos Vinicius V, Lima, M.L., da Silva, J.F., Olivares, F.L., de Souza Filho, G.A., 2009. Identification and characterization of Gluconacetobacter diazotrophicus mutants defective in the solubilization of phosphorus and zinc. Arch. Microbiol. 191, 477–483. https://doi.org/10.1007/s00203-009-0472-0

Iordachescu, M., Imai, R., 2008. Trehalose Biosynthesis in Response to Abiotic Stresses. J. Integr. Plant Biol. 50, 1223–1229. https://doi.org/10.1111/j.1744-7909.2008.00736.x

Itelima, Bang, W.J., Onyimba, I.A., Sila, Egbere, O.J., 2018. Bio-fertilizers as key player in enhancing soil fertility and crop productivity: A Review 6, 73–83. https://doi.org/10.26765/DRJAFS.2018.4815

Justice, S.S., Hunstad, D.A., Cegelski, L., Hultgren, S.J., 2008. Morphological plasticity as a bacterial survival strategy. Nat. Rev. Microbiol. 6, 162–168. https://doi.org/10.1038/nrmicro1820

Kudva, R., Denks, K., Kuhn, P., Vogt, A., Müller, M., Koch, H.-G., 2013. Protein translocation across the inner membrane of Gram-negative bacteria: the Sec and Tat

dependent protein transport pathways. Res. Microbiol. 164, 505–534. https://doi.org/10.1016/j.resmic.2013.03.016

Lyu, Z.X., Zhao, X.S., 2015. Periplasmic quality control in biogenesis of outer membrane proteins. Biochem. Soc. Trans. 43, 133–138. https://doi.org/10.1042/BST20140217

Martinez, J.L., Sánchez, M.B., Martínez-Solano, L., Hernandez, A., Garmendia, L., Fajardo, A., Alvarez-Ortega, C., 2009. Functional role of bacterial multidrug efflux pumps in microbial natural ecosystems. FEMS Microbiol. Rev. https://doi.org/10.1111/j.1574-6976.2008.00157.x

Mas, G., Thoma, J., Hiller, S., 2019. The Periplasmic Chaperones Skp and SurA, in: Subcellular Biochemistry. Springer New York, pp. 169–186. https://doi.org/10.1007/978-3-030-18768-2_6

Miller, K.J., Wood, J.M., 1996. Osmoadaptation by rhizosphere bacteria. Annu. Rev. Microbiol. https://doi.org/10.1146/annurev.micro.50.1.101

Mitchell, A.M., Silhavy, T.J., 2019. Envelope stress responses: balancing damage repair and toxicity. Nat. Rev. Microbiol. https://doi.org/10.1038/s41579-019-0199-0

Ortiz, M.E., Bleckwedel, J., Fadda, S., Picariello, G., Hebert, E.M., Raya, R.R., Mozzi, F., 2017. Global Analysis of Mannitol 2-Dehydrogenase in Lactobacillus reuteri CRL 1101 during Mannitol Production through Enzymatic, Genetic and Proteomic Approaches. PLoS One 12, e0169441. https://doi.org/10.1371/journal.pone.0169441

Passamani, L.Z., Bertolazi, A.A., Ramos, A.C., Santa-Catarina, C., Thelen, J.J., Silveira, V., 2018. Embryogenic Competence Acquisition in Sugar Cane Callus Is Associated with

Differential H+-Pump Abundance and Activity. J. Proteome Res. 17, 2767–2779. https://doi.org/10.1021/acs.jproteome.8b00213

Popham, D.L., Young, K.D., 2003a. Role of penicillin-binding proteins in bacterial cell morphogenesis. Curr. Opin. Microbiol. https://doi.org/10.1016/j.mib.2003.10.002

Popham, D.L., Young, K.D., 2003b. Role of penicillin-binding proteins in bacterial cell morphogenesis. Curr. Opin. Microbiol. 6, 594–599. https://doi.org/10.1016/j.mib.2003.10.002

Rodrigues, E.P., Soares, C. de P., Galvão, P.G., Imada, E.L., Simões-Araújo, J.L., Rouws, L.F.M., de Oliveira, A.L.M., Vidal, M.S., Baldani, J.I., 2016. Identification of genes involved in indole-3-acetic acid biosynthesis by Gluconacetobacter diazotrophicus PAL5 strain using transposon mutagenesis. Front. Microbiol. https://doi.org/10.3389/fmicb.2016.01572

Rollauer, S.E., Sooreshjani, M.A., Noinaj, N., Buchanan, S.K., 2015. Outer membrane protein biogenesis in Gram-negative bacteria. Philos. Trans. R. Soc. B Biol. Sci. 370, 20150023. https://doi.org/10.1098/rstb.2015.0023

Saravanan, V.S., Madhaiyan, M., Osborne, J., Thangaraju, M., Sa, T.M., 2008. Ecological Occurrence of Gluconacetobacter diazotrophicus and Nitrogen-fixing Acetobacteraceae Members: Their Possible Role in Plant Growth Promotion. Microb. Ecol. 55, 130–140. https://doi.org/10.1007/s00248-007-9258-6

Saravanan, V.S., Madhaiyan, M., Thangaraju, M., 2007. Solubilization of zinc compounds by the diazotrophic, plant growth promoting bacterium Gluconacetobacter diazotrophicus. Chemosphere 66, 1794–1798. https://doi.org/10.1016/j.chemosphere.2006.07.067

Saulou-Bérion, C., Gonzalez, I., Enjalbert, B., Audinot, J.-N., Fourquaux, I., Jamme, F., Cocaign-Bousquet, M., Mercier-Bonin, M., Girbal, L., 2015. Escherichia coli under Ionic Silver Stress: An Integrative Approach to Explore Transcriptional, Physiological and Biochemical Responses. PLoS One 10, e0145748. https://doi.org/10.1371/journal.pone.0145748

Spiess, C., Beil, A., Ehrmann, M., 1999. A temperature-dependent switch from chaperone to protease in a widely conserved heat shock protein. Cell 97, 339–347. https://doi.org/10.1016/S0092-8674(00)80743-6

Stevenson, A., Cray, J.A., Williams, J.P., Santos, R., Sahay, R., Neuenkirchen, N., McClure, C.D., Grant, I.R., Houghton, J.D., Quinn, J.P., Timson, D.J., Patil, S. V., Singhal, R.S., Antón, J., Dijksterhuis, J., Hocking, A.D., Lievens, B., Rangel, D.E.N., Voytek, M.A., Gunde-Cimerman, N., Oren, A., Timmis, K.N., McGenity, T.J., Hallsworth, J.E., 2015. Is there a common water-activity limit for the three domains of life. ISME J. https://doi.org/10.1038/ismej.2014.219

Stevenson, A., Hallsworth, J.E., 2014. Water and temperature relations of soil Actinobacteria. Environ. Microbiol. Rep. https://doi.org/10.1111/1758-2229.12199

Sugawara, M., Cytryn, E.J., Sadowsky, M.J., 2010. Functional role of Bradyrhizobium japonicum trehalose biosynthesis and metabolism genes during physiological stress and nodulation. Appl. Environ. Microbiol. https://doi.org/10.1128/AEM.02483-09

Tang, J., Jia, J., Chen, Y., Huang, X., Zhang, X., Zhao, L., Hu, W., Wang, C., Lin, C., Wu, Z., 2018. Proteomic Analysis of Vibrio parahaemolyticus Under Cold Stress. Curr. Microbiol. 75, 20–26. https://doi.org/10.1007/s00284-017-1345-4

Tapia-Hernández, A., Bustillos-Cristales, M.R., Jiménez-Salgado, T., Caballero-Mellado, J., Fuentes-Ramírez, L.E., 2000. Natural endophytic occurrence of Acetobacter diazotrophicus in pineapple plants. Microb. Ecol. https://doi.org/10.1007/s002489900190

Tejera, N.A., Ortega, E., Gonzalez-Lopez, J., Lluch, C., 2003. Effect of some abiotic factors on the biological activity of Gluconacetobacter diazotrophicus. J. Appl. Microbiol. 95, 528–535. https://doi.org/10.1046/j.1365-2672.2003.02007.x

Trček, J., Jernejc, K., Matsushita, K., 2007. The highly tolerant acetic acid bacterium Gluconacetobacter europaeus adapts to the presence of acetic acid by changes in lipid composition, morphological properties and PQQ-dependent ADH expression. Extremophiles 11, 627–635. https://doi.org/10.1007/s00792-007-0077-y

Velázquez-Hernández, M.L., Baizabal-Aguirre, V.M., Cruz-Vázquez, F., Trejo-Contreras, M.J., Fuentes-Ramírez, L.E., Bravo-Patiño, A., Cajero-Juárez, M., Chávez-Moctezuma, M.P., Valdez-Alarcón, J.J., 2011. Gluconacetobacter diazotrophicus levansucrase is involved in tolerance to NaCl, sucrose and desiccation, and in biofilm formation. Arch. Microbiol. 193, 137–149. https://doi.org/10.1007/s00203-010-0651-z

Wonderling, L.D., Wilkinson, B.J., Bayles, D.O., 2004. The htrA (degP) Gene of Listeria monocytogenes 10403S Is Essential for Optimal Growth under Stress Conditions. Appl. Environ. Microbiol. https://doi.org/10.1128/AEM.70.4.1935-1943.2004

Wright, B.W., Kamath, K.S., Krisp, C., Molloy, M.P., 2019. Proteome profiling of Pseudomonas aeruginosa PAO1 identifies novel responders to copper stress. BMC Microbiol. 19, 69. https://doi.org/10.1186/s12866-019-1441-7

Zahid, N., Schweiger, P., Galinski, E., Deppenmeier, U., 2015. Identification of mannitol as compatible solute in Gluconobacter oxydans. Appl. Microbiol. Biotechnol. 99, 5511–5521. https://doi.org/10.1007/s00253-015-6626-x

Zhang, S., Cheng, Y., Ma, J., Wang, Y., Chang, Z., Fu, X., 2019. DegP degrades a wide range of substrate proteins in Escherichia coli under stress conditions. Biochem. J. https://doi.org/10.1042/BCJ20190446

4. CHAPTER 3

THE RESISTANCE OF THE PLANT GROWTH-PROMOTING BACTERIUM *Gluconacetobacter diazotrophicus* TO HIGH-SUCROSE INVOLVES OSMOTOLERANCE AND SUGAR-TOLERANCE MECHANISMS

4.1 Abstract

Sugar-rich environments represent an important challenge for microorganisms. The osmotic and molecular imbalances resulting from this condition severely limit microbial metabolism and growth. *Gluconacetobacter diazotrophicus* is one of the most sugar-tolerant prokaryotes, able to grow in the presence of sucrose concentrations up to 30%. However, the mechanisms that control its resistance to such conditions remain poorly exploited. The present work investigated the key mechanisms of resistance to high-sucrose in *G. diazotrophicus***.** Comparative proteomics was applied to investigate the main functional pathways regulated in *G. diazotrophicus* when cultivated in the presence of sucrose. Among 191 proteins regulated by high-sucrose, regulatory pathways related to sugar metabolism, nutrient uptake, compatible solute synthesis, amino acid metabolism, and proteolytic system were highlighted. The role of such pathways on high-sucrose resistance was investigated by mutagenesis analysis and revealed that the knockout mutants Δ*zwf* (sugar metabolism), Δ*tbdr* (nutrients uptake), Δ*mtlK* (compatible solute synthesis), Δ*pepN* (proteolytic system), Δ*metH* (amino acid metabolism), and Δ*ilvD* (amino acid metabolism), became more sensitive to high-sucrose. Together, our results identified the mechanisms involved in response to high-sucrose in *G. diazotrophicus*, shedding light on the combination of osmotolerance and sugar-tolerance mechanisms.

4.2 Introduction

Sugar-rich environments are widespread in the microbial habitats. This condition challenges bacterial life through multiple aspects, such as the imbalance on macromolecular systems and decreased water activity (Oliveira et al., 2017; Lievens et al., 2015). High-sugar conditions occur naturally in the environment, such as plant tissues and juices, plant exudates, fruits, and honey. However, they can also occur artificially in the industry of sugar-rich products (Lievens *et al.*, 2015). Despite the challenging conditions of these environments, several microorganisms species can survive under such circumstances (Lievens *et al.*, 2015). For this, these microorganisms may rely on resistance mechanisms for both high-sugar levels and low water activity.

The decrease in water activity resulting from the exposure to solutes, including sugars, leads to an osmotic imbalance on microorganism cells, which can cause the efflux of water, turgor pressure loss, decrease in metabolic functions, and ultimately culminate in cell death (Esbelin *et al.*, 2018). One of the most described mechanisms to counteract such effects involves the synthesis of compatible solutes within microbial cells, which rebalance the solute levels between intra- and extracellular spaces (Bremer and Krämer, 2019). Although the mechanisms related to low water activity resistance are widely described, less is known about how microorganisms deal with the excess of sugar.

The plant growth-promoting bacterium (PGPB) *Gluconacetobacter diazotrophicus* is classified as one of the most sugar-tolerant prokaryotes (Cavalcante and Dobereiner, 1988; Stevenson *et al.*, 2015). It was first isolated from sugarcane, and colonizes mainly the sugarcane apoplast, where the sucrose content can vary between 20-30% (Vladimir A. Cavalcante and Dobereiner, 1988). This ability to live in a sugar-rich environment makes *G. diazotrophicus* a potential source of new osmotolerance and high-sugar resistance mechanisms.

G. diazotrophicus has also been isolated from pineapple (*Ananas comosus*), sweet potato (*Ipomoea batatas*), and coffee plants (*Coffea arabica*) (Madhaiyan *et al.*, 2004; Luna *et al.*, 2010). Among its main beneficial mechanisms as PGPB are the nitrogen fixation, phytohormones production, and nutrient solubilization (Saravanan *et al.*, 2007; Pedraza, 2008; Rodrigues *et al.*, 2016). The sequencing of *the G. diazotrophicus* genome revealed osmotolerance mechanisms also found in bacterial species that are non-resistant to high-sugar environments (Bertalan *et al.*, 2009). Thus, new molecular analyzes are necessary to explore the mechanisms involved with the high resistance of *G. diazotrophicus* to such conditions.

Boniolo et al. (2009) showed that the addition of the compatible solute glycine betaine to *G. diazotrophicus* cultures counteract the inhibitory effect of the ionic osmotic stressor NaCl. Leandro et al. (2020) demonstrated that, when exposed to PEG-400, a non-ionic osmotic stressor, *G. diazotrophicus* turns down the proteins responsible for nutrient uptake, modifies its cellular envelope structure, and activates the biosynthesis of compatible solutes. However, the molecular mechanisms specifically modulated in *G. diazotrophicus* in response to high-sugar environments remain unclear.

The present work investigated the mechanisms of *G. diazotrophicus* involved in the response and resistance to high sucrose concentrations. The effects of such conditions on cell morphology and viability were investigated by epifluorescence microscopy. The molecular mechanisms regulated in response to high sucrose concentrations were investigated by comparative proteomics, and the proteins essential for resistance to sugar stress were identified by using knockout mutants.

4.3 Results

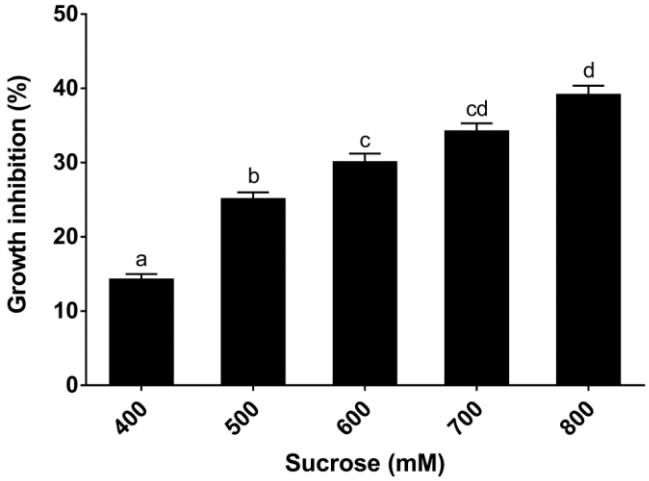

Fig. 1 Sucrose inhibits *G. diazotrophicus* growth. *G. diazotrophicus* was cultivated for 12 h in liquid medium supplemented with different concentrations of sucrose, and its growth performance was analyzed through optical density. Means followed by different letters are significantly different from each other at 5% probability level by Tukey test.

4.3.1 Effects of sucrose on *G. diazotrophicus* growth, morphology, and cell viability

Aiming to evaluate the effects of sucrose on *G. diazotrophicus* growth, morphology, and cell viability, bacterial cultures were grown under sucrose concentrations ranging from 0 to 800 mM.

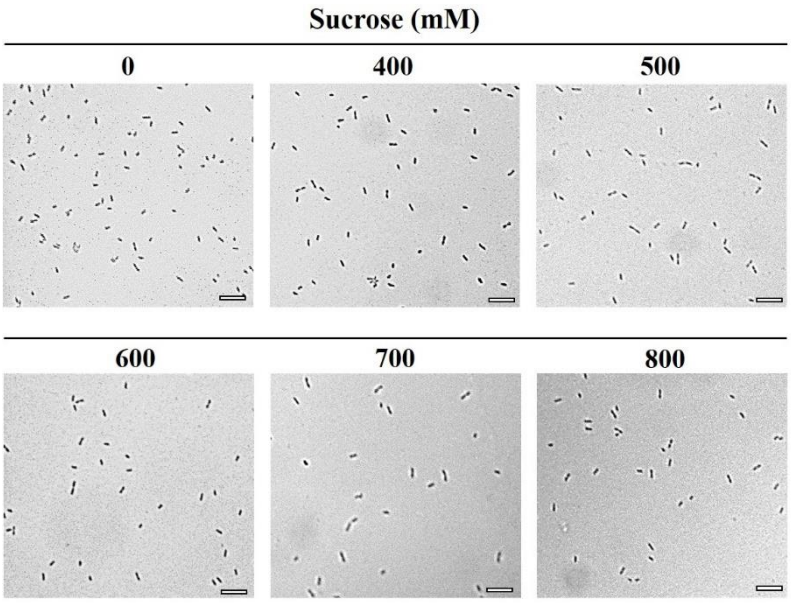

Fig.2 Morphological effects of sucrose on *G. diazotrophicus* cells. *G. diazotrophicus* was cultivated for 12 h in liquid medium supplemented with different dilutions of sucrose, and its morphological changes were analyzed through optical microscopy. *Bar* 5 µM.

G. diazotrophicus growth was inhibited by all sucrose concentrations tested, ranging from 14% inhibition, at 400 mM sucrose, to 40% inhibition, at 800 mM (Fig. 1). None of the sugar concentrations caused apparent morphological changes to bacterial cells (Fig. 2).

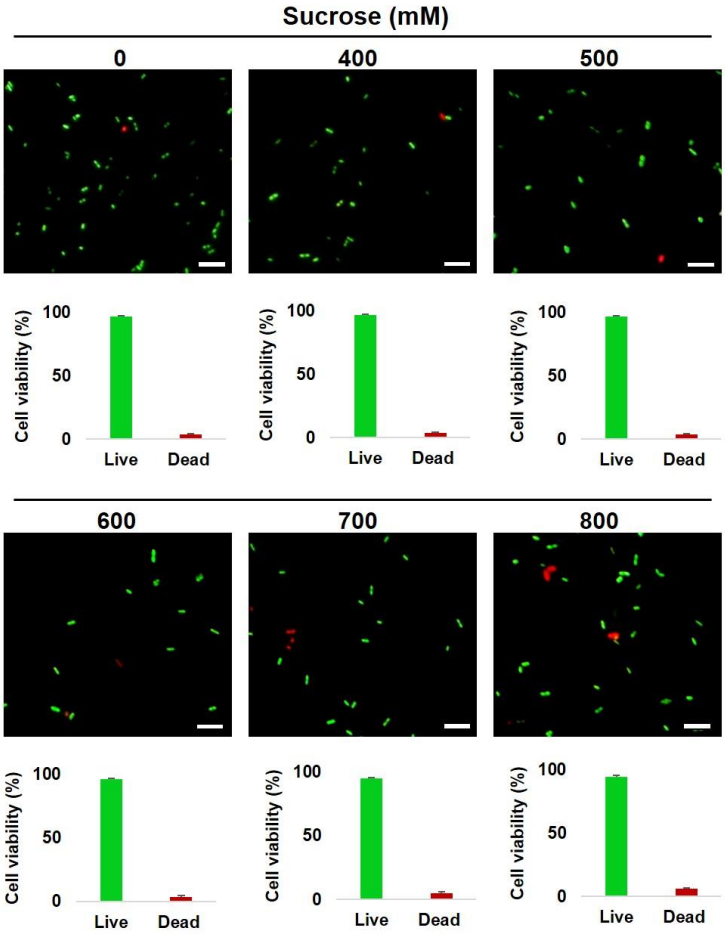

Fig. 3 Sucrose effects on *G. diazotrophicus* cell viability. *G. diazotrophicus* was cultivated for 12 h in liquid medium supplemented with different dilutions of sucrose, and its cell viability was analyzed through epifluorescence analysis. The proportion of living (green) and dead (red) cells in the different dilutions of PEG-400 was plotted. *Bar* 5 µM.

Additionally, epifluorescence microscopy analyses show that sucrose *slightly* affects the cell viability of *G. diazotrophicus*, even at the highest concentrations of sucrose tested (Fig. 3).

These results indicate that, despite the inhibitory effect of high-sucrose on *G. diazotrophicus* growth, bacterial cells contain adaptative mechanisms that allow cell

viability maintenance. So, the treatment with 600 mM sucrose was selected to further analyses of the molecular aspects of the bacterial response to high-sucrose by proteomic analyses.

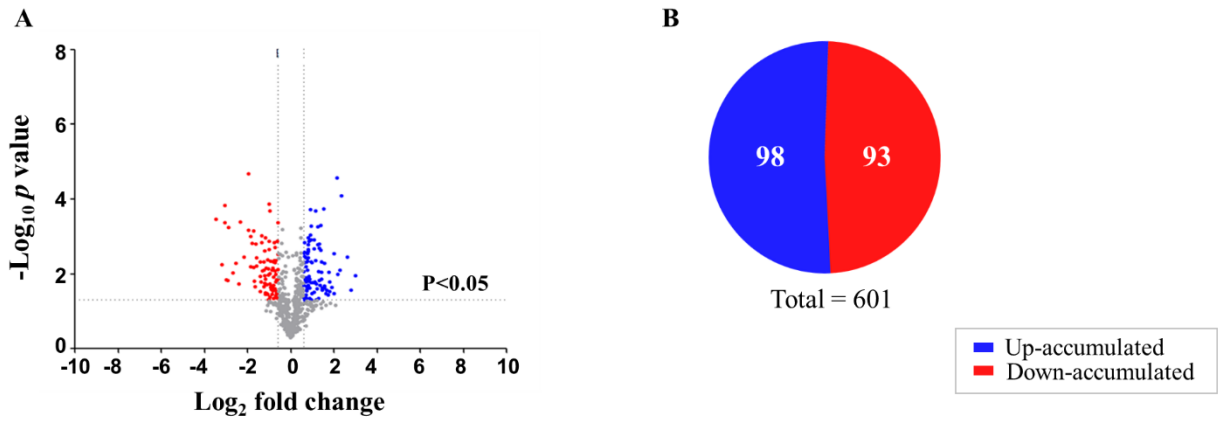

Fig. 2 High-sucrose concentration changes the proteome profile of *G. diazotrophicus*. Volcano plot of all identified proteins was performed (A). The spots represent differential abundance (log2 fold change) of identified proteins in the function of statistical significance (-log10 p value), and up-accumulated, down-accumulated and non-regulated proteins are represented by blue, red, and grey spots, respectively. A graphical representation of the proportion of differentially accumulated proteins (DAPs) increased and decreased was also performed (B).

4.3.2 Changes in the proteome profile of *G. diazotrophicus* in response to high-sucrose

To investigate the mechanisms regulated in *G. diazotrophicus* under a high-sucrose environment, total protein extracts from bacterial cells, cultivated in the presence and absence of 600 mM sucrose, were analyzed by comparative proteomics. A total of 601 proteins were identified, of which 191 (~30%) were differentially accumulated (Table S1, Fig. 2A). Among regulated proteins, 98 were up-accumulated, while 93 were down-accumulated in response to sucrose (Fig. 2B).

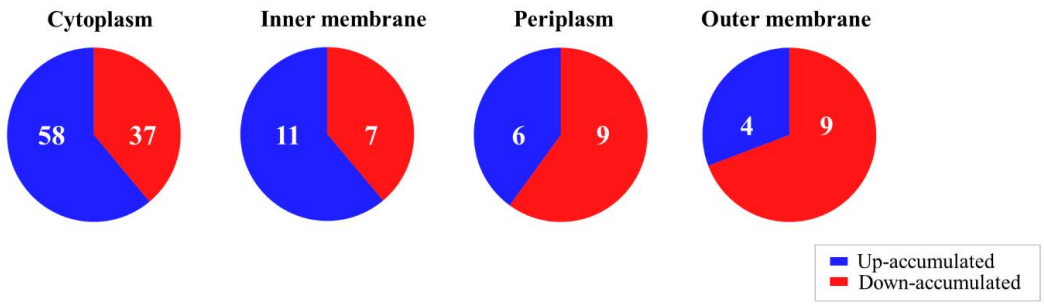

Fig. 3 High sucrose concentration changes the protein profile of the cellular compartments of *G. diazotrophicus*. Differentially accumulated proteins (DAPs) were classified by predicted subcellular localization (Cytoplasm; Inner Membrane; Periplasm; Outer Membrane) with FUEL-mLoc software.

The 191 proteins differentially accumulated in response to sucrose were categorized through its predicted localization (see methods). As shown in Fig. 3, most of the regulated proteins are located in the cytoplasm and inner membrane, with a higher proportion of up-accumulated proteins. Proteins from the outer membrane and periplasm were mainly down-accumulated in response to sucrose.

4.3.3 Functional pathways regulated in *G. diazotrophicus* in response to high-sucrose

Five functional pathways regulated during the *G. diazotrophicus* response to high-sucrose were identified through the functional categorization of DAPs: sugar metabolism, nutrients uptake, osmotic adjustment, amino acid metabolism, and proteolytic system. Such pathways are described below.

Table 1 Functional pathways regulated in *G. diazotrophicus* cells exposed to high-sucrose

Accession	Description	Fold Change
a. *Sugar metabolism*		
A9H0G0	Glucose-6-phosphate 1-dehydrogenase (Zwf)	2.78
A9HI04	Glucokinase (Glk)	2.95
A9H320	Bifunctional transaldolase/phosoglucose isomerase (Tal/Pgi)	3.75
A9HSH5	Alpha-D-glucose phosphate-specific phosphoglucomutase (Pgm)	1.83
A9HJ42	6-phosphogluconolactonase (Pgl)	1.64
A9H324	6-phosphogluconate dehydrogenase, decarboxylating (Gnd)	1.64
A9H317	Transketolase (TktA)	3.05
A9HGX3	Phosphoketolase	4.79
A9HJB2	Dihydrolipoyl acetyltransferase	4.47
A9HJA9	Pyruvate dehydrogenase E1 (PdhB)	3.97
A9HNN4	NAD(P)-dependent alcohol dehydrogenase (Adh)	2.11
A9HNA5	Alcohol dehydrogenase (AdhP)	3.39
A9H4V7	Aldehyde Dehydrogenase (AldA)	2.17
A9HL52	Gluconolactonase	1.70
A9HBF6	Galactose mutarotase (GalM)	2.64
b. *Nutrients uptake*		
A9HPE7	sn-glycerol-3-phosphate ABC transporter ATP-binding protein (UgpC)	0.51
A9HPE1	Sugar ABC transporter substrate-binding protein	0.12
A9HPF6	Carbohydrate porin (OprB)	0.12
A9HNP0	D-xylose ABC transporter, periplasmic substrate-binding (XylF)	0.28
A9HPB9	ABC transporter substrate-binding protein (RbsB)	0.25
A9HPK6	D-ribose-binding periplasmic protein (RbsB)	0.11
A9H932	TonB-dependent receptor	1.53
A9H7M7	TonB-dependent receptor	0.13
A9HEU6	TonB-dependent receptor	0.27
A9HDZ9	TonB-dependent receptor	0.42
A9H7L3	TonB-dependent siderophore receptor	0.11
c. *Osmotic adjustment*		
A9HBU3	Trehalose 6-phosphate phosphatase (OtsB)	1.52
A9HBL5	Mannitol 2-dehydrogenase (MtlK)	6.8
A9HBX1	Pyrroline-5-carboxylate reductase (ProC)	1.64
d. *Amino acids metabolism*		
A9HNX4	5-methyltetrahydropteroyltriglutamate--homocysteine methyltransferase (MetE)	7.94
A9HNY2	Methylenetetrahydrofolate reductase (MetF)	4.0
A9GZJ4	Ketol-acid reductoisomerase (NADP(+)) (IlvC)	3.13
A9HCQ4	Homoserine dehydrogenase 1	2.07
e. *Proteolytic system*		
A9HEL6	M1 family metallopeptidase - aminopeptidase N (PepN)	1.74
A9HFU5	M1 family metallopeptidase - aminopeptidase N (PepN)	1.75
A9HN12	M61 family metallopeptidase (aminopeptidase)	2.05
A9HP02	M3 family metallopeptidase (dipeptidyl carboxypeptidase - dcp)	1.53
A9HRE6	M13 family metallopeptidase - endopeptidase (PepO)	1.92
A9HKD9	M32 family metallopeptidase (carboxypeptidase)	1.61
A9HS00	Serine peptidase S10 (carboxypeptidase)	1.74

4.3.3.1 Sugar metabolism

Among the proteins up-accumulated in response to high sucrose, 15 participates in pathways involved with sugar metabolism (Table 1). Six proteins are components of glucose catabolism (glycolysis): Zwf (A9H0G0), Gnd (A9H324), Glk (A9HI04), Tal/Pgi (A9H320), Pgl (A9HJ42), and Pgm (A9HSH5); two belongs to Pyruvate dehydrogenase complex: Dihydrolipoyl acetyltransferase (A9HJB2) and PdhB (A9HJA9); and three participates in the two-step pathway of ethanol oxidation: Adh (A9HNN4), AdhP (A9HNA5) and AldA (A9H4V7). Additionally, the proteins Gluconolactonase (A9Hl52) and GalM (A9HBF6), essentials to gluconic acid production and galactose metabolism, respectively, were also up-accumulated. These results indicate that, in response to high-sucrose, *G. diazotrophicus* intensifies sugar metabolism, producing gluconic acid and oxidizing ethanol.

4.3.3.2 Nutrients uptake

The functional pathway with the second-highest number of proteins regulated in response to high-sucrose is related to nutrients uptake. Among the down-accumulated proteins, 11 are related to sugar, iron, and other nutrients uptake (Table 1). Among these, six are involved with sugar uptake (A9HPE7, A9HPE1, A9HPF6, A9HNP0, A9HPB9, and A9HPK6), four are TonB-dependent receptors – TBDRs (A9H932, A9H7M7, A9HEU6, and A9HDZ9), and one is a TonB-dependent siderophore receptor (A9H7L3), involved with iron and other nutrients uptake. These results indicate that *G. diazotrophicus* turns down the uptake of sugar and other nutrients in response to a high-sucrose environment.

4.3.3.3 Compatible solute synthesis

Three proteins involved with compatible solutes synthesis were up-accumulated in *G. diazotrophicus* in response to high-sucrose: OtsB (A9HBU3), MtlK (A9HBL5), and ProC (A9HBX1) (Table 1). The regulation of proteins related to the synthesis of three different classes of compatible solutes suggests that a variety of these compounds may be required for *G. diazotrophicus* resistance to high-sucrose.

4.3.3.4 Amino acid metabolism

Among the cytoplasmic proteins up-accumulated in response to sucrose, four are directly involved in amino acid metabolism (Table 1). Among these, two participates in the methionine biosynthetic pathway: MetE (A9HNX4) and MetF (A9HNY2); one participates in the homoserine synthesis: Homoserine dehydrogenase 1 (A9HCQ4); and one is involved in the biosynthesis of branched-chain amino acids (BCAA): IlvC (A9GZJ4).

4.3.3.5 Proteolytic system

Seven proteins with proteolytic activity were up-accumulated in *G. diazotrophicus* in response to sucrose (Table 1). Among these, six belongs to the family of metallopeptidases: M1 aminopeptidases N - PepN (A9HEL6, A9HFU5), M61 aminopeptidase (A9HN12), M3 dipeptidyl carboxypeptidase – Dcp (A9HP02), M13 endopeptidase – PepO (A9HRE6), M32 carboxypeptidase (A9HKD9), and one is a serine peptidase: Carboxypeptidase S10 (A9HS00), indicating that the exposure to a high-sucrose environment leads to the activation of proteolytic systems in *G. diazotrophicus*.

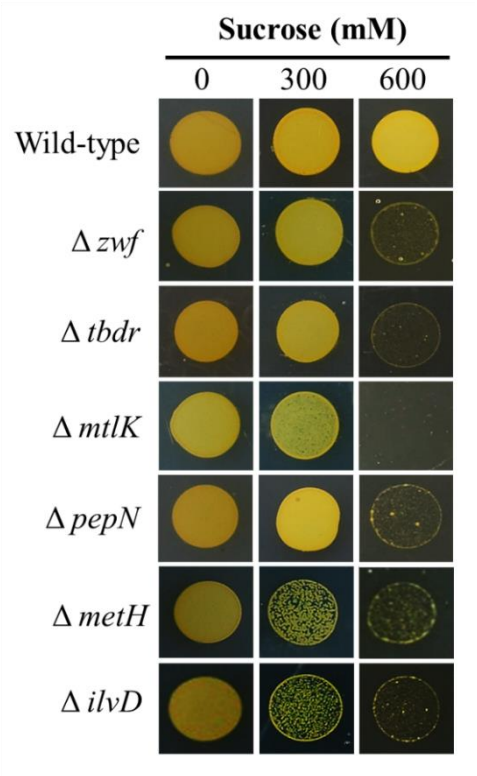

Fig. 4 Reverse genetics analysis revealed essential genes to high sucrose concentration resistance in *G. diazotrophicus*. Knock-out mutants of *G. diazotrophicus* defectives in the synthesis of proteins related to protein functional groups identified in our proteomic analyses were selected to perform the sucrose resistance assay. Results were registered after five days of sucrose exposure.

4.3.4 Reverse genetics analysis revealed essential proteins for *G. diazotrophicus* resistance to high-sucrose

The five above-mentioned functional pathways revealed by the proteomic analyses as regulated by high-sucrose were tested about its role on *G. diazotrophicus* resistance to such conditions. To this, a "*G. diazotrophicus* knockout mutants library" was accessed to identify strains defectives for key proteins of such pathways. As a result, we select the knockout mutant strains related to sugar metabolism (Δ*zwf*), nutrients uptake (Δ*tbdr*), compatible solute synthesis (Δ*mtlK*), amino acid metabolism (Δ*metH*, Δ*ilvD*), and proteolytic system (Δ*pepN*). Thereby, a reverse genetic approach was performed

comparing the growth of the wild-type strain of *G. diazotrophicus* with the knockout mutant strains under moderate (300 mM) and high (600 mM) sucrose concentrations.

As shown in Fig. 4, all the knockout mutants were sensitive to the high sucrose concentration tested. This result confirms that the functional pathways revealed by the proteomic analyses have a key role on *G. diazotrophicus* resistance to high-sucrose.

4.4 Discussion

The present work investigated the key mechanisms involved in the resistance of *G. diazotrophicus* to high-sucrose. Our analyses showed that, although high-sucrose inhibit the growth of *G. diazotrophicus*, no evident effects on bacterial cell morphology or cell viability were observed. Proteomic analyses highlighted the regulation of several proteins involved with sugar metabolism, nutrients uptake, compatible solute synthesis, amino acid metabolism, and proteolytic system. The use of knockout mutants revealed the essential role of such pathways for *G. diazotrophicus* resistance to high-sucrose.

The proteomic analyses of *G. diazotrophicus* responses to high-sucrose showed the up-accumulation of several proteins related to sugar metabolism and the down-accumulation of proteins related to sugar import. Such a result suggests that the bacteria activate both the sucrose conversion and sugar import restriction to avoid its excess into the cytoplasm. *G. diazotrophicus* is not able to import sucrose, so it utilizes the extracellular enzyme levansucrase to break sucrose into glucose and fructose, which are uptake by the cell (Alvarez and Martinez-Drets, 1995). Here, reverse genetics analysis showed that the lack of the protein Glucose-6-phosphate 1-dehydrogenase (Zwf) affects the resistance of *G. diazotrophicus* to high-sucrose. Zwf is an essential component for glucose breakdown once it integrates the oxidative phase of the pentose-phosphate pathway (Saavedra and Sesma, 2005).

Proteomics also revealed the down-accumulation of proteins involved with nutrients uptake. A similar response was observed in *G. diazotrophicus* cells as a resistance mechanism against the osmotic stress caused by PEG-400, probably to avoid the entry of the harmful compounds in bacterial cells (Leandro et al., 2020). In the present work, the sensibility of Δ*tbdr* to sucrose suggests that the uptake of nutrients is necessary to homeostasis maintenance in *G. diazotrophicus*. The down-accumulation of proteins

related to nutrients uptake may be a side effect of mechanisms that aim to reduce the excessive sugar entrance into bacterial cells.

Three proteins involved with the *de novo* synthesis of the compatible solutes mannitol (MtlK), trehalose (OtsB), and proline (ProC) were up-accumulated in our proteomic analyses. The protein MtlK is an essential component of *G. diazotrophicus* resistance to osmotic stress caused by PEG-400 (Leandro *et al.*, 2020). Here, the lack of protein MtlK severely affects the resistance of *G. diazotrophicus* to high sucrose concentrations. Thus, although previous works demonstrate that *G. diazotrophicus* did not accumulate significant levels of compatible solutes (Hartmann *et al.*, 1991), our results show that proteins that participate in the synthesis of such compounds may have a crucial role in the resistance to high-sucrose in this bacterium.

The proteomic analyses also revealed the up-accumulation of proteins of the proteolytic system. Such activation may represent a bacterial response mechanism to hyperosmotic environments, leading to the accumulation of amino acids into the cytoplasm to act as compatible solutes (Piuri *et al.*, 2003; Le Marrec *et al.*, 2007). However, proteolytic systems also have a wide range of functions within bacterial cells, such as protein turnover and the release of free amino acids to support other metabolic processes. Our reverse genetic analysis revealed that the lack of PepN peptidase affects the resistance of *G. diazotrophicus* to high-sucrose. Such results justify further studies to explore the specific role of proteolytic pathways on bacterial resistance to high-sucrose.

MetE and MetF, two proteins involved in *de novo* methionine biosynthesis, were up-accumulated in our proteomic analyses. The last step of *de novo* methionine biosynthesis is catalyzed by either cobalamin (B12)-independent methionine synthase (MetE) or B12-dependent methionine synthase (MetH) (Weissbach and Brot, 1991). The assays with knockout mutants showed that the lack of MetH affects the resistance of *G.*

diazotrophicus to sucrose, even at the moderate sucrose concentration tested. So, the activity of MetE does not compensate for the lack of MetH under such conditions. The catalytic activity of MetH has been demonstrated to be more efficient than MetE (Gonzalez *et al.*, 1992; Matthews *et al.*, 2003). Reverse genetic analysis also demonstrates that the lack of IlvD, an essential component in the *de novo* branched-chain amino acids (BCAAs) biosynthesis, affects *G. diazotrophicus* even at the moderate sucrose concentration (300 mM). Although some amino acids are described as compatible solutes in bacteria, this is not the case of methionine and BCAAs. The metabolism of these amino acids is linked to bacterial central metabolism, which involves several essential processes, such as protein synthesis and DNA and RNA methylation (Ferla and Patrick, 2014; Amorim Franco and Blanchard, 2017). Thus, these results indicate that methionine and BCAAs have a key role in *G. diazotrophicus* resistance to high-sucrose, probably supporting bacterial central metabolism.

Table 2. *G. diazotrophicus* proteins up-accumulated in response to both sucrose and sugarcane co-cultivation

Accession	Description
A9H320	Bifunctional transaldolase/phosoglucose isomerase (Tal/Pgi)
A9H317	Transketolase (TktA)
A9H324	6-phosphogluconate dehydrogenase, decarboxylating (Gnd)
A9HGX3	Phosphoketolase
A9HL52	Gluconolactonase
A9H932	TonB-dependent receptor
A9GZJ4	Ketol-acid reductoisomerase (NADP(+)) (IlvC)
A9HNX4	5-methyltetrahydropteroyltriglutamate--homocysteine methyltransferase (MetE)
A9HFU5	M1 family metallopeptidase - aminopeptidase N (PepN)
A9HHS4	Large-conductance mechanosensitive channel (MscL)
A9HED6	OmpW family protein (OmpW)
A9H5P1	Bacteriocin protein
A9H9C0	Adenosine kinase
A9HAP4	Hypothetical protein

Lery et al. (2011) utilized the proteomics approach to explore the mechanisms regulated in *G. diazotrophicus* during the association with sugarcane. Comparing our

results with such proteomic data revealed 14 proteins that are regulated both in response to high-sucrose and during the association with sugarcane plants (Table 2). Among these proteins, nine belong to the functional pathways of sugar metabolism, nutrient uptake, amino acid metabolism, and proteolytic system, with an emphasis on TBDR, IlvC, MetE, and PepN. Our analysis using knockout mutants showed that such pathways are essential for *G. diazotrophicus* resistance to high-sucrose. Thus, these results highlight that resistance to high-sucrose is a crucial component of the mechanisms activated by *G. diazotrophicus* during its association with sugar-rich plant hosts.

The main *G. diazotrophicus* mechanisms of response to high-sucrose, revealed by proteomic and reverse genetic analyses, are summarized in a schematic illustration (Fig. 5). We propose that high-sucrose strongly activates the glycolysis pathway of *G. diazotrophicus* to metabolize the excess of sugar that entered the cell, leading to the production of gluconic acid and the oxidation of ethanol. Moreover, *G. diazotrophicus* turns down the accumulation of proteins related to nutrients uptake to avoid the excess of sugar entrance into bacterial cells. *G. diazotrophicus* activates the *de novo* synthesis of compatible solutes to adjust its osmotic balance. The activation of the proteolytic system may represent a strategy to release amino acids within bacterial cells. *G. diazotrophicus* also activates the *de novo* synthesis of methionine and BCAAs, from bacterial central metabolism, which involves protein synthesis and the regulation of DNA and RNA.

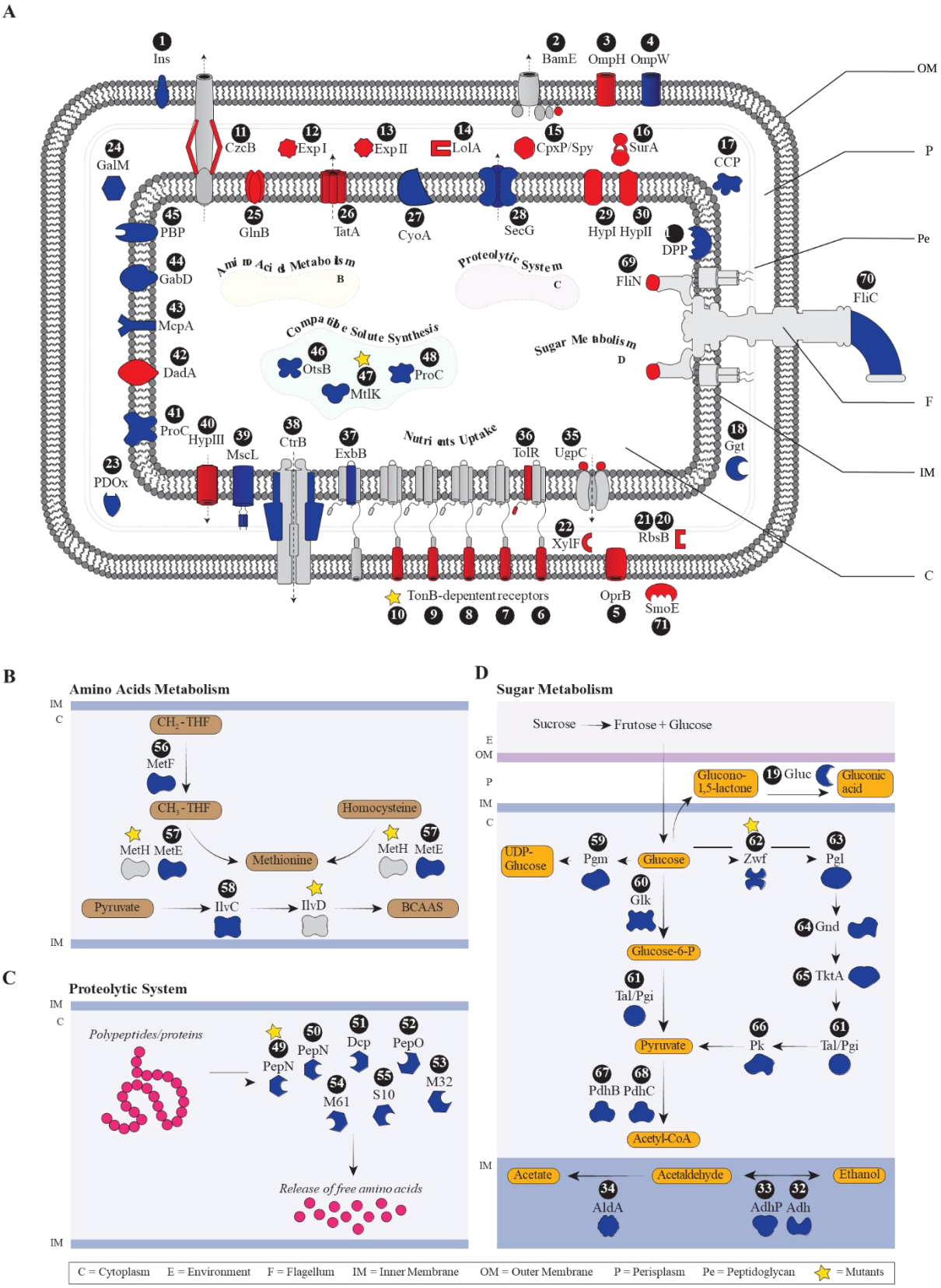

Fig. 5 Schematic illustration of the main responses of *G. diazotrophicus* to high-sugar. Red and blue forms represent proteins classified as down-accumulated and up-accumulated, respectively, and grey forms represent non-regulated proteins (A). Cytoplasmic functional groups with more than three proteins were separately illustrated (B, C, D).

Taken together, our results identified molecular mechanisms of *G. diazotrophicus* resistance to high-sucrose, shedding light on two ways of metabolic response that are related to osmotolerance and the metabolism of the excess of sugar. These findings contribute to understanding the resistance to high-sugar in bacteria and open new perspectives for the understanding of its association with sugar-rich hosts.

4.5 Materials and methods

4.5.1 Stock preparation of bacterial strains

G. diazotrophicus PAL5 wild-type strain used in this study was obtained in the culture collection of the Universidade Estadual do Norte Fluminense Darcy Ribeiro (UENF, Campos dos Goytacazes, Rio de Janeiro State, Brazil). The knockout mutants of *G. diazotrophicus* PAL5, defective in the synthesis of proteins Zwf (A9HEX0 - Δ*zwf*), MtlK (A9HBL5 - Δ*mtlK*), PepN (A9HEL6 - Δ*pepN*), MetH (A9HFG3 - Δ*metH*), IlvD (A9HA40 - Δ*ilvD*), and a TonB-dependent receptor (A9HNM4 - Δ*tbdr*), were obtained from the "*G. diazotrophicus* PAL5 Tn5 insertion mutant library" of the Laboratório de Biotecnologia - UENF (Aline C. Intorne *et al.*, 2009). Stock cultures were prepared as previously described (Oliveira et al., 2016) and samples were stored in 25% glycerol at -80°C.

4.5.2 High-sucrose exposure assays

Osmotic stress was performed as previously described (Oliveira et al., 2016) with some modifications. Specifically, the sucrose (Sucrose for molecular biology, Sigma Chemical Co., St. Louis, MO, USA) stock solutions were previously prepared at a concentration twice the desired final concentration and autoclaved. Strains were grown in DYGS medium (in g/L: glucose:2; yeast extract: 2; peptone: 1.5; glutamic acid:1.3; K_2HPO_4: 0.5; $MgSO_4.7H_2O$: 0.5; pH 6.0) until OD_{600} of 1.0. After centrifugation, the cells were suspended into 2X DYGS at OD_{600} 0.2, and 25 mL was mixed with an equal volume of sucrose stock solutions and incubated under stirring (250 rpm min^{-1}, 30 °C). OD_{600} measurements were performed after 12 h, and 2 mL aliquots were kept for microscopy analysis

4.5.3 Microscopy analyses

2 mL of cell culture of *G. diazotrophicus* submitted to different sucrose concentrations were centrifuged (3 min; 10.000 g; 25 °C), and the resultant pellets were washed three times with saline solution [0.85% (w/v) NaCl]. 100 µL of 0.8% (w/v) agarose were added in the center of the glass slides before adding bacterial cells.

For morphological analysis, 5 µL of each washed bacterial suspension was applied onto the solidified agarose in the glass slides, covered with coverslips, and observed in the microscope (Carl Zeiss Axion Imager A.2 Microscope). To capture the images, the software Carl Zeiss Axion Vision Software 4.8.2 was used.

The washed cells were stained for cell viability analysis using the Live/Dead Bacterial Viability Kit (*Bac*LightTM, Thermo Fisher Scientific, U.S.), following fabricant recommendations. After staining, 5 µL of each bacterial suspension was applied onto the solidified agarose in the glass slides, covered with coverslips, and observed in the microscope (Carl Zeiss Axion Imager A.2 Microscope). Six fields of glass slides per treatment were used to count live and dead bacterial cells.

4.5.4 Protein extraction

Three biological samples of *G. diazotrophicus* cells, exposed and non-exposed (control) to 600 mM sucrose, were used for protein extract preparation. Each sample corresponded to each treatment sample (20 mL). The extraction methods were performed as previously described (Damerval *et al.*, 1986), and the final protein concentration of each sample was estimated with 2-D Quant Kit (2-D Quant Kit - G.E. Healthcare Life Sciences).

4.5.5 Protein digestion and mass spectrometry analysis

Protein digestion was performed as previously described (Passamani *et al.*, 2018). After digestion, the samples were transferred to Total Recovery Vials (Waters), and peptide/sample (1 µg) was used for mass spectrometry analysis. Afterward, a nanoAcquity UPLC connected to a Synapt G2-Si HDMS mass spectrometer (Waters) was used for the ESI-LC-MS/MS analyses performed as previously described [24].

4.5.6 Proteomic data analyses

For spectral processing and database searching, the software ProteinLynx Global Server (PLGS; version 3.0.2) and ISOQuant were used. The spectral processing on PLGS software was performed with previously described settings (Leandro *et al.*, 2020). The proteomics data were processed against the *G. diazotrophicus* RIOGENE proteome database (www.uniprot.org/proteomes/UP000001176).

The analysis of comparative label-free quantification was performed with ISOQuant software with previously described settings and algorithms (Distler *et al.*, 2014, 2016). The TOP3 identification was used to perform label-free quantification, with the multidimensional normalization process implemented within ISOQuant. The detailed ISOQuant processing parameters configuration is provided in Table S1.

After ISOQuant analysis, only the proteins present or absent (for unique proteins) in all three biological samples were selected for differential abundance analysis. The data were analyzed using Student's t-test (two-tailed). Differentially accumulated proteins (DAPs) ($P < 0.05$) were considered up-accumulated if the fold change (F.C.) was higher than 1.5 and down-accumulated if the F.C. was lesser than 0.667.

The prediction of the subcellular localization (outer membrane, periplasm, cytoplasmic membrane, or cytoplasm) of the identified DAPs was performed using

FUEL-mLoc software (http://bioinfo.eie.polyu.edu.hk/FUEL-mLoc/). Additionally, DAPs were manually categorized into protein functional groups based on the information available in the literature.

4.5.7 Reverse genetics analysis

Reverse genetics analysis was performed by the inoculation of 5 mL of cells from glycerol stocks of *G. diazotrophicus* wild-type and insertional mutant strains in 45 mL of LGI medium (1L: 5 g sucrose; 0.2 g K_2HPO_4; 0.6 g KH_2PO_4; 0.2 g $MgSO_4.7H_2O$; 0.02 g $CaCl_2.2H_2O$; 0.002 g $Na_2MoO_4.2H_2O$; 0.01 g $FeCl_3$; pH 6.0) (Vladimir A. Cavalcante and Dobereiner, 1988) within Erlenmeyer flasks (250 mL). After that, cultures were grown under constant stirring (250 rpm min^{-1}, 30 °C) until they reached OD_{600nm} 1.0. Then, cultures were arranged on a 96-well microplate and plated on LGI solid medium supplemented with sucrose with a 96-pin replicator (Boekel, Fisher Scientific, Pittsburgh, PA, USA). The plates were maintained at 30 °C for five days. Then, results were registered.

4.6 References

Alvarez, B., Martinez-Drets, G., 1995. Metabolic characterization of Acetobacter diazotrophicus. Can. J. Microbiol. https://doi.org/10.1139/m95-126

Amorim Franco, T.M., Blanchard, J.S., 2017. Bacterial Branched-Chain Amino Acid Biosynthesis: Structures, Mechanisms, and Drugability. Biochemistry. https://doi.org/10.1021/acs.biochem.7b00849

Bertalan, M., Albano, R., de Pádua, V., Rouws, L., Rojas, C., Hemerly, A., Teixeira, K., Schwab, S., Araujo, J., Oliveira, A., França, L., Magalhães, V., Alquéres, S., Cardoso, A., Almeida, W., Loureiro, M., Nogueira, E., Cidade, D., Oliveira, D., Simão, T., Macedo, Jacyara, Valadão, A., Dreschsel, M., Freitas, F., Vidal, M., Guedes, H., Rodrigues, E., Meneses, C., Brioso, P., Pozzer, L., Figueiredo, D., Montano, H., Junior, J., de Souza Filho, G., Martin Quintana Flores, V., Ferreira, B., Branco, A., Gonzalez, P., Guillobel, H., Lemos, M., Seibel, L., Macedo, José, Alves-Ferreira, M., Sachetto-Martins, G., Coelho, A., Santos, E., Amaral, G., Neves, A., Pacheco, A., Carvalho, D., Lery, L., Bisch, P., Rössle, S.C., Ürményi, T., Rael Pereira, A., Silva, R., Rondinelli, E., von Krüger, W., Martins, O., Baldani, J., Ferreira, P.C., 2009. Complete genome sequence of the sugarcane nitrogen-fixing endophyte Gluconacetobacter diazotrophicus Pal5. BMC Genomics 10, 450. https://doi.org/10.1186/1471-2164-10-450

Bremer, E., Krämer, R., 2019. Responses of microorganisms to osmotic stress. Annu. Rev. Microbiol. https://doi.org/10.1146/annurev-micro-020518-115504

Cavalcante, V.A., Dobereiner, J., 1988. A new acid-tolerant nitrogen-fixing bacterium associated with sugarcane. Plant Soil 108, 23–31. https://doi.org/10.1007/BF02370096

Damerval, C., De Vienne, D., Zivy, M., Thiellement, H., 1986. Technical improvements in two-dimensional electrophoresis increase the level of genetic variation detected in wheat-seedling proteins. Electrophoresis 7, 52–54. https://doi.org/10.1002/elps.1150070108

de Oliveira, M.V. V., Intorne, A.C., Vespoli, L. de S., Andrade, L.F., Pereira, L. de M., Rangel, P.L., de Souza Filho, G.A., 2017. Essential role of K+ uptake permease (Kup) for resistance to sucrose-induced stress in Gluconacetobacter diazotrophicus PAl 5. Environ. Microbiol. Rep. 9, 85–90. https://doi.org/10.1111/1758-2229.12503

De Oliveira, M.V. V., Intorne, A.C., Vespoli, L. de S., Madureira, H.C., Leandro, M.R., Pereira, T.N.S., Olivares, F.L., Berbert-Molina, M.A., De Souza Filho, G.A., 2016. Differential effects of salinity and osmotic stress on the plant growth-promoting bacterium Gluconacetobacter diazotrophicus PAL5. Arch. Microbiol. 198, 287–294. https://doi.org/10.1007/s00203-015-1176-2

Distler, U., Kuharev, J., Navarro, P., Levin, Y., Schild, H., Tenzer, S., 2014. Drift time-specific collision energies enable deep-coverage data-independent acquisition proteomics. Nat. Methods 11, 167–170. https://doi.org/10.1038/nmeth.2767

Distler, U., Kuharev, J., Navarro, P., Tenzer, S., 2016. Label-free quantification in ion mobility-enhanced data-independent acquisition proteomics. Nat. Protoc. 11, 795–812. https://doi.org/10.1038/nprot.2016.042

Esbelin, J., Santos, T., Hébraud, M., 2018. Desiccation: An environmental and food industry stress that bacteria commonly face. Food Microbiol. https://doi.org/10.1016/j.fm.2017.07.017

Ferla, M.P., Patrick, W.M., 2014. Bacterial methionine biosynthesis. Microbiol. (United Kingdom). https://doi.org/10.1099/mic.0.077826-0

Gonzalez, J.C., Banerjee, R. V., Huang, S., Sumner, J.S., Matthews, R.G., 1992. Comparison of Cobalamin-independent and Cobalamin-Dependent Methionine Synthases from Escherichia coli : Two Solutions to the Same Chemical Problem. Biochemistry. https://doi.org/10.1021/bi00141a013

Hartmann, A., Prabhu, S.R., Galinski, E.A., 1991. Osmotolerance of diazotrophic rhizosphere bacteria. Plant Soil. https://doi.org/10.1007/BF02187440

Intorne, A.C., de Oliveira, M.V. V., Lima, M.L., da Silva, J.F., Olivares, F.L., de Souza Filho, G.A., 2009. Identification and characterization of Gluconacetobacter diazotrophicus mutants defective in the solubilization of phosphorus and zinc. Arch. Microbiol. 191, 477–483. https://doi.org/10.1007/s00203-009-0472-0

Le Marrec, C., Bon, E., Lonvaud-Funel, A., 2007. Tolerance to high osmolality of the lactic acid bacterium Oenococcus oeni and identification of potential osmoprotectants. Int. J. Food Microbiol. 115, 335–342. https://doi.org/10.1016/j.ijfoodmicro.2006.12.039

Leandro, M., Andrade, L., Vespoli, L., Moreira, J., Pimentel, V., Soares, F., Passamani, L., Silveira, V., de Souza Filho, G., 2020. Comparative proteomics reveals essential mechanisms for osmotolerance in Gluconacetobacter diazotrophicus. Res. Microbiol. https://doi.org/10.1016/j.resmic.2020.09.005

Lievens, B., Hallsworth, J.E., Pozo, M.I., Belgacem, Z. Ben, Stevenson, A., Willems, K.A., Jacquemyn, H., 2015. Microbiology of sugar-rich environments: Diversity, ecology and system constraints. Environ. Microbiol. https://doi.org/10.1111/1462-2920.12570

Luna, M.F., Galar, M.L., Aprea, J., Molinari, M.L., Boiardi, J.L., 2010. Colonization of sorghum and wheat by seed inoculation with Gluconacetobacter diazotrophicus. Biotechnol. Lett. 32, 1071–1076. https://doi.org/10.1007/s10529-010-0256-2

Madhaiyan, M., Saravanan, V.S., Jovi, D.B.S.S., Lee, H., Thenmozhi, R., Hari, K., Sa, T., 2004. Occurrence of Gluconacetobacter diazotrophicus in tropical and subtropical plants of Western Ghats, India. Microbiol. Res. 159, 233–243. https://doi.org/10.1016/j.micres.2004.04.001

Matthews, R.G., Smith, A.E., Zhou, Z.S., Taurog, R.E., Bandarian, V., Evans, J.C., Ludwig, M., 2003. Cobalamin-Dependent and Cobalamin-Independent Methionine Synthases: Are There Two Solutions to the Same Chemical Problem? Helv. Chim. Acta. https://doi.org/10.1002/hlca.200390329

Passamani, L.Z., Bertolazi, A.A., Ramos, A.C., Santa-Catarina, C., Thelen, J.J., Silveira, V., 2018. Embryogenic Competence Acquisition in Sugar Cane Callus Is Associated with Differential H+-Pump Abundance and Activity. J. Proteome Res. 17, 2767–2779. https://doi.org/10.1021/acs.jproteome.8b00213

Pedraza, R.O., 2008. Recent advances in nitrogen-fixing acetic acid bacteria. Int. J. Food Microbiol. https://doi.org/10.1016/j.ijfoodmicro.2007.11.079

Piuri, M., Sanchez-Rivas, C., Ruzal, S.M., 2003. Adaptation to high salt in Lactobacillus: role of peptides and proteolytic enzymes. J. Appl. Microbiol. 95, 372–379. https://doi.org/10.1046/j.1365-2672.2003.01971.x

Rodrigues, E.P., Soares, C. de P., Galvão, P.G., Imada, E.L., Simões-Araújo, J.L., Rouws, L.F.M., de Oliveira, A.L.M., Vidal, M.S., Baldani, J.I., 2016. Identification of genes involved in indole-3-acetic acid biosynthesis by Gluconacetobacter diazotrophicus PAL5

strain using transposon mutagenesis. Front. Microbiol. https://doi.org/10.3389/fmicb.2016.01572

Saavedra, L., Sesma, F., 2005. Atypical genetic locus associated with the zwf gene encoding the glucose 6-phosphate dehydrogenase from Enterococcus mundtii CRL35. Curr. Microbiol. https://doi.org/10.1007/s00284-004-4454-9

Saravanan, V.S., Madhaiyan, M., Thangaraju, M., 2007. Solubilization of zinc compounds by the diazotrophic, plant growth promoting bacterium Gluconacetobacter diazotrophicus. Chemosphere 66, 1794–1798. https://doi.org/10.1016/j.chemosphere.2006.07.067

Stevenson, A., Cray, J.A., Williams, J.P., Santos, R., Sahay, R., Neuenkirchen, N., McClure, C.D., Grant, I.R., Houghton, J.D., Quinn, J.P., Timson, D.J., Patil, S. V., Singhal, R.S., Antón, J., Dijksterhuis, J., Hocking, A.D., Lievens, B., Rangel, D.E.N., Voytek, M.A., Gunde-Cimerman, N., Oren, A., Timmis, K.N., McGenity, T.J., Hallsworth, J.E., 2015. Is there a common water-activity limit for the three domains of life. ISME J. https://doi.org/10.1038/ismej.2014.219

Weissbach, H., Brot, N., 1991. Regulation of methionine synthesis in Escherichia coli. Mol. Microbiol. https://doi.org/10.1111/j.1365-2958.1991.tb01905.x

5. CONCLUSIONS

In the present work, we aim to elucidate the molecular mechanisms regulated in *G. diazotrophicus* in response to different osmo-challenging conditions. As shown in Figure 3, although there are particularities of response to each osmo-challenging condition, there is a significant number of overlapping proteins and mechanisms regulated in *G. diazotrophicus*. The protein overlap is observed mainly between osmotic stress and salt stress responses, demonstrating a high degree of similarity between the molecular mechanisms regulated in *G. diazotrophicus* in response to both osmotic and salt stress. On the other hand, most proteins regulated in *G. diazotrophicus* response to high-sugar were unique to this condition, demonstrating that, although there is an osmotic challenge under this condition, most of the molecular responses are associated with other aspects inherent to a sugar-rich environment. It is important to highlight that *G. diazotrophicus* does not metabolize PEG or NaCl, but metabolize sucrose, producing organic acids and ethanol. Therefore, many of the molecular mechanisms that are unique to high-sucrose response may be associated with bacterial adaptation to sugar metabolism products. Moreover, the down-accumulation of proteins related to nutrients uptake in response to all conditions tested demonstrates that such a mechanism is one of the hallmarks of *G. diazotrophicus* response to osmo-challenging environments.

A

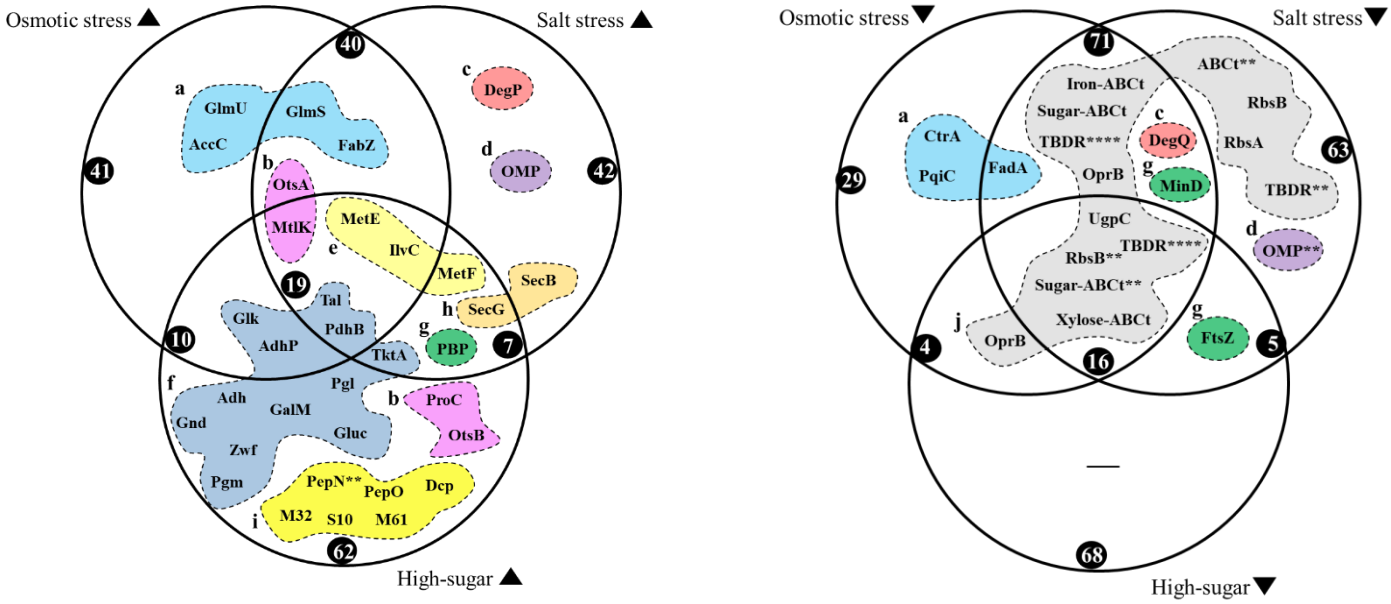

a – *Cel envelope metabolism* **b** – *Compatible solutes synthesis* **c** - *Protein quality control* **d** – *Efflux pump systems*

e – *Amino acids metabolism* **f** – *Sugar metabolism* **g** – *Cell division and elongation* **h** – *Protein export*

i – *Preoteolytic system* **j** – *Nutrients uptake*

B

Table 1. Essential genes to tolerance to osmo-challenging environments in *G. diazotrophicus*

	Osmotic stress	Salt stress	High-sugar
Δ*accC*	*	**n.r.**	**n.r.**
Δ*degP*	**n.r.**	*	**n.r.**
Δ*ilvD*	**n.r.**	**n.r.**	*
Δ*metH*	**n.r.**	**n.r.**	*
Δ*mtlK*	*	*	*
Δ*otsA*	*	-	**n.r.**
Δ*pepN*	**n.r.**	**n.r.**	*
Δ*oprB*	*	*	-
Δ*tbdr*	*	*	*
Δ*zwf*	**n.r.**	**n.r.**	*

* essential; - not essential; **nr** non-regulated on proteomic analysis

Fig. 3 Integrated overview of molecular responses of *G. diazotrophicus* to different osmo-challenging conditions. (A) Venny diagram of proteins up- (▲) and down-accumulated (▼) in response to osmotic stress, salt stress and high-sugar. The numbers inside black circles indicate the number of proteins regulated. Proteins inside dotted forms compose functional pathways

highlighted in our proteomic analyses. Asterisks indicate number of homologous proteins regulated. Colors indicate different functional pathway groups (B) The responses to osmotic stress, salt stress and high-sugar of the knock-out mutants related to functional pathways highlighted in our proteomic analyses were compared and disposed in a table.

There are also overlaps and specificities with the proteins that compose the functional pathways from *G. diazotrophicus* highlighted in our proteomic analyses (Fig. 3A). All the three osmo-challenging conditions tested in the present work led to the activation of proteins related to compatible solute synthesis. MtlK, related to mannitol synthesis, was the only protein from this functional pathway regulated in common between all the three conditions. The mutagenesis analyses showed that *mtlK* is essential to *G. diazotrophicus* tolerance to osmotic stress, salt stress, and high-sugar (Fig. 3B). The up-accumulation of DegP, from protein quality control system and OMP, from efflux pump systems, were unique to bacterial response to salt stress. Similarly, the activation of the proteolytic system was unique to bacterial response to high-sugar (Fig. 3A). Therefore, the essential role of some genes varies according to the nature of the osmo-challenging condition. Our results highlight the essential role of *accC* to osmotic stress tolerance, *degP* to salt stress tolerance; and *pepN* and *zwf* to high-sugar tolerance in *G. diazotrophicus* (Fig. 3B).

The present work shed light on the molecular mechanisms of *G. diazotrophicus* that are specific to each osmo-challenging condition analyzed and those that are common among these. Moreover, our results point to essential genes of *G. diazotrophicus* tolerance to osmo-challenging environments, opening perspectives for its use in further genetic transfer to other species aiming to stress resistance improvement.

6. REFERENCES

Adesemoye, A.O., Torbert, H.A., and Kloepper, J.W. (2009) Plant growth-promoting rhizobacteria allow reduced application rates of chemical fertilizers. *Microb Ecol* **58**: 921–929.

Alvarez, B. and Martinez-Drets, G. (1995) Metabolic characterization of Acetobacter diazotrophicus. *Can J Microbiol*.

Amorim Franco, T.M. and Blanchard, J.S. (2017) Bacterial Branched-Chain Amino Acid Biosynthesis: Structures, Mechanisms, and Drugability. *Biochemistry* **56**: 5849–5865.

Barcarolo, M.V., Garavaglia, B.S., Thomas, L., Marondedze, C., Gehring, C., Gottig, N., and Ottado, J. (2019) Proteome changes and physiological adaptations of the phytopathogen Xanthomonas citri subsp. citri under salt stress and their implications for virulence. *FEMS Microbiol Ecol* **95**:.

Bednarska, N.G., Schymkowitz, J., Rousseau, F., and Van Eldere, J. (2013) Protein aggregation in bacteria: The thin boundary between functionality and toxicity. *Microbiol (United Kingdom)* **159**: 1795–1806.

Bertalan, M., Albano, R., de Pádua, V., Rouws, L., Rojas, C., Hemerly, A., et al. (2009) Complete genome sequence of the sugarcane nitrogen-fixing endophyte Gluconacetobacter diazotrophicus Pal5. *BMC Genomics* **10**: 450.

Boniolo, F.S., Rodrigues, R.C., Delatorre, E.O., da Silveira, M.M., Flores, V.M.Q., and Berbert-Molina, M.A. (2009) Glycine Betaine Enhances Growth of Nitrogen-Fixing Bacteria Gluconacetobacter diazotrophicus PAL5 Under Saline Stress Conditions. *Curr Microbiol* **59**: 593–599.

Bremer, E. and Krämer, R. (2019) Responses of microorganisms to osmotic stress. *Annu Rev Microbiol* **73**: 313–334.

Campbell, J.W. and Cronan, J.E. (2001) Bacterial Fatty Acid Biosynthesis: Targets for Antibacterial Drug Discovery. *Annu Rev Microbiol*.

Cavalcante, Vladimir A. and Dobereiner, J. (1988) A new acid-tolerant nitrogen-fixing bacterium associated with sugarcane. *Plant Soil* **108**: 23–31.

Cavalcante, Vladimir A and Dobereiner, J. (1988) A new acid-tolerant nitrogen-fixing bacterium associated with sugarcane. *Plant Soil* **108**: 23–31.

Cesari, A.B., Paulucci, N.S., Biasutti, M.A., Morales, G.M., and Dardanelli, M.S. (2018) Changes in the lipid composition of Bradyrhizobium cell envelope reveal a rapid response to water deficit involving lysophosphatidylethanolamine synthesis from phosphatidylethanolamine in outer membrane. *Res Microbiol*.

Chang, Z. (2016) The function of the DegP (HtrA) protein: Protease versus chaperone. *IUBMB Life* **68**: 904–907.

Clausen, T., Kaiser, M., Huber, R., and Ehrmann, M. (2011) HTRA proteases: Regulated proteolysis in protein quality control. *Nat Rev Mol Cell Biol* **12**: 152–162.

Conti, J., Viola, M.G., and Camberg, J.L. (2015) The bacterial cell division regulators MinD and MinC form polymers in the presence of nucleotide. *FEBS Lett* **589**: 201–206.

Csonka, L.N. (1989) Physiological and Genetic Responses of Bacteria to Osmotic Stress.

Damerval, C., De Vienne, D., Zivy, M., and Thiellement, H. (1986) Technical improvements in two-dimensional electrophoresis increase the level of genetic variation detected in wheat-seedling proteins. *Electrophoresis* **7**: 52–54.

Distler, U., Kuharev, J., Navarro, P., Levin, Y., Schild, H., and Tenzer, S. (2014) Drift time-specific collision energies enable deep-coverage data-independent acquisition

proteomics. *Nat Methods* **11**: 167–170.

Distler, U., Kuharev, J., Navarro, P., and Tenzer, S. (2016) Label-free quantification in ion mobility-enhanced data-independent acquisition proteomics. *Nat Protoc* **11**: 795–812.

Dong, Z., Mccully, M.E., and Canny, M.J. (1997) Does Acetobacter diazotrophicus Live and Move in the Xylem of Sugarcane Stems ? Anatomical and Physiological Data.

Ekiert, D.C., Bhabha, G., Isom, G.L., Greenan, G., Ovchinnikov, S., Henderson, I.R., et al. (2017) Architectures of Lipid Transport Systems for the Bacterial Outer Membrane. *Cell*.

Errington, J., Daniel, R.A., and Scheffers, D.-J. (2003) Cytokinesis in Bacteria. *Microbiol Mol Biol Rev*.

Esbelin, J., Santos, T., and Hébraud, M. (2018) Desiccation: An environmental and food industry stress that bacteria commonly face. *Food Microbiol* **69**: 82–88.

FAO-UN (2017) World fertilizer trends and outlook to 2020. *Food Agric Organ United Nations*.

FAO (1994) FAO IRRIGATION AND DRAINAGE PAPER: Water Quality for Agriculture.

Fenchel, T. and Finlay, B.J. (2004) The ubiquity of small species: Patterns of local and global diversity. *Bioscience* **54**: 777–784.

Ferla, M.P. and Patrick, W.M. (2014) Bacterial methionine biosynthesis. *Microbiol (United Kingdom)* **160**: 1571–1584.

Flannagan, R.S., Aubert, D., Kooi, C., Sokol, P.A., and Valvano, M.A. (2007) Burkholderia cenocepacia Requires a Periplasmic HtrA Protease for Growth under Thermal and Osmotic Stress and for Survival In Vivo †. *Infect Immun* **75**: 1679–

1689.

Fujita, Y., Matsuoka, H., and Hirooka, K. (2007) Regulation of fatty acid metabolism in bacteria. *Mol Microbiol*.

Ge, X., Wang, R., Ma, J., Liu, Y., Ezemaduka, A.N., Chen, P.R., et al. (2014) DegP primarily functions as a protease for the biogenesis of β-barrel outer membrane proteins in the Gram-negative bacterium *Escherichia coli*. *FEBS J* **281**: 1226–1240.

De Geyter, J., Tsirigotaki, A., Orfanoudaki, G., Zorzini, V., Economou, A., and Karamanou, S. (2016) Protein folding in the cell envelope of Escherichia coli. *Nat Microbiol* **1**:.

Ghai, I. and Ghai, S. (2017) Exploring bacterial outer membrane barrier to combat bad bugs. *Infect Drug Resist*.

Gonzalez, J.C., Banerjee, R. V., Huang, S., Sumner, J.S., and Matthews, R.G. (1992) Comparison of Cobalamin-independent and Cobalamin-Dependent Methionine Synthases from Escherichia coli : Two Solutions to the Same Chemical Problem. *Biochemistry*.

Griffiths, R.I., Whiteley, A.S., O'Donnell, A.G., and Bailey, M.J. (2003) Physiological and Community Responses of Established Grassland Bacterial Populations to Water Stress. *Appl Environ Microbiol*.

Hallsworth, J.E. (2018) Stress-free microbes lack vitality. *Fungal Biol*.

Hartmann, A., Prabhu, S.R., and Galinski, E.A. (1991) Osmotolerance of diazotrophic rhizosphere bacteria. *Plant Soil*.

Van Heijenoort, J. (2001) Recent advances in the formation of the bacterial peptidoglycan monomer unit. *Nat Prod Rep* **18**: 503–519.

Held, C. and Sadowski, G. (2016) Compatible solutes: Thermodynamic properties

relevant for effective protection against osmotic stress. *Fluid Phase Equilib* **407**: 224–235.

Hoffmann, T., Schütz, A., Brosius, M., Völker, A., Völker, U., and Bremer, E. (2002) High-salinity-induced iron limitation in Bacillus subtilis. *J Bacteriol*.

Hoyer, J., Bartel, J., Gómez-Mejia, A., Rohde, M., Hirschfeld, C., Heß, N., et al. (2018) Proteomic response of Streptococcus pneumoniae to iron limitation. *Int J Med Microbiol* **308**: 713–721.

Intorne, Aline C, De Oliveira, M. V V, Lima, M.L., da Silva, J.F., Olivares, F.L., de Souza Filho, G.A., et al. (2009) Identification and characterization of *Gluconacetobacter diazotrophicus* mutants defective in the solubilization of phosphorus and zinc. *Arch Microbiol* **191**: 477–483.

Intorne, Aline C., de Oliveira, M.V. V., Lima, M.L., da Silva, J.F., Olivares, F.L., and de Souza Filho, G.A. (2009) Identification and characterization of Gluconacetobacter diazotrophicus mutants defective in the solubilization of phosphorus and zinc. *Arch Microbiol* **191**: 477–483.

Iordachescu, M. and Imai, R. (2008) Trehalose Biosynthesis in Response to Abiotic Stresses. *J Integr Plant Biol* **50**: 1223–1229.

Itelima, Bang, W.J., Onyimba, I.A., Sila, and Egbere, O.J. (2018) Bio-fertilizers as key player in enhancing soil fertility and crop productivity: A Review. **6**: 73–83.

Jimenez-Salgado, T., Fuentes-Ramirez, L.E., Tapia-Hernandez, A., Mascarua-Esparza, M.A., Martinez-Romero, E., and Caballero-Mellado, J. (1997) Coffea arabica L., a new host plant for Acetobacter diazotrophicus, and isolation of other nitrogen-fixing acetobacteria. *Appl Environ Microbiol*.

Justice, S.S., Hunstad, D.A., Cegelski, L., and Hultgren, S.J. (2008) Morphological plasticity as a bacterial survival strategy. *Nat Rev Microbiol* **6**: 162–168.

Karimzadeh, J., Alikhani, H.A., Etesami, H., and Pourbabaei, A.A. (2020) Improved Phosphorus Uptake by Wheat Plant (Triticum aestivum L.) with Rhizosphere Fluorescent Pseudomonads Strains Under Water-Deficit Stress. *J Plant Growth Regul*.

Kudva, R., Denks, K., Kuhn, P., Vogt, A., Müller, M., and Koch, H.-G. (2013) Protein translocation across the inner membrane of Gram-negative bacteria: the Sec and Tat dependent protein transport pathways. *Res Microbiol* **164**: 505–534.

Larue, K., Ford, R.C., Willis, L.M., and Whitfield, C. (2011) Functional and structural characterization of polysaccharide co-polymerase proteins required for polymer export in ATP-binding cassette transporter-dependent capsule biosynthesis pathways. *J Biol Chem*.

Leandro, M., Andrade, L., Vespoli, L., Moreira, J., Pimentel, V., Soares, F., et al. (2020) Comparative proteomics reveals essential mechanisms for osmotolerance in Gluconacetobacter diazotrophicus. *Res Microbiol*.

Lennen, R.M. and Pfleger, B.F. (2012) Engineering Escherichia coli to synthesize free fatty acids. *Trends Biotechnol*.

Levin, P.A., Shim, J.J., and Grossman, A.D. (1998) Effect of minCD on FtsZ ring position and polar septation in Bacillus subtilis. *J Bacteriol*.

Lievens, B., Hallsworth, J.E., Pozo, M.I., Belgacem, Z. Ben, Stevenson, A., Willems, K.A., and Jacquemyn, H. (2015) Microbiology of sugar-rich environments: Diversity, ecology and system constraints. *Environ Microbiol*.

Loffhagen, N., Härtig, C., Benndorf, D., and Babel, W. (2002) Effects of Growth Temperature and Lipophilic Carbon Sources on the Fatty Acid Composition and Membrane Lipid Fluidity of Acinetobacter calcoaceticus 69V. *Acta Biotechnol* **22**: 235–243.

Luna, M.F., Galar, M.L., Aprea, J., Molinari, M.L., and Boiardi, J.L. (2010) Colonization of sorghum and wheat by seed inoculation with Gluconacetobacter diazotrophicus. *Biotechnol Lett* **32**: 1071–1076.

Lyu, Z.X. and Zhao, X.S. (2015) Periplasmic quality control in biogenesis of outer membrane proteins. *Biochem Soc Trans* **43**: 133–138.

Madhaiyan, M., Saravanan, V.S., Jovi, D.B.S.S., Lee, H., Thenmozhi, R., Hari, K., and Sa, T. (2004) Occurrence of Gluconacetobacter diazotrophicus in tropical and subtropical plants of Western Ghats, India. *Microbiol Res* **159**: 233–243.

Magnuson, K., Jackowski, S., Rock, C.O., and Cronan, J.E. (1993) Regulation of fatty acid biosynthesis in Escherichia coli. *Microbiol Rev*.

Le Marrec, C., Bon, E., and Lonvaud-Funel, A. (2007) Tolerance to high osmolality of the lactic acid bacterium Oenococcus oeni and identification of potential osmoprotectants. *Int J Food Microbiol* **115**: 335–342.

Martinez, J.L., Sánchez, M.B., Martínez-Solano, L., Hernandez, A., Garmendia, L., Fajardo, A., and Alvarez-Ortega, C. (2009) Functional role of bacterial multidrug efflux pumps in microbial natural ecosystems. *FEMS Microbiol Rev*.

Mas, G., Thoma, J., and Hiller, S. (2019) The Periplasmic Chaperones Skp and SurA. In, *Subcellular Biochemistry*. Springer New York, pp. 169–186.

Masi, M., Réfregiers, M., Pos, K.M., and Pagès, J.M. (2017) Mechanisms of envelope permeability and antibiotic influx and efflux in Gram-negative bacteria. *Nat Microbiol*.

Matthews, R.G., Smith, A.E., Zhou, Z.S., Taurog, R.E., Bandarian, V., Evans, J.C., and Ludwig, M. (2003) Cobalamin-Dependent and Cobalamin-Independent Methionine Synthases: Are There Two Solutions to the Same Chemical Problem? *Helv Chim Acta*.

Miller, K.J. and Wood, J.M. (1996) Osmoadaptation by rhizosphere bacteria. *Annu Rev Microbiol*.

Mitchell, A.M. and Silhavy, T.J. (2019) Envelope stress responses: balancing damage repair and toxicity. *Nat Rev Microbiol* **17**: 417–428.

Murínová, S. and Dercová, K. (2014) Response mechanisms of bacterial degraders to environmental contaminants on the level of cell walls and cytoplasmic membrane. *Int J Microbiol*.

Nikaido, H. (2003) Molecular Basis of Bacterial Outer Membrane Permeability Revisited. *Microbiol Mol Biol Rev*.

de Oliveira, M.V. V., Intorne, A.C., Vespoli, L. de S., Andrade, L.F., Pereira, L. de M., Rangel, P.L., and de Souza Filho, G.A. (2017) Essential role of K+ uptake permease (Kup) for resistance to sucrose-induced stress in *Gluconacetobacter diazotrophicus* PAl 5. *Environ Microbiol Rep* **9**: 85–90.

De Oliveira, M.V. V., Intorne, A.C., Vespoli, L. de S., Madureira, H.C., Leandro, M.R., Pereira, T.N.S., et al. (2016) Differential effects of salinity and osmotic stress on the plant growth-promoting bacterium Gluconacetobacter diazotrophicus PAL5. *Arch Microbiol* **198**: 287–294.

Ortiz, M.E., Bleckwedel, J., Fadda, S., Picariello, G., Hebert, E.M., Raya, R.R., and Mozzi, F. (2017) Global Analysis of Mannitol 2-Dehydrogenase in Lactobacillus reuteri CRL 1101 during Mannitol Production through Enzymatic, Genetic and Proteomic Approaches. *PLoS One* **12**: e0169441.

Passamani, L.Z., Bertolazi, A.A., Ramos, A.C., Santa-Catarina, C., Thelen, J.J., and Silveira, V. (2018) Embryogenic Competence Acquisition in Sugar Cane Callus Is Associated with Differential H+-Pump Abundance and Activity. *J Proteome Res* **17**: 2767–2779.

Paul, D. (2013) Osmotic stress adaptations in rhizobacteria. *J Basic Microbiol* **53**: 101–110.

de Paula Soares, C., Rodrigues, E.P., de Paula Ferreira, J., Simões Araújo, J.L., Rouws, L.F.M., Baldani, J.I., and Vidal, M.S. (2015) Tn5 insertion in the tonB gene promoter affects iron-related phenotypes and increases extracellular siderophore levels in Gluconacetobacter diazotrophicus. *Arch Microbiol* **197**: 223–233.

Pedraza, R.O. (2008) Recent advances in nitrogen-fixing acetic acid bacteria. *Int J Food Microbiol*.

Piuri, M., Sanchez-Rivas, C., and Ruzal, S.M. (2003) Adaptation to high salt in Lactobacillus: role of peptides and proteolytic enzymes. *J Appl Microbiol* **95**: 372–379.

Popham, D.L. and Young, K.D. (2003a) Role of penicillin-binding proteins in bacterial cell morphogenesis. *Curr Opin Microbiol* **6**: 594–599.

Popham, D.L. and Young, K.D. (2003b) Role of penicillin-binding proteins in bacterial cell morphogenesis. *Curr Opin Microbiol* **6**: 594–599.

Rodrigues, E.P., Soares, C. de P., Galvão, P.G., Imada, E.L., Simões-Araújo, J.L., Rouws, L.F.M., et al. (2016) Identification of genes involved in indole-3-acetic acid biosynthesis by Gluconacetobacter diazotrophicus PAL5 strain using transposon mutagenesis. *Front Microbiol*.

Rodrigues Neto, J., Malavolta, J.R.V.A., and Victor, O. (1986) Meio simples para o isolamento e cultivo de Xanthomonas campestris pv. Citri TIPO B. *Suma Phytopathol* **12**: 16.

Rollauer, S.E., Sooreshjani, M.A., Noinaj, N., and Buchanan, S.K. (2015) Outer membrane protein biogenesis in Gram-negative bacteria. *Philos Trans R Soc B Biol Sci* **370**: 20150023.

Saavedra, L. and Sesma, F. (2005) Atypical genetic locus associated with the zwf gene encoding the glucose 6-phosphate dehydrogenase from Enterococcus mundtii CRL35. *Curr Microbiol*.

Saravanan, V.S., Madhaiyan, M., Osborne, J., Thangaraju, M., and Sa, T.M. (2008) Ecological Occurrence of Gluconacetobacter diazotrophicus and Nitrogen-fixing Acetobacteraceae Members: Their Possible Role in Plant Growth Promotion. *Microb Ecol* **55**: 130–140.

Saravanan, V.S., Madhaiyan, M., and Thangaraju, M. (2007) Solubilization of zinc compounds by the diazotrophic, plant growth promoting bacterium Gluconacetobacter diazotrophicus. *Chemosphere* **66**: 1794–1798.

Saulou-Bérion, C., Gonzalez, I., Enjalbert, B., Audinot, J.-N., Fourquaux, I., Jamme, F., et al. (2015) Escherichia coli under Ionic Silver Stress: An Integrative Approach to Explore Transcriptional, Physiological and Biochemical Responses. *PLoS One* **10**: e0145748.

Shabala, L., Bowman, J., Brown, J., Ross, T., McMeekin, T., and Shabala, S. (2009) Ion transport and osmotic adjustment in Escherichia coli in response to ionic and non-ionic osmotica. *Environ Microbiol* **11**: 137–148.

de Souza, R., Ambrosini, A., and Passaglia, L.M.P. (2015) Plant growth-promoting bacteria as inoculants in agricultural soils. *Genet Mol Biol*.

Spiess, C., Beil, A., and Ehrmann, M. (1999) A temperature-dependent switch from chaperone to protease in a widely conserved heat shock protein. *Cell* **97**: 339–347.

Stenberg, F., Chovanec, P., Maslen, S.L., Robinson, C. V., Ilag, L.L., Von Heijne, G., and Daley, D.O. (2005) Protein complexes of the Escherichia coli cell envelope. *J Biol Chem*.

Stevenson, A., Cray, J.A., Williams, J.P., Santos, R., Sahay, R., Neuenkirchen, N., et al.

(2015) Is there a common water-activity limit for the three domains of life. *ISME J*.

Stevenson, A. and Hallsworth, J.E. (2014) Water and temperature relations of soil Actinobacteria. *Environ Microbiol Rep*.

Sugawara, M., Cytryn, E.J., and Sadowsky, M.J. (2010) Functional role of Bradyrhizobium japonicum trehalose biosynthesis and metabolism genes during physiological stress and nodulation. *Appl Environ Microbiol*.

Tang, J., Jia, J., Chen, Y., Huang, X., Zhang, X., Zhao, L., et al. (2018) Proteomic Analysis of Vibrio parahaemolyticus Under Cold Stress. *Curr Microbiol* **75**: 20–26.

Tapia-Hernández, A., Bustillos-Cristales, M.R., Jiménez-Salgado, T., Caballero-Mellado, J., and Fuentes-Ramírez, L.E. (2000) Natural endophytic occurrence of Acetobacter diazotrophicus in pineapple plants. *Microb Ecol*.

Tejera, N.A., Ortega, E., Gonzalez-Lopez, J., and Lluch, C. (2003) Effect of some abiotic factors on the biological activity of Gluconacetobacter diazotrophicus. *J Appl Microbiol* **95**: 528–535.

Tejera, Noel A., Ortega, E., González-López, J., and Lluch, C. (2003) Effect of some abiotic factors on the biological activity of Gluconacetobacter diazotrophicus. *J Appl Microbiol* **95**: 528–535.

Trček, J., Jernejc, K., and Matsushita, K. (2007) The highly tolerant acetic acid bacterium Gluconacetobacter europaeus adapts to the presence of acetic acid by changes in lipid composition, morphological properties and PQQ-dependent ADH expression. *Extremophiles* **11**: 627–635.

Velázquez-Hernández, M.L., Baizabal-Aguirre, V.M., Cruz-Vázquez, F., Trejo-Contreras, M.J., Fuentes-Ramírez, L.E., Bravo-Patiño, A., et al. (2011) Gluconacetobacter diazotrophicus levansucrase is involved in tolerance to NaCl,

sucrose and desiccation, and in biofilm formation. *Arch Microbiol* **193**: 137–149.

Vriezen, J.A.C., De Bruijn, F.J., and Nüsslein, K. (2007) Responses of rhizobia to desiccation in relation to osmotic stress, oxygen, and temperature. *Appl Environ Microbiol*.

Watt, M., Silk, W.K., and Passioura, J.B. (2006) Rates of root and organism growth, soil conditions, and temporal and spatial development of the rhizosphere. In, *Annals of Botany*.

Weissbach, H. and Brot, N. (1991) Regulation of methionine synthesis in Escherichia coli. *Mol Microbiol*.

Wonderling, L.D., Wilkinson, B.J., and Bayles, D.O. (2004) The htrA (degP) Gene of Listeria monocytogenes 10403S Is Essential for Optimal Growth under Stress Conditions. *Appl Environ Microbiol*.

Wood, J.M., Rosenthal, A.Z., Gralla, J., Greie, J.-C., Booth, I.R., and Altendorf, K. (2009) Osmotic Stress. *EcoSal Plus* **3**:.

Wright, B.W., Kamath, K.S., Krisp, C., and Molloy, M.P. (2019) Proteome profiling of Pseudomonas aeruginosa PAO1 identifies novel responders to copper stress. *BMC Microbiol* **19**: 69.

Yoon, Y., Lee, H., Lee, S., Kim, S., and Choi, K.H. (2015) Membrane fluidity-related adaptive response mechanisms of foodborne bacterial pathogens under environmental stresses. *Food Res Int*.

Zahid, N., Schweiger, P., Galinski, E., and Deppenmeier, U. (2015) Identification of mannitol as compatible solute in Gluconobacter oxydans. *Appl Microbiol Biotechnol* **99**: 5511–5521.

Zammit, C.M., Mangold, S., Rao Jonna, V., Mutch, L.A., Watling, H.R., Dopson, M., and Watkin, E.L.J. (2012) Bioleaching in brackish waters-effect of chloride ions on

the acidophile population and proteomes of model species. *Appl Microbiol Biotechnol* **93**: 319–329.

Zhang, S., Cheng, Y., Ma, J., Wang, Y., Chang, Z., and Fu, X. (2019) DegP degrades a wide range of substrate proteins in Escherichia coli under stress conditions. *Biochem J*.

Zhang, Y.M. and Rock, C.O. (2008) Membrane lipid homeostasis in bacteria. *Nat Rev Microbiol*.

7. SUPPLEMENTARY MATERIAL

7.1 Supplementary material from Chapter 1

Table S1 Detailed ISOQuant processing configuration

Parameter	Value
isoquant.pluginQueue.name	design project and run ISOQuant analysis
process.peptide.deplete.PEP_FRAG_2	false
process.peptide.deplete.CURATED_0	false
process.peptide.statistics.doSequenceSearch	false
process.emrt.minIntensity	1000
process.emrt.minMass	500
process.emrt.rt.alignment.match.maxDeltaMass.ppm	10
process.emrt.rt.alignment.match.maxDeltaDriftTime	2
process.emrt.rt.alignment.normalizeReferenceTime	false
process.emrt.rt.alignment.maxProcesses	8
process.emrt.rt.alignment.referenceRun.selectionMethod	AUTO
process.emrt.clustering.preclustering.orderSequence	MTMTMT
process.emrt.clustering.preclustering.maxDistance.mass.ppm	6.06E-6
process.emrt.clustering.preclustering.maxDistance.time.min	0,202
process.emrt.clustering.preclustering.maxDistance.drift	2,02
process.emrt.clustering.distance.unit.mass.ppm	6.0E-6
process.emrt.clustering.distance.unit.time.min	0,2
process.emrt.clustering.distance.unit.drift.bin	2
process.emrt.clustering.dbscan.minNeighborCount	2
process.identification.peptide.minReplicationRate	2
process.identification.peptide.minScore	6
process.identification.peptide.minOverallMaxScore	6
process.identification.peptide.minSequenceLength	6
process.identification.peptide.acceptType.PEP_FRAG_1	true
process.identification.peptide.acceptType.IN_SOURCE	false
process.identification.peptide.acceptType.MISSING_CLEAVAGE	true
process.identification.peptide.acceptType.NEUTRAL_LOSS_H20	false
process.identification.peptide.acceptType.NEUTRAL_LOSS_NH3	false
process.identification.peptide.acceptType.PEP_FRAG_2	true
process.identification.peptide.acceptType.DDA	false
process.identification.peptide.acceptType.VAR_MOD	true
process.identification.peptide.acceptType.PTM	true
process.annotation.peptide.maxSequencesPerEMRTCluster	1
process.annotation.protein.resolveHomology	true
process.annotation.peptide.maxFDR	0,01
process.annotation.useSharedPeptides	all
process.normalization.lowess.bandwidth	0,3
process.normalization.orderSequence	XPIR
process.normalization.minIntensity	3000
process.quantification.peptide.minMaxScorePerCluster	6
process.quantification.peptide.acceptType.IN_SOURCE	false
process.quantification.peptide.acceptType.MISSING_CLEAVAGE	true
process.quantification.peptide.acceptType.NEUTRAL_LOSS_H20	false
process.quantification.peptide.acceptType.NEUTRAL_LOSS_NH3	false
process.quantification.peptide.acceptType.PEP_FRAG_1	true
process.quantification.peptide.acceptType.PEP_FRAG_2	true
process.quantification.peptide.acceptType.VAR_MOD	true
process.quantification.peptide.acceptType.PTM	true
process.quantification.peptide.acceptType.DDA	false
process.quantification.topx.degree	3
process.quantification.topx.allowDifferentPeptides	true

process.quantification.minPeptidesPerProtein	2
process.quantification.absolute.standard.entry	ENO1_YEAST
process.quantification.absolute.standard.fmol	50
process.quantification.topx.allowDifferentPeptides	true
process.quantification.absolute.standard.entry	ENO1_YEAST
process.quantification.absolute.standard.fmol	50
process.quantification.maxProteinFDR	0,01

Table S2 Proteins identified in *G. diazotrophicus* exposed to PEG-400

Description	Acces.	IC Control1	IC Control2	IC Control3	IC PEG 1	IC PEG2	IC PEG3	T test
1-deoxy-D-xylulose-5-phosphate synthase	A9HIR0	9654	11030	10237	18171	20445	21278	0,0018
2,3,4,5-tetrahydropyridine-2,6-dicarboxylate N-succinyltransferase	A9HKR5	17728	17666	12283	18947	26181	28810	0,0387
2-nitropropane dioxygenase	A9HF38	5482	5277	5010	9161	16361	16003	0,0333
2-oxoglutarate dehydrogenase E1 component	A9HFG6	3713	3881	3027	14599	19675	17436	0,0048
30S ribosomal protein S1	A9H459	39648	47724	35654	53408	71726	66210	0,0157
30S ribosomal protein S6	RS6	3931	3143	2431	10329	13167	10991	0,0017
3-hydroxyacyl-[acyl-carrier-protein] dehydratase FabZ	FABZ	2832	3167	4575	7785	4929	5188	0,0488
3-phosphoshikimate 1-carboxyvinyltransferase	A9H466	15390	15140	17047	28180	27244	27849	0,0003
4-hydroxy-3-methylbut-2-en-1-yl diphosphate synthase (flavodoxin)	ISPG	4961	6982	5922	13459	13258	12410	0,0008
50S ribosomal protein L10	RL10	65663	42144	49111	108091	106917	79321	0,0101
50S ribosomal protein L15	RL15	7448	7996	5344	23515	17932	35461	0,0327
5-methyltetrahydropteroyltriglutamate--homocysteine methyltransferase	A9HNX4	13650	16176	14609	36648	34040	38839	0,0004
6,7-dimethyl-8-ribityllumazine synthase	A9HDF5	10130	11219	11139	17908	18313	17208	7E-05
6-phosphogluconate dehydrogenase NAD-binding	A9HL10	7546	7322	7872	28723	29979	31658	0,0005
7-cyano-7-deazaguanine synthase	QUEC	5588	5135	4708	9606	8229	9149	0,0013
Acetoin(Diacetyl) reductase	A9HHS9	11996	12500	12531	28361	31230	30169	0,0008
Acetyltransferase component of pyruvate dehydrogenase complex	A9HJB2	16766	19250	12642	22584	33486	31347	0,0199
Aconitate hydratase	A9HEZ2	74972	76484	56600	102219	116632	117654	0,0036
Adenosylhomocysteinase	A9HFJ7	13661	16003	12697	26676	38450	37291	0,0135
Alcohol dehydrogenase	A9HNA5	17422	25541	17759	29326	42019	49730	0,0299
Alcohol dehydrogenase zinc-binding domain protein	A9HE22	4867	5581	4846	5936	8787	8993	0,0485
Aldehyde Dehydrogenase	A9H4V7	97112	88276	96370	129455	151451	156716	0,0084
Aldehyde dehydrogenase protein	A9H192	4596	4704	4373	9191	10953	11403	0,0057
Aldo/keto reductase family	A9HF59	14254	14037	14104	22114	20236	21329	0,0027
Alpha,alpha-trehalose-phosphate synthase (UDP-forming)	A9HBU6	8901	7241	6972	16769	15693	16349	0,0005
Amidophosphoribosyltransferase	A9H4K2	4770	6943	5538	9660	9779	10671	0,0048
Arginine biosynthesis bifunctional protein ArgJ	A9HAU1	4998	7924	5731	10855	10194	13102	0,0071
Arginine--tRNA ligase	A9HLH8	2963	2264	2840	6435	6402	9118	0,0151
Aspartate--tRNA(Asp/Asn) ligase	A9HLJ4	4229	5196	3143	8866	15152	11915	0,0198
Aspartokinase	A9HJ44	4993	6526	7713	10492	10528	12575	0,0053
ATP synthase subunit beta	ATPB	80259	105445	61588	106323	120479	147821	0,0368
Bifunctional protein GlmU	GLMU	8656	6837	5848	16881	20788	21046	0,0015
Biotin carboxylase protein	A9HEX0	33851	22140	20867	36175	55782	46315	0,0241
Carbamoyl-phosphate synthase large chain	A9H1P7	3453	4011	3590	8803	10639	11829	0,0071
Carboxymethylenebutenolidase	A9HK54	20463	23079	20537	38288	37235	40692	0,0001
Chaperone protein DnaJ	DNAJ	5546	5681	3385	10748	12482	14045	0,002
Chaperone protein DnaK	DNAK	105036	131879	131292	164772	175528	####	0,0196
Chaperone protein HtpG	A9HLJ9	19630	24778	21570	40757	51653	47163	0,0035
Chemoreceptor mcpA (Methyl-accepting chemotaxis protein)	A9HHE0	14031	16127	14940	23233	29710	28556	0,0094
Conserved protein	A9H3Z0	3615	3756	3874	8621	8364	8461	7E-07
D-2-hydroxyacid dehydrogensase	A9HDT4	114319	107563	92881	181177	231695	####	0,0052
Dehydrogenase	A9H159	5863	4208	6855	8257	8637	8797	0,029
Deoxyuridine 5'-triphosphate nucleotidohydrolase	A9HI24	16355	15103	14814	25136	20761	23751	0,0085
Dihydrolipoyl dehydrogenase	A9HJB6	14528	9352	15901	23977	27054	29057	0,0035
Dihydrolipoyl dehydrogenase	A9HFH1	37130	38785	34190	103271	109509	113732	0,0002
Dihydrolipoyllysine-residue succinyltransferase	A9HFG9	83365	70284	69047	179383	161694	161657	0,0002
Electron transfer flavoprotein-ubiquinone oxidoreductase	A9HEE4	11926	12165	10292	25959	39604	34746	0,0146
Elongation factor G	A9HS02	24102	27025	18735	38228	56146	52759	0,0139
Endoribonuclease L-PSP	A9HBS7	14716	22718	25026	42269	35889	44795	0,0042
Ferrochelatase	A9HEQ4	13295	12985	11969	20985	20472	19773	8E-05
FeS assembly protein SufB	A9HRY9	1985	2339	1782	4253	6001	5224	0,0088
Fumarate hydratase class I	A9HBG7	13750	10556	13731	49551	51006	49979	8E-05
Geranyltranstransferase	A9HIR3	17825	18796	15872	26054	26514	27275	0,0018
Glucokinase	A9HI04	28982	28088	31902	46325	61957	61477	0,0147
Glucose-6-phosphate 1-dehydrogenase	A9H326	11712	12817	10894	28427	29861	30298	1E-05
Glutamine--fructose-6-phosphate aminotransferase [isomerizing]	A9HI49	6138	6812	5008	29803	25959	28260	0,0003
Glutaredoxin	A9HJG8	80535	65185	57455	106072	109606	106180	0,0127

Glycosyl transferase group 1	A9HNQ7	1461	1491	1881	5475	5981	6843	0,0021
GMP synthase [glutamine-hydrolyzing]	A9H085	3710	4515	2919	6354	7962	7190	0,0031
GTP-binding protein TypA/BipA	A9H9C1	6259	7786	4225	10109	21117	17056	0,039
Histidine--tRNA ligase	SYH	10066	11230	9418	22010	19114	20184	0,0006
Indole-3-glycerol phosphate synthase	A9HJA0	15921	16413	14977	24945	24169	23010	0,0002
Inosine-guanosine kinase	A9H9C0	6643	6993	7275	13390	13164	13812	8E-06
Isochorismatase hydrolase	A9H559	4112	4207	4915	9160	8521	9008	0,0001
Isocitrate dehydrogenase (NAD(+))	A9HJQ1	50557	46548	40967	93396	102141	59497	0,0448
Ketol-acid reductoisomerase (NADP(+))	ILVC	11925	13750	11762	24776	25472	28346	0,0006
Leucine--tRNA ligase	A9HMQ5	3026	3046	2334	3413	5019	4565	0,0331
Lipase protein	A9HBK6	27088	26000	30557	57848	44143	47817	0,0118
Lysine--tRNA ligase	A9HK29	4725	4962	4771	8373	10532	10673	0,0102
Malate dehydrogenase (Oxaloacetate-decarboxylating) (NADP(+))	A9HH05	6367	6137	4127	15833	21228	15949	0,0059
Mannitol 2-dehydrogenase	A9HBL5	21648	32962	31332	61574	68224	68660	0,0009
NAD(P)H nitroreductase	A9H8I9	5915	6583	9631	16117	15385	13371	0,0038
NADH-quinone oxidoreductase	A9HRT3	14146	13968	11743	26156	30161	32062	0,0023
NADH-quinone oxidoreductase subunit B 2	NUOB2	27866	33093	33195	50719	49814	53150	0,0009
NADH-quinone oxidoreductase subunit C	A9HRU1	19917	19728	19922	39013	35465	35819	0,0022
NADH-ubiquinone/plastoquinone oxidoreductase chain 6	A9HRS8	3305	4020	3289	4857	5218	6505	0,0199
Oligoendopeptidase F	A9HSA2	5270	4793	4444	9024	9281	9239	0,0007
Peptidase M24	A9HJP9	10641	9626	10646	21088	15857	19289	0,0134
Phenylalanine--tRNA ligase beta subunit	A9H165	11742	12560	10595	15644	19135	20472	0,0146
Phosphoribosylformylglycinamidine synthase subunit PurL	A9HJG3	6704	7469	6436	12055	15125	15160	0,0068
Phosphoribosylformylglycinamidine synthase subunit PurQ	A9HJG0	14467	9712	9384	26880	24844	22705	0,0018
Polyribonucleotide nucleotidyltransferase	PNP	19114	23901	17079	30968	41164	40261	0,0079
Probable malate:quinone oxidoreductase	A9HKZ6	5159	5237	4234	8887	10523	9113	0,0015
Putative 2-keto-4-pentenoate hydratase-like	A9HDT5	20919	25917	22798	37189	46493	48072	0,0073
Putative aldehyde dehydrogenase A	A9HEG7	1536	1378	1264	11763	12169	16261	0,0069
Putative cytochrome c551 peroxidase	A9HK81	5582	4362	4477	8632	8304	8171	0,0032
Putative nitrogen fixation protein	A9HFA7	25413	16591	20537	27279	34272	33230	0,017
Putative phosphoglycolate phosphatase	A9HJN8	3145	2841	3567	4984	4871	4742	0,0047
Putative ribosomal RNA small subunit methyltransferase B	A9HID3	2989	2652	2744	6502	6010	5240	0,0048
Putative xanthine dehydrogenase iron-sulfur-binding subunit	A9H189	7637	9297	9301	19804	18097	18373	0,0001
Pyruvate dehydrogenase E1 component subunit beta	A9HJA9	33049	41431	24661	48895	65757	54689	0,0139
Ribose-5-phosphate isomerase A	A9H338	16507	18082	16652	34238	42022	40060	0,0045
Ribose-phosphate pyrophosphokinase	A9HBZ3	7957	9451	7671	15411	17365	15811	0,0003
Ribosome-binding ATPase YchF	A9HC06	6496	7345	6481	14948	13559	11915	0,0053
S-(hydroxymethyl)glutathione dehydrogenase	A9HIP1	13297	14072	10730	31660	42158	39018	0,0048
S-formylglutathione hydrolase	A9HIP3	1538	1582	1330	2898	2979	3498	0,003
Succinate dehydrogenase flavoprotein subunit	A9HFD7	19428	21162	15521	38480	58251	54847	0,0139
Succinate-semialdehyde dehydrogenase	A9H549	30322	37862	30023	110457	108236	####	1E-05
Superoxide dismutase	A9HL14	50345	15504	29127	70701	61704	58660	0,0369
Thiamine-phosphate pyrophosphorylase	A9HI58	14252	15123	15262	28869	25946	25388	0,0025
Thiazole synthase	THIG	22340	20340	16461	36157	38911	35873	0,0013
Transaldolase	A9H320	79700	80220	67267	151910	180834	####	0,0013
Transcription termination/antitermination protein NusA	A9HF12	11395	11965	8424	17632	16157	17845	0,0068
Tryptophan synthase alpha chain	TRPA	36668	40644	38751	62110	56190	72211	0,014
Tryptophan synthase beta chain	A9HE87	17992	17773	15104	28352	28782	29679	0,0011
Uncharacterized protein	A9HBG4	7343	9327	9301	15737	11423	14576	0,0182
Uncharacterized protein	A9HJK6	3513	9446	3525	32475	30895	25949	0,0005
Uncharacterized protein	A9HLD4	2758	2576	2207	3933	4531	4062	0,0013
Uncharacterized protein	A9H9H3	7067	5620	7136	11609	12042	12558	0,001
Xanthine phosphoribosyltransferase	A9H0R0	6741	6601	5289	14555	10468	12257	0,0113
2-isopropylmalate synthase	A9HMA2	30103	30153	25926	14222	12718	12960	0,0022
3'(2'),5'-bisphosphate nucleotidase CysQ	A9H1J6	14043	16465	14972	5724	5587	6471	0,0012
30S ribosomal protein S8	RS8	94261	77303	108440	46490	30050	35840	0,0057
30S ribosomal protein S9	A9H812	57163	48320	63512	37275	32539	40395	0,0145
SDR family oxidoreductase	A9HPF0	31849	36597	27571	14624	16870	19931	0,0067
50S ribosomal protein L1	RL1	77417	73297	69477	49215	31458	36014	0,0062
50S ribosomal protein L11	RL11	32850	25228	26987	14053	15598	15899	0,0119
50S ribosomal protein L5	A9H3M8	96141	75807	95036	27126	31439	31380	0,0048
sn-glycerol-3-phosphate ABC transporter ATP-binding protein UgpC	A9HPE7	55771	59603	49596	17619	18004	19453	0,0025
Acetylornithine aminotransferase	A9HFT8	41494	38087	43222	16008	17806	16276	0,0007
Adenylate kinase	KAD	36155	26647	25905	9676	11573	10706	0,0132
Alkyl hydroperoxide reductase AhpD	AHPD	44270	42213	39543	26152	25433	30296	0,001
Alkyl hydroperoxide reductase/ Thiol specific antioxidant/ Mal allergen	A9H3W7	34226	21885	22436	11547	13667	14425	0,0392
Alpha/beta hydrolase, chloride peroxidase	A9H000	30402	28298	31229	15860	13269	14775	0,0001
Amidinotransferase	A9HNM6	9294	9418	9336	5883	5982	6025	3E-07
Anthranilate phosphoribosyltransferase	A9HJ97	14779	14482	13380	5946	6896	6598	0,0001
ATP synthase subunit delta	ATPD	14426	11096	6253	2353	2715	1990	0,0364
Bacteriocin protein	A9H5P1	33337	33115	25740	15297	19380	19591	0,0098
Carboxymethylenebutenolidase	A9H121	11905	12630	13098	4623	5207	5934	8E-05
Carboxy-terminal protease protein	A9H3A3	55542	51197	53196	20090	17765	20922	2E-05
Catalase	A9GZZ4	194730	170405	104876	66797	81743	93770	0,0478
J domain-containing protein	A9HAH3	39668	33178	43735	20344	19903	22282	0,0115
Choloylglycine hydrolase	A9H2I4	6931	8475	8303	2212	2230	2796	0,0017
Chorismate synthase	AROC	5613	4549	4461	2227	1974	2282	0,0068

Cold-shock DNA-binding domain protein	A9HK34	15766	16600	19171	2989	4196	4138	0,0012
Conjugal transfer	A9HT68	86724	70706	69436	37293	33821	36359	0,0082
Circularly permuted type 2 ATP-grasp protein GN	A9H282	15245	13002	13658	7301	8193	8147	0,0025
SIMPL domain-containing protein GN	A9HFQ7	30178	25354	32555	13846	12222	12283	0,006
Lipid A deacylase LpxR family protein GN	A9HIX3	47600	47323	56548	19729	21004	23020	0,0032
CRISPR-associated protein, Cse4 family	A9HLC8	26973	27332	26409	8438	9329	7267	8E-05
Cysteine synthase	A9HAE5	39743	36767	39038	27547	22188	26143	0,0024
Dipeptidyl-peptidase	A9H090	59700	46316	53567	36170	34217	33157	0,0174
D-ribose-binding periplasmic protein	A9HPK6	133803	120500	141151	23077	23397	24708	0,0015
DSBA oxidoreductase	A9HIK8	18265	9055	9879	3929	3767	3705	0,0499
dTDP-4-dehydrorhamnose 3,5-epimerase	A9H3H9	9021	8003	7955	4925	4988	5406	0,0024
D-xylose ABC transporter, periplasmic substrate-binding protein	A9HNP0	140312	137276	124315	33586	30883	33346	0,0009
Electron transport protein SCO1/SenC	A9H4T2	14304	13920	14430	8463	9725	9821	0,002
Endoribonuclease L-PSP	A9HC24	15810	14048	12961	8881	9817	9503	0,0097
Exodeoxyribonuclease III Xth	A9HIE6	11700	8286	7661	3795	4447	3437	0,0225
Sugar ABC transporter substrate-binding protein	A9HPE1	117396	110781	113835	4487	5007	3575	8E-05
Ferritin Dps family protein	A9HB55	25359	23280	32647	5193	6646	5954	0,008
Flagellar L-ring protein	A9HHH1	8476	7543	9896	4269	4794	5166	0,0095
Flavin oxidoreductase	A9H2N2	47945	44036	45580	31093	25021	27117	0,001
Flavin-dependent thymidylate synthase	A9HBG1	18045	15190	16649	11387	10728	9870	0,0037
FMN-dependent NADH-azoreductase	AZOR	12103	11490	9183	6600	5687	7433	0,0107
Fructose-bisphosphate aldolase class 1	A9H6A5	80938	73480	62321	18599	20819	21042	0,0047
Ribose ABC transporter GN	A9HPM0	7221	6709	6583	3061	2658	2768	0,0001
Gamma-glutamyltranspeptidase	A9HM18	26353	27064	35028	15986	19821	21270	0,0216
Gluconate 2-dehydrogenase (Acceptor)	A9HK15	97541	87250	85367	56250	56136	61001	0,0031
Glutamate--tRNA ligase 1	SYE1	13258	10704	8625	3303	8803	5621	0,039
Glutamine amidotransferase of anthranilate synthase	A9HJ94	14735	12982	11676	5660	5204	5226	0,0055
Glutathione peroxidase	A9HKB6	9330	8838	6096	1786	1866	1745	0,0123
Glycerol-3-phosphate dehydrogenase	A9HHX8	22313	21537	13140	7335	12761	11558	0,0416
Lipoprotein	A9HPJ3	26674	26564	31133	16422	16342	17064	0,0075
Metal-dependent carboxypeptidase	A9HKD9	7876	7169	6916	3784	3957	5098	0,0027
Methylamine dehydrogenase heavy chain	A9H2X8	15420	17195	22185	8295	8227	8232	0,0193
Molybdenum cofactor biosynthesis protein B	A9HAM8	18104	14344	13024	6837	8440	9966	0,0138
Nitrogen regulatory protein P-II	A9HMD4	29278	27081	25728	18695	16471	19372	0,0014
Octanoyltransferase	A9HJ12	6716	7850	7329	4301	3798	3713	0,0012
Ornithine carbamoyltransferase	A9HFT5	17731	17301	17329	9479	9510	10850	0,0009
Outer membrane protein assembly factor BamA	A9HKV0	23373	17503	19143	9610	12234	12678	0,0111
Outer membrane protein assembly factor BamD	A9H0L0	10227	14443	10729	1593	1431	1688	0,0081
Oxygen-dependent coproporphyrinogen-III oxidase	A9HK65	15889	13723	16914	8364	11880	10322	0,0093
Peptide methionine sulfoxide reductase MsrA	A9HI15	23076	15984	14340	8092	10948	10644	0,0429
Iron ABC transporter substrate-binding protein	A9HK76	33352	27478	34327	10055	10113	10355	0,0048
Sugar ABC transporter substrate-binding protein	A9HPB9	163399	156770	176417	62084	52036	57258	0,0003
Periplasmic serine endoprotease DegQ	A9HBK9	19462	19862	22964	14001	12553	12504	0,005
Phosphoenolpyruvate carboxykinase (ATP)	A9H8M9	17023	16390	14957	5727	6178	6083	0,0012
PKHD-type hydroxylase GDI1238/Gdia	Y1238	56758	35779	45751	7753	8730	11724	0,0114
Polyphenol oxidase	A9HBY8	17099	14071	13491	7524	10893	8646	0,0088
Porin OprB	A9HAM5	11698	10565	12020	6151	7509	8166	0,0031
Porin	A9HPF6	16134	14615	17207	2774	3636	2801	0,0006
PrkA serine protein kinase	A9HIB1	25954	24381	15475	6730	11592	8397	0,0205
Acetyl-CoA C-acyltransferase (Acetoacetyl-CoA thiolase)	A9HE46	6955	6232	6049	3009	2626	2526	0,0006
Putative aldo-keto reductase	A9HQR7	10116	10203	11481	6835	5044	6043	0,0013
Putative conjugal transfer	A9HSY7	14273	9479	12068	4249	3798	4704	0,0137
Putative DNA-binding response regulator mtrA	A9HIE2	18916	20140	21095	8872	8411	10435	0,0001
Putative L-amino-acid oxidase	A9HN63	16864	15791	16636	7463	9678	9080	0,0011
Putative NAD dependent epimerase	A9H2U3	10100	9876	8439	2980	3310	3605	0,0018
Putative oxidoreductase	A9HM21	20107	14706	15329	3284	3540	3870	0,0078
Sugar ABC transporter substrate-binding protein	A9H577	76805	66814	81078	15381	12917	15656	0,0018
Putative polysaccharide export protein	A9HMV6	28977	29427	37583	25319	18670	19542	0,0201
Putative regulatory protein	A9HF98	22586	21942	19857	9000	7871	7958	0,0005
Putative ribonuclease D	A9HKL8	6485	6414	6842	2863	3448	3407	0,0001
Putative thioredoxin protein	A9HSA5	38172	20616	21474	4004	5055	4062	0,0295
Putative TonB-dependent receptor	A9HDZ9	7493	5416	5544	1651	1833	2175	0,0098
Putative tonB-dependent receptor	A9HE38	114344	117560	139966	42731	54445	49114	0,0025
Putative tonB-dependent receptor	A9HEU6	109797	104767	115235	31779	35326	42360	4E-05
Putative TonB-dependent receptor	A9HNM4	16703	14455	18560	2905	2943	3193	0,0037
Putative TonB-dependent receptor	A9H7L3	23309	19260	17889	7176	7758	9798	0,004
Putative tonB-dependent receptor protein	A9H7M7	42522	35380	44423	4372	4736	6383	0,0021
Putative two component response regulator	A9HH92	7232	6812	7363	3814	3290	3385	5E-05
Putative Ubiquinol-cytochrome c reductase	A9H861	21667	19846	19235	9337	12562	12190	0,0015
Quinolinate synthase A	A9H8C0	40460	39360	39638	22258	21703	25282	0,0012
Ribosomal RNA large subunit methyltransferase E	A9HIS5	9384	8704	9476	6180	5776	5912	0,0007
Ribulokinase	A9HPD7	26783	23735	26854	5827	7132	6797	0,0005
Rieske (2Fe-2S) domain protein	A9HL46	36484	25811	24150	7428	9489	6639	0,0138
RNA-binding protein Hfq	HFQ	21680	22681	31246	8494	7990	7052	0,0137
Serine hydroxymethyltransferase	A9HRP5	39844	36746	28758	9377	11327	10696	0,0076
Serine--tRNA ligase	SYS	32201	23622	31223	16510	13641	15714	0,0139
Site-determining protein	A9HLY3	115052	168128	96062	36864	37949	87500	0,0303

S-methyl-5'-thioadenosine phosphorylase	A9HK57	48109	65191	47740	33919	31685	36160	0,0345
Succinate--CoA ligase [ADP-forming] subunit alpha	A9HRF1	26605	22293	20499	10222	9588	10619	0,0084
Tol-Pal system protein TolB	A9HB04	95765	102937	99343	52356	62439	65534	0,0016
TonB-dependent receptor	A9H932	39188	30956	33429	12958	21339	20818	0,0059
TonB-dependent receptor	A9H7L9	8142	7346	8209	2125	2524	2769	1E-04
Transcription termination/antitermination protein NusG	A9H988	35642	32564	35613	17394	16458	18785	0,0002
Transcriptional regulator LysR	A9H0A8	79618	75054	69701	36341	42211	41464	0,0006
Tryptophan--tRNA ligase	A9HIP8	8307	11380	8949	5721	4574	5652	0,0161
Two-component response regulator	A9HFR4	25207	25319	24704	10879	10999	12066	4E-05
MYG1 family protein	A9H8I6	14154	12695	12090	1916	2250	2203	0,0013
Membrane integrity-associated transporter subunit PqiC	A9H986	17327	21717	25795	9783	12405	15200	0,0215
Sulfurtransferase	A9HAE9	10978	11523	13550	4888	5658	4776	0,0035
YfdX family protein	A9HCT2	25310	23505	14170	11974	12093	9741	0,05
Uncharacterized protein	A9HIF7	4447	4476	6303	2371	2043	3207	0,017
NAD(P)/FAD-dependent oxidoreductase	A9HJS1	17454	15097	16868	7469	8343	7652	0,0015
Sugar ABC transporter substrate-binding protein	A9HPC7	6086	5756	5519	2385	2241	2016	8E-05
Ankyrin repeat domain-containing protein	A9H3D7	14471	13041	14606	6926	8301	5734	0,0012
Uncharacterized protein	A9H3X9	20699	19749	21744	11923	11642	11303	0,001
TrbG/VirB9 family P-type conjugative transfer protein	A9HSZ4	24623	23360	23123	10797	9766	9720	2E-05
Cof-like hydrolase	A9H332	67713	63822	65568	46126	44535	40908	0,0003
Methylenetetrahydrofolate reductase	A9HNY2	8037	8551	6800	5110	5285	5420	0,0183
Putative rare lipoprotein A	A9HI92	7146	5606	7398	5014	3838	4783	0,0195
Outer-membrane lipoprotein carrier protein	A9H103	10415	8605	10455	7407	5061	7643	0,0213
Putative pyruvate dehydrogenase E2 component	A9HHP4	15752	14862	16983	10535	10749	11394	0,0036
Alcohol dehydrogenase GroES domain protein	A9H073	10127	10082	10880	6607	7397	7461	0,0005
Secretion protein, HlyD-family	A9HA48	10511	9387	9295	6939	6544	6757	0,0058
Pyridine nucleotide-disulphide oxidoreductase	A9HDE6	66822	64584	66248	41744	46281	49545	0,0041
Putative ABC transporter ATP-binding protein in rpoN region	A9HKM9	14984	13072	16242	10854	10040	10179	0,0168
Cof-like hydrolase	A9H329	6436	5413	5098	3929	3899	4164	0,0249
Putative dehydrogenase	A9HQE8	19837	18848	20781	13901	14223	14069	0,004
Putative L-asparaginase II protein	A9HE73	29167	24523	30460	20221	19183	20888	0,0198
TonB-dependent Receptor protein	A9HFV5	112497	105040	121352	74257	82709	86633	0,0035
HAD-superfamily hydrolase, subfamily IA, variant 3	A9HDX4	13391	13553	12037	9968	8596	9580	0,0025
Putative 3-oxoacyl-[acyl-carrier-protein] reductase	A9H2M9	38057	34332	35739	23322	26898	27908	0,0028
Conserved protein	A9H314	22481	21408	23243	15376	16470	16904	0,0005
DEAD/DEAH box helicase domain protein	A9H0S9	16900	15624	15575	13134	10338	11501	0,0084
Peptidase protein	A9HET1	18463	17435	20859	11246	14996	15157	0,0187
Glycerol kinase	A9HHY3	144661	147592	128599	91669	109247	####	0,0051
Phosphoglycolate phosphatase	A9HI43	30102	29703	25985	22900	19099	21359	0,0064
Uncharacterized protein	A9HM07	13706	11577	15341	10982	9364	9986	0,0354
Conserved protein	A9HS96	15806	13844	18073	11201	11882	12611	0,0347
Transcription elongation factor GreA	A9H1Q0	9443	10579	10447	7834	7789	7183	0,0035
NAD(P)H dehydrogenase (quinone)	NQOR	27064	28612	28101	21459	17730	23915	0,0271
Histidinol-phosphate aminotransferase	HIS8	13922	14756	15678	10963	11347	11127	0,0077
Conserved protein	A9HSH2	40000	44243	49992	28923	37343	35058	0,0235
Putative membrane protein	A9H806	12865	12349	15255	8788	10916	11426	0,0309
Pyrrolo-quinoline quinone	A9H134	33945	31109	39166	22614	28771	29413	0,0359
Putative transporter protein	A9H3U2	4905	4677	4966	3409	3839	4032	0,0072
50S ribosomal protein L4	RL4	23763	20618	18279	15455	18885	15045	0,0481
Flagellar motor switch protein FliN	A9HHD1	35280	36085	43291	32674	28207	31032	0,0388
Aldose 1-epimerase	A9HBF6	13984	11548	14508	9601	11581	10929	0,0411
Uncharacterized protein	A9GZL6	11119	10340	9765	9119	8913	7025	0,0352
Putative glutamyl-tRNA(Gln) amidotransferase subunit A	A9HJR7	36985	38656	39474	25610	33479	33422	0,0464
2-octaprenyl-6-methoxyphenol hydroxylase	A9HMD1	7820	7753	7884	6440	6020	6493	0,0035
UDP-N-acetylmuramoyl-L-alanyl-D-glutamate--2,6-diaminopimelate ligase	A9H0H5	6873	5642	6195	4864	4752	5555	0,0301
50S ribosomal protein L25	RL25	57489	59186	58487	44175	53167	45178	0,0291
Protein RecA	A9HM16	11925	13491	10974	8924	10222	10610	0,0381
Putative gamma-glutamyltranspeptidase	A9HJR4	13482	13841	16374	12371	11046	12399	0,0418
Protein TolR	A9HAZ8	27090	25765	30080	23487	21642	23254	0,0227
Type II and III secretion system protein	A9HHL5	13905	11986	13635	9444	11457	12029	0,0472
Oxidoreductase	A9HAF3	83766	79655	84949	66716	71467	69881	0,0017
Glycine cleavage system aminomethyltransferase T	A9HM51	38024	40765	43492	35384	35295	32066	0,0165
3-methyl-2-oxobutanoate hydroxymethyltransferase	PANB	11101	11260	12089	9032	9753	10213	0,0086
3-mercaptopyruvate sulfurtransferase	A9HJI4	19220	18743	22094	18718	16579	15486	0,0473
2-ketogluconate reductase	A9H3Y4	25579	25848	27790	21045	23628	22381	0,0083
Phosphate-binding protein PstS	A9H9X2	44737	40834	45846	33812	38758	38771	0,0205
Putative phosphate acetyltransferase	A9HL01	6536	5637	5959	4901	5737	4896	0,0436
Peptide chain release factor 2	A9HF65	11828	12212	13408	11962	10111	10465	0,0468
Putative metallopeptidase	A9HRE6	23708	21341	23681	20184	21659	20370	0,0454
Mammalian cell entry related domain protein	A9H983	8998	8495	8659	7692	8402	8007	0,03
Cysteine desulfurase	A9HRY2	27869	28101	28017	27295	26640	25642	0,0448
Uncharacterized protein	A9HRD5	27407	26169	28436	30685	31108	29948	0,0109
ATPase associated with various cellular activities AAA	A9H3C6	23741	21480	25135	27580	24935	26594	0,0487
Putative molybdopterin biosynthesis protein moeA	A9HJ67	9281	8387	8402	10088	9728	9684	0,0222
Enolase-phosphatase E1	MTNC	9162	9392	9326	9966	10678	11053	0,026
DNA-directed RNA polymerase subunit alpha	RPOA	67606	78847	69426	82672	80421	82957	0,0476
Conserved protein	A9HM79	60100	52608	54736	65284	66559	59805	0,0286

Methylthioribose-1-phosphate isomerase	A9HLJ6	11089	12002	13246	13152	13791	14697	0,045
Conserved protein	A9HHA4	78034	81490	92543	98094	93469	97829	0,046
Bifunctional enzyme IspD/IspF	A9HLU2	19925	19913	21288	25331	22644	22842	0,0224
NADH-quinone oxidoreductase chain E	A9HRT6	10021	12001	11170	12805	13251	12477	0,0375
Putative glycyl aminopeptidase	A9HN12	33759	32762	34447	36978	39819	41079	0,0149
Carbamoyl-phosphate synthase small chain	A9H1P4	17745	16454	18653	21484	18718	21538	0,0332
Signal recognition particle receptor FtsY	A9HM31	6747	6379	6796	7536	7887	7867	0,0016
Acetylglutamate kinase	ARGB	19453	16723	17966	19409	21993	22065	0,0291
Putative N-carbamoyl-L-amino acid amidohydrolase	A9HJT7	8631	7417	7400	9333	9346	8869	0,0318
Inositol-1-monophosphatase	A9HRD4	24061	25937	21519	28510	28216	27482	0,0367
Beta sliding clamp	A9HI34	28194	29233	28027	32163	34037	34710	0,0048
Transcriptional regulator, IclR family/regucalcin	A9HL52	14438	14237	17250	16979	18535	19264	0,0374
3-oxoacyl-[acyl-carrier-protein] reductase	A9HRE0	33499	32029	35414	36712	39510	44853	0,0456
Putative pilus assembly protein	A9HHL8	10753	9848	9527	12895	11713	11611	0,0108
Outer membrane efflux protein	A9H3U0	3843	4005	4414	5219	4827	4816	0,0089
4-diphosphocytidyl-2-C-methyl-D-erythritol kinase	ISPE	18908	16056	19482	23256	20745	22157	0,0225
Ferredoxin--NADP reductase	FENR	18832	18526	19414	24195	22053	22751	0,0065
Peptidyl-prolyl cis-trans isomerase	A9HIQ1	108659	99311	125994	135399	135885	135149	0,0453
Orotidine 5'-phosphate decarboxylase	A9HES3	8828	8143	10331	11071	10889	11410	0,0408
Aminotransferase	A9HSE7	7978	8121	6415	8962	9053	9718	0,0345
Putative ribitol 2-dehydrogenase	A9HPG2	82582	83483	85378	108264	98171	108591	0,0101
Biotin carboxyl carrier protein of acetyl-CoA carboxylase	A9HEX3	57038	53814	55736	72613	68381	68295	0,001
Putative 2-amino-3-ketobutyrate coenzyme A ligase	A9HMR4	9985	10427	7596	11529	12339	11496	0,0485
Glucose-1-phosphate thymidylyltransferase	A9HH12	9202	9719	7011	10440	10730	11606	0,0474
Enolase	ENO	112018	108879	100720	126908	140959	####	0,0043
FeS assembly protein SufC	A9HRY6	33257	27079	33313	41090	38148	39567	0,0204
Gluconate 5-dehydrogenase	A9H995	58009	57373	63478	73644	74471	78968	0,0018
Acetyl-coenzyme A carboxylase carboxyl transferase subunit beta	ACCD	9529	8226	11592	11613	13646	12109	0,0472
Enoyl-CoA hydratase/isomerase	A9HE55	16801	15796	17895	22184	19870	22240	0,0056
Serine protease	A9HEK6	83759	69192	80154	98561	96441	####	0,0132
4-hydroxy-tetrahydrodipicolinate synthase	DAPA	18181	17092	19749	24528	21824	23905	0,0054
ATP synthase subunit alpha	ATPA	97406	102779	92992	116361	130060	####	0,0046
Elongation factor Tu	EFTU	309804	302816	307380	444036	####	####	0,0376
Aminopeptidase	A9HFU5	54324	45088	39382	58407	59907	60794	0,0437
Protein-L-isoaspartate O-methyltransferase	A9HI07	57667	45632	59537	74622	66262	69808	0,0233
Putative Aldose 1-epimerase	A9HDX0	7687	9745	10869	12658	11655	12311	0,0427
ATP phosphoribosyltransferase regulatory subunit	A9HLQ2	14900	13718	17135	18856	20053	20468	0,0143
Threonylcarbamoyl-AMP synthase	A9H1J9	12476	13148	12605	16130	16803	16944	0,0002
Oxidoreductase domain protein	A9HDU1	108085	93086	100795	127646	127455	####	0,0032
Bifunctional purine biosynthesis protein PurH	A9HDN9	26598	23338	22909	33343	27590	34745	0,0267
Putaive gamma-glutamyltranspeptidase	A9H4A8	8810	6884	9544	11175	10653	11333	0,0357
Fe-S protein, radical SAM family	A9HA97	26252	25748	25833	30600	37223	35027	0,0248
Putative nitroreductase family protein	A9GZY4	12328	10279	12862	17463	14598	15065	0,0156
Acetyl-CoA hydrolase	A9HIK2	20421	20385	16538	20844	28487	26995	0,0477
Glucose-6-phosphate 1-dehydrogenase	A9HFE6	49320	53553	54679	70537	64305	74943	0,0075
Phosphatidylserine decarboxylase proenzyme	PSD	18143	21315	21184	26873	27146	26918	0,011
Enoyl-[acyl-carrier-protein] reductase [NADH]	A9H0U5	14017	16884	13892	18338	21819	20069	0,0107
Oxidoreductase (Aldo/keto reductase) protein	A9H614	8210	10336	8618	12209	12715	11602	0,0122
Carbonic anhydrase	A9HL77	56138	50310	49275	70564	66119	72864	0,0018
Methionine--tRNA ligase	A9HIA3	3692	3491	3049	4288	4737	4751	0,0047
Probable phosphoketolase	A9HGX3	45322	46278	40020	50511	65697	61377	0,0301
1-(5-phosphoribosyl)-5-[(5-phosphoribosylamino)methylideneamino]	A9GZX2	11328	11000	12761	15070	15636	16685	0,0025
Fructose-1,6-bisphosphatase	A9HCQ2	120293	93689	103971	134172	141805	156713	0,0104
Dihydroorotase	A9H142	8327	9617	8714	10264	12937	13133	0,0287
Peptidase protein, modulator of DNA gyrase	A9HEU1	10393	10620	9143	13375	14730	13364	0,0021
Elongation factor Ts	A9HRQ5	73228	64359	49401	87649	82333	87750	0,0344
Transcriptional regulator protein	A9HF00	10247	9944	7984	12176	13022	13843	0,0088
ATP synthase epsilon chain	ATPE	22486	22320	24593	30340	36807	29022	0,0276
Inositol-1-monophosphatase	A9H6E0	16834	17027	15705	22567	23976	23078	0,0002
Putative penicillin-binding protein	A9H435	14837	14420	16274	20808	21456	21833	0,0011
Glutamyl-tRNA(Gln) amidotransferase subunit A	A9HRI9	27002	27739	22686	34281	36916	37941	0,0037
Malonyl CoA-acyl carrier protein transacylase	A9HRE1	31361	34126	33767	48055	47158	44933	0,0002
Putative amidohydrolase	A9HMC5	19364	13515	17043	24054	22530	23983	0,0233
Cysteine synthase	A9HFX5	19618	19935	18362	27422	28576	26125	0,0006
ATP-dependent Clp protease ATP-binding subunit ClpX	CLPX	12243	12276	12258	14225	19701	18355	0,0442
Pyruvate, phosphate dikinase	A9HEP2	3820	5121	3302	4826	6376	6244	0,039
Uroporphyrinogen decarboxylase	DCUP	15295	13872	15432	19200	22375	22142	0,0061
Aldo/keto reductase	A9HH27	16821	16279	14952	22398	19384	27395	0,0438
D-3-phosphoglycerate dehydrogenase	A9HIU7	4267	4183	3226	4682	6707	5493	0,0392
Preprotein translocase, YajC subunit	A9HL42	14343	12113	15767	22091	18946	20038	0,0058
RNA-metabolising metallo-beta-lactamase protein	A9HRR8	70454	66929	66011	99817	93573	101713	0,0007
Peptidyl-prolyl cis-trans isomerase D	A9HJ89	16876	13953	16874	26503	21417	21691	0,0139
Pyruvate dehydrogenase E1 component subunit alpha	A9HJA6	16006	15104	14485	23233	19489	23993	0,0139
Outer membrane protein	A9H3F7	6721	7082	7634	11313	9433	10774	0,0069
Citrate synthase	A9HII7	51608	44848	42151	60537	71177	72495	0,0059
3-oxoacyl-[acyl-carrier-protein] reductase	A9HIY5	43094	50699	50547	64405	74890	73969	0,0033
Transketolase	A9H317	132450	137477	118157	177855	####	####	0,0018

Uncharacterized protein	A9HKE4	10772	12211	12826	17939	17127	17956	0,0022
Alanine--tRNA ligase	A9HL73	3086	3617	2892	4040	5693	4648	0,0315
Glucokinase protein	A9HIS0	49383	44815	49610	40470	43493	45829	0,0505
Phosphoribosylglycinamide formyltransferase	A9HJV2	5188	5296	5308	5897	5385	5774	0,0522
Peptidase, family M16	A9HKF0	13411	11424	12224	11369	10555	10629	0,0526
Adenine deaminase	A9HNM9	7440	5444	6301	4406	4857	5437	0,0527
Molybdopterin biosynthesis protein moeB	A9HEI1	7294	8057	9220	10677	9135	9373	0,0534
Aminotransferase class-III	A9HJT9	9842	12936	12015	7843	8978	10502	0,0541
Gluconate 2-dehydrogenase (Acceptor)	A9HBC6	6970	6194	6592	7806	6904	7198	0,055
NADP oxidoreductase coenzyme F420-dependent	A9HL93	18881	22546	27343	17424	15866	15879	0,0554
Thioredoxin	A9HA92	29802	14873	15180	4736	6677	11047	0,0568
Glycine dehydrogenase (decarboxylating)	A9HM48	3078	3428	2870	3744	6605	5597	0,0578
Uncharacterized protein	A9HRF9	6889	5237	9678	3383	4190	4157	0,0585
Conserved protein	A9HBT6	10132	9012	11374	13241	10664	13418	0,0589
Dihydroorotate dehydrogenase (quinone)	A9HBE5	23555	30697	26009	35461	30133	30839	0,059
50S ribosomal protein L9	RL9	61911	41998	35129	25772	23482	27943	0,0604
ATP-dependent Clp protease proteolytic subunit	A9HRV4	60726	63940	41538	33819	40717	39957	0,0612
Delta-aminolevulinic acid dehydratase	A9HRP9	13814	13864	14027	15554	14359	16443	0,0613
Pyruvate kinase	A9HEH3	73304	74485	75620	94557	107083	148817	0,0614
Aminotransferase	A9HCQ6	15415	15206	13467	11729	12936	14084	0,0627
NADH dehydrogenase/NAD(P)H nitroreductase rutE	A9HFB0	8322	9044	12656	13863	13237	12726	0,064
Putative phosphatidylethanolamine N-methyltransferase	A9HKI4	15442	13307	14503	13829	10383	9172	0,064
Conservev protein	A9GZU8	22739	19524	14528	11416	15682	12849	0,0641
Aminotransferase	A9HSE9	57721	48684	48451	43174	43595	45989	0,0641
Alcohol dehydrogenase	A9HBQ8	2470	3541	2316	6671	7139	15249	0,0643
Protease protein	A9HAN0	30121	18464	20462	32932	30409	32070	0,0647
Threonine synthase	A9HKE7	14408	15564	16506	11263	14083	14289	0,066
Trigger factor	TIG	99098	97247	83449	80848	79815	84505	0,0678
Glycine--tRNA ligase beta subunit	A9HM86	8316	6684	5716	7401	10692	9436	0,0703
Adenylosuccinate synthetase	PURA	34640	31908	37246	32660	30975	29790	0,0704
Universal stress protein	A9H0V0	66508	56243	51492	54751	42518	44839	0,0704
Uncharacterized protein	A9HHW9	18362	15671	23023	22054	24454	25002	0,0705
dCTP deaminase	A9HFN2	22106	22161	26046	43254	30700	28214	0,0709
Multidrug resistance protein A	A9H3B5	14110	15090	14416	13510	13874	14246	0,0726
Probable cytosol aminopeptidase	A9H1J4	13611	19483	11667	16953	21341	27638	0,0746
NADH-quinone oxidoreductase subunit F	A9HRT4	1938	1781	1985	2440	8194	7289	0,075
Ubiquinone biosynthesis O-methyltransferase	A9HJ43	14277	16901	17170	14824	14672	12096	0,0766
Putative Outer membrane protein oprM	A9HEG4	15550	16161	18855	15459	13706	14878	0,0766
ATP-dependent zinc metalloprotease FtsH	A9HB14	8352	9440	9007	9049	10407	10867	0,0768
ATP-dependent Clp protease proteolytic subunit	A9HCR1	44989	63190	50951	72188	59945	62369	0,077
Ubiquinol oxidase subunit 2	A9HK01	65596	65717	65452	60716	64725	63404	0,077
Putative serine carboxypeptidase	A9HS00	10215	11148	13017	10811	9279	8832	0,0777
ATP-dependent protease ATPase subunit HslU	A9H199	13099	12454	7898	8265	7099	7374	0,0779
Putative threonine dehydratase catabolic	A9H381	4430	4231	4747	4543	5944	6052	0,0779
UTP--glucose-1-phosphate uridylyltransferase	A9HJ15	106678	90822	79911	106130	114136	####	0,0784
Phosphoribosylamine--glycine ligase	A9H4P1	9049	8933	7456	8766	10530	9939	0,0788
Glycosyl transferase group 1	A9HLZ7	33269	31552	31124	32611	38703	35761	0,0794
Putative GAF sensor protein	A9HP16	9870	7337	8315	4811	7033	7761	0,0825
Acyl-[acyl-carrier-protein]--UDP-N-acetylglucosamine O-acyltransferase	A9HKU0	16154	14522	18813	14789	12645	14353	0,0829
Putative haloacid dehalogenase-like hydrolase	A9HBE7	22395	18512	23779	28141	23664	23797	0,0835
Multifunctional fusion protein	A9H0J6	19060	22543	16256	10330	11209	19048	0,0843
Putative aerobic cobaltochelatase cobS subunit	A9HJ01	22810	26713	23028	26425	26853	27172	0,0849
Nitrilase/cyanide hydratase	A9GZH7	8134	15199	10711	6249	7498	7635	0,0864
ABC transporter ATP-binding protein	A9H4G2	11380	10737	7664	10798	13548	12431	0,0895
Phosphoglucomutase/phosphomannomutase alpha/beta/alpha domain I	A9H070	52456	52773	53591	43479	51234	49822	0,0909
50S ribosomal protein L19	RL19	24046	31177	23056	26468	37623	34927	0,091
1-deoxy-D-xylulose 5-phosphate reductoisomerase	A9HKV5	9646	10512	8573	9636	12012	11625	0,0911
3-oxoacyl-[acyl-carrier-protein] synthase 2	A9HRD7	40427	45908	34736	45367	46016	48370	0,0933
Uncharacterized protein	A9HMQ8	5422	5324	8095	4824	4062	4705	0,0939
Ribosome maturation factor RimP	RIMP	25303	23445	30799	23439	21022	22643	0,0969
NADP-dependent L-serine/L-allo-threonine dehydrogenase	A9H4E8	83631	67996	68713	85644	79810	83545	0,097
Bifunctional NAD(P)H-hydrate repair enzyme	A9HRW0	7446	6037	7004	6244	5283	6410	0,0978
TonB-dependent receptor	A9HFL0	10281	8295	9035	9237	11053	11631	0,0993
Thioredoxin protein	A9H2A4	35505	30882	30787	34648	35376	35761	0,1014
50S ribosomal protein L7/L12	RL7	212894	100739	74420	198607	221111	####	0,1021
Aspartyl/glutamyl-tRNA(Asn/Gln) amidotransferase subunit B	A9HRI7	7950	8000	5717	8184	9421	8156	0,1038
Cold shock-like protein cspE	A9HIW8	96850	63429	79882	96744	104646	90303	0,1049
Uncharacterized protein	A9HT76	60471	110879	83866	60771	55436	60123	0,1057
Cold-shock DEAD box protein A homolog	A9HRW6	5577	6550	3844	5266	8823	7870	0,1061
Folate-binding protein YgfZ	A9H151	16479	14691	15798	13517	4685	13284	0,1075
Conserved protein	A9HF41	12055	13241	14298	9192	12345	12376	0,1077
Uncharacterized protein	A9HBZ1	10594	8506	11260	8413	8149	9444	0,1083
Outer membrane protein	OMPC	209496	262664	239220	203702	####	####	0,1095
Alcohol dehydrogenase [acceptor]	A9HK12	54247	48458	48507	39066	45621	49895	0,1108
Probable transcriptional regulatory protein GDI0798	A9HAV2	26476	28403	31677	20383	25491	28311	0,1111
50S ribosomal protein L3	RL3	18391	13876	30701	15839	9161	12226	0,1119
Oxidoreductase protein	A9HL82	4685	4517	4247	4281	4336	4180	0,1122

Glucose-6-phosphate 1-dehydrogenase	A9H0G0	37830	39660	33088	28981	35154	34531	0,1127
Protein-export protein SecB	SECB	31442	52286	47362	57561	57573	48075	0,1136
Glucans biosynthesis protein G	A9HBM4	25689	23930	26902	25028	31530	29743	0,1149
tRNA pseudouridine synthase B	TRUB	13223	11216	14552	12516	10239	11175	0,1164
Protein TonB	A9HF68	10333	12084	14138	12524	14458	15225	0,1225
ATP synthase gamma chain	ATPG	45780	44307	57688	44109	40197	43115	0,1232
Methionyl-tRNA formyltransferase	FMT	6753	7034	7269	5479	5174	7274	0,1247
Aspartate-semialdehyde dehydrogenase	A9HFE5	25322	27076	27004	28890	26401	27797	0,128
50S ribosomal protein L16	RL16	10854	7385	16035	7200	7287	8238	0,132
NADPH dehydrogenase	A9H535	18379	23650	24809	14575	21307	19880	0,1323
Acetyl-coenzyme A carboxylase carboxyl transferase subunit alpha	ACCA	58853	48157	60641	65063	61218	58965	0,1353
Conserved protein	A9H9B9	7873	19261	6392	36170	7168	29164	0,1377
30S ribosomal protein S5	RS5	10676	6186	22495	7354	6443	4010	0,1379
Efflux transporter, RND family, MFP subunit	A9HEF9	30726	31278	35607	35795	32750	36288	0,1401
Hopanoid-associated sugar epimerase	A9HGZ6	40498	34373	28159	26745	30785	30068	0,1416
Tyrosine--tRNA ligase	A9HMK2	16694	15612	11823	15839	16885	17803	0,1419
Cell division protein FtsZ	A9H0K4	27164	33097	26171	23816	26242	27177	0,1469
Triosephosphate isomerase	TPIS	28175	25602	28655	27602	28777	32416	0,1488
2,3-bisphosphoglycerate-independent phosphoglycerate mutase	A9H397	115598	107227	105141	107258	107345	95171	0,1539
Putative short-chain dehydrogenase	A9HAC6	9824	12122	10287	10821	11814	12771	0,1539
Putative D-3-phosphoglycerate dehydrogenase	A9HFV9	15663	12549	14477	12367	12741	13846	0,154
Proline--tRNA ligase	A9HRR5	23529	20962	16900	15334	19185	18700	0,1546
Thiamine biosynthesis oxidoreductase thiO	A9HI52	20377	17747	17246	17249	15979	18053	0,1554
Ribokinase	A9H0C5	6261	5816	7555	5238	5767	6413	0,1556
Glycosyl transferase	A9HH55	42961	38912	50550	36657	41035	41191	0,1597
N-acetyl-gamma-glutamyl-phosphate reductase	A9HLR0	30659	25632	28072	27186	24164	27020	0,1629
Putative prolyl-tRNA synthetases	A9HBP4	3586	3250	3492	2672	3511	3195	0,1633
Putative dihydro-orotase protein	A9GZR4	15386	15201	15182	16228	14887	16694	0,1679
6-phosphogluconate dehydrogenase, decarboxylating	A9H324	168528	140141	162242	139570	140873	####	0,1691
Uncharacterized protein	A9HAF1	13660	12702	17960	13994	12505	11855	0,1732
Bifunctional protein FolD	FOLD	24001	20878	26075	23296	18988	22283	0,1735
6-phosphogluconolactonase	A9H335	63021	24533	26815	26690	20409	22355	0,1762
Leucyl aminopeptidase	A9HJY3	10144	10513	10374	7887	8593	11072	0,1763
Nucleoside diphosphate kinase	NDK	56319	48407	66715	47561	53369	51527	0,1781
Insulinase protein	A9H438	26054	22343	20110	17282	21959	22120	0,1843
Putative phosphoserine aminotransferase	A9HLQ7	4468	6283	4500	5102	6407	5950	0,1843
Isocitrate dehydrogenase [NADP]	A9HBR3	25739	27521	17186	21075	18529	20392	0,1948
D-amino acid dehydrogenase	A9HMX8	25501	27892	24835	24775	25303	25151	0,1971
Glycine cleavage system H protein	A9HM50	5438	36328	39212	11843	18261	16493	0,2003
Electron transfer flavoprotein subunit beta	A9HEE6	65441	52447	53716	49037	53065	56140	0,2038
Inositol-3-phosphate synthase	A9H8S7	89079	76017	89207	92146	83277	93697	0,21
Elongation factor P	EFP	39283	32493	38796	38379	30581	33145	0,2118
Glyceraldehyde-3-phosphate dehydrogenase	A9HM29	284746	258204	252376	259405	####	####	0,2155
10 kDa chaperonin	A9HK46	24936	55695	50811	35881	27334	39782	0,2161
Putative amine oxidase	A9HGY5	4702	5851	4847	4845	5881	6017	0,2179
Uncharacterized protein	A9HMQ3	48937	56329	68820	56076	51946	49036	0,2183
Uncharacterized protein	A9H8H8	47881	45010	79291	42272	50368	47806	0,2192
Aminotransferase	A9H801	6016	5208	4318	4220	5190	4654	0,2218
Phosphoglycerate kinase	A9HM30	137521	135067	150272	133410	141271	134136	0,2221
Uncharacterized protein	A9H6W0	16413	17927	22684	21215	19964	21203	0,2229
Putative 2Fe-2S ferredoxin	A9HMI7	32438	31558	51109	29599	58093	55708	0,2249
Homoserine dehydrogenase	A9HCQ4	23215	25908	22908	24178	26601	24321	0,2278
S-adenosylmethionine synthase	METK	39688	38773	43113	39170	41166	36775	0,2311
Cytokinin riboside 5'-monophosphate phosphoribohydrolase	A9HEM3	23769	35275	40617	20253	33604	30257	0,2323
4-hydroxythreonine-4-phosphate dehydrogenase	A9HET4	9510	9193	12815	8588	9973	9792	0,2332
PEBP family protein	A9HBI3	35600	19492	24754	21848	24004	21472	0,2363
30S ribosomal protein S11	RS11	2816	4532	8704	4050	3356	4036	0,2363
UPF0303 protein GDI1201	A9HDU3	37038	31830	37740	33023	33698	35003	0,2398
Chemotaxis response regulator protein-glutamate methylesterase	A9HHG0	30135	24896	26832	26473	24539	26772	0,2409
Inosine-5'-monophosphate dehydrogenase	A9HID1	57449	65009	36395	46826	68818	68162	0,25
30S ribosomal protein S2	RS2	117359	93982	127530	112508	98851	####	0,2544
Putative MotA/TolQ/ExbB proton channel family protein	A9H6D5	4570	3185	3219	2341	3914	3327	0,2566
OmpW family protein	A9HED6	54519	21016	37644	48212	43444	44107	0,2595
Thioredoxin reductase	A9H0A5	15736	19201	12125	17694	18212	15917	0,263
Putative short-chain dehydrogenase	A9HLW8	36992	35163	35949	37475	27841	36404	0,2795
Succinate-semialdehyde dehydrogenase [NADP+]	A9HNC1	37410	23685	38136	33798	38177	37095	0,2813
Uncharacterized protein	A9HHE4	6455	5120	6402	4970	5783	6165	0,2824
Uncharacterized protein	A9HJX9	34136	36249	45578	44239	4992	40951	0,2849
Biopolymer transport protein ExbD/TolR	A9HF92	22445	12429	13981	21205	11066	7128	0,2906
2-dehydro-3-deoxyphosphooctonate aldolase	A9HJ79	8287	7295	6827	7325	8196	7793	0,2925
NADH dehydrogenase (Ubiquinone)	A9HKL6	21163	19679	18301	18034	19632	19706	0,2939
FAD linked oxidase domain protein	A9H1K4	17157	14729	15573	16042	15811	17052	0,2959
Peptidoglycan-associated protein	A9HB05	281723	104147	189930	161641	152103	####	0,307
Preprotein translocase, SecG subunit	A9HJ83	10232	10122	14984	9796	11676	10954	0,3073
Electron transfer flavoprotein alpha subunit	A9HEE9	65426	52787	59138	68835	48280	75049	0,3098
30S ribosomal protein S3	RS3	8732	1710	15509	9090	5159	4616	0,3112
Uncharacterized protein	A9HET8	6841	9482	13304	9751	12037	11125	0,3138

Dehydrogenase (Zinc-binding alcohol dehydrogenase)	A9H246	15343	19306	14058	15022	18283	18366	0,3189
Putative rod shape-determining protein mreB	A9HM98	12948	21198	18582	13341	24302	21322	0,3196
UDP-3-O-acylglucosamine N-acyltransferase	A9HKU5	11420	10944	12651	10071	12275	15073	0,3221
Inorganic pyrophosphatase	A9H4G5	163546	206490	251700	211348	####	####	0,3266
Putative 6-phosphogluconolactonase	A9HJ42	11702	10289	10101	8231	11090	11150	0,3266
Putative FeS assembly protein SufD	A9HRY4	13654	12739	10106	10345	12234	12112	0,3274
Histidinol dehydrogenase	A9HFM4	6689	5343	4505	4984	6085	6513	0,3406
Orotate phosphoribosyltransferase	A9HII0	36595	30606	37398	32775	33275	35400	0,3414
Conseved protein	A9H247	5998	7432	9116	8447	6257	6337	0,3432
Conserved protein	A9HBW8	18686	15550	14268	20776	13407	17398	0,3534
Uncharacterized protein	A9HCR3	6940	7381	8178	7436	7138	7453	0,3555
Glutamine synthetase	A9H7Z5	165905	264154	202616	232424	####	####	0,3574
60 kDa chaperonin 2	CH602	23250	21704	10776	20583	17907	21855	0,3692
Nicotinate-nucleotide pyrophosphorylase	A9H8C5	25666	25007	25645	22469	26095	26335	0,3717
Glutamate--cysteine ligase	A9H108	11496	11750	10010	9720	11306	11446	0,3765
4-hydroxy-3-methylbut-2-enyl diphosphate reductase	A9HS93	20290	19117	16707	17782	22583	12615	0,3798
Trehalose 6-phosphate phosphatase	A9HBU3	23037	19707	24450	24552	23808	20565	0,3863
60 kDa chaperonin 1	CH601	282648	231308	237526	231522	####	####	0,3864
Branched-chain-amino-acid aminotransferase	A9HNB7	41439	62399	28588	36834	42715	43043	0,3867
Phosphoribosylformylglycinamidine synthase subunit PurS	A9HJF5	29095	31848	39141	31123	36378	35661	0,3915
Putative outer membrane protein	A9H9Q6	16556	21537	20439	19580	20071	20281	0,3938
50S ribosomal protein L14	RL14	52351	41583	22446	39564	42727	42171	0,3939
Transcription termination factor Rho	A9HE94	15876	15892	11764	9081	22097	15757	0,3992
OmpA/MotB domain protein	A9GZP4	39607	38346	44697	75723	27849	31769	0,4047
Adenylyl-sulfate kinase	A9H0W3	5240	5031	3690	3966	5469	5026	0,4065
Conserved protein	A9HAR7	13091	10975	13807	11436	12898	12846	0,4138
Phosphoglucomutase	A9HSH5	56982	51480	52314	47382	54655	56449	0,4142
Uridylate kinase	A9HKW8	50307	46224	46511	50379	45472	45811	0,4172
Peptidase	A9HEL6	21018	20254	35546	29772	21103	22393	0,4237
Signal recognition particle protein	A9HS68	24100	26713	26101	23535	25939	26789	0,4356
Ubiquinone/menaquinone biosynthesis C-methyltransferase UbiE	A9HI27	40827	34214	37148	33631	40697	39344	0,4364
Biopolymer transport exbB protein	A9HF70	108746	133872	134935	115621	150103	118229	0,4434
Phosphoglycerate mutase	A9HBZ6	31890	29231	34477	39430	36500	22193	0,4457
Gamma-glutamyl phosphate reductase	A9HC10	4499	6151	4266	3392	6326	5648	0,4481
Dihydroxy-acid dehydratase	A9HA40	8169	7339	7340	6547	8066	8510	0,4492
50S ribosomal protein L6	RL6	34619	38326	25047	30975	35170	33523	0,4516
Alkyl hydroperoxide reductase/ Thiol specific antioxidant/ Mal allergen	A9H8D6	259795	207552	204001	226335	####	####	0,4522
Peptidase U62 modulator of DNA gyrase	A9HKF2	12041	11720	16720	15512	13567	10707	0,4594
Alcohol dehydrogenase zinc-binding domain protein	A9HNN4	19630	19659	16969	14742	21285	20798	0,47
Gluconokinase	A9HSC5	4905	4169	3594	3985	4448	4139	0,4715
Uncharacterized protein	A9H0Y9	33299	30629	41563	32132	38369	35850	0,4719
Aminopeptidase	A9HMM0	44991	42614	42629	42165	41612	46119	0,4745
Lipoprotein SmpA/OmlA family	A9HS35	17704	24189	28560	24052	21889	23843	0,4754
Phosphoribosylformylglycinamidine cyclo-ligase	A9HJV0	24407	28617	25707	19944	32046	27438	0,4776
Surface antigen protein	A9HAP4	47946	24250	20281	29604	32733	31787	0,4776
Argininosuccinate synthase	ASSY	49911	47312	40609	43291	47245	47864	0,4777
Zinc-type alcohol dehydrogenase-like protein	A9H2A8	10725	10328	17175	13058	14234	10523	0,4796
Uncharacterized protein	A9HEH6	6269	9113	8190	8025	8200	7214	0,4819
Ferredoxin--NADP reductase	A9HLF6	13438	9778	15404	15326	11317	12224	0,4851
Signal peptidase I	A9HKX7	5633	6142	6609	6954	5462	5942	0,4937
ATP-dependent protease subunit HslV	A9H1A3	38937	16101	35948	18740	22125	49550	0,4941
Putative ribose/galactose/methyl galactoside import ATP-binding protein	A9HPL1	9523	9608	5492	1	1	1	0,0132
Signal peptidase I	A9H4M0	9314	8899	8582	1	1	1198	0,0001
Putative transcriptional regulator, rrf2 family	A9HRZ0	6975	6445	7501	1	1	1034	7E-05
D-ribose-binding protein	A9HFZ1	9666	6861	10020	1	1	1504	0,0026
Putative sulfotransferase	A9HQQ2	8439	6665	4221	1	1144	1114	0,017
Guanylate kinase	A9HDA8	10109	6702	6578	1	1393	1458	0,0082
Putative phosphoenolpyruvate carboxylase	A9HRZ5	1346	1	2396	3602	2602	2460	0,0632
Uncharacterized protein	A9HBI5	46530	1	38399	11415	26160	14849	0,2675

*Acces. = Uniprot accession code; IC = Ion counts.

Table S3 - Detailed information of proteins from schematic illustration of *G. diazotrophicus* responses to osmotic stress

Localization	Accession	Description	Abbreviation	Number
Outer Membrane	A9HMV6	Polysaccharide export protein	CtrA	1
	A9H986	Membrane integrity-associated transporter subunit	PqiC	2
	A9HE38	TonB-dependent receptor	TonB-dependent receptor	3
	A9HNM4	TonB-dependent receptor	TonB-dependent receptor	4
	A9H7M7	TonB-dependent receptor	TonB-dependent receptor	5
	A9H7L9	TonB-dependent receptor	TonB-dependent receptor	6
	A9HEU6	TonB-dependent receptor	TonB-dependent receptor	7
	A9H7L3	TonB-dependent receptor	TonB-dependent receptor	8

	A9HDZ9	TonB-dependent receptor	TonB-dependent receptor	9
	A9H932	TonB-dependent receptor	TonB-dependent receptor	10
	A9HPF6	Porin	OprB	11
	A9HAM5	Porin	OprB	12
	A9HKV0	Outer membrane protein assembly factor	BamA	13
	A9H0L0	Outer membrane protein assembly factor	BamD	14
	A9HHH1	Flagellar L-ring protein	FlgH	15
Periplasmic	A9HK76	Iron ABC transporter substrate-binding protein	IBP	16
	A9H577	Sugar ABC transporter substrate-binding protein	Sugar ABC	17
	A9HPC7	Sugar ABC transporter substrate-binding protein	Sugar ABC	18
	A9HPE1	Sugar ABC transporter substrate-binding protein	Sugar ABC	19
	A9HNP0	D-xylose ABC transporter substrate-binding protein	XylF	20
	A9HPB9	Periplasmic binding protein/LacI Transcriptional regulator	RbsB	21
	A9HPK6	D-ribose-binding periplasmic protein	RbsB	22
	A9HB04	Tol-Pal system protein	TolB	23
	A9HL14	Superoxide dismutase	SodB	24
	A9HK81	Cytochrome c551 peroxidase precursor	CCP	25
	A9HBK9	Periplasmic serine endoprotease	DegQ	26
	A9H3H9	dTDP-4-dehydrorhamnose 3,5-epimerase	RfbC	27
	A9HSZ4	Uncharaterized protein	Unc	28
	A9H2X8	Methylamine dehydrogenase heavy chain precursor	MauB	29
	A9HKB6	Glutathione peroxidase	GPx	30
Inner Membrane	A9HFD7	Succinate dehydrogenase flavoprotein subunit	SdhA	31
	A9HMD4	Nitrogen regulatory protein P-II	GlnK	32
	A9HHE0	Chemoreceptor Methyl-accepting chemotaxis protein	McpA	33
	A9H9A1	ATPD ATP synthase subunit delta	AtpH	34
	A9HPJ3	Lipoprotein	MetQ	35
	A9HK15	Gluconate 2-dehydrogenase (Acceptor)	AdhB	36
	A9H192	Aldehyde dehydrogenase protein	XdhB	37
	A9HSY7	Putative conjugal transfer	TrbI	38
	A9H090	Dipeptidyl-peptidase	DPP	39
	A9H559	Isochorismatase hydrolase	ISH	40
	A9H3A3	Carboxy-terminal protease protein	CTPP	41
	A9HPE7	ABC transporter related	ABC	42
	A9HRU3	NUOB2 NADH-quinone oxidoreductase subunit B 2	NuoB2	43
	A9HRS8	NADH-ubiquinone/plastoquinone oxidoreductase chain 6	NuoJ	44
Cytoplasmic	A9HRU1	NADH-quinone oxidoreductase subunit C	NuoC	45
	A9HRT3	NADH-quinone oxidoreductase	NuoG	46
	A9HBU6	Alpha,alpha-trehalose-phosphate synthase	OtsA	47
	A9HBL5	Mannitol 2-dehydrogenase	MtlK	48
	A9HKU2	3-hydroxyacyl-[acyl-carrier-protein] dehydratase	FabZ	49
	A9HEX0	Biotin carboxylase protein	AccC	50
	A9HI49	Glutamine--fructose-6-phosphate aminotransferase	GlmS	51
	A9HI46	GlmU Bifunctional protein	GlmU	52
	A9HE46	Acetyl-CoA C-acyltransferase	FadA	53
	A9HLY3	Septum site-determining protein	MinD	54

7.2 Supplementary material from Chapter 2

Table S1 Detailed live and dead cells counting of *G. diazotrophicus* wild-type and Δ*degP* exposed to NaCl

								Avarage	SD
0 mM NaCl GDwt	**Number of live cells**	115	123	127	118	122	113	119,67	5,278888772
	Number of dead cells	8	5	6	5	7	6	6,17	1,169045194
	Total of cells	123	128	133	123	129	119	125,83	5,076087732
	Percentage of live cells	93,50	96,09	95,49	95,93	94,57	94,96	95,09	0,970107335
	Percentage of dead cells	6,50	3,91	4,51	4,07	5,43	5,04	4,91	0,970107335

								Avarage	SD
50 mM NaCl GDwt	**Number of live cells**	124	135	103	127	131	132	125,33	11,60459679
	Number of dead cells	18	16	8	10	12	18	13,67	4,273952113
	Total of cells	142	151	111	137	143	150	139,00	14,68332387
	Percentage of live cells	87,32	89,40	92,79	92,70	91,61	88,00	90,30	2,393283735
	Percentage of dead cells	12,68	10,60	7,21	7,30	8,39	12,00	9,70	2,393283735

								Avarage	SD
100 mM NaCl GDwt	**Number of live cells**	97	87	93	104	97	105	97,17	6,765106552
	Number of dead cells	3	4	5	3	5	7	4,50	1,516575089
	Total of cells	100	91	98	107	102	112	101,67	7,284687136
	Percentage of live cells	97,00	95,60	94,90	97,20	95,10	93,75	95,59	1,317188092
	Percentage of dead cells	3,00	4,40	5,10	2,80	4,90	6,25	4,41	1,317188092

								Avarage	SD
150 mM NaCl GDwt	**Number of live cells**	53	67	52	57	68	72	61,50	8,5498538
	Number of dead cells	3	5	5	6	6	5	5,00	1,095445115
	Total of cells	56	72	57	63	74	77	66,50	9,049861877
	Percentage of live cells	94,64	93,06	91,23	90,48	91,89	93,51	92,47	1,548568213
	Percentage of dead cells	5,36	6,94	8,77	9,52	8,11	6,49	7,53	1,548568213

								Avarage	SD
200 mM NaCl GDwt	**Number of live cells**	7	6	9	7	7	8	7,33	1,032795559
	Number of dead cells	6	8	4	6	6	12	7,00	2,75680975
	Total of cells	13	14	13	13	13	20	14,33	2,804757862
	Percentage of live cells	53,85	42,86	69,23	53,85	53,85	40,00	52,27	10,33707162
	Percentage of dead cells	46,15	57,14	30,77	46,15	46,15	60,00	47,73	10,33707162

								Avarage	SD
250 mM NaCl GDwt	**Number of live cells**	14	16	11	16	17	16	15,00	2,19089023
	Number of dead cells	49	60	42	37	61	49	49,67	9,542885657
	Total of cells	63	76	53	53	78	65	64,67	10,7827022
	Percentage of live cells	22,22	21,05	20,75	30,19	21,79	24,62	23,44	3,578432085
	Percentage of dead cells	77,78	78,95	79,25	69,81	78,21	75,38	76,56	3,578432085

								Avarage	SD
0 mM NaCl Δ*degP*	**Number of live cells**	115	123	127	118	122	113	119,67	5,278888772
	Number of dead cells	8	5	6	5	7	6	6,17	1,169045194
	Total of cells	123	128	133	123	129	119	125,83	5,076087732
	Percentage of live cells	93,50	96,09	95,49	95,93	94,57	94,96	95,09	0,970107335
	Percentage of dead cells	6,50	3,91	4,51	4,07	5,43	5,04	4,91	0,970107335

								Avarage	SD
50 mM NaCl Δ*degP*	**Number of live cells**	124	135	103	127	131	132	125,33	11,60459679
	Number of dead cells	18	16	8	10	12	18	13,67	4,273952113
	Total of cells	142	151	111	137	143	150	139,00	14,68332387
	Percentage of live cells	87,32	89,40	92,79	92,70	91,61	88,00	90,30	2,393283735
	Percentage of dead cells	12,68	10,60	7,21	7,30	8,39	12,00	9,70	2,393283735

								Avarage	SD
100 mM NaCl Δ*degP*	**Number of live cells**	53	67	52	57	68	72	61,50	8,5498538
	Number of dead cells	43	45	48	57	49	52	49,00	5,019960159
	Total of cells	96	112	100	114	117	124	110,50	10,57827963
	Percentage of live cells	55,21	59,82	52,00	50,00	58,12	58,06	55,54	3,865010682
	Percentage of dead cells	44,79	40,18	48,00	50,00	41,88	41,94	44,46	3,865010682

								Avarage	SD
150 mM NaCl Δ*degP*	**Number of live cells**	3	5	5	6	6	5	5,00	1,095445115
	Number of dead cells	53	45	55	42	41	39	45,83	6,645800679
	Total of cells	56	50	60	48	47	44	50,83	6,013872851
	Percentage of live cells	5,36	10,00	8,33	12,50	12,77	11,36	10,05	2,831142908
	Percentage of dead cells	94,64	90,00	91,67	87,50	87,23	88,64	89,95	2,831142908

								Avarage	SD
200 mM NaCl Δ*degP*	**Number of live cells**	10	25	30	30	32	31	26,33	8,358628277
	Number of dead cells	124	135	103	127	131	132	125,33	11,60459679
	Total of cells	134	160	133	157	163	163	151,67	14,2501462
	Percentage of live cells	7,46	15,63	22,56	19,11	19,63	19,02	17,23	5,269577843
	Percentage of dead cells	92,54	84,38	77,44	80,89	80,37	80,98	82,77	5,269577843

								Avarage	SD
250 mM NaCl Δ*degP*	**Number of live cells**	1	2	1	3	2	1	1,67	0,816496581
	Number of dead cells	98	100	99	97	95	93	97,00	2,607680962
	Total of cells	99	102	100	100	97	94	98,67	2,804757862
	Percentage of live cells	1,01	1,96	1,00	3,00	2,06	1,06	1,68	0,807197399
	Percentage of dead cells	98,99	98,04	99,00	97,00	97,94	98,94	98,32	0,807197399

*GDwt = *G. diazotrophicus* wild-type

Table S2 Detailed ISOQuant processing configuration

Parameter	Value
isoquant.pluginQueue.name	design project and run ISOQuant analysis
process.peptide.deplete.PEP_FRAG_2	false
process.peptide.deplete.CURATED_0	false
process.peptide.statistics.doSequenceSearch	false
process.emrt.minIntensity	1000
process.emrt.minMass	500
process.emrt.rt.alignment.match.maxDeltaMass.ppm	10
process.emrt.rt.alignment.match.maxDeltaDriftTime	2
process.emrt.rt.alignment.normalizeReferenceTime	false
process.emrt.rt.alignment.maxProcesses	8
process.emrt.rt.alignment.referenceRun.selectionMethod	AUTO
process.emrt.clustering.preclustering.orderSequence	MTMTMT
process.emrt.clustering.preclustering.maxDistance.mass.ppm	6.06E-6
process.emrt.clustering.preclustering.maxDistance.time.min	0,202
process.emrt.clustering.preclustering.maxDistance.drift	2,02
process.emrt.clustering.distance.unit.mass.ppm	6.0E-6
process.emrt.clustering.distance.unit.time.min	0,2
process.emrt.clustering.distance.unit.drift.bin	2
process.emrt.clustering.dbscan.minNeighborCount	2
process.identification.peptide.minReplicationRate	2
process.identification.peptide.minScore	6
process.identification.peptide.minOverallMaxScore	6
process.identification.peptide.minSequenceLength	6
process.identification.peptide.acceptType.PEP_FRAG_1	true
process.identification.peptide.acceptType.IN_SOURCE	false
process.identification.peptide.acceptType.MISSING_CLEAVAGE	true
process.identification.peptide.acceptType.NEUTRAL_LOSS_H20	false
process.identification.peptide.acceptType.NEUTRAL_LOSS_NH3	false
process.identification.peptide.acceptType.PEP_FRAG_2	true
process.identification.peptide.acceptType.DDA	false
process.identification.peptide.acceptType.VAR_MOD	true
process.identification.peptide.acceptType.PTM	true
process.annotation.peptide.maxSequencesPerEMRTCluster	1
process.annotation.protein.resolveHomology	true
process.annotation.peptide.maxFDR	0,01
process.annotation.useSharedPeptides	all
process.normalization.lowess.bandwidth	0,3
process.normalization.orderSequence	XPIR
process.normalization.minIntensity	3000
process.quantification.peptide.minMaxScorePerCluster	6
process.quantification.peptide.acceptType.IN_SOURCE	false
process.quantification.peptide.acceptType.MISSING_CLEAVAGE	true
process.quantification.peptide.acceptType.NEUTRAL_LOSS_H20	false
process.quantification.peptide.acceptType.NEUTRAL_LOSS_NH3	false

process.quantification.peptide.acceptType.PEP_FRAG_1	true
process.quantification.peptide.acceptType.PEP_FRAG_2	true
process.quantification.peptide.acceptType.VAR_MOD	true
process.quantification.peptide.acceptType.PTM	true
process.quantification.peptide.acceptType.DDA	false
process.quantification.topx.degree	3
process.quantification.topx.allowDifferentPeptides	true
process.quantification.minPeptidesPerProtein	2
process.quantification.absolute.standard.entry	ENO1_YEAST
process.quantification.absolute.standard.fmol	50
process.quantification.topx.allowDifferentPeptides	true
process.quantification.absolute.standard.entry	ENO1_YEAST
process.quantification.absolute.standard.fmol	50
process.quantification.maxProteinFDR	0,01

Table S2 Proteins identified in *G. diazotrophicus* exposed to salt stress

Description	Accession	IC Control 1	IC Control 2	IC Control 3	IC NaCl 1	IC NaCl 2	IC NaCl 3
Aldehyde Dehydrogenase (AldA)	A9H4V7	97112	88276	96370	139962	148862	134485
Conserved protein (GDI0283)	A9H314	22481	21408	23243	37737	34072	29152
Alanine--tRNA ligase (AlaS)	A9HL73	3086	3617	2892	5573	4609	4254
Uroporphyrinogen decarboxylase (HemE)	DCUP	15295	13872	15432	22178	21610	23577
Methionine--tRNA ligase (MetG)	A9HIA3	3692	3491	3049	6090	5067	4431
Thiamine-phosphate pyrophosphorylase (ThiE)	A9HI58	14252	15123	15262	22577	22009	23473
Succinate-semialdehyde dehydrogenase [NADP+] (GabD)	A9HNC1	37410	23685	38136	48632	46846	56050
Ribosome-binding ATPase (YchF)	A9HC06	6496	7345	6481	9976	10456	10648
dCTP deaminase (Dcd)	A9HFN2	22106	22161	26046	41037	36901	29665
50S ribosomal protein L10 (RplJ)	RL10	65663	42144	49111	69188	70324	100836
NADH-quinone oxidoreductase subunit C (NouC)	A9HRU1	19917	19728	19922	30376	28516	32595
Orotidine 5'-phosphate decarboxylase (PyrF)	A9HES3	8828	8143	10331	14387	11811	15921
Histidine--tRNA ligase (HisS)	SYH	10066	11230	9418	13734	14992	18816
FeS assembly protein (SufB)	A9HRY9	1985	2339	1782	2966	3018	3481
Putative penicillin-binding protein (PBP)	A9H435	14837	14420	16274	25427	21625	23858
4-hydroxythreonine-4-phosphate dehydrogenase (PdxA)	A9HET4	9510	9193	12815	18817	15856	15404
1-deoxy-D-xylulose 5-phosphate reductoisomerase (Dxr)	A9HKV5	9646	10512	8573	15569	15599	14622
Phosphoglycerate mutase (GpmB)	A9HBZ6	31890	29231	34477	46212	57714	49786
UPF0303 protein (GDI1201)	A9HDU3	37038	31830	37740	56435	62359	52789
60 kDa chaperonin 2 (GroL2)	CH602	23250	21704	10776	29775	31467	28779
Alcohol dehydrogenase (Adh)	A9HBQ8	2470	3541	2316	5358	3860	4376
Polyribonucleotide nucleotidyltransferase (Pnp)	PNP	19114	23901	17079	30995	33279	34218
Cysteine synthase (GDI1480)	A9HFX5	19618	19935	18362	31862	31576	32625
Uncharacterized protein (GDI1335)	A9HET8	6841	9482	13304	17832	17779	14092
Glycine dehydrogenase (decarboxylating) (GcvP)	A9HM48	3078	3428	2870	5607	5050	5165
Putative 2-keto-4-pentenoate hydratase-like (GDI1198)	A9HDT5	20919	25917	22798	32519	49109	36451
Putative nitroreductase family protein (GDI0074)	A9GZY4	12328	10279	12862	21249	19517	19409
Transketolase (TktA)	A9H317	132450	137477	118157	221890	229899	211334
Phosphoglycolate phosphatase (gpH)	A9HI43	30102	29703	25985	49292	45849	51484
Aspartate--tRNA(Asp/Asn) ligase (AspS)	A9HLJ4	4229	5196	3143	6634	7918	7112
Serine protease (DegP)	A9HEK6	83759	69192	80154	132679	140887	128492
Uncharacterized protein (GDI1748)	A9HHW9	18362	15671	23023	40855	25172	32959

Inosine-guanosine kinase	A9H9C0	6643	6993	7275	11924	11812	12715
Elongation factor G	A9HS02	24102	27025	18735	43392	41183	38402
Putative xanthine dehydrogenase	A9H189	7637	9297	9301	17795	16751	11733
Putative phosphoglycolate phosphatase	A9HJN8	3145	2841	3567	5395	5524	6057
Preprotein translocase (SecG)	A9HJ83	10232	10122	14984	22650	21084	19229
Conserved protein (GDI0912)	A9HBT6	10132	9012	11374	15649	20317	18781
Aldehyde dehydrogenase	A9H192	4596	4704	4373	7147	9619	7936
Protein-export protein (SecB)	A9HK92	31442	52286	47362	78396	71229	87364
Carboxymethylenebutenolidase	A9HK54	20463	23079	20537	41213	34464	40755
D-2-hydroxyacid dehydrogensase	A9HDT4	114319	107563	92881	182586	176090	219795
Conserved protein	A9HFQ7	30178	25354	32555	38919	69600	56292
Uncharacterized protein	A9HBG4	7343	9327	9301	18253	17555	13224
Succinate-semialdehyde dehydrogenase (GabD)	A9H549	30322	37862	30023	57619	61817	66077
Probable cytosol aminopeptidase (PepA)	A9H1J4	13611	19483	11667	23217	28764	33039
NADP oxidoreductase coenzyme F420-dependent	A9HL93	18881	22546	27343	44624	46591	40912
Uncharacterized protein	A9HCR3	6940	7381	8178	16065	14675	12848
S-(hydroxymethyl)glutathione dehydrogenase (FrmA)	A9HIP1	13297	14072	10730	24214	26306	23325
Dihydrolipoyl dehydrogenase (LpdA)	A9HJB6	14528	9352	15901	26200	22430	28966
Indole-3-glycerol phosphate synthase (TrpC)	A9HJA0	15921	16413	14977	30427	31367	33150
NAD(P)H nitroreductase (GDI0595)	A9H8I9	5915	6583	9631	16136	14984	13609
Conserved protein	A9H3Z0	3615	3756	3874	7951	7248	7781
Putative aldehyde dehydrogenase A (aldA)	A9HEG7	1536	1378	1264	2912	2976	2702
50S ribosomal protein (RplP)	RL16	10854	7385	16035	20676	25273	25615
Phosphoribosylformylglycinamidine synthase (PurQ)	A9HJG0	14467	9712	9384	22458	20009	27753
Alpha,alpha-trehalose-phosphate synthase (OtsA)	A9HBU6	8901	7241	6972	13775	15150	20060
Isochorismatase hydrolase	A9H559	4112	4207	4915	8885	9295	9882
Chaperone protein (HtpG)	A9HLJ9	19630	24778	21570	47427	50014	45809
Gluconokinase	A9HSC5	4905	4169	3594	9155	11671	7067
Deoxyuridine 5'-triphosphate nucleotidohydrolase	A9HI24	16355	15103	14814	35066	34753	32243
Glutaredoxin	A9HJG8	80535	65185	57455	138882	166821	144351
Methylenetetrahydrofolate reductase (MetF)	A9HNY2	8037	8551	6800	10827	20508	20708
Pyruvate dehydrogenase E1 component subunit beta (PdhB)	A9HJA9	33049	41431	24661	83493	66289	73171
Putative prolyl-tRNA synthetases OS	A9HBP4	3586	3250	3492	8160	8631	6589
Chemoreceptor (McpA)	A9HHE0	14031	16127	14940	40051	31162	31422
Endoribonuclease L-PSP	A9HBS7	14716	22718	25026	46280	45845	51740
Putative nitrogen fixation protein (NifU)	A9HFA7	25413	16591	20537	42514	58301	47381
Fumarate hydratase class I (FumA)	A9HBG7	13750	10556	13731	29954	30432	30100
Ribose-5-phosphate isomerase A (RpiA)	A9H338	16507	18082	16652	41603	40359	40133
Acetyltransferase (PdhC)	A9HJB2	16766	19250	12642	39841	39614	36890
30S ribosomal protein S5 (RpsE)	RS5	10676	6186	22495	30198	33168	30895
Transaldolase (Tal)	A9H320	79700	80220	67267	184248	165922	200293
Glutamine--fructose-6-phosphate aminotransferase	A9HI49	6138	6812	5008	15593	13225	15630
Mannitol 2-dehydrogenase (MtlK)	A9HBL5	21648	32962	31332	74971	70313	68546
50S ribosomal protein L15	RL15	7448	7996	5344	14074	18353	21221
Uncharacterized protein	A9H9H3	7067	5620	7136	18995	15901	16652
30S ribosomal protein S3	RS3	8732	1710	15509	21729	19146	26769
Uncharacterized protein	A9H6W0	16413	17927	22684	53579	43764	54077
Outer membrane efflux protein	A9H3U0	3843	4005	4414	9343	10771	12459
Arginine--tRNA ligase	A9HLH8	2963	2264	2840	7034	7738	7739
NADH-quinone oxidoreductase subunit F (NouF)	A9HRT4	1938	1781	1985	5153	5109	6295
Glucose-6-phosphate 1-dehydrogenase (Zwf)	A9H326	11712	12817	10894	32591	29798	41657
Acetoin(Diacetyl) reductase	A9HHS9	11996	12500	12531	40849	34204	34442
30S ribosomal protein S6	RS6	3931	3143	2431	7809	10520	10533
GMP synthase [glutamine-hydrolyzing]	A9H085	3710	4515	2919	12153	11139	10544
Ketol-acid reductoisomerase (NADP(+)) (IlvC)	ILVC	11925	13750	11762	40923	37797	34960
3-hydroxyacyl-[acyl-carrier-protein] dehydratase (FabZ)	FABZ	2832	3167	4575	13325	12519	6294
NADH-ubiquinone (NouJ)	A9HRS8	3305	4020	3289	10776	10950	11319
Lysine--tRNA ligase (LysS)	A9HK29	4725	4962	4771	16861	14559	14422
Phosphoribosylformylglycinamidine synthase (PurL)	A9HJG3	6704	7469	6436	23330	21076	21539
Flagellar motor protein (MotA)	A9H6D5	4570	3185	3219	11987	12266	12044
Adenosylhomocysteinase	A9HFJ7	13661	16003	12697	47422	51294	45928
Malate dehydrogenase (Oxaloacetate-decarboxylating)	A9HH05	6367	6137	4127	19056	12444	26181

Carbamoyl-phosphate synthase large chain	A9H1P7	3453	4011	3590	11988	13533	13958
6-phosphogluconate dehydrogenase NAD-binding	A9HL10	7546	7322	7872	32274	27324	26809
2-oxoglutarate dehydrogenase E1 component (SucA)	A9HFG6	3713	3881	3027	10005	16201	19087
5-methyltetrahydropteroyltriglutamate (MetE)	A9HNX4	13650	16176	14609	148169	160930	147906
TonB-dependent siderophore receptor	A9H7L3	23309	19260	17889	-1	-1	-1
TonB-dependent siderophore receptor	A9HNM4	16703	14455	18560	-1	-1	-1
Signal peptidase I	A9H4M0	9314	8899	8582	-1	-1	-1
D-ribose-binding protein (RbsB)	A9HFZ1	9666	6861	10020	-1	-1	-1
Putative ribose import ATP-binding protein (RbsA)	A9HPL1	9523	9608	5492	-1	-1	-1
TonB-dependent siderophore receptor	A9H7L9	8142	7346	8209	-1	-1	-1
Putative sulfotransferase	A9HQQ2	8439	6665	4221	-1	-1	-1
TonB-dependent siderophore receptor	A9HDZ9	7493	5416	5544	-1	-1	-1
Uncharacterized protein OS	A9HPC7	6086	5756	5519	-1	-1	-1
Uncharacterized protein OS	A9HLD4	2758	2576	2207	-1	-1	-1
Extracellular solute-binding protein family 1 OS	A9HPE1	117396	110781	113835	3969	3225	3293
TonB-dependent siderophore receptor	A9H7M7	42522	35380	44423	2159	1992	1750
Putative periplasmic binding proteins	A9H577	76805	66814	81078	7016	3799	6396
D-ribose-binding periplasmic protein (RbsB)	A9HPK6	133803	120500	141151	17092	11926	14950
D-xylose ABC transporter (XylF)	A9HNP0	140312	137276	124315	19312	14455	16919
TonB-dependent siderophore receptor	A9HEU6	109797	104767	115235	14223	14777	13624
Rieske (2Fe-2S) domain protein	A9HL46	36484	25811	24150	4229	4694	3193
Phosphoenolpyruvate carboxykinase (PckA)	A9H8M9	17023	16390	14957	2151	2126	2536
PrkA serine protein kinase	A9HIB1	25954	24381	15475	3815	3450	2959
Methylamine dehydrogenase heavy chain (MauB)	A9H2X8	15420	17195	22185	2293	3687	2793
CRISPR-associated protein, Cse4 family	A9HLC8	26973	27332	26409	3868	5594	4174
Outer membrane protein assembly factor (BamA)	A9HKV0	23373	17503	19143	3862	4347	3934
Putative L-amino-acid oxidase	A9HN63	16864	15791	16636	2503	3611	3913
Uncharacterized protein	A9HJS1	17454	15097	16868	3758	2967	4041
Multidrug resistance protein A (EmrA)	A9H3B5	14110	15090	14416	2836	3812	3213
ATP synthase subunit delta (AtpH)	ATPD	14426	11096	6253	2120	3462	1669
Dipeptidyl-peptidase	A9H090	59700	46316	53567	10858	14126	11986
Periplasmic binding protein (RbsB)	A9HPB9	163399	156770	176417	40637	38288	39886
Alcohol dehydrogenase (GroES)	A9H073	10127	10082	10880	2749	2229	2488
TonB-dependent siderophore receptor	A9HFL0	10281	8295	9035	2525	2564	1551
Peptidase	A9HEL6	21018	20254	35546	5854	6459	6376
Site-determining protein (MinD)	A9HLY3	115052	168128	96062	32975	29296	30220
Uncharacterized protein	A9H8I6	14154	12695	12090	2332	4719	2485
Periplasmic binding protein	A9HK76	33352	27478	34327	7184	9279	7477
Porin	A9HAM5	11698	10565	12020	3311	3254	2373
Conserved protein	A9H282	15245	13002	13658	3491	3728	3735
TonB-dependent siderophore receptor OS	A9HE38	114344	117560	139966	25427	37456	34608
Outer membrane protein assembly factor (BamD)	A9H0L0	10227	14443	10729	2388	4792	2687
Uncharacterized protein	A9HJX9	34136	36249	45578	4251	2323	26074
3'(2'),5'-bisphosphate nucleotidase (CysQ)	A9H1J6	14043	16465	14972	4198	4520	4320
Putative Ubiquinol-cytochrome c reductase	A9H861	21667	19846	19235	5002	5962	6535
Uncharacterized protein	A9HSZ4	24623	23360	23123	4588	9540	6479
Transcription termination factor (Rho)	A9HE94	15876	15892	11764	3642	4409	4569
Succinate--CoA ligase [ADP-forming] subunit alpha (SucD)	A9HRF1	26605	22293	20499	7178	6392	6603
Flagellar L-ring protein	A9HHH1	8476	7543	9896	2855	2410	2461
Putative pyruvate dehydrogenase E2 component	A9HHP4	15752	14862	16983	4566	4685	5335
Alcohol dehydrogenase (AdhA)	A9HK12	54247	48458	48507	15031	16983	15081
Putative two component response regulator	A9HH92	7232	6812	7363	2056	2201	2420
DEAD/DEAH box helicase domain protein	A9H0S9	16900	15624	15575	4403	5341	5810
TonB-dependent siderophore receptor	A9HFV5	112497	105040	121352	35291	40373	35382
D-amino acid dehydrogenase	A9HMX8	25501	27892	24835	10476	7570	7607
Uncharacterized protein	A9HM07	13706	11577	15341	5084	4144	4125
50S ribosomal protein	A9H3M8	96141	75807	95036	20558	39699	28112
2-isopropylmalate synthase	A9HMA2	30103	30153	25926	8882	10309	9488
Conservev protein	A9GZU8	22739	19524	14528	7249	6883	4945
50S ribosomal protein L4	RL4	23763	20618	18279	5195	7876	7987
50S ribosomal protein L14	RL14	52351	41583	22446	9935	8171	21877
Adenylate kinase	KAD	36155	26647	25905	9186	13889	8143

ABC transporter related	A9HPE7	55771	59603	49596	27269	16756	15212
Fructose-bisphosphate aldolase class 1	A9H6A5	80938	73480	62321	16222	39222	23676
Conjugal transfer	A9HT68	86724	70706	69436	28128	27856	29925
Outer membrane protein (OprM)	A9HEG4	15550	16161	18855	6105	6580	6506
Serine--tRNA ligase	SYS	32201	23622	31223	10298	13813	9005
tRNA pseudouridine synthase B	TRUB	13223	11216	14552	4286	5284	5319
Insulinase protein	A9H438	26054	22343	20110	9524	8852	8723
Conserved protein	A9HIX3	47600	47323	56548	19934	20561	19896
Isocitrate dehydrogenase [NADP]	A9HBR3	25739	27521	17186	8283	9816	10217
Chorismate synthase	AROC	5613	4549	4461	1849	2072	1980
PKHD-type hydroxylase	Y1238	56758	35779	45751	17381	26036	12757
Uncharacterized protein	A9HCT2	25310	23505	14170	11185	7042	7540
50S ribosomal protein L25	RL25	57489	59186	58487	23775	23858	25189
3-oxoacyl-[acyl-carrier-protein] reductase	A9HPF0	31849	36597	27571	13835	14385	12236
Putative oxidoreductase	A9HM21	20107	14706	15329	6634	9228	5396
Type II and III secretion system protein	A9HHL5	13905	11986	13635	4794	6244	5764
50S ribosomal protein L6	RL6	34619	38326	25047	12759	13128	16380
Oxygen-dependent coproporphyrinogen-III oxidase	A9HK65	15889	13723	16914	5884	8269	6052
Putative serine carboxypeptidase	A9HS00	10215	11148	13017	4750	5495	4812
Cold-shock DEAD box protein A homolog	A9HRW6	5577	6550	3844	2112	2339	2590
Putative aldo-keto reductase	A9HQR7	10116	10203	11481	4674	4453	4893
Metal-dependent carboxypeptidase	A9HKD9	7876	7169	6916	2873	3132	3685
Catalase	A9GZZ4	194730	170405	104876	69498	68732	69294
Tol-Pal system protein TolB	A9HB04	95765	102937	99343	52042	40217	39456
Glutathione peroxidase	A9HKB6	9330	8838	6096	3219	4901	2605
Ribosomal RNA large subunit methyltransferase E	A9HIS5	9384	8704	9476	3695	4014	4515
Carboxy-terminal protease protein	A9H3A3	55542	51197	53196	24919	24679	21436
Putative NAD dependent epimerase	A9H2U3	10100	9876	8439	4086	4651	3964
Ribulokinase	A9HPD7	26783	23735	26854	17175	11088	6747
Exodeoxyribonuclease III Xth	A9HIE6	11700	8286	7661	4067	4026	4763
Phenylalanine--tRNA ligase beta subunit	A9H165	11742	12560	10595	4972	5324	5938
Glycerol-3-phosphate dehydrogenase	A9HHX8	22313	21537	13140	8457	10948	7205
TonB-dependent siderophore receptor	A9H932	39188	30956	33429	15674	16110	16933
Gluconate 2-dehydrogenase (Acceptor)	A9HK15	97541	87250	85367	42862	47947	37553
Putaive gamma-glutamyltranspeptidase	A9H4A8	8810	6884	9544	3554	4076	4420
ATP-dependent protease ATPase subunit HslU	A9H199	13099	12454	7898	5422	5425	5138
Glutamine synthetase	A9H7Z5	165905	264154	202616	105173	116773	87505
Uncharacterized protein	A9HKE4	10772	12211	12826	5655	6156	5726
Putative pilus assembly protein	A9HHL8	10753	9848	9527	4686	4582	5526
Tryptophan--tRNA ligase	A9HIP8	8307	11380	8949	3417	5308	5553
Oxidoreductase protein	A9HL82	4685	4517	4247	2211	1900	2657
Putative conjugal transfer	A9HSY7	14273	9479	12068	6219	6660	5191
Ferritin Dps family protein	A9HB55	25359	23280	32647	11725	18923	11225
Putative Acetyl-CoA acetyltransferase	A9HE46	6955	6232	6049	3452	2986	3482
Serine hydroxymethyltransferase	A9HRP5	39844	36746	28758	18557	20578	15234
Cold shock-like protein (CspE)	A9HIW8	96850	63429	79882	39192	43016	42322
Putative DNA-binding response regulator (MtrA)	A9HIE2	18916	20140	21095	7780	10899	12523
Molybdopterin biosynthesis protein (MoeB)	A9HEI1	7294	8057	9220	4587	3593	4596
Transcriptional regulator LysR	A9H0A8	79618	75054	69701	37556	43181	37681
Peptide chain release factor 2	A9HF65	11828	12212	13408	6327	6997	6455
Putative regulatory protein	A9HF98	22586	21942	19857	10618	14201	9240
Oxidoreductase	A9HAF3	83766	79655	84949	44057	42034	45600
NAD(P)H dehydrogenase (quinone)	NQOR	27064	28612	28101	15362	15330	13736
Transcription termination/antitermination protein (NusG)	A9H988	35642	32564	35613	17268	19736	18565
Serine endoprotease (DegQ)	A9HBK9	19462	19862	22964	11450	10884	11814
Trigger factor	TIG	99098	97247	83449	49405	54102	50320
Cold-shock DNA-binding domain protein	A9HK34	15766	16600	19171	9577	8748	10157
Putative ribonuclease	A9HKL8	6485	6414	6842	3473	3196	4268
Proline--tRNA ligase	A9HRR5	23529	20962	16900	10646	11549	11862
Quinolinate synthase A (NadA)	A9H8C0	40460	39360	39638	22114	22482	21686
50S ribosomal protein L11 (RplK)	RL11	32850	25228	26987	15416	16754	15203
Fucose operon fucU protein (FucU)	A9HPM0	7221	6709	6583	4303	3403	3775

50S ribosomal protein L1 (RplA)	RL1	77417	73297	69477	44234	44819	35519
Histidinol-phosphate aminotransferase	HIS8	13922	14756	15678	7800	8922	8419
Cell division protein (FtsZ)	A9H0K4	27164	33097	26171	17474	15312	16212
Octanoyltransferase	LIPB	6716	7850	7329	3603	4888	4022
Secretion protein, HlyD-family	A9HA48	10511	9387	9295	4458	7013	5289
Anthranilate phosphoribosyltransferase	A9HJ97	14779	14482	13380	9074	6634	8978
Amidinotransferase	A9HNM6	9294	9418	9336	5174	5368	5704
Folate-binding protein (YgfZ)	A9H151	16479	14691	15798	9702	8441	9201
Uncharacterized protein	A9H3D7	14471	13041	14606	8364	9039	7429
Flavin-dependent thymidylate synthase	A9HBG1	18045	15190	16649	7669	10320	11748
Aminotransferase class-III	A9HJT9	9842	12936	12015	7146	6055	7572
ATP synthase subunit alpha	ATPA	97406	102779	92992	58479	57196	60901
Putative amidohydrolase	A9HMC5	19364	13515	17043	9007	9789	11282
Putative L-asparaginase II protein	A9HE73	29167	24523	30460	16932	16338	17548
Pyridine nucleotide-disulphide oxidoreductase	A9HDE6	66822	64584	66248	38313	41325	40180
Flavin oxidoreductase	A9H2N2	47945	44036	45580	24574	28842	30779
1-deoxy-D-xylulose-5-phosphate synthase OS	A9HIR0	9654	11030	10237	6354	6157	6628
Ornithine carbamoyltransferase OS	A9HFT5	17731	17301	17329	11277	10286	10949
Putative ABC transporter ATP-binding protein	A9HKM9	14984	13072	16242	8462	9581	9628
Methionyl-tRNA formyltransferase OS	FMT	6753	7034	7269	3699	5245	4267
ABC transporter ATP-binding protein OS	A9H4G2	11380	10737	7664	5981	6819	6020
Acetylornithine aminotransferase OS	A9HFT8	41494	38087	43222	28346	23233	26128
30S ribosomal protein S1 OS	A9H459	39648	47724	35654	23701	27156	27033
Cysteine synthase OS	A9HAE5	39743	36767	39038	24197	25792	23503
Methylthioribose-1-phosphate isomerase OS	A9HLJ6	11089	12002	13246	7711	7283	8132
S-methyl-5'-thioadenosine phosphorylase OS	A9HK57	48109	65191	47740	33300	34051	35197
ATP synthase gamma chain OS	ATPG	45780	44307	57688	27128	32637	34758
Putative N-carbamoyl-L-amino acid amidohydrolase OS	A9HJT7	8631	7417	7400	4684	5269	5123
Outer-membrane lipoprotein carrier protein OS	A9H103	10415	8605	10455	6936	5750	6301
Putative outer membrane protein OS	A9H9Q6	16556	21537	20439	10491	13298	14107
Outer membrane protein OS	OMPC	209496	262664	239220	180685	167597	118855
Oxidoreductase (Aldo/keto reductase) protein OS	A9H614	8210	10336	8618	4814	5819	7313
Aspartate-semialdehyde dehydrogenase OS	A9HFE5	25322	27076	27004	16309	16881	19276
Glycerol kinase OS	A9HHY3	144661	147592	128599	94185	90170	95076
50S ribosomal protein L19 OS	RL19	24046	31177	23056	18098	15470	18409
Glycine cleavage system aminomethyltransferase T OS	A9HM51	38024	40765	43492	27849	25285	28438
Putative 6-phosphogluconolactonase OS	A9HJ42	11702	10289	10101	6008	7785	7688
Elongation factor Ts OS	A9HRQ5	73228	64359	49401	35650	39076	51594
Aminopeptidase OS	A9HMM0	44991	42614	42629	29849	28557	30249
Aldo/keto reductase family OS	A9HF59	14254	14037	14104	8380	9543	10954
Hopanoid-associated sugar epimerase OS	A9HGZ6	40498	34373	28159	24757	21609	24344
Bifunctional NAD(P)H-hydrate repair enzyme OS	A9HRW0	7446	6037	7004	4435	4524	5190
Aconitate hydratase OS	A9HEZ2	74972	76484	56600	49083	49748	45427
Conserved protein OS	A9HHA4	78034	81490	92543	55680	57793	62094
Transcriptional regulator protein OS	A9HF00	10247	9944	7984	6261	6382	6990
Protein RecA OS	A9HM16	11925	13491	10974	7989	8303	9338
Peptidase protein OS	A9HET1	18463	17435	20859	12636	14473	12900
S-adenosylmethionine synthase OS	METK	39688	38773	43113	26949	26436	32372
Glutamate--cysteine ligase OS	A9H108	11496	11750	10010	7031	8442	8150
HAD-superfamily hydrolase, subfamily IA, variant 3 OS	A9HDX4	13391	13553	12037	7566	9676	10597
Bifunctional purine biosynthesis protein PurH OS	A9HDN9	26598	23338	22909	16476	16838	18983
Nitrogen regulatory protein P-II OS	A9HMD4	29278	27081	25728	23279	18007	17714
Carboxymethylenebutenolidase OS	A9H121	11905	12630	13098	8374	8687	10098
Phosphate-binding protein PstS OS	A9H9X2	44737	40834	45846	32889	30104	31899
Peptidase, family M16 OS	A9HKF0	13411	11424	12224	7499	10444	9013
Chemotaxis response regulator protein	A9HHG0	30135	24896	26832	21949	14791	23223
Aldo/keto reductase OS	A9HH27	16821	16279	14952	12181	12254	10944
Dihydroxy-acid dehydratase OS	A9HA40	8169	7339	7340	5773	5126	6005
Uncharacterized protein OS	A9HRD5	27407	26169	28436	20487	18752	21480
Glucans biosynthesis protein G OS	A9HBM4	25689	23930	26902	19712	18915	18091
Electron transfer flavoprotein subunit beta OS	A9HEE6	65441	52447	53716	41233	43369	43017
60 kDa chaperonin 1 OS	CH601	282648	231308	237526	181738	184277	193931

2,3-bisphosphoglycerate-independent	A9H397	115598	107227	105141	70179	89301	85549
Putative GAF sensor protein OS	A9HP16	9870	7337	8315	6939	5283	6860
Efflux transporter, RND family, MFP subunit OS	A9HEF9	30726	31278	35607	23582	23135	27056
Putative metallopeptidase OS	A9HRE6	23708	21341	23681	16512	17822	17620
Acetyl-coenzyme A carboxylase carboxyl	ACCA	58853	48157	60641	45094	38666	43330
Fe-S protein, radical SAM family OS	A9HA97	26252	25748	25833	18605	20552	19940
Conserved protein OS	A9HSH2	40000	44243	49992	36694	31203	34887
Protein TolR OS	A9HAZ8	27090	25765	30080	18724	25698	19100
FAD linked oxidase domain protein OS	A9H1K4	17157	14729	15573	11873	12486	12053
Signal recognition particle protein OS	A9HS68	24100	26713	26101	21387	17074	20646
Uncharacterized protein OS	A9H3X9	20699	19749	21744	18013	15063	14880
Signal peptidase I OS	A9HKX7	5633	6142	6609	4928	4597	4752
Aminotransferase OS	A9HSE9	57721	48684	48451	39114	40454	40977
Putative dihydro-orotase protein OS	A9GZR4	15386	15201	15182	12684	10908	12079
Alkyl hydroperoxide reductase AhpD OS	AHPD	44270	42213	39543	31377	35655	31505
Threonine synthase OS	A9HKE7	14408	15564	16506	11935	11840	12846
Adenylosuccinate synthetase OS	PURA	34640	31908	37246	26889	27798	27210
Alpha/beta hydrolase, chloride peroxidase OS	A9H000	30402	28298	31229	22501	26198	22309
Phosphoglucomutase OS	A9HSH5	56982	51480	52314	45132	43353	39108
Glucokinase protein OS	A9HIS0	49383	44815	49610	39992	34020	40146
Putative short-chain dehydrogenase OS	A9HLW8	36992	35163	35949	29098	26216	30664
Conserved protein OS	A9HF41	12055	13241	14298	9666	11814	10094
Glycosyl transferase group 1 OS	A9HLZ7	33269	31552	31124	24436	25093	27441
Threonylcarbamoyl-AMP synthase OS	A9H1J9	12476	13148	12605	9961	9597	11172
Lipoprotein OS	A9HPJ3	26674	26564	31133	24659	21928	21320
Orotate phosphoribosyltransferase OS	A9HII0	36595	30606	37398	26535	28089	29669
Flagellar motor switch protein FliN OS	A9HHD1	35280	36085	43291	32684	30500	29274
Two-component response regulator OS	A9HFR4	25207	25319	24704	17892	22705	20434
Phosphoglucomutase/phosphomannomutase	A9H070	52456	52773	53591	45856	42148	41333
Glyceraldehyde-3-phosphate dehydrogenase OS	A9HM29	284746	258204	252376	215819	220456	211580
Putative 3-oxoacyl-[acyl-carrier-protein] reductase OS	A9H2M9	38057	34332	35739	30634	29535	28446
Triosephosphate isomerase OS	TPIS	28175	25602	28655	24060	20978	23341
DNA-directed RNA polymerase subunit alpha OS	RPOA	67606	78847	69426	56845	60940	61816
Mammalian cell entry related domain protein OS	A9H983	8998	8495	8659	7409	6851	7588
Leucyl aminopeptidase OS	A9HJY3	10144	10513	10374	8602	9468	8373
Aminotransferase OS	A9HCQ6	15415	15206	13467	13071	11675	13084
Putative glycyl aminopeptidase OS	A9HN12	33759	32762	34447	27761	30690	28898
ATP-dependent zinc metalloprotease FtsH OS	A9HB14	8352	9440	9007	7640	7310	8268
ATP synthase epsilon chain OS	ATPE	22486	22320	24593	21328	19140	19712
Putative dehydrogenase OS	A9HQE8	19837	18848	20781	17458	18794	18315
Uridylate kinase OS	A9HKW8	50307	46224	46511	44128	42423	45726
Ferredoxin--NADP reductase OS	FENR	18832	18526	19414	18138	17558	18158
2-nitropropane dioxygenase OS	A9HF38	5482	5277	5010	5840	5721	5475
Phosphoglycerate kinase OS	A9HM30	137521	135067	150272	163825	154668	153725
Putative glutamyl-tRNA(Gln) amidotransferase subunit A OS	A9HJR7	36985	38656	39474	47041	42080	41935
Homoserine dehydrogenase OS	A9HCQ4	23215	25908	22908	29261	27197	25971
Putative ribosomal RNA small subunit methyltransferase B OS	A9HID3	2989	2652	2744	3000	3150	3496
3-oxoacyl-[acyl-carrier-protein] reductase OS	A9HRE0	33499	32029	35414	41395	36280	38951
Putative phosphatidylethanolamine N-methyltransferase OS	A9HKI4	15442	13307	14503	17059	16862	16341
Phosphatidylserine decarboxylase proenzyme OS	PSD	18143	21315	21184	22911	22380	25490
Citrate synthase OS	A9HII7	51608	44848	42151	57682	51506	55724
Dihydrolipoyl dehydrogenase OS	A9HFH1	37130	38785	34190	43465	39668	47984
4-diphosphocytidyl-2-C-methyl-D-erythritol kinase OS	ISPE	18908	16056	19482	22071	19603	23338
Alcohol dehydrogenase zinc-binding domain protein OS	A9HNN4	19630	19659	16969	23906	23085	20540
Carbonic anhydrase OS	A9HL77	56138	50310	49275	64077	66555	56790
Ferrochelatase OS	A9HEQ4	13295	12985	11969	14287	14710	17060
Peptidyl-prolyl cis-trans isomerase OS	A9HIQ1	108659	99311	125994	131295	139913	133413
Enolase OS	ENO	112018	108879	100720	141782	131760	121962
Malonyl CoA-acyl carrier protein transacylase OS	A9HRE1	31361	34126	33767	42902	38462	41084
Cysteine desulfurase OS	A9HRY2	27869	28101	28017	32403	34269	37084
Outer membrane protein OS	A9H3F7	6721	7082	7634	8822	8971	8871
Thiazole synthase OS	THIG	22340	20340	16461	25270	22396	26583

Transcriptional regulator, IclR family/regucalcin OS	A9HL52	14438	14237	17250	20945	17592	19273
Gluconate 5-dehydrogenase OS	A9H995	58009	57373	63478	79294	74635	71404
Probable transcriptional regulatory protein GDI0798 OS	A9HAV2	26476	28403	31677	39018	36773	33499
Tryptophan synthase alpha chain OS	TRPA	36668	40644	38751	52180	49366	45284
Peptidase M24 OS	A9HJP9	10641	9626	10646	13457	11972	14627
Gluconate 2-dehydrogenase (Acceptor) OS	A9HBC6	6970	6194	6592	9152	8188	8288
Glucokinase OS	A9HI04	28982	28088	31902	42875	33974	38661
Biotin carboxyl carrier protein of acetyl-CoA carboxylase OS	A9HEX3	57038	53814	55736	76679	66079	73980
Enoyl-CoA hydratase/isomerase OS	A9HE55	16801	15796	17895	21432	21420	23104
ATP-dependent Clp protease ATP-binding subunit ClpX OS	CLPX	12243	12276	12258	17746	15239	15310
Glutamyl-tRNA(Gln) amidotransferase subunit A OS	A9HRI9	27002	27739	22686	37524	27948	36557
NADH-quinone oxidoreductase subunit B 2 OS	NUOB2	27866	33093	33195	43567	40546	40407
Acetylglutamate kinase OS	ARGB	19453	16723	17966	24451	23101	24574
6,7-dimethyl-8-ribityllumazine synthase OS	A9HDF5	10130	11219	11139	16441	12651	14222
NADH-quinone oxidoreductase OS	A9HRT3	14146	13968	11743	16965	18459	17885
3-oxoacyl-[acyl-carrier-protein] reductase OS	A9HIY5	43094	50699	50547	69417	61749	62152
Succinate dehydrogenase flavoprotein subunit OS	A9HFD7	19428	21162	15521	24981	25350	24895
Amidophosphoribosyltransferase OS	A9H4K2	4770	6943	5538	7967	7592	7575
Putative haloacid dehalogenase-like hydrolase OS	A9HBE7	22395	18512	23779	29431	25612	32872
Trehalose 6-phosphate phosphatase OS	A9HBU3	23037	19707	24450	31194	33013	28124
Conserved protein OS	A9HAR7	13091	10975	13807	17298	16481	18320
Putative threonine dehydratase catabolic OS	A9H381	4430	4231	4747	5838	5695	7026
S-formylglutathione hydrolase OS	A9HIP3	1538	1582	1330	2246	2212	1734
Beta sliding clamp OS	A9HI34	28194	29233	28027	43385	34509	42268
Transcription termination/antitermination protein NusA OS	A9HF12	11395	11965	8424	16252	14581	14302
Protein-L-isoaspartate O-methyltransferase OS	A9HI07	57667	45632	59537	80963	75983	75200
Carbamoyl-phosphate synthase small chain OS	A9H1P4	17745	16454	18653	24566	23943	26935
RNA-metabolising metallo-beta-lactamase protein OS	A9HRR8	70454	66929	66011	98647	94399	104977
Preprotein translocase, YajC subunit OS	A9HL42	14343	12113	15767	20875	20411	21020
Nicotinate-nucleotide pyrophosphorylase OS	A9H8C5	25666	25007	25645	33420	36307	43179
NADP-dependent L-serine/L-allo-threonine dehydrogenase OS	A9H4E8	83631	67996	68713	113198	109690	103215
Lipase protein OS	A9HBK6	27088	26000	30557	42779	45428	35703
Uncharacterized protein OS	A9HMQ8	5422	5324	8095	4291	3424	3785
Ribosome maturation factor RimP OS	RIMP	25303	23445	30799	21857	22638	18310
Ribokinase OS	A9H0C5	6261	5816	7555	5719	4838	5236
1-(5-phosphoribosyl)-5-[(5-phosphoribosylamino)	A9GZX2	11328	11000	12761	15639	12247	16029
Argininosuccinate synthase OS	ASSY	49911	47312	40609	38522	38706	38789
PEBP family protein OS	A9HBI3	35600	19492	24754	41074	36732	37762
30S ribosomal protein S9 OS	A9H812	57163	48320	63512	39989	37375	53135
Dihydroorotase OS	A9H142	8327	9617	8714	9659	10217	9490
Lipoprotein SmpA/OmlA family OS	A9HS35	17704	24189	28560	13767	16501	17698
Uncharacterized protein OS	A9HBZ1	10594	8506	11260	12655	11017	12600
OmpA/MotB domain protein OS	A9GZP4	39607	38346	44697	39108	30558	25965
Protein TonB OS	A9HF68	10333	12084	14138	6973	10906	9569
Pyruvate dehydrogenase E1 component subunit alpha OS	A9HJA6	16006	15104	14485	18344	18849	25665
Acetyl-coenzyme A carboxylase carboxyl transferase subunit	ACCD	9529	8226	11592	16488	10450	15134
Oligoendopeptidase F OS	A9HSA2	5270	4793	4444	6342	8079	11772
ATP synthase subunit beta OS	ATPB	80259	105445	61588	52706	48822	52942
Uncharacterized protein OS	A9H0Y9	33299	30629	41563	44404	43275	40477
Transcription elongation factor GreA OS	A9H1Q0	9443	10579	10447	9722	7956	6552
Putative Aldose 1-epimerase OS	A9HDX0	7687	9745	10869	6845	6650	8466
Aminopeptidase OS	A9HFU5	54324	45088	39382	35533	35790	36424
RNA-binding protein Hfq OS	HFQ	21680	22681	31246	19042	20768	8373
Uncharacterized protein OS	A9HAE9	10978	11523	13550	11531	8214	6399
Uncharacterized protein OS	A9HEH6	6269	9113	8190	5759	6098	5941
Uncharacterized protein OS	A9HT76	60471	110879	83866	45752	53851	57281
Glucose-6-phosphate 1-dehydrogenase OS	A9H0G0	37830	39660	33088	34462	32164	31132
Inositol-1-monophosphatase OS	A9H6E0	16834	17027	15705	20056	16825	21029
Phosphoribosylformylglycinamidine synthase subunit PurS OS	A9HJF5	29095	31848	39141	41804	35372	44344
Dehydrogenase OS	A9H159	5863	4208	6855	4922	3666	3298
Conserved protein OS	A9HBW8	18686	15550	14268	19515	17045	20921
ATP-dependent Clp protease proteolytic subunit OS	A9HCR1	44989	63190	50951	57868	63912	76098

Superoxide dismutase OS	A9HL14	50345	15504	29127	36181	99176	72568
Electron transport protein SCO1/SenC OS	A9H4T2	14304	13920	14430	10115	13742	7899
2-octaprenyl-6-methoxyphenol hydroxylase OS	A9HMD1	7820	7753	7884	8332	9710	11728
Thiamine biosynthesis oxidoreductase thiO OS	A9HI52	20377	17747	17246	17907	14613	15941
Glycosyl transferase group 1 OS	A9HNQ7	1461	1491	1881	1681	2018	2043
30S ribosomal protein S11 OS	RS11	2816	4532	8704	8278	7473	10973
DSBA oxidoreductase OS	A9HIK8	18265	9055	9879	5153	9073	5324
Ferredoxin--NADP reductase OS	A9HLF6	13438	9778	15404	15509	39354	25728
Bifunctional enzyme IspD/IspF OS	A9HLU2	19925	19913	21288	18112	19775	19722
NADH dehydrogenase/NAD(P)H nitroreductase rutE OS	A9HFB0	8322	9044	12656	13329	12587	12055
Putative molybdopterin biosynthesis protein moeA OS	A9HJ67	9281	8387	8402	7661	7188	8640
Probable phosphoketolase OS	A9HGX3	45322	46278	40020	47664	48281	47037
Signal recognition particle receptor FtsY OS	A9HM31	6747	6379	6796	5816	6202	6602
Thioredoxin protein OS	A9H2A4	35505	30882	30787	28962	22614	31063
Biopolymer transport protein ExbD/TolR OS	A9HF92	22445	12429	13981	11035	10896	9162
Oxidoreductase domain protein OS	A9HDU1	108085	93086	100795	92431	93136	91514
Putative ribitol 2-dehydrogenase OS	A9HPG2	82582	83483	85378	60391	72936	82071
Putative thioredoxin protein OS	A9HSA5	38172	20616	21474	17083	22299	7025
50S ribosomal protein L3 OS	RL3	18391	13876	30701	30442	29373	31326
Putative phosphoserine aminotransferase OS	A9HLQ7	4468	6283	4500	5997	6250	6332
Uncharacterized protein OS	A9HIF7	4447	4476	6303	4559	3524	3786
Putative membrane protein OS	A9H806	12865	12349	15255	12725	11831	10991
Alcohol dehydrogenase OS	A9HNA5	17422	25541	17759	23544	26670	24911
Tyrosine--tRNA ligase OS	A9HMK2	16694	15612	11823	13128	10474	12454
Ubiquinol oxidase subunit 2 OS	A9HK01	65596	65717	65452	81573	71865	67017
Aminotransferase OS	A9H801	6016	5208	4318	4290	3019	4896
Putative polysaccharide export protein OS	A9HMV6	28977	29427	37583	23248	26820	30196
4-hydroxy-tetrahydrodipicolinate synthase OS	DAPA	18181	17092	19749	19215	19201	21968
3-methyl-2-oxobutanoate hydroxymethyltransferase OS	PANB	11101	11260	12089	7068	7948	11807
Electron transfer flavoprotein-ubiquinone oxidoreductase OS	A9HEE4	11926	12165	10292	12055	12302	15067
Putative 2-amino-3-ketobutyrate coenzyme A ligase OS	A9HMR4	9985	10427	7596	7311	7227	8894
Ubiquinone biosynthesis O-methyltransferase OS	A9HJ43	14277	16901	17170	12982	13257	16197
Tryptophan synthase beta chain OS	A9HE87	17992	17773	15104	18511	18143	24382
Universal stress protein OS	A9H0V0	66508	56243	51492	53717	49446	49030
Ubiquinone/menaquinone biosynthesis	A9HI27	40827	34214	37148	35188	34458	33036
Adenylyl-sulfate kinase OS	A9H0W3	5240	5031	3690	3528	3958	4084
Glucose-6-phosphate 1-dehydrogenase OS	A9HFE6	49320	53553	54679	47140	47387	52766
NADH-quinone oxidoreductase chain E OS	A9HRT6	10021	12001	11170	13690	11728	11507
Nucleoside diphosphate kinase OS	NDK	56319	48407	66715	40531	48892	54338
2,3,4,5-tetrahydropyridine-2,6-dicarboxylate	A9HKR5	17728	17666	12283	24239	15559	20858
UDP-N-acetylmuramoyl-L-alanyl-D-glutamate	A9H0H5	6873	5642	6195	6836	6776	6838
3-phosphoshikimate 1-carboxyvinyltransferase OS	A9H466	15390	15140	17047	17065	16017	17602
Peptidoglycan-associated protein OS	A9HB05	281723	104147	189930	135189	80652	116479
Xanthine phosphoribosyltransferase OS	A9H0R0	6741	6601	5289	6079	10833	17632
Uncharacterized protein OS	A9H8H8	47881	45010	79291	38439	44668	37804
Cof-like hydrolase OS	A9H329	6436	5413	5098	6940	7775	5458
Elongation factor P OS	EFP	39283	32493	38796	32352	33518	34607
Isocitrate dehydrogenase (NAD(+)) OS	A9HJQ1	50557	46548	40967	44337	58035	70307
Elongation factor Tu OS	EFTU	309804	302816	307380	263877	312367	276781
Bacteriocin protein OS	A9H5P1	33337	33115	25740	33932	35701	33944
Putative 2Fe-2S ferredoxin OS	A9HMI7	32438	31558	51109	55624	41009	48579
Nitrilase/cyanide hydratase OS	A9GZH7	8134	15199	10711	7763	8773	8211
Putative aerobic cobaltochelatase cobS subunit OS	A9HJ01	22810	26713	23028	23860	21073	21693
Peptidase protein, modulator of DNA gyrase OS	A9HEU1	10393	10620	9143	7204	9261	9949
Pyrrolo-quinoline quinone OS	A9H134	33945	31109	39166	30520	33754	29629
Inosine-5'-monophosphate dehydrogenase OS	A9HID1	57449	65009	36395	43609	39204	39589
Inositol-1-monophosphatase OS	A9HRD4	24061	25937	21519	30336	23018	27550
Alcohol dehydrogenase zinc-binding domain protein OS	A9HE22	4867	5581	4846	9204	4669	6971
Histidinol dehydrogenase OS	A9HFM4	6689	5343	4505	4828	4939	4065
50S ribosomal protein L9 OS	RL9	61911	41998	35129	29831	45672	28716
2-dehydro-3-deoxyphosphooctonate aldolase OS	A9HJ79	8287	7295	6827	7332	8950	8375
Peptide methionine sulfoxide reductase MsrA OS	A9HI15	23076	15984	14340	12925	18167	9205

4-hydroxy-3-methylbut-2-enyl diphosphate reductase OS	A9HS93	20290	19117	16707	19968	14479	12469
Aminotransferase OS	A9HSE7	7978	8121	6415	8208	7561	9460
Chaperone protein DnaJ OS	DNAJ	5546	5681	3385	3909	3301	4391
UTP--glucose-1-phosphate uridylyltransferase OS	A9HJ15	106678	90822	79911	100943	106592	100676
Arginine biosynthesis bifunctional protein ArgJ OS	A9HAU1	4998	7924	5731	7056	8344	6827
Ribose-phosphate pyrophosphokinase OS	A9HBZ3	7957	9451	7671	9355	8539	9407
3-oxoacyl-[acyl-carrier-protein] synthase 2 OS	A9HRD7	40427	45908	34736	45287	44533	43856
dTDP-4-dehydrorhamnose 3,5-epimerase OS	A9H3H9	9021	8003	7955	9407	10974	7987
Cytokinin riboside 5'-monophosphate	A9HEM3	23769	35275	40617	39791	41048	37858
Zinc-type alcohol dehydrogenase-like protein OS	A9H2A8	10725	10328	17175	8806	11187	9866
D-3-phosphoglycerate dehydrogenase OS	A9HIU7	4267	4183	3226	3755	4443	5555
ATP-dependent Clp protease proteolytic subunit OS	A9HRV4	60726	63940	41538	52140	49884	35893
Glycosyl transferase OS	A9HH55	42961	38912	50550	47926	46085	51085
Conserved protein OS	A9H9B9	7873	19261	6392	38802	7352	20149
Conserved protein OS	A9HM79	60100	52608	54736	53402	61454	77456
Multifunctional fusion protein OS	A9H0J6	19060	22543	16256	18312	12303	18800
Delta-aminolevulinic acid dehydratase OS	A9HRP9	13814	13864	14027	16464	12801	16988
Branched-chain-amino-acid aminotransferase OS	A9HNB7	41439	62399	28588	44130	25147	28243
OmpW family protein OS	A9HED6	54519	21016	37644	13426	13923	44573
ATP phosphoribosyltransferase regulatory subunit OS	A9HLQ2	14900	13718	17135	19812	14296	17229
Dehydrogenase (Zinc-binding alcohol dehydrogenase) OS	A9H246	15343	19306	14058	21398	16954	16714
ATPase associated with various cellular activities	A9H3C6	23741	21480	25135	22741	23077	20776
Alkyl hydroperoxide reductase	A9H3W7	34226	21885	22436	21343	26504	16505
Aspartyl/glutamyl-tRNA(Asn/Gln) amidotransferase subunit	A9HRI7	7950	8000	5717	8196	7991	7879
Pyruvate kinase OS	A9HEH3	73304	74485	75620	76665	77843	73331
Electron transfer flavoprotein alpha subunit OS	A9HEE9	65426	52787	59138	54653	42637	61492
Uncharacterized protein OS	A9HMQ3	48937	56329	68820	51763	50632	53872
Uncharacterized protein OS	A9HHE4	6455	5120	6402	6045	5584	4793
Dihydrolipoyllysine-residue succinyltransferase	A9HFG9	83365	70284	69047	63188	95873	99275
Enoyl-[acyl-carrier-protein] reductase [NADH] OS	A9H0U5	14017	16884	13892	18403	13307	18522
Probable malate:quinone oxidoreductase OS	A9HKZ6	5159	5237	4234	3991	3440	5433
NADPH dehydrogenase OS	A9H535	18379	23650	24809	20437	19957	20940
N-acetyl-gamma-glutamyl-phosphate reductase OS	A9HLR0	30659	25632	28072	30968	27179	30992
Acyl-[acyl-carrier-protein]--UDP-N-acetylglucosamine	A9HKU0	16154	14522	18813	15736	15690	14589
Uncharacterized protein OS	A9GZL6	11119	10340	9765	11964	8363	22252
Protease protein OS	A9HAN0	30121	18464	20462	27005	25030	26643
10 kDa chaperonin OS	A9HK46	24936	55695	50811	43463	26287	35369
Aldose 1-epimerase OS	A9HBF6	13984	11548	14508	12553	10681	13844
Acetyl-CoA hydrolase OS	A9HIK2	20421	20385	16538	21107	14601	16365
Putative rare lipoprotein A OS	A9HI92	7146	5606	7398	6375	5811	6661
FMN-dependent NADH-azoreductase OS	AZOR	12103	11490	9183	8764	12637	7780
Putative FeS assembly protein SufD OS	A9HRY4	13654	12739	10106	11934	10929	11238
Phosphoribosylamine--glycine ligase OS	A9H4P1	9049	8933	7456	6404	9180	7906
Gamma-glutamyltranspeptidase OS	A9HM18	26353	27064	35028	29978	26599	25501
6-phosphogluconate dehydrogenase, decarboxylating OS	A9H324	168528	140141	162242	133111	168572	141994
Aspartokinase OS	A9HJ44	4993	6526	7713	12407	8923	3510
Polyphenol oxidase OS	A9HBY8	17099	14071	13491	14247	13239	14737
30S ribosomal protein S2 OS	RS2	117359	93982	127530	95519	106800	114223
Phosphoribosylformylglycinamidine cyclo-ligase OS	A9HJV0	24407	28617	25707	29319	20558	23233
4-hydroxy-3-methylbut-2-en-1-yl diphosphate synthase	ISPG	4961	6982	5922	5697	7238	6304
Uncharacterized protein OS	A9HJK6	3513	9446	3525	3134	4800	4690
Peptidyl-prolyl cis-trans isomerase D OS	A9HJ89	16876	13953	16874	14059	18862	17904
Biopolymer transport exbB protein OS	A9HF70	108746	133872	134935	127560	119292	115404
FeS assembly protein SufC OS	A9HRY6	33257	27079	33313	33880	30536	32959
Endoribonuclease L-PSP OS	A9HC24	15810	14048	12961	17437	12228	8877
Conserved protein OS	A9HS96	15806	13844	18073	14715	17381	13077
Putative phosphate acetyltransferase OS	A9HL01	6536	5637	5959	4983	7032	5075
Putative short-chain dehydrogenase OS	A9HAC6	9824	12122	10287	10694	9145	11107
6-phosphogluconolactonase OS	A9H335	63021	24533	26815	30896	35397	30074
Glycine--tRNA ligase beta subunit OS	A9HM86	8316	6684	5716	6075	6912	9208
Pyruvate, phosphate dikinase OS	A9HEP2	3820	5121	3302	4310	4620	4038
50S ribosomal protein L7/L12 OS	RL7	212894	100739	74420	134407	201812	110998

3-mercaptopyruvate sulfurtransferase OS	A9HJI4	19220	18743	22094	20557	20192	17713
7-cyano-7-deazaguanine synthase OS	QUEC	5588	5135	4708	5258	4546	6303
Chaperone protein DnaK OS	DNAK	105036	131879	131292	126600	110959	119765
Adenine deaminase OS	A9HNM9	7440	5444	6301	6854	4956	6515
Chaperone protein dnaJ OS	A9HAH3	39668	33178	43735	37464	42831	39976
Phosphoribosylglycinamide formyltransferase OS	A9HJV2	5188	5296	5308	3982	6484	6201
Glutamine amidotransferase of anthranilate synthase OS	A9HJ94	14735	12982	11676	13344	15326	12055
UDP-3-O-acylglucosamine N-acyltransferase OS	A9HKU5	11420	10944	12651	13079	11172	11552
Fructose-1,6-bisphosphatase OS	A9HCQ2	120293	93689	103971	100662	102469	125969
Thioredoxin OS	A9HA92	29802	14873	15180	25109	21093	19040
2-ketogluconate reductase OS	A9H3Y4	25579	25848	27790	28083	23362	26232
Bifunctional protein FolD OS	FOLD	24001	20878	26075	22465	21690	25010
Geranyltranstransferase OS	A9HIR3	17825	18796	15872	18380	17093	16018
Dihydroorotate dehydrogenase (quinone) OS	A9HBE5	23555	30697	26009	22913	26805	28297
Alkyl hydroperoxide reductase	A9H8D6	259795	207552	204001	228039	246320	214516
Enolase-phosphatase E1 OS	MTNC	9162	9392	9326	9745	8541	9281
Peptidase U62 modulator of DNA gyrase OS	A9HKF2	12041	11720	16720	8419	13647	16132
NADH dehydrogenase (Ubiquinone) OS	A9HKL6	21163	19679	18301	18658	18053	21427
Uncharacterized protein OS	A9HRF9	6889	5237	9678	5715	8025	6972
Putative transporter protein OS	A9H3U2	4905	4677	4966	4400	5507	4352
Putative amine oxidase OS	A9HGY5	4702	5851	4847	4577	4825	5654
Putative D-3-phosphoglycerate dehydrogenase OS	A9HFV9	15663	12549	14477	14489	13452	14050
Molybdenum cofactor biosynthesis protein B OS	A9HAM8	18104	14344	13024	13364	19944	10022
Putative rod shape-determining protein mreB OS	A9HM98	12948	21198	18582	18545	15587	16984
Cof-like hydrolase OS	A9H332	67713	63822	65568	54680	76465	62013
Inorganic pyrophosphatase OS	A9H4G5	163546	206490	251700	230819	200761	172536
GTP-binding protein TypA/BipA OS	A9H9C1	6259	7786	4225	6169	7365	5420
30S ribosomal protein S8 OS	RS8	94261	77303	108440	81720	105350	86638
Surface antigen protein OS	A9HAP4	47946	24250	20281	33731	29683	33579
Conseved protein OS	A9H247	5998	7432	9116	7311	7194	7596
Biotin carboxylase protein OS	A9HEX0	33851	22140	20867	19943	20734	33446
Gamma-glutamyl phosphate reductase OS	A9HC10	4499	6151	4266	3708	6112	4821
Leucine--tRNA ligase OS	A9HMQ5	3026	3046	2334	2328	2770	3243
Bifunctional protein GlmU OS	GLMU	8656	6837	5848	6684	5093	9297
Uncharacterized protein OS	A9H986	17327	21717	25795	12543	33869	19543
Putative transcriptional regulator, rrf2 family OS	A9HRZ0	6975	6445	7501	6872	9423	4399
Inositol-3-phosphate synthase OS	A9H8S7	89079	76017	89207	86664	80738	87436
Thioredoxin reductase OS	A9H0A5	15736	19201	12125	17253	13322	16711
Uncharacterized protein OS	A9HAF1	13660	12702	17960	15837	12809	15833
Putative gamma-glutamyltranspeptidase OS	A9HJR4	13482	13841	16374	14873	14189	14711
Glycine cleavage system H protein OS	A9HM50	5438	36328	39212	28042	27949	25797
Glucose-1-phosphate thymidylyltransferase OS	A9HH12	9202	9719	7011	8687	8678	8601
ATP-dependent protease subunit HslV OS	A9H1A3	38937	16101	35948	23768	44672	22331
Putative phosphoenolpyruvate carboxylase OS	A9HRZ5	1346	-1	2396	8444	7145	8067
Porin OS	A9HPF6	16134	14615	17207	1947	1813	-1
Glutamate--tRNA ligase 1 OS	SYE1	13258	10704	8625	1662	2030	-1
Guanylate kinase OS	A9HDA8	10109	6702	6578	-1	2698	-1
Choloylglycine hydrolase OS	A9H2I4	6931	8475	8303	2064	-1	1519
Putative cytochrome c551 peroxidase OS	A9HK81	5582	4362	4477	-1	2491	1699
Uncharacterized protein OS	A9HBI5	46530	-1	38399	55666	53227	43435

*IC= Ion Counts

Table S3 - Detailed information of proteins from schematic illustration of the main responses of *G. diazotrophicus* to salt stress

Localization	Accession	Description	Protein Name
Outer Membrane	A9H3U0	Outer membrane efflux protein	Omp
	A9HHH1	Flagellar L-ring protein	FlgH
	A9HAM5	Porin	OprB
	A9H438	Insulinase protein	Ins
	A9HKV0	Outer membrane protein assembly factor	BamA
	A9H0L0	Outer membrane protein assembly factor	BamD
	A9H9Q6	Outer membrane protein	Omp
	A9HEG4	Outer membrane protein	Omp
	OMPC	Outer membrane protein	OmpC
	A9HNM4	TonB-dependent receptor	TonB-dependent receptor
	A9H7M7	TonB-dependent receptor	TonB-dependent receptor
	A9H7L9	TonB-dependent receptor	TonB-dependent receptor
	A9HE38	TonB-dependent receptor	TonB-dependent receptor
	A9HEU6	TonB-dependent receptor	TonB-dependent receptor
	A9H7L3	TonB-dependent receptor	TonB-dependent receptor
	A9HFL0	TonB-dependent receptor	TonB-dependent receptor
	A9HDZ9	TonB-dependent receptor	TonB-dependent receptor
	A9HFV5	TonB-dependent receptor	TonB-dependent receptor
	A9H932	TonB-dependent receptor	TonB-dependent receptor
Periplasm	A9HEK6	Serine protease	DegP
	A9HBK9	Serine protease	DegQ
	A9HB04	Tol-Pal system protein	TolB
	A9H103	Outer-membrane lipoprotein carrier protein	LolA
	A9HKB6	Glutathione peroxidase	GPx
	A9HNP0	D-xylose ABC transporter, periplasmic substrate-binding protein	XylF
	A9HK12	Alcohol dehydrogenase [acceptor]	AdhA
	A9H4A8	Gamma-glutamyltranspeptidase	Ggt
	A9HSZ4	Uncharacterized protein	Unc
	A9HPB9	D-ribose-binding periplasmic protein	RbsB
	A9HPB9	D-ribose-binding periplasmic protein	RbsB
	A9HFZ1	D-ribose-binding protein	RbsB
	A9HDE6	Pyridine nucleotide-disulphide oxidoreductase	PDOx
	A9HA48	Secretion protein	HlyD
	A9H577	Periplasmic binding protein	Per
	A9HJ97	Anthranilate phosphoribosyltransferase	TrpD
Inner Membrane	A9HRS8	NADH-quinone oxidoreductase subunit J	NouJ
	A9HJ83	Preprotein translocase	SecG
	A9HHE0	Chemoreceptor	McpA
	A9H6D5	Flagellar motor protein	MotA
	A9HNC1	Succinate-semialdehyde dehydrogenase [NADP+]	GabD
	A9H192	Xanthine dehydrogenase family protein molybdopterin-binding subunit	XdhB
	A9HL93	Oxidoreductase	Oxi
	A9H435	Penicillin-binding protein	PBP
	A9HPL1	Ribose import ATP-binding protein	RbsA
	A9HMX8	D-amino acid dehydrogenase	DadA
	A9H4M0	Signal peptidase I Spase I	LepB
	A9HPE7	ABC transporter related	ABCt
	A9H3B5	Multidrug resistance protein A	EmrA
	A9H3A3	Carboxy-terminal protease protein	CPr
	A9HM07	Uncharacterized protein	Unc
	A9H090	Dipeptidyl-peptidase	DPe
	A9HHL8	Putative pilus assembly protein	Pilus
	A9H0K4	Cell division protein	FtsZ
Cytoplasm	A9HRU1	NADH-quinone oxidoreductase subunit C	NouC
	A9HRT4	NADH-quinone oxidoreductase subunit F	NouF
	SECB	Protein-export protein	SecB
	A9HBL5	Mannitol 2-dehydrogenase	MtlK
	A9HBU6	Alpha,alpha-trehalose-phosphate synthase	OtsA
	ATPA	ATP synthase subunit alpha	AtpA
	ATPG	ATP synthase gamma chain	AtpG
	ATPD	ATP synthase subunit delta	AtpH
	A9H4G2	ABC transporter ATP-binding protein	ATPb
	A9HKM9	ABC transporter ATP-binding protein	ATPb

* Unc = Uncharacterized protein

7.3 Supplementary material from Chapter 3

Table S1 Detailed ISOQuant processing configuration

Parameter	Value
isoquant.pluginQueue.name	design project and run ISOQuant analysis
process.peptide.deplete.PEP_FRAG_2	false
process.peptide.deplete.CURATED_0	false
process.peptide.statistics.doSequenceSearch	false
process.emrt.minIntensity	1000
process.emrt.minMass	500
process.emrt.rt.alignment.match.maxDeltaMass.ppm	10
process.emrt.rt.alignment.match.maxDeltaDriftTime	2
process.emrt.rt.alignment.normalizeReferenceTime	false
process.emrt.rt.alignment.maxProcesses	8
process.emrt.rt.alignment.referenceRun.selectionMethod	AUTO
process.emrt.clustering.preclustering.orderSequence	MTMTMT
process.emrt.clustering.preclustering.maxDistance.mass.ppm	6.06E-6
process.emrt.clustering.preclustering.maxDistance.time.min	0,202
process.emrt.clustering.preclustering.maxDistance.drift	2,02
process.emrt.clustering.distance.unit.mass.ppm	6.0E-6
process.emrt.clustering.distance.unit.time.min	0,2
process.emrt.clustering.distance.unit.drift.bin	2
process.emrt.clustering.dbscan.minNeighborCount	2
process.identification.peptide.minReplicationRate	2
process.identification.peptide.minScore	6
process.identification.peptide.minOverallMaxScore	6
process.identification.peptide.minSequenceLength	6
process.identification.peptide.acceptType.PEP_FRAG_1	true
process.identification.peptide.acceptType.IN_SOURCE	false
process.identification.peptide.acceptType.MISSING_CLEAVAGE	true
process.identification.peptide.acceptType.NEUTRAL_LOSS_H20	false
process.identification.peptide.acceptType.NEUTRAL_LOSS_NH3	false
process.identification.peptide.acceptType.PEP_FRAG_2	true
process.identification.peptide.acceptType.DDA	false
process.identification.peptide.acceptType.VAR_MOD	true
process.identification.peptide.acceptType.PTM	true
process.annotation.peptide.maxSequencesPerEMRTCluster	1
process.annotation.protein.resolveHomology	true
process.annotation.peptide.maxFDR	0,01
process.annotation.useSharedPeptides	all
process.normalization.lowess.bandwidth	0,3
process.normalization.orderSequence	XPIR
process.normalization.minIntensity	3000
process.quantification.peptide.minMaxScorePerCluster	6
process.quantification.peptide.acceptType.IN_SOURCE	false
process.quantification.peptide.acceptType.MISSING_CLEAVAGE	true
process.quantification.peptide.acceptType.NEUTRAL_LOSS_H20	false
process.quantification.peptide.acceptType.NEUTRAL_LOSS_NH3	false
process.quantification.peptide.acceptType.PEP_FRAG_1	true
process.quantification.peptide.acceptType.PEP_FRAG_2	true
process.quantification.peptide.acceptType.VAR_MOD	true
process.quantification.peptide.acceptType.PTM	true
process.quantification.peptide.acceptType.DDA	false
process.quantification.topx.degree	3
process.quantification.topx.allowDifferentPeptides	true
process.quantification.minPeptidesPerProtein	2

process.quantification.absolute.standard.entry	ENO1_YEAST
process.quantification.absolute.standard.fmol	50
process.quantification.topx.allowDifferentPeptides	true
process.quantification.absolute.standard.entry	ENO1_YEAST
process.quantification.absolute.standard.fmol	50
process.quantification.maxProteinFDR	0,01

Table S2 Proteins identified in *G. diazotrophicus* exposed to high-sucrose

Description	Acces.	IC Control1	IC Control2	IC Control3	IC PEG 1	IC PEG2	IC PEG3	T test
2,3,4,5-tetrahydropyridine-2,6-dicarboxylate N-succinyltransferase	A9HKR5	11204	6950	7546	17582	13796	27224	0,04958523
3-oxoacyl-[acyl-carrier-protein] reductase	A9HIY5	39388	30424	31108	54731	50189	62374	0,00468331
4-diph phocytidyl-2-C-methyl-D-erythritol kinase	ISPE	7578	6474	7058	17637	19913	18003	0,00049212
4-hydroxy-3-methylbut-2-enyl diph phate reductase	A9HS93	9064	7554	6425	19021	17629	18332	0,00055154
50S rib omal protein L3	RL3	34745	32804	45468	79024	88917	70379	0,00216948
5-methyltetrahydropteroyltriglutamate	A9HNX4	8130	15128	15821	101848	79346	129379	0,011029
6-ph phogluconate dehydrogenase NAD-binding	A9HL10	8715	9797	13329	44410	46422	48160	2,7485E-05
6-ph phogluconate dehydrogenase, decarboxylating	A9H324	193861	149538	151076	298444	202985	310930	0,03653929
Acetoin(Diacetyl) reductase	A9HHS9	18325	15725	17390	30728	31899	34086	0,00018734
Acetyltransferase component of pyruvate dehydrogenase complex	A9HJB2	7206	5434	5612	27139	21614	32972	0,01033022
Alcohol dehydrogenase	A9HNA5	26151	18987	20228	71895	60852	88902	0,00901218
Alcohol dehydrogenase zinc-binding domain protein	A9HNN4	12543	5561	7870	16849	14102	23962	0,03074935
Aldehyde Dehydrogenase	A9H4V7	84215	57498	70150	147796	124498	187958	0,01609115
Ald e 1-epimerase	A9HBF6	33392	31543	31600	68504	87292	99336	0,01357412
Aminopeptidase	A9HFU5	42557	34399	38149	66651	56851	77564	0,01405815
ATP-dependent Clp protease ATP-binding subunit ClpX	CLPX	10396	6524	6192	16987	13291	22843	0,02525978
Bacteriocin protein	A9H5P1	24325	19304	21948	36150	34128	46005	0,01538275
Biopolymer transport exbB protein	A9HF70	69941	59713	62683	163730	152324	193211	0,00481298
Carbamoyl-ph phate synthase small chain	A9H1P4	31472	30591	30173	56990	55783	51841	0,00133895
Carboxymethylenebutenolidase	A9HK54	16124	11831	12504	33683	26880	43575	0,02014816
Chaperone protein DnaJ	DNAJ	14258	14747	14160	26441	29222	27738	0,0012196
Chaperone protein HtpG	A9HLJ9	18821	13881	13983	42389	35272	59308	0,02285663
Chemoreceptor mcpA (Methyl-accepting chemotaxis protein)	A9HHE0	16284	5973	7441	21868	16831	34043	0,04420578
Chemotaxis response regulator protein-glutamate methylesterase	A9HHG0	12964	8970	11906	16333	14196	21904	0,04811125
Cof-like hydrolase	A9H329	23820	22199	13348	30639	31282	28131	0,03889904
Conserved protein	A9HHA4	20063	14111	22356	25317	26855	37310	0,04071001
dCTP deaminase	A9HFN2	14430	12618	16558	25799	29059	28291	0,00051414
DEAD/DEAH box helicase domain protein	A9H0S9	10611	6934	9831	15074	12226	18554	0,02840839
Delta-aminolevulinic acid dehydratase	A9HRP9	12812	9542	7544	17314	14494	19320	0,01374663
Dihydrolipoyl dehydrogenase	A9HFH1	53166	31530	30617	69387	50784	90351	0,04554609
Dipeptidyl-peptidase	A9H090	33897	26314	27571	49763	53945	50621	0,00164159
Electron transfer flavoprotein-ubiquinone oxidoreductase	A9HEE4	2987	3332	4756	11372	8356	17056	0,03623241
Endoribonuclease L-PSP	A9HBS7	8538	10748	11906	15275	20217	20902	0,01175973
Enoyl-CoA hydratase/isomerase	A9HE55	7076	6630	8035	10759	11036	11337	0,0027595
Exodeoxyribonuclease III Xth	A9HIE6	7075	8730	7851	11929	11690	13242	0,00145999
Fe-S protein, radical SAM family	A9HA97	14016	10232	13952	23014	20985	22442	0,00371289
Flagellin	A9HH66	13843	20435	20898	44293	41217	43985	0,00161658
Glucokinase	A9HI04	10286	9533	3326	21177	22675	24652	0,00508835
Gluc e-6-ph phate 1-dehydrogenase	A9H0G0	28745	15958	19716	52641	46984	79997	0,02500581
Hom erine dehydrogenase	A9HCQ4	11832	5845	8217	17004	14547	22144	0,01680465
In ine-guan ine kinase	A9H9C0	6397	4674	4846	12664	10828	15378	0,00857618
In itol-1-monoph phatase	A9HRD4	12695	8375	8556	18370	17361	22149	0,00486861
Insulinase protein	A9H438	14989	14722	16183	24085	27658	23184	0,0063247
Ketol-acid reductoisomerase (NADP(+))	ILVC	11001	8603	10835	29565	23868	42093	0,02686876
Large-conductance mechan ensitive channel	A9HHS4	12951	11738	19783	23441	25930	31044	0,01196253
Lysine--tRNA ligase	A9HK29	2446	1933	2521	5476	4777	7082	0,01468368
Mannitol 2-dehydrogenase	A9HBL5	17376	9580	9252	72547	58268	116118	0,02662344
Metal-dependent carboxypeptidase	A9HKD9	11726	8688	8840	16466	12955	17841	0,01642981
Methylenetetrahydrofolate reductase	A9HNY2	8994	8236	6923	31005	29127	36638	0,00286048
NADH-quinone oxidoreductase	A9HRT3	7174	3635	4361	25290	23845	27022	8,0492E-05
NADP-dependent L-serine/L-allo-threonine dehydrogenase	A9H4E8	91170	89786	88205	141599	144837	131165	0,00263247
OmpW family protein	A9HED6	85413	90826	84744	159247	172210	155198	0,00092425
Oxidoreductase domain protein	A9HDU1	48141	30401	41883	68497	60802	77875	0,00787418
Peptidase	A9HEL6	23097	19813	23122	38669	41647	34728	0,00251608
Ph phoglucomutase	A9HSH5	69065	35568	36632	90916	73793	95100	0,0240899
Preprotein translocase, SecG subunit	A9HJ83	13868	13946	18268	25159	32365	22714	0,02011144
Probable ph phoketolase	A9HGX3	20438	11938	16421	77628	62360	94015	0,0080024
Putaive gamma-glutamyltranspeptidase	A9H4A8	15647	18561	18792	27796	34730	25067	0,02227434
Putative 6-ph phogluconolactonase	A9HJ42	8008	8305	7019	13161	11426	13768	0,00368106
Putative aerobic cobaltochelatase cobS subunit	A9HJ01	14802	10986	10135	25195	22971	27233	0,00121873

Putative capsule polysaccharide export inner-membrane protein ctrB	A9HMV0	5554	4188	3971	8046	7340	11710	0,03359982
Putative cytochrome c551 peroxidase	A9HK81	4535	5054	5350	11218	15507	13279	0,00915348
Putative exodeoxyribonuclease III	A9HLI8	7261	6040	5601	10425	11156	11080	0,0022102
Putative glycyl aminopeptidase	A9HN12	20563	15892	19837	46345	42413	52249	0,00160945
Putative metallopeptidase	A9HRE6	33427	29638	35597	61229	57278	71346	0,00483794
Putative methyltransferase protein	A9HNX8	1947	1595	2110	11902	9849	12888	0,00357866
Putative molybdenum transport protein modE	A9HJC5	11344	13381	14504	25582	36303	26006	0,01819556
Putative nitrogen fixation protein	A9HFA7	34548	32332	35749	52100	61297	49039	0,01289577
Putative penicillin-binding protein	A9H435	17880	11774	10289	23345	20939	28388	0,01353333
Putative peptidyl-dipeptidase dcp	A9HP02	5816	5036	5570	8065	7840	9273	0,00504133
Putative serine carboxypeptidase	A9HS00	9051	9718	8495	15694	17004	14822	0,00110102
Pyridine nucleotide-disulphide oxidoreductase	A9HDE6	71022	58229	59211	95990	83155	104225	0,00851674
Pyrroline-5-carboxylate reductase	A9HBX1	7965	8845	8740	13593	16559	11889	0,02569297
Pyruvate dehydrogenase E1 component subunit beta	A9HJA9	10549	5255	5346	25820	18692	39454	0,03274814
RNA-metabolising metallo-beta-lactamase protein	A9HRR8	41930	25007	29186	86006	63230	112094	0,02343586
S-(hydroxymethyl)glutathione dehydrogenase	A9HIP1	13157	7825	9666	31733	25579	47848	0,02891141
Serine--tRNA ligase	SYS	16774	13389	14879	44687	40053	44975	0,00017855
Succinate dehydrogenase flavoprotein subunit	A9HFD7	12174	7358	10190	18921	15397	23269	0,01712005
Succinate-semialdehyde dehydrogenase [NADP+]	A9HNC1	14169	7955	5055	22844	18138	33793	0,02739021
Succinate-semialdehyde dehydrogenase	A9H549	15032	8316	9198	35110	29246	48962	0,01614858
Surface antigen protein	A9HAP4	115810	132901	94583	180607	212082	189396	0,00291355
Thiazole synthase	THIG	10825	7590	8619	13007	12775	19250	0,04420475
TonB-dependent receptor	A9H932	38264	33894	38844	56990	61540	52026	0,0034491
Transaldolase	A9H320	48423	25347	24198	129453	80641	157776	0,02250436
Transcriptional regulator, IclR family/regucalcin	A9HL52	23010	17833	18198	32681	33270	34453	0,00459931
Transketolase	A9H317	77048	47408	52408	176309	120616	243352	0,03397672
Trehal e 6-ph phate ph phatase	A9HBU3	27640	27778	29362	45439	47092	36713	0,02033778
Ubiquinol oxidase subunit 2	A9HK01	36874	43093	45002	62374	64304	79977	0,0125293
Ubiquinone/menaquinone bi ynthesis C-methyltransferase UbiE	A9HI27	18196	15075	22266	28915	27292	36015	0,01252627
Uncharacterized protein	A9H234	9164	11539	12249	14836	17804	19746	0,01254787
Uncharacterized protein	A9HCT2	47299	35388	56115	73491	78386	67261	0,01413095
Uncharacterized protein	A9HIN9	6482	5377	6894	15316	14914	18220	0,00226824
Uncharacterized protein	A9HKE4	13022	12816	13305	28782	31091	25926	0,00431968
Uncharacterized protein	A9HP51	3327	4032	3474	13455	10358	8187	0,0207619
Uncharacterized protein	A9H730	13504	13723	14121	33050	37209	32913	0,00206845
Uncharacterized protein	A9H738	6204	7997	8248	11387	13663	8983	0,04285208
Uncharacterized protein	A9H9H3	8956	11954	12478	18636	28287	16569	0,04912247
UPF0303 protein GDI1201	A9HDU3	28450	28083	27327	63304	63600	60194	0,00020385
10 kDa chaperonin	A9HPH9	45514	56180	55631	17520	19828	9968	0,00071962
50S rib omal protein L17	RL17	27957	26052	32730	8231	15800	4497	0,00622558
50S rib omal protein L28	RL28	58096	52942	57965	42883	43155	25380	0,0362753
50S rib omal protein L31	RL31	53705	54976	62754	20341	43041	28305	0,02070501
60 kDa chaperonin 2	CH602	29315	21305	17181	12078	8476	10908	0,03318804
ABC transporter related	A9HPE7	36893	30182	31315	15357	21957	13747	0,00457644
ATP-dependent Clp protease adapter protein ClpS	A9H4B8	11635	15077	12224	6036	7741	4579	0,00427272
Bacterioferritin	A9H7G6	157545	140353	138233	82282	100727	25623	0,03481113
Cell division protein FtsZ	A9H0K4	51597	57829	51410	38320	32782	33502	0,00134801
Chaperone SurA	A9H1L4	58666	57154	54021	35700	36177	26042	0,00484634
Cold shock protein (Fragment)	A5YJ14	65436	70796	46509	32482	37213	7468	0,02163122
Conserved protein	A9HBX6	59375	65559	64832	30388	34942	32208	0,00020983
D-amino acid dehydrogenase	A9HMX8	14070	11225	13566	6716	6921	7552	0,00780346
Deoxyuridine 5'-triph phate nucleotidohydrolase	A9HI24	25708	28764	29338	16725	21106	13807	0,01013641
D-rib e-binding periplasmic protein	A9HPK6	199885	183706	183666	21371	23980	22101	0,00042606
D-xyl e ABC transporter, periplasmic substrate-binding protein	A9HNP0	154029	153002	156989	45154	56108	32477	0,00152362
Efflux transporter, RND family, MFP subunit	A9HN17	9323	15029	13272	6195	9865	7192	0,04329757
ETC complex I subunit conserved region	A9H0R5	7882	12959	8997	6361	6843	3902	0,04588143
Extracellular solute-binding protein family 1	A9HPE1	68997	67438	72412	9089	8103	7926	0,00014709
Ferritin Dps family protein	A9HB55	26593	24087	24503	17859	17921	13299	0,0076246
Flagellar motor switch protein FliN	A9HHD1	43660	47582	49074	20599	31898	18546	0,00991185
Fuc e operon fucU protein	A9HPM0	6396	5349	5558	3491	3092	3494	0,00439263
Gamma-glutamyltranspeptidase	A9HM18	67850	87218	73723	49795	57623	36474	0,01428541
Glyoxalase/bleomycin resistance protein/dioxygenase	A9H2I1	12303	14665	13696	5104	6798	3884	0,00093843
Integration h t factor subunit beta	IHFB	36340	30417	30833	17956	23562	9365	0,02295826
LexA repressor	LEXA	5994	7295	8722	3848	4305	2495	0,01049841
Lipoprotein SmpA/OmlA family	A9HS35	37348	38623	43181	24344	27242	20620	0,00198326
NAD(P)H dehydrogenase (quinone)	NQOR	31135	31439	28506	14615	16615	13871	0,00013523
Organic solvent tolerance protein	A9HKM6	11355	13914	12922	6963	8368	8224	0,00440166
Outer membrane protein assembly factor BamD	A9H0L0	39050	42983	44454	24660	31780	14081	0,02866108
Outer membrane protein	A9HKU8	162704	167314	196477	36304	53890	14873	0,00041487
Outer-membrane lipoprotein carrier protein	A9H103	10263	12931	12565	6312	8857	6241	0,00815212
Peptide methionine sulfoxide reductase MsrA	A9HI15	84295	91438	82551	57723	62923	48955	0,0029287
Periplasmic binding protein/LacI transcriptional regulator	A9HPB9	244896	237447	225179	61632	67059	53530	2,0497E-05
Peroxidase	A9HPI6	12654	14517	14277	5925	7621	4860	0,00108425
Porin	A9HPF6	11355	9527	15744	1418	1487	1751	0,01418744
Protein GrpE	A9HEA5	28063	34441	43205	16608	23325	13542	0,01835262
Protein TolR	A9HAZ8	37767	41066	38227	24249	27757	26062	0,00042441
Putative 3-oxoacyl-[acyl-carrier-protein] reductase	A9H2M9	58545	42593	43746	31490	27892	32692	0,03311848

Putative DNA-binding protein HU	A9HR15	39523	51730	55854	16728	22231	9789	0,00364745
Putative exported protein	A9HM38	25863	27131	33503	13371	15935	3428	0,01149925
Putative exported protein	A9H7E6	16269	20414	24824	7981	12490	6106	0,01129724
Putative nitrogen regulatory protein	A9H7Z8	48005	50565	48326	31591	36042	23333	0,01638514
Putative outer membrane protein	A9H4M9	111150	119238	119238	56713	90640	51309	0,02460678
Putative periplasmic binding proteins	A9H577	66932	74659	75275	7007	7779	4926	0,00034607
Putative pyruvate dehydrogenase E2 component	A9HHP4	15231	15814	15057	6280	8354	3961	0,00808467
Putative rare lipoprotein A	A9HI92	13332	19029	18657	9905	12362	6874	0,02050391
Putative ribitol 2-dehydrogenase	A9HPG2	94366	83306	80662	19184	25378	22189	0,00066869
Putative ribonuclease D	A9HKL8	11210	16812	12377	7664	7951	5825	0,02552347
Putative R /MUCR transcriptional regulator protein	A9HR22	7930	10619	11431	2142	1918	1029	0,00507531
Putative sporulation protein	A9HLH5	8385	14280	16616	4179	7796	2813	0,02911956
Putative TonB-dependent receptor	A9HDZ9	10346	10737	13609	4557	5507	4483	0,00778056
Putative tonB-dependent receptor	A9HEU6	145564	130017	137548	37913	37974	37911	0,00100874
Putative TonB-dependent receptor	A9H7L3	27589	24008	33345	2882	3021	3463	0,00560119
Putative tonB-dependent receptor protein	A9H7M7	62495	57278	65888	7419	9752	8099	0,00057913
Putative transcriptional regulator protein	A9H0C0	128498	146004	145004	60479	69467	28427	0,00484306
Putative transcriptional Regulator, MarR family	A9HJY0	34831	29055	28845	13351	14839	7869	0,00144073
Putative transcriptional regulator, rrf2 family	A9HRZ0	12038	12167	14790	6572	6250	5974	0,00731873
Putative transcriptional regulator, TetR family	A9H9Q2	10931	12013	12249	6993	9163	5832	0,01573887
Putative transcriptional regulatory protein, MerR family	A9HS23	19616	24323	23863	13209	17534	6238	0,03561024
Rib ome-recycling factor	RRF	140589	166881	151859	104984	124094	57216	0,04328126
RNA polymerase-binding transcription factor DksA	A9H9Q9	23397	27940	30671	8245	12497	5789	0,00156007
R /MUCR transcriptional regulator protein	A9HFC1	55869	67033	69672	38019	51761	27068	0,02517215
Sec-independent protein translocase protein TatA	TATA	27902	37136	51442	12143	18133	6888	0,02148488
Succinate--CoA ligase [ADP-forming] subunit alpha	A9HRF1	31245	22793	30180	8613	7190	9492	0,00678605
Transcription antitermination protein NusB	A9HHZ2	11496	17239	17895	7489	12597	3787	0,042054
Translation initiation factor IF-3	A9HFP7	16055	18313	24143	11040	15785	8969	0,03777943
Tri eph phate isomerase	TPIS	45225	48188	40147	21016	24292	21386	0,0022279
Ubiquinone bi ynthesis O-methyltransferase	A9HJ43	17998	20740	18202	11069	12474	10189	0,00142993
Uncharacterized protein	A9GZL6	54277	51582	58025	20968	35927	13125	0,01743334
Uncharacterized protein	A9HAF1	22866	23940	21838	13889	16046	11482	0,00498452
Uncharacterized protein	A9HB09	26982	26164	35623	6385	9202	4127	0,00358537
Uncharacterized protein	A9HFF2	22589	25656	39452	6483	7210	2668	0,01837039
Uncharacterized protein	A9HFW9	47062	74663	73240	29536	37211	7788	0,01658307
Uncharacterized protein	A9HH94	42345	48733	52470	22903	39272	8680	0,04961971
Uncharacterized protein	A9HIF7	4582	4916	6180	2088	2819	1688	0,00473496
Uncharacterized protein	A9HIX9	27959	29295	30293	14523	20072	4221	0,03500623
Uncharacterized protein	A9HJ39	12056	16440	15451	8070	10477	6925	0,01200357
Uncharacterized protein	A9HJR9	39184	48840	62602	8724	10325	4253	0,00951843
Uncharacterized protein	A9HMM2	146824	149707	144406	106515	119367	66119	0,04457835
Uncharacterized protein	A9HMQ3	93733	103232	101606	68774	75924	52111	0,01349455
Uncharacterized protein	A9HPS1	17196	19590	26839	6695	7641	5205	0,01541206
Uncharacterized protein	A9HRJ8	22669	38832	39396	5374	5668	2409	0,01497803
Uncharacterized protein	A9HS71	31970	39805	46354	18498	25376	8750	0,01373879
Uncharacterized protein	A9H1P1	25461	30511	31904	14621	23391	4520	0,04796088
Uncharacterized protein	A9H3D7	35807	42388	42011	17626	22533	12193	0,00242853
Uncharacterized protein	A9H470	9713	13150	14352	7492	8731	6609	0,02868431
Uncharacterized protein	A9H4L3	10364	12395	12220	6536	6033	4914	0,00133575
Uncharacterized protein	A9H4N6	13373	18821	15296	8196	10591	3259	0,0191745
Uncharacterized protein	A9HT05	15302	19333	23930	4172	9453	2394	0,00650508
Uncharacterized protein	A9HT76	150079	196817	200341	77958	114991	54858	0,00702607
UPF0434 protein GDI0182/Gdia_2252	Y182	35600	41085	46829	22946	27959	19017	0,00697721
YceI family protein	A9HFY2	28387	30489	34453	17778	19974	3685	0,03206071
Secretion protein, HlyD-family	A9HA48	19033	21057	18872	13250	14796	11404	0,00376682
Conserved protein	A9HID9	18145	20424	23119	14289	16291	10778	0,01775976
DNA-binding protein HU	A9HRU7	211363	230996	167535	141859	163220	110453	0,02892895
Uncharacterized protein	A9HRD5	41052	38789	39950	26349	31594	23737	0,01223972
Putative Outer membrane protein oprM	A9HEG4	17293	15292	15189	10084	11617	10937	0,00284997
Biotin carboxyl carrier protein of acetyl-CoA carboxylase	A9HEX3	85634	97826	95012	63047	80497	48371	0,03719767
Putative membrane protein	A9HAA2	62215	58305	59678	44491	50882	29278	0,04873245
DNA-directed RNA polymerase subunit omega	RPOZ	71416	56965	51542	39310	51221	36340	0,04075765
Uncharacterized protein	A9H3Z8	18078	22580	25071	15481	18476	12456	0,03809646
Putative endoribonuclease protein	A9HN59	28516	32748	34460	23278	26713	17724	0,02458842
Thioredoxin protein	A9H2A4	39576	42260	44395	28058	33381	28447	0,00302427
Uncharacterized protein	A9H0Y9	59696	68539	65443	47123	57019	34580	0,04541512
Lipase protein	A9HBK6	22180	19673	19506	16355	16296	12659	0,01388805
dTDP-4-dehydrorhamn e 3,5-epimerase	A9H3H9	16334	15334	14052	11443	12530	9797	0,00968245
Outer membrane protein	A9H3F7	8041	7393	7688	5610	6178	5418	0,0014907
Putative polysaccharide export protein	A9HMV6	50531	57142	57282	40906	49521	32824	0,04224919
Rib ome maturation factor RimP	RIMP	23907	27586	29218	18171	25161	17665	0,04797011
Uncharacterized protein	A9HHE4	15191	15861	14550	11439	13586	9468	0,03901365
Putative dihydro-orotase protein	A9GZR4	14184	13341	13352	10697	9531	11007	0,00325464
Adenylate kinase	KAD	51604	54769	56432	36797	49532	38218	0,03688425
2-isopropylmalate synthase	A9HMA2	19278	16420	16896	13740	11018	15511	0,03407794
Threonylcarbamoyl-AMP synthase	A9H1J9	8535	8752	10549	6774	7457	7119	0,03313289
Putative ABC transporter ATP-binding protein in rpoN region	A9HKM9	15341	14558	13426	11645	12584	9014	0,034089

FAD linked oxidase domain protein	A9H1K4	15966	13681	13437	11729	10731	10604	0,01866239
Acetylglutamate kinase	ARGB	20303	19129	20360	15583	15606	14792	0,00063757
TonB-dependent Receptor protein	A9HFV5	134712	121171	144472	99459	108272	100323	0,01539119
Tol-Pal system protein TolB	A9HB04	98275	86679	100131	72891	68610	78245	0,00847495
Outer membrane protein assembly factor BamA	A9HKV0	20285	17359	22712	15617	16061	15071	0,04737161
Cold-shock DNA-binding domain protein	A9HK34	126258	105823	131912	85703	112340	84493	0,04434515
Putative exported protein	A9HDN7	26972	28584	28046	18010	23422	24125	0,04096706
Uracil ph phorib yltransferase	A9H391	15132	17840	18233	13489	14700	12308	0,02306167
Glycine cleavage system H protein	A9HM50	22054	19657	16958	15996	16842	13786	0,0471442
Uncharacterized protein	A9H8I6	18752	17359	17155	15736	14981	12726	0,02393681
In itol-3-ph phate synthase	A9H8S7	92248	90145	81587	76433	72485	69632	0,01198545
Putative DNA-binding response regulator mtrA	A9HIE2	17688	17262	17194	13619	15040	14648	0,00607788
Multidrug resistance protein A	A9H3B5	10838	9759	9056	7967	8648	8052	0,03438296
Alcohol dehydrogenase [acceptor]	A9HK12	83970	71557	87691	65197	64959	73502	0,04781323
Multifunctional fusion protein	A9H0J6	35486	32674	36444	27479	33411	27083	0,04757249
Gluconate 2-dehydrogenase (Acceptor)	A9HK15	153813	149223	139531	129442	122851	123083	0,00904069
Acetylornithine aminotransferase	A9HFT8	17649	16653	17742	14881	14212	15206	0,00260035
Putative outer membrane protein	A9H9Q6	14263	14602	14884	13291	13590	12965	0,00347373
N-acetyl-gamma-glutamyl-ph phate reductase	A9HLR0	14994	14896	16173	14320	14058	14115	0,04801716
Bifunctional protein FolD	FOLD	25401	23567	24517	22606	22540	22922	0,03498816
NADH-quinone oxidoreductase chain E	A9HRT6	30654	30484	30673	32445	33088	32484	0,00321105
Hydroxyacylglutathione hydrolase	A9H1G0	11781	12641	12092	13240	13825	13406	0,0080447
50S rib omal protein L1	RL1	58630	57784	64429	63347	66639	70479	0,04484782
50S rib omal protein L10	RL10	121500	122593	116259	138249	135814	129271	0,00755789
DNA-directed RNA polymerase subunit alpha	RPOA	103002	96151	88227	108138	102389	115777	0,04414085
Two-component response regulator	A9HFR4	22625	23764	22303	25756	28063	24413	0,0401148
NADH-quinone oxidoreductase subunit C	A9HRU1	22573	21444	19731	25690	23133	24895	0,02079983
Transcriptional regulator, CarD family	A9HIN7	31743	32557	31136	36493	40079	34944	0,03157372
50S rib omal protein L19	RL19	90314	80846	77416	93604	105997	93580	0,02925392
6-ph phogluconolactonase	A9H335	88020	87451	94472	109047	107080	102796	0,00277739
Uncharacterized protein	A9HM07	16786	14791	15328	18494	19503	17494	0,01314293
Putative D-3-ph phoglycerate dehydrogenase	A9HFV9	21816	22859	21218	25814	27914	24336	0,02108288
Thioredoxin reductase	A9H0A5	17710	16935	15595	20206	19145	20217	0,00978531
Bifunctional enzyme IspD/IspF	A9HLU2	24718	24929	23731	29341	27869	29987	0,00315799
Ph phoglycerate kinase	A9HM30	185659	174380	162543	215927	192988	216190	0,01463562
Trigger factor	TIG	148672	135932	129509	171675	147537	180319	0,04070283
Conserved protein	A9HBW8	12887	11022	11603	13231	14305	15444	0,02154181
Carboxymethylenebutenolidase	A9H121	5591	6542	6265	8351	7304	6709	0,04593082
Biopolymer transport protein ExbD/TolR	A9HF92	37978	30272	35761	43895	42646	40739	0,03083103
S-aden ylmethionine synthase	METK	57277	47377	52295	62935	63274	67564	0,01579821
Conserved protein	A9HBT6	11863	13364	12243	15656	16970	13770	0,03313854
Cof-like hydrolase	A9H332	52397	45559	46338	61664	57068	61338	0,00689579
Thiamine-ph phate pyroph phorylase	A9HI58	9191	7994	7896	9714	9910	11677	0,02957577
Orotate ph phorib yltransferase	A9HII0	37751	32202	30981	45909	38308	42280	0,0240978
Conserved protein	A9HRX3	29430	32302	31320	36380	42280	38191	0,01419902
Alpha/beta hydrolase, chloride peroxidase	A9H000	14128	11573	14834	15702	18449	16981	0,02616347
Cysteine synthase	A9HFX5	26881	24554	25127	30292	32323	34846	0,00896392
Carbonic anhydrase	A9HL77	70227	59332	58381	81476	78628	80731	0,01896738
Adenyl uccinate synthetase	PURA	36926	26855	32252	42029	38498	43080	0,0343404
Gluconate 5-dehydrogenase	A9H995	39634	29408	37719	45053	43129	49376	0,03058273
FMN-dependent NADH-azoreductase	AZOR	26017	20023	23411	30246	26923	32328	0,02340702
ATP synthase gamma chain	ATPG	20524	15587	18482	23659	22970	23968	0,02986597
D-2-hydroxyacid dehydrogensase	A9HDT4	156730	136099	131555	184729	165213	203576	0,01951113
Glucans bi ynthesis protein G	A9HBM4	32911	24278	35800	38331	42059	41215	0,04933275
Dihydrolipoyllysine-residue succinyltransferase component of 2-oxoglutarate dehydrogenase complex	A9HFG9	86721	78474	77839	108867	97293	112643	0,0073817
Acyl-[acyl-carrier-protein]--UDP-N-acetylgluc amine O-acyltransferase	A9HKU0	14028	12228	14514	17447	18092	19204	0,00362681
Peptidase protein	A9HET1	19553	18109	17186	26400	23051	24207	0,00430834
50S rib omal protein L6	RL6	50643	42617	56469	68250	60986	71953	0,0155657
2-dehydro-3-deoxyph phooctonate aldolase	A9HJ79	8864	9077	8316	11039	10978	13391	0,02619436
Ph phorib ylformylglycinamidine synthase subunit PurQ	A9HJG0	15541	14251	16232	21679	22526	18412	0,01568813
ATP-dependent protease subunit HslV	A9H1A3	5439	4295	4263	7235	5876	5949	0,02306482
Ph phoglycerate mutase	A9HBZ6	32693	37243	37585	51631	44556	50811	0,00557104
Putative sulfotransferase	A9HQQ2	18070	16537	22332	24757	22901	30288	0,03567527
Uncharacterized protein	A9HHW9	26508	27934	29900	37888	43951	33687	0,03064354
Putative 2-keto-4-pentenoate hydratase-like	A9HDT5	30103	29956	26610	40385	40872	38135	0,00106766
Superoxide dismutase	A9HL14	139048	151844	136085	189174	198299	201583	0,00059834
UTP--gluc e-1-ph phate uridylyltransferase	A9HJ15	49237	43856	42618	64153	57846	65445	0,00272898
Citrate synthase	A9HII7	51655	37663	35782	59898	48354	64839	0,04209073
Putative FeS assembly protein SufD	A9HRY4	17112	13445	12695	20688	16760	23080	0,03560873
Nucle ide diph phate kinase	NDK	67464	84677	58661	108244	100604	86923	0,02377508
50S rib omal protein L5	A9H3M8	64851	61006	62733	90972	93913	82282	0,00567065
Dihydroorotate dehydrogenase (quinone)	A9HBE5	15218	11424	14171	18972	18843	20340	0,011496
Hydrolase, TatD family	A9HIA6	9254	9722	8420	12938	14776	11589	0,01773183
Gluconokinase	A9HSC5	29436	30110	33186	46379	47188	40336	0,00535918
Major royal jelly protein	A9HBE2	7120	6770	5509	10201	8380	9503	0,00808034
PKHD-type hydroxylase GDI1238/Gdia_1949	Y1238	52978	42201	52659	76315	70476	71193	0,00492592
Oxygen-dependent coproporphyrinogen-III oxidase	A9HK65	12437	11430	13201	18325	16198	20280	0,01181949

Molybdenum cofactor bi ynthesis protein B	A9HAM8	26365	25791	21970	33319	41735	35153	0,0121809
Aminopeptidase	A9HMM0	30719	25869	23096	36839	33939	48202	0,03781832
Ph phorib ylformylglycinamidine cyclo-ligase	A9HJV0	11723	7977	10397	13961	13699	17279	0,01798919
Isochorismatase hydrolase	A9H559	5828	7314	7005	9686	11840	8582	0,02771291
2-ketogluconate reductase	A9H3Y4	14479	13547	13436	14576	15082	14409	0,05125054
50S rib omal protein L11	RL11	83720	76698	94806	90805	107692	102537	0,0517817
Pyrrolo-quinoline quinone	A9H134	32093	27863	35659	24152	29460	22916	0,05180878
Uridylate kinase	A9HKW8	8119	6567	9404	13634	16296	26385	0,05191213
Cysteine desulfurase	A9HRY2	13685	9352	9975	18266	13571	23454	0,05231309
ATP synthase subunit b	A9HDM7	29012	32304	29238	16042	23895	4883	0,05243086
Ph phoglucomutase/ph phomannomutase alpha/beta/alpha domain I	A9H070	36829	28349	35747	23017	21551	31177	0,05265604
UDP-3-O-acylgluc amine N-acyltransferase	A9HKU5	53252	56774	61304	42031	53885	37580	0,05267954
N5-carboxyaminoimidazole ribonucleotide mutase	A9HHQ7	15226	18535	13340	11692	12926	10677	0,05332892
GTP-binding protein TypA/BipA	A9H9C1	10588	5149	5333	14245	9815	20210	0,05364033
Alkyl hydroperoxide reductase AhpD	AHPD	60594	58272	56835	45184	55457	51660	0,05416551
In ine-5'-monoph phate dehydrogenase	A9HID1	23670	15511	15433	36925	22189	43220	0,05482777
Ph phate-binding protein PstS	A9H9X2	60588	56829	58093	55005	56373	55562	0,05484068
NADP oxidoreductase coenzyme F420-dependent	A9HL93	23882	28778	29246	16660	25411	14313	0,05564855
Polyribonucleotide nucleotidyltransferase	PNP	12314	5054	5857	20401	12742	31485	0,05574915
Putative oxidoreductase	A9HM21	55031	56027	56729	45603	46622	29041	0,05579283
Conjugal transfer	A9HT68	81035	77657	84275	69524	75959	58343	0,0567584
Preprotein translocase, YajC subunit	A9HL42	39664	38896	40661	37763	34105	37931	0,05688492
Peptidyl-prolyl cis-trans isomerase	A9HIQ1	100684	114787	118445	98358	103196	83122	0,05706108
Putative exported protein	A9H8Y9	25679	45514	40369	20579	28099	18594	0,05737769
Conserved protein	A9HHR5	56042	64468	58890	38414	46243	10508	0,05795746
30S rib omal protein S16	RS16	51152	70003	80087	48327	49989	39496	0,05832643
Catalase	A9GZZ4	244529	220736	238446	277781	278457	361921	0,0584965
50S rib omal protein L14	RL14	110579	89795	82382	123057	125583	101874	0,05862923
Uncharacterized protein	A9HJF8	50130	64445	60272	39385	53365	27870	0,05903704
ATP synthase subunit b	ATPF	34100	33489	39253	24120	25142	3331	0,05903756
Enolase	ENO	143019	93880	86175	162453	135352	226918	0,05913714
FeS assembly protein SufC	A9HRY6	19811	14494	21390	24998	20908	30069	0,05970217
Reversed Sequence 2559	REVERSE2559	8135	11372	7742	4270	7519	6511	0,05980785
Aden ylhomocysteinase	A9HFJ7	4087	2959	3222	10275	7348	18442	0,06039842
Serine protease	A9HEK6	154147	159099	142773	173993	174191	155290	0,0604209
Uncharacterized protein	A9H732	21785	15090	22501	15718	15224	11316	0,06095438
Serine hydroxymethyltransferase	A9HRP5	41528	26601	29107	47387	37839	60598	0,06143273
PrkA serine protein kinase	A9HIB1	15984	8880	12518	28832	20904	48441	0,06212518
Uncharacterized protein	A9HJS1	13294	8185	13134	16830	13041	19852	0,06263
Indole-3-glycerol ph phate synthase	A9HJA0	20482	20347	17337	50109	25490	36361	0,06267806
Ferredoxin	A9HJZ0	7257	11129	8538	3526	7963	5482	0,06319636
NADH dehydrogenase (Ubiquinone)	A9HKL6	12320	9510	10347	12528	11829	14668	0,06413127
Histidinol dehydrogenase	A9HFM4	4184	3470	3612	5974	4695	8266	0,06439178
Protein RecA	A9HM16	13480	11046	11477	15518	13858	20295	0,06456872
Uncharacterized protein	A9HLI9	18675	15361	28040	12290	14265	8777	0,0647329
Transcriptional regulator LysR	A9H0A8	23810	14964	20354	32434	24783	46329	0,06494667
Cold shock-like protein cspE	A9HIW8	311017	331851	274485	265080	286028	249032	0,06672096
Beta sliding clamp	A9HI34	16755	11413	10110	17808	14811	21718	0,06685611
Acetyl-CoA hydrolase	A9HIK2	17766	5682	6453	31239	25037	68207	0,06765469
Rib ome-binding ATPase YchF	A9HC06	4119	1671	1702	9115	3317	10866	0,06783036
Universal stress protein	A9H0V0	18193	14176	18181	19995	18794	24888	0,06819251
3-oxoacyl-[acyl-carrier-protein] reductase	A9HRE0	38129	32988	34069	28855	32161	32887	0,06825374
Putative DNA binding protein	A9HQJ8	22189	26049	26248	14926	22840	9050	0,06838016
NADPH-dependent 7-cyano-7-deazaguanine reductase	A9H9B4	23378	25425	16933	16926	17475	13859	0,06842335
Threonine synthase	A9HKE7	29482	18714	13890	9990	8594	10512	0,06884984
Arginin uccinate synthase	ASSY	25519	14917	17450	37231	29391	64109	0,06887184
Uncharacterized protein	A9H9H6	17181	9695	9960	33616	33628	14081	0,06924777
Nitrogen regulatory protein P-II	A9HMD4	54645	61182	54512	66149	67739	57847	0,06956777
HAD-superfamily hydrolase, subfamily IA, variant 3	A9HDX4	5753	6744	7268	5079	6141	5474	0,0701012
Single-stranded DNA-binding protein	A9HM62	62243	58310	55387	37639	55843	30734	0,07012692
Conserved protein	A9H282	8240	6265	8153	4978	4824	7241	0,0704793
Conserved protein	A9HAR7	24953	27485	24869	19107	24574	15277	0,07085281
Transcription termination/antitermination protein NusA	A9HF12	11610	5814	5700	13498	11501	23978	0,07112927
Conserved protein	A9HFQ7	18596	22531	27930	15996	20675	13395	0,07188901
Uncharacterized protein	A9HC33	64541	69358	64793	57424	64152	50039	0,07267509
Elongation factor G	A9HS02	48514	39234	35986	89053	53894	128527	0,07300408
Iron-sulfur cluster assembly accessory protein	A9HRX5	16993	19333	24647	13985	18726	11958	0,07393952
ATP synthase subunit delta	ATPD	26327	31014	21036	15539	24836	13661	0,07397952
ATP-dependent Clp protease proteolytic subunit	A9HRV4	57488	46124	51961	61972	57573	79226	0,07410354
Nitrilase/cyanide hydratase	A9GZH7	8351	6419	7775	6554	5599	6654	0,07531032
Aconitate hydratase	A9HEZ2	51829	23379	30813	66970	42241	94033	0,07559212
Uncharacterized protein	A9H0M6	4478	5699	3364	2853	3926	2312	0,0772895
Periplasmic binding protein	A9HK76	20402	19363	20298	23047	24567	20368	0,07859532
Putative chemotaxis protein cheY	A9HHE7	53001	61085	65998	45588	58215	37372	0,07870951
Periplasmic serine endoprotease DegP-like	A9HBK9	42316	43889	42918	33532	40994	25814	0,07931932
Conserved protein	A9H9B9	65986	68674	68956	62188	63063	49043	0,07952458
3-mercaptopyruvate sulfurtransferase	A9HJI4	14142	14234	14871	18178	14709	19278	0,08010186

Uncharacterized protein	A9HBI5	33494	47874	38101	45302	53459	47325	0,08093155
Electron transfer flavoprotein alpha subunit	A9HEE9	84735	86730	85611	83849	75421	81803	0,08244643
Threonine--tRNA ligase	SYT	4387	2775	4276	8865	5765	15979	0,08276369
Glyc yl transferase	A9HH55	25720	18353	28648	28933	28008	36783	0,08331347
3-ph ph hikimate 1-carboxyvinyltransferase	A9H466	226076	235950	231926	228112	166806	154491	0,08333247
In itol-1-monoph phatase	A9H6E0	7074	6158	7677	8073	8038	11178	0,08337317
Uncharacterized protein	A9H3X9	68825	81078	78326	82277	117858	93010	0,08337595
RNA-binding protein Hfq	HFQ	104235	109349	101856	77828	100246	55075	0,08341354
Putative haloacid dehalogenase-like hydrolase	A9HBE7	21183	20691	22111	20951	20446	19235	0,08363635
Integration h t factor subunit alpha	A9HS25	37500	41755	45027	24303	40914	19443	0,08512507
50S rib omal protein L7/L12	RL7	328257	265399	264401	227018	267615	147766	0,08519974
Gluconate 2-dehydrogenase (Acceptor)	A9H186	11111	6999	5345	10327	10258	13351	0,08538845
Tryptophan synthase beta chain	A9HE87	7779	6365	7282	9015	7732	11650	0,0860119
Putative short-chain dehydrogenase	A9HLW8	31545	34946	39529	28275	34548	24720	0,08675079
Putative thioredoxin protein	A9HSA5	72352	79616	77218	63650	75311	55126	0,08700232
Alkyl hydroperoxide reductase AhpD	A9HFF9	43649	38447	35375	34063	37073	26612	0,08731385
Glyceraldehyde-3-ph phate dehydrogenase	A9HM29	274333	229185	232744	304285	254199	359912	0,08742269
Glutamyl-tRNA(Gln) amidotransferase subunit A	A9HRI9	11419	6689	6928	14300	11360	25946	0,08806224
Isocitrate dehydrogenase (NAD(+))	A9HJQ1	58914	42957	44950	86382	52351	112602	0,08830999
Nucleoid-associated protein GDI3467/Gdia_2910	Y3467	43473	56609	59456	39378	51336	33401	0,08865349
ATP synthase subunit alpha	ATPA	63769	46885	46859	72661	53425	81280	0,09018433
ATP synthase subunit beta	ATPB	52607	23250	25603	52543	41902	82400	0,09065165
Ph phopantetheine-binding	A9HRB7	24039	23384	21385	19274	20743	10981	0,09191798
NADH dehydrogenase/NAD(P)H nitroreductase rutE	A9HFB0	12359	9938	11211	14728	16113	11140	0,09405723
Oxidoreductase	A9HAF3	21997	18104	17963	22647	21644	21346	0,0946913
Uncharacterized protein	A9H0W6	8772	9912	9745	7036	9224	4746	0,09469568
S-methyl-5'-thioaden ine ph phorylase	A9HK57	29996	20066	23054	27990	28314	34082	0,094859
Putative multidrug resistance protein mdtA	A9H3E8	6246	19162	17659	5654	7716	6076	0,09539391
Glutamate--tRNA ligase 1	SYE1	28066	20707	25424	41257	35689	24722	0,09565001
Fruct e-bisph phate aldolase class 1	A9H6A5	172530	153148	140460	204970	195410	154585	0,09571059
Flagellar protein FliL	A9HHK6	9550	9023	9762	7409	9438	8143	0,09624968
Biotin carboxylase protein	A9HEX0	11713	5935	7164	16005	8961	23517	0,09626546
Chaperone protein DnaK	DNAK	190488	141431	136661	196399	164725	211202	0,097257
Probable transcriptional regulatory protein GDI0798	A9HAV2	37152	35746	34750	34183	31538	23139	0,0983262
Glutamine synthetase	A9H7Z5	167004	174400	101160	117269	78466	116599	0,09882426
Cell division topological specificity factor	MINE	11196	30288	29178	12447	16565	7427	0,09917282
Geranyltranstransferase	A9HIR3	39095	33147	30727	29520	30866	28816	0,10066725
Uncharacterized protein	A9HEH6	5133	7357	6277	5075	5881	3619	0,10215774
Putative Antibiotic bi ynthesis monooxygenase	A9HM53	5827	6856	7014	8466	10401	6661	0,10329965
Uncharacterized protein	A9HB99	150199	114065	150592	105225	135916	74911	0,10354015
Cytokinin rib ide 5'-monoph phate ph phoribohydrolase	A9HEM3	11184	14685	18271	15982	24673	18334	0,10614748
Acetyl-coenzyme A carboxylase carboxyl transferase subunit alpha	ACCA	48759	58796	44588	59077	58484	57348	0,10614969
Ph phoglycolate ph phatase	A9HI43	29785	42660	42007	48727	56976	38795	0,10690516
Uncharacterized protein	A9H6W0	13605	15914	16251	12729	15271	10683	0,10950061
Peptide chain release factor 2	A9HF65	19833	21586	19731	19075	20029	16508	0,10993389
ATP synthase epsilon chain	ATPE	14534	17961	21137	9444	17536	13511	0,11134548
OmpA/MotB domain protein	A9GZP4	56095	65523	69688	45937	54520	63120	0,11211314
Electron transport protein SCO1/SenC	A9H4T2	20699	19654	19563	20633	24313	20943	0,11397492
Cytidylate kinase	A9H463	9529	10524	10480	6121	10467	3190	0,11502135
30S rib omal protein S1	A9H459	42270	19249	20410	44196	28210	56612	0,11575186
ATP-dependent Clp protease proteolytic subunit	A9HCR1	89554	92283	92130	98963	95985	90821	0,11726517
Putative Thiol:disulfide interchange protein tlpA	A9HRH3	9703	11020	10097	12749	14725	10044	0,11852927
Transcription termination factor Rho	A9HE94	6557	4139	4711	9073	4799	12504	0,11879472
50S rib omal protein L24	RL24	30910	40651	34317	28352	31898	31651	0,11966776
Porin	A9HAM5	14736	13151	22645	11470	12975	11649	0,12047107
Putative L-asparaginase II protein	A9HE73	23784	25460	24909	18965	25156	21225	0,12095276
Zinc-type alcohol dehydrogenase-like protein	A9H2A8	24337	22268	21946	21730	22001	21194	0,1216657
4-hydroxy-tetrahydrodipicolinate synthase	DAPA	21161	17324	20350	20870	20990	27244	0,12336973
Alkyl hydroperoxide reductase/ Thiol specific antioxidant/ Mal allergen	A9H8D6	340215	357900	318385	383862	411906	331695	0,12749373
Transcription elongation factor GreA	A9H1Q0	52977	59346	63937	71374	87214	57601	0,12811628
Putative exported protein	A9HAK6	14439	22969	25687	9016	20943	13941	0,12849161
6,7-dimethyl-8-ribityllumazine synthase	A9HDF5	18083	15316	28439	14492	13587	14995	0,12854541
30S rib omal protein S11	RS11	6618	6461	9864	16231	15379	6138	0,13139168
Cys-tRNA(Pro)/Cys-tRNA(Cys) deacylase	A9H4K8	9242	12261	11808	8150	11541	5676	0,13142868
Cysteine synthase	A9HAE5	60275	67961	48429	64482	70805	67268	0,13231393
Conserved protein	A9HIX3	56283	56845	68031	48187	61576	49158	0,13434724
Bifunctional protein GlmU	GLMU	3757	3080	3035	3527	4039	6663	0,13549428
Quinolinate synthase A	A9H8C0	22148	15432	18619	22600	18664	29163	0,13629099
Uncharacterized protein	A9HBG4	11258	10608	10071	11728	16023	11089	0,13676737
Conserved protein	A9H314	10904	16411	19434	11828	12833	11164	0,14019521
Tyr ine--tRNA ligase	A9HMK2	8315	4154	4196	8007	5504	12169	0,14145536
Putative toluene tolerance	A9HBF1	58214	61384	58913	54818	60627	51553	0,14147113
Peptidase, family M16	A9HKF0	7969	5426	5332	8024	6132	11456	0,14240443
30S rib omal protein S9	A9H812	100199	92137	110185	118789	130930	96630	0,14350559
Peptidyl-prolyl cis-trans isomerase D	A9HJ89	17005	16808	15211	18311	17180	27562	0,14478591
RNA pyroph phohydrolase	RPPH	7009	8536	7445	10712	12149	6845	0,14547584
Aldo/keto reductase	A9HH27	8585	4584	7087	8186	7109	10543	0,1481731

Putative membrane protein	A9HEQ1	35369	85711	55735	35514	56013	20959	0,15115415
Lipoprotein	A9HPJ3	19351	17172	18331	18080	20063	19829	0,1532978
Protein-export protein SecB	SECB	80753	45498	87740	88683	106144	75423	0,15468813
Proline--tRNA ligase	A9HRR5	9836	5558	7810	10433	7363	17162	0,1550003
Site-determining protein	A9HLY3	65299	51842	54274	55180	37208	53879	0,15513229
Aspartyl/glutamyl-tRNA(Asn/Gln) amidotransferase subunit C	GATC	39288	37704	40820	36616	39077	25952	0,15573804
Ph phorib ylamine--glycine ligase	A9H4P1	8038	6880	6003	7625	7141	8795	0,15851251
Putative GAF sensor protein	A9HP16	7839	9022	5162	5131	7277	4943	0,16346887
Putative Ubiquinol-cytochrome c reductase	A9H861	7317	8242	11979	7598	7416	7078	0,16514996
50S rib omal protein L18	RL18	15308	15671	19429	28247	36581	12491	0,16556361
Ferric uptake regulation protein	A9HFC2	24028	24203	24207	24155	22690	15913	0,16576232
Uroporphyrinogen decarboxylase	DCUP	11936	10051	13415	12244	12601	14562	0,16853091
Putative hydrolase protein	A9H9D0	5786	5876	5692	7539	7767	5151	0,17093544
30S rib omal protein S2	RS2	142920	132077	146485	93036	145599	126124	0,17147517
50S rib omal protein L4	RL4	47720	43181	50187	63763	63697	40893	0,17756089
Efflux transporter, RND family, MFP subunit	A9HEF9	57112	52193	49320	43440	55820	44758	0,17860717
Uncharacterized protein	A9HJX9	77660	12399	53671	61513	79232	70259	0,18039634
Flavin-dependent thymidylate synthase	A9HBG1	12457	10855	10799	11828	11561	17234	0,18092684
NADH-quinone oxidoreductase subunit B 2	NUOB2	8051	8215	7071	9057	9043	7351	0,18100541
Uncharacterized protein	A9HDE3	43885	51750	52789	41501	53210	28101	0,18198587
Nicotinate-nucleotide pyroph phorylase	A9H8C5	25835	18779	20692	24697	20702	34967	0,18461024
Pyruvate kinase	A9HEH3	71122	47843	52485	88237	42487	108628	0,18484922
Malonyl CoA-acyl carrier protein transacylase	A9HRE1	27757	21948	20687	28513	22709	27745	0,18624044
Alkyl hydroperoxide reductase/ Thiol specific antioxidant/ Mal allergen	A9H3W7	41356	48232	40169	50048	59252	39908	0,18655766
Conserved protein	A9HM79	31828	39288	42749	28609	42635	17879	0,18829634
DSBA oxidoreductase	A9HIK8	85068	88345	98460	84683	93092	70284	0,18840952
2,3-bisph phoglycerate-independent ph phoglycerate mutase	A9H397	94863	82215	86023	91167	86772	104433	0,1922907
Elongation factor Tu	EFTU	298852	261525	355153	342867	295367	388800	0,19347669
Glucokinase protein	A9HIS0	55227	44025	46697	53240	47074	60330	0,19629846
Ferrochelatase	A9HEQ4	9813	8466	11791	10240	10931	12208	0,19687251
Glyc yl transferase group 1	A9HLZ7	15749	9877	13650	13731	13233	23925	0,19713197
Carboxy-terminal protease protein	A9H3A3	96186	100564	96004	92266	100916	81160	0,19836974
ATPase associated with various cellular activities AAA_3	A9H3C6	14680	22525	23122	20294	25755	23445	0,19941594
50S rib omal protein L9	RL9	135436	129575	134715	133301	140152	134192	0,20273935
Gamma-glutamyl ph phate reductase	A9HC10	8920	6322	7502	8278	7367	10224	0,20452181
Uncharacterized protein	A9H986	20988	33767	23200	24231	25841	11100	0,20655224
Putative transporter protein	A9H3U2	10594	7842	8173	9603	9010	10856	0,20685952
Putative N-formylglutamate amidohydrolase	A9HRH2	8144	9877	8998	8009	9777	4743	0,2106721
Branched-chain-amino-acid aminotransferase	A9HNB7	26091	17671	22145	24490	19971	36668	0,2149564
Putative nitrogen fixation protein nifU	A9HRX9	20382	21180	21831	20134	22144	14892	0,21979427
Putative amidohydrolase	A9HMC5	33089	34751	36147	34281	34903	30600	0,21991173
Succinate dehydrogenase iron-sulfur subunit	A9HFD5	41733	41316	43292	47433	51086	38468	0,22221192
Uncharacterized protein	A9HFS9	19879	17809	6555	8936	14225	9118	0,22331747
30S rib omal protein S8	RS8	48229	50357	62230	58016	64199	52522	0,22489615
Ph phate-specific transport system accessory protein PhoU	A9HS74	16964	17612	18090	17174	18189	11425	0,22553757
Conserved protein	A9HSH2	168632	143046	159016	155838	159044	121395	0,23600668
Hopanoid-associated sugar epimerase	A9HGZ6	15914	11255	15052	16590	12931	17434	0,23603815
Putative chemotaxis protein cheY	A9HHG3	37276	53570	39620	47508	33943	32645	0,23854519
Outer membrane protein	OMPC	473840	482042	441529	482229	437819	429183	0,24080526
Putative dehydrogenase	A9HQE8	16266	14984	13527	15090	13457	14041	0,24134116
Glycerol kinase	A9HHY3	87327	44870	53831	44740	27651	71573	0,24174553
Ph phoaden ine ph ph ulfate reductase	A9H0V9	15274	13990	13442	14365	14958	5946	0,24275799
Tryptophan synthase alpha chain	TRPA	31523	35123	32238	31367	35799	36097	0,242938
Uncharacterized protein	A9HBZ1	12408	11619	11605	12298	37209	8576	0,24634251
50S rib omal protein L30	A9H3K9	52147	60810	45680	51643	55476	32672	0,24946787
Uncharacterized protein	A9HJK6	19260	20737	18282	18771	20042	17066	0,25782307
Chaperone protein dnaJ	A9HAH3	70508	62978	66154	74021	78900	60163	0,25921022
Putative transcriptional regulator	A9HFX3	8961	8209	8372	8583	9057	4586	0,25927676
Gluconokinase	A9H341	4845	8713	10103	6650	8178	4999	0,26512761
NADH:ubiquinone oxidoreductase 17.2 kD subunit	A9HBT3	21592	25241	24869	22537	26619	14167	0,26594702
ATP-dependent zinc metalloprotease FtsH	A9HB14	13624	10218	10410	11673	10745	15566	0,2698273
PEBP family protein	A9HBI3	58622	43911	47841	44994	52066	42685	0,27044977
Aspartate-semialdehyde dehydrogenase	A9HFE5	18651	13615	16194	15191	10868	17508	0,27081079
Gluc e-6-ph phate 1-dehydrogenase	A9HFE6	20105	10756	14127	18229	10869	26695	0,2718847
Signal recognition particle protein	A9HS68	11686	9953	15688	9720	12775	10926	0,27268113
Putative regulatory protein	A9HF98	20586	21459	20962	21276	22768	11092	0,27449121
RpsU-divergently transcribed protein	A9HS45	6437	6234	7472	7340	8392	5972	0,28002919
Putative general stress response protein	A9H3E6	30008	33820	49249	27854	37783	34698	0,28256252
60 kDa chaperonin 1	CH601	277554	231461	232741	297089	258113	231945	0,28397637
Pyridoxal ph phate home tasis protein	A9HMN4	6038	6926	5294	7653	7130	5166	0,28401181
Protease protein	A9HAN0	43021	17835	36621	38899	36859	36947	0,28573746
ATP-dependent protease ATPase subunit HslU	A9H199	14334	11506	12219	26007	9850	12270	0,28754992
Putative peroxiredoxin mC	A9H0U0	4205	60964	46868	39026	61983	45632	0,29027087
Methylthioribul e-1-ph phate dehydratase	MTNB	9220	9569	8656	8597	10394	9525	0,29189884
Xanthine ph phorib yltransferase	A9H0R0	23571	22133	24038	30025	35234	15660	0,29503488
30S rib omal protein S12	RS12	12418	60380	49890	30595	75839	50433	0,29609784
Putative 2Fe-2S ferredoxin	A9HMI7	44032	50624	43458	42452	51565	34152	0,29691963

Histone family protein DNA-binding protein	A9HP12	9381	12464	23931	12497	36643	12740	0,29860911
Uncharacterized protein	A9HRF9	6488	11424	15291	7396	13775	6114	0,30054288
Uncharacterized protein	A9HAQ6	23899	23607	23194	21165	27734	15056	0,30092667
Flavin oxidoreductase	A9H2N2	45724	35548	34560	42255	35565	45755	0,30482596
Aminotransferase	A9HSE9	43512	33730	34396	38955	32694	49864	0,30669622
Uncharacterized protein	A9H4T8	49695	58766	52045	50303	61977	33223	0,30873478
Conserved protein	A9H0X1	9102	10271	8354	8789	9882	7787	0,31717077
Putative glutamyl-tRNA(Gln) amidotransferase subunit A	A9HJR7	22130	17037	15392	19652	17208	21398	0,31761756
Folate-binding protein YgfZ	A9H151	2441	3351	2745	3027	2363	3893	0,33042644
Dehydrogenase (Zinc-binding alcohol dehydrogenase)	A9H246	21549	15074	16720	19109	14558	24670	0,3318015
Anthranilate ph phorib yltransferase	A9HJ97	11153	10116	9411	9674	7491	11634	0,33293552
Putative tonB-dependent receptor	A9HE38	125185	116321	114214	118198	115666	116896	0,33726915
Polyphenol oxidase	A9HBY8	11140	15359	16437	16988	17877	11526	0,33849879
30S rib omal protein S19	RS19	75586	74706	96174	83768	102524	74110	0,34623712
Uncharacterized protein	A9HCR3	18608	7777	13531	14651	14176	15388	0,34633196
Elongation factor Ts	A9HRQ5	120690	113430	80385	96911	121228	115010	0,34649479
Transcriptional regulatory protein	A9HEA8	13350	10233	14835	14826	18148	9247	0,34715365
30S rib omal protein S7	RS7	12116	24757	28376	30089	41689	7878	0,34725655
CRISPR-associated protein, Cse4 family	A9HLC8	14432	9311	10727	11843	9394	16442	0,35009863
Fruct e-1,6-bisph phatase	A9HCQ2	158560	126289	130923	152612	123523	157408	0,35300892
3'(2'),5'-bisph phate nucleotidase CysQ	A9H1J6	10244	10389	11238	11060	10552	10685	0,35442174
Cytochrome c class I	A9HIC3	20078	25030	28612	24014	31082	10947	0,35938919
Ferredoxin--NADP reductase	FENR	26186	11346	12094	14991	15827	12786	0,36003583
Phenylalanine--tRNA ligase alpha subunit	SYFA	18887	13675	14685	17185	13934	18524	0,36159993
tRNA pseudouridine synthase B	TRUB	32113	33850	25171	32046	31853	22584	0,36238386
50S rib omal protein L13	A9H809	23391	17386	21978	37329	28587	7644	0,36239935
Tryptophan--tRNA ligase	A9HIP8	13355	12254	12742	16067	14361	10086	0,36327523
30S rib omal protein S3	RS3	13554	18386	25629	27728	32313	7201	0,36544097
Biopolymer transport protein ExbD/TolR	A9HF93	27775	30244	31840	26683	53475	21418	0,36637774
50S rib omal protein L25	RL25	130088	143320	138416	138445	140880	125833	0,36643323
10 kDa chaperonin	A9HK46	180282	180203	181660	154781	188732	220654	0,36837617
NADH-quinone oxidoreductase subunit I	A9HRS9	22392	27700	17534	28432	25577	18172	0,36915038
3-oxoacyl-[acyl-carrier-protein] synthase 2	A9HRD7	39017	29812	33243	34064	29188	44574	0,36926444
Glutaredoxin	A9HJG8	92269	105429	111547	107411	122746	90821	0,36987352
Rib omal RNA small subunit methyltransferase E	A9H111	6925	5948	6980	6315	6839	6292	0,37187278
Uncharacterized protein	A9HBB9	50719	126090	139820	107293	117477	57465	0,37527896
UDP-N-acetylmuramoyl-L-alanyl-D-glutamate--2,6-diaminopimelate ligase	A9H0H5	7295	6466	6237	6762	6214	6646	0,37552022
Lipoprotein-releasing system ATP-binding protein LolD	A9HRR2	5218	3912	4065	4725	4434	4477	0,37878873
Putative histidine triad (HIT) protein	A9GZW3	17467	20651	26715	12240	26295	21431	0,38060321
3-isopropylmalate dehydratase small subunit	LEUD	11107	12958	13752	12680	16241	10684	0,38194946
Inorganic pyroph phatase	A9H4G5	94547	132783	126654	126689	125277	113970	0,38771734
Uncharacterized protein	A9HF96	77423	92566	96357	83242	96007	80176	0,38777043
30S rib omal protein S5	RS5	31876	60922	67768	41663	79106	22891	0,39628739
Protein TonB	A9HF68	53101	53534	51271	58107	54955	47644	0,39716018
Uncharacterized protein	A9HLE3	12837	14794	17231	13233	18573	10956	0,4019074
BolA family protein	A9HJG6	9295	11197	10778	10663	14471	7770	0,40484514
Ph phatidylserine decarboxylase proenzyme	PSD	19039	15952	18536	17619	21197	16083	0,40669304
Endoribonuclease L-PSP	A9HC24	52306	56063	54455	50379	60511	54319	0,40965199
Isocitrate dehydrogenase [NADP]	A9HBR3	12833	6335	7395	7616	5973	11124	0,40985033
Uncharacterized protein	A9HAE9	64469	72708	68711	70854	77484	51604	0,41331638
Transcription termination/antitermination protein NusG	A9H988	52251	67153	54773	61289	69575	48569	0,41545708
50S rib omal protein L16	RL16	28516	34907	50776	34522	59693	9266	0,41927142
Glycine cleavage system aminomethyltransferase T	A9HM51	26172	17607	21148	22330	18104	26782	0,4197107
ATP ph phorib yltransferase regulatory subunit	A9HLQ2	14469	14749	12768	15527	15333	9940	0,42682713
Electron transfer flavoprotein subunit beta	A9HEE6	75048	65975	61407	66963	69169	68815	0,42736651
Uncharacterized protein	A9HSZ4	29020	28733	28515	28638	31126	27210	0,4283109
Putatiev lipoprotein vacJ	A9HBF3	14236	14741	13494	15114	14325	12548	0,43040489
30S rib omal protein S6	RS6	60197	81043	77937	82146	105965	15440	0,43367791
Putative Antibiotic bi ynthesis monooxygenase	A9HP28	43763	46099	46786	36372	68045	26207	0,44407807
30S rib omal protein S17	A9H3N6	12395	16463	16333	18341	22657	6532	0,44434186
Putative conjugal transfer	A9HSY7	21392	23507	22081	22164	26143	17518	0,44666593
Uncharacterized protein	A9H8H8	113057	119192	109083	106737	127014	104239	0,44822211
Putative xanthine dehydrogenase iron-sulfur-binding subunit	A9H189	6815	10925	10106	9041	11529	7888	0,45387774
Glycerol-3-ph phate dehydrogenase	A9HHX8	24655	13540	17246	17724	14677	24522	0,457807
Thioredoxin	A9HA92	147550	167303	169262	161671	182914	134546	0,46108262
Peptidoglycan-associated protein	A9HB05	379542	285557	229537	329643	334464	212229	0,4615083
Rieske (2Fe-2S) domain protein	A9HL46	7094	11580	15001	14493	13201	6868	0,46629702
30S rib omal protein S10	RS10	10835	59553	61936	47883	59476	20061	0,47012211
Protein-L-isoaspartate O-methyltransferase	A9HI07	66162	68516	73786	67151	75079	65452	0,47389226
Ph phorib ylformylglycinamidine synthase subunit PurS	A9HJF5	38780	40777	34691	34635	47171	33458	0,47405634
Conservev protein	A9GZU8	48306	36311	42922	42414	38577	45760	0,47598985
Elongation factor P	EFP	13725	38997	45928	31764	40127	24897	0,47889885
Peptidyl-prolyl cis-trans isomerase	A9HM70	219986	190981	194664	209058	237797	162573	0,48060836
50S rib omal protein L15	RL15	50784	31179	104908	93461	63979	33338	0,48265534
Conserved protein	A9H137	11989	11263	12503	12533	15734	7797	0,4843344
Putative peptide methionine sulfoxide reductase	A9H394	17975	17215	17028	19126	18277	14705	0,49060963
Beta-lactamase-like protein	A9HC31	11593	11903	11308	11360	14663	8889	0,49241217

Adenyl uccinate lyase	A9HJE7	18719	15508	15324	18053	17804	13796	0,49275427
Putative transcriptional regulatory protein ompR	A9HS40	10086	10602	10233	11060	10572	9281	0,4982656
Uncharacterized protein	A9HSC1	11612	35213	32630	1	8525	1	0,03620487
Putative membrane protein	A9HS08	5476	5638	11421	1535	2044	1	0,03631627
Uncharacterized protein	A9H9E8	6138	6236	6517	1209	3483	1	0,02100601
Glutaredoxin	A9HJ33	26942	28026	28155	20134	16412	1	0,06410517
Uncharacterized protein	A9HH52	18913	14226	22496	18337	1	1	0,08427753

Table S3 - Detailed information of proteins from schematic illustration *G. diazotrophicus* responses to high-sucrose

Localization	Accession	Description	Abbreviation	Number
Outer Membrane	A9H438	Insulinase protein (Zinc protease)	Ins (PqqL)	1
	A9HS35	Lipoprotein	BamE	2
	A9HKU8	Outer membrane protein	OmpH	3
	A9HED6	Outer membrane protein	OmpW	4
	A9HPF6	Putative porin B precursor	OprB	5
	A9H7L3	TonB-dependent siderophore receptor (Iron complex outermembrane receptor membrane)	TonB	6
	A9H932	TonB-dependent receptor (Vitamin B12 transporter)	TonB	7
	A9HDZ9	TonB-dependent receptor (Iron complex outermembrane receptor membrane)	TonB	8
	A9HEU6	TonB-dependent receptor (Catecholate siderophore receptor)	TonB	9
	A9HNM4	TonB-dependent receptor (Iron complex outermembrane receptor membrane)	TonB	10
Periplasm	A9HN17	Secretion protein, HlyD-family (Membrane fusion protein, heavy metal efflux system)	CzcB	11
	A9HM38	Putative exported protein	ExpI	12
	A9H7E6	Putative exported protein (YfdX family protein)	ExpII	13
	A9H103	Putative outer-membrane lipoprotein carrier protein	LolA	14
	A9HS71	Conserved hypothetical protein (Periplasmatic protein CpxP/Spy)	CpxP/Spy	15
	A9H1L4	Peptidyl-prolyl cis-trans isomerase SurA	SurA	16
	A9HK81	Putative cytochrome c551 peroxidase precursor (Cytochrome c peroxidase)	CCP	17
	A9H4A8	Gamma-glutamyltranspeptidase/glutathione hydrolase	Ggt	18
	A9HL52	Transcriptional regulator, IcIR family/regucalcin (Xylono-1,5-lactonase)	Gluc	19
	A9HPB9	Putative D-ribose-binding protein precursor	RbsB	20
	A9HPK6	D-ribose-binding periplasmic protein precursor	RbsB	21
	A9HNP0	D-xylose ABC transporter, periplasmic substrate-binding	XylF	22
	A9HDE6	Pyridine nucleotide-disulphide oxidoreductase (sulfide:quinone oxidoreductase)	PDOx	23
	A9HBF6	Putative aldose 1-epimerase precursor	GalM	24
Inner Membrane	A9H7Z8	P-II family nitrogen regulator	GlnB	25
	A9H8F8	Twin-arginine translocase TatA/TatE family subunit (Sec-indepedent protein translocase protein TatA)	TatA	26
	A9HK01	Ubiquinol oxidase subunit 2 precursor (Cytochrome o ubiquinol oxidase subunit II)	CyoA	27
	A9HJ83	Protein translocase subunit SecG	SecG	28
	A9HMM2	Conserved hypothetical protein (Uncharacterized protein)	HypI	29
	A9HT76	Hypothetical protein (Gly-zipper_YMGG domain-containing protein)	HypII	30
	A9H090	Depeptidy-peptidase (Uncharacterized protein)	DPP	31

	A9HNN4	NAD(P)-dependent alcohol dehydrogenase	Adh	32
	A9HNA5	Alcohol dehydrogenase (propanol-preferring)	AdhP	33
	A9H4V7	Aldehyde dehydrogenase	AldA	34
	A9HPE7	Sugar uptake ABC transporter ATP-binding protein (Multiple sugar transport system ATP-binding protein)	UgpC	35
	A9HAZ8	Biopolymer transport protein TolR	TolR	36
	A9HF70	Biopolymer transport exbB protein	ExbB	37
	A9HMV0	Capsule polysaccharide export inner-membrane protein	CtrB	38
	A9HHS4	Large-conductance mechanosensitive channel	MscL	39
	A9HIN9	Conserved hypothetical protein (ion channel-forming bestrophin family protein)	HypIII	40
	A9HBX1	Pyrroline-5-carboxylate reductase	ProC	41
	A9HMX8	D-amino acid dehydrogenase small subunit)	DadA	42
	A9HHE0	Methyl-accepting chemotaxis protein (Chemoreceptor mcpA)	McpA	43
	A9HNC1	Succinate-semialdehyde dehydrogenase [NADP+]	GabD	44
	A9H435	Putative penicillin-binding protein (Beta-lactamase)	PBP	45
	A9HBU3	Trehalose 6-phosphate phosphatase	OtsB	46
	A9HBL5	Mannitol 2-dehydrogenase	MtlK	47
	A9HBX1	Putative pyrroline-5-carboxylate reductase	ProC	48
	A9HEL6	M1 family metallopeptidase - aminopeptidase N	PepN	49
	A9HFU5	M1 family metallopeptidase - aminopeptidase N	PepN	50
	A9HP02	M3 family metallopeptidase - dipeptidyl carboxypeptidase (Putative peptidyl-dipeptidase dcp)	Dcp	51
	A9HRE6	M13 family metallopeptidase: neprilysin family (Putative metallopeptidase)	PepO	52
	A9HKD9	M32 family metallopeptidase - carboxypeptidase Taq family (Thermostable carboxypeptidase 1)	M32	53
	A9HN12	M61 family metallopeptidase - aminopeptidase (Putative glycyl aminopeptidase)	M61	54
	A9HS00	Serine peptidase S10 - carboxypeptidase (Putative serine carboxypeptidase)	S10	55
	A9HNY2	Methylenetetrahydrofolate reductase (NADPH)	MetF	56
Cytoplasm	A9HNX4	5-methyltetrahydropteroyltriglutamate--homocysteine methyltransferase	MetE	57
	A9GZJ4	Ketol-acid reductoisomerase (NADP(+))	IlvC	58
	A9HCQ4	Homoserine dehydrogenase	HoM	
	A9HSH5	Alpha-D-glucose phosphate-specific phosphoglucomutase (Phosphoglucomutase)	Pgm	59
	A9HI04	Glucokinase	Glk	60
	A9H320	Bifunctional transaldolase/phosoglucose isomerase (Transaldolase - Transladolase/glucose-6-phosphate isomerase)	Tal	61
	A9H0G0	Glucose-6-phosphate 1-dehydrogenase	Zwf	62
	A9HJ42	6-phosphogluconolactonase	Pgl	63
	A9H324	6-phosphogluconate dehydrogenase	Gnd	64
	A9H317	Transketolase	TktA	65
	A9HGX3	Phosphoketolase (Xylulose-5-phosphate/fructose-6-phosphate phosphoketolase)	Pk	66
	A9HJA9	Pyruvate dehydrogenase E1 component subunit beta	PdhB	67

	A9HJB2	Dihydrolipoamid acetyltransferase component of pytuvate dehydrogenase complex (Pyruvate dehydrogenase E2 component (dehydrolipoamide acetyltranferase)	PdhC	68
Cytoplasmic/Flagellar	A9HHD1	Flagellar motor switch protein FliN	FliN	69
Extracellular/Flagellar	A9HH66	Putative flagellin C	FliC	70
Extracellular	A9HPE1	Sorbitol/mannitol transport system substrate-binding protein	SmoE	71